Clinical Studies on Jaw Bone Regeneration

Wu, Vivian

2023

DOI (link to publisher)
10.5463/thesis.309

document version
Publisher's PDF, also known as Version of record

CLINICAL STUDIES ON JAW BONE REGENERATION

Application of Autologous Bone Grafts, Bone Substitutes, and Adipose Stem Cells

VIVIAN WU

The studies described in this thesis were carried out at the section Oral Cell Biology of the Academic Centre for Dentistry Amsterdam (ACTA), University of Amsterdam and Vrije Universiteit Amsterdam, Amsterdam Movement Sciences, Amsterdam, The Netherlands, and at the department of Oral and Maxillofacial Surgery/Oral Pathology, Amsterdam University Medical Centers and ACTA, Vrije Universiteit Amsterdam, Amsterdam Movement Sciences, Amsterdam, The Netherlands.

The printing of this thesis was kindly supported by:
Academisch Centrum Tandheelkunde Amsterdam (ACTA)
Koninklijke Nederlandse Maatschappij tot Bevordering der Tandheelkunde (KNMT)
Nederlandse Vereniging voor Orale Implantologie (NVOI)
Nobel Biocare Benelux
Straumann Group Nederland
Dentsply Sirona Benelux
Dam Medical B.V.
Orfeokliniek
Tandartspraktijk Wu

Cover painting:	Maartje Zwart
Layout and design:	Hans Schaapherder, persoonlijkproefschrift.nl
Printed by:	Ipskamp Printing | proefschriften.net
ISBN:	978-94-6473-159-0
DOI:	http://doi.org/10.5463/thesis.309

VRIJE UNIVERSITEIT

Clinical Studies on Jaw Bone Regeneration

Application of Autologous Bone Grafts, Bone Substitutes, and Adipose Stem Cells

ACADEMISCH PROEFSCHRIFT

ter verkrijging van de graad Doctor of Philosophy aan
de Vrije Universiteit Amsterdam,
op gezag van de rector magnificus
prof.dr. J.J.G. Geurts,
in het openbaar te verdedigen
ten overstaan van de promotiecommissie
van de Faculteit der Tandheelkunde
op dinsdag 3 oktober 2023 om 13.45 uur
in een bijeenkomst van de universiteit,
De Boelelaan 1105

door
Vivian Wu
geboren te Amsterdam

promotoren:	prof.dr. J. Klein Nulend prof.dr. E.A.J.M. Schulten
copromotoren:	dr. M.N. Helder dr. N. Bravenboer
promotiecommissie:	dr. A.D. Bakker prof.dr. G.M. Raghoebar prof.dr. K. de Groot prof.dr.ir. S.C.G. Leeuwenburgh prof.dr. J.W.M. Niessen prof.dr. P.A. Nolte prof.dr. I. Heyligers

The most effortful forms of slow thinking
are those that require you to think fast.

Daniel Kahneman

CONTENTS

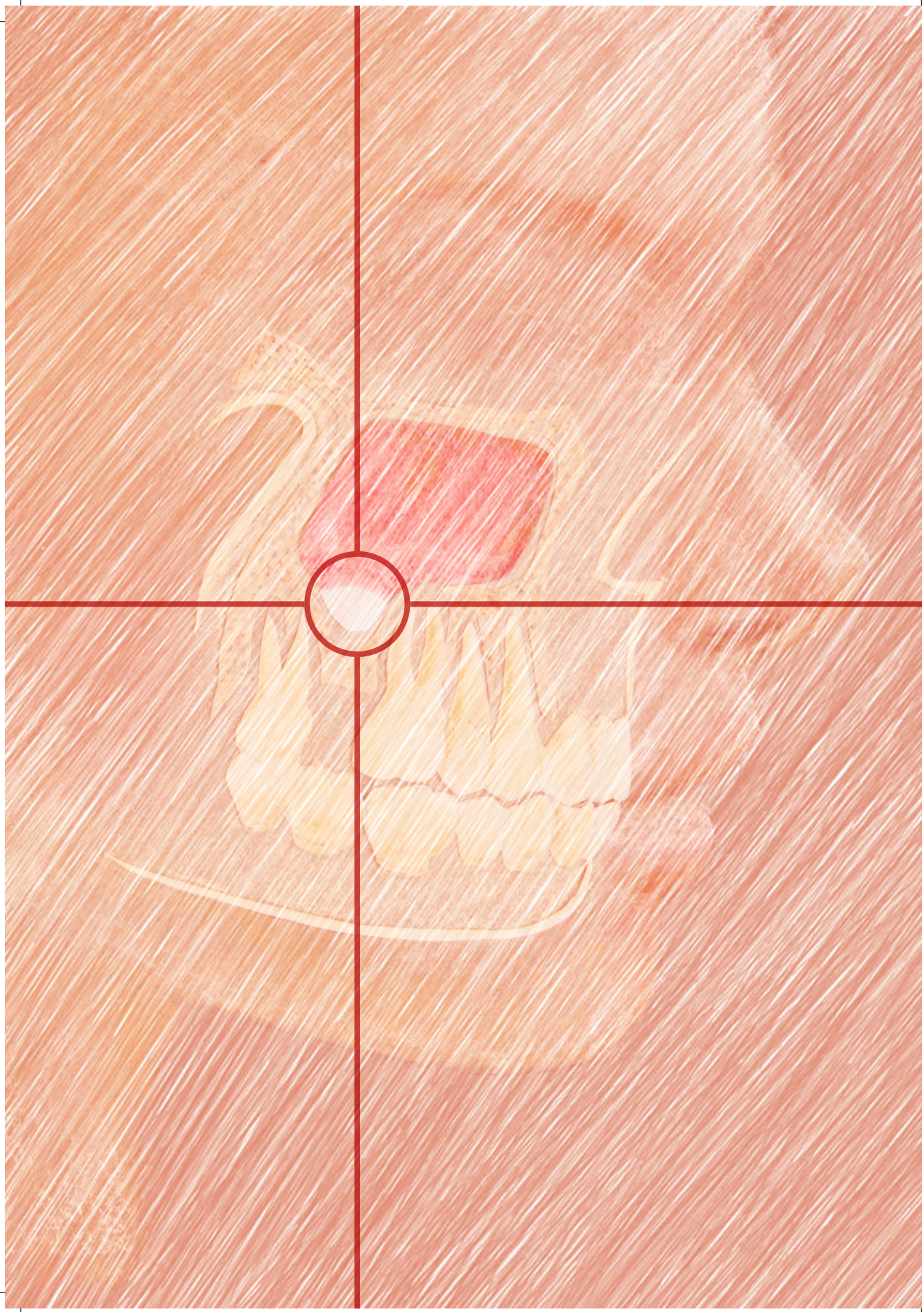

CHAPTER 1

General introduction

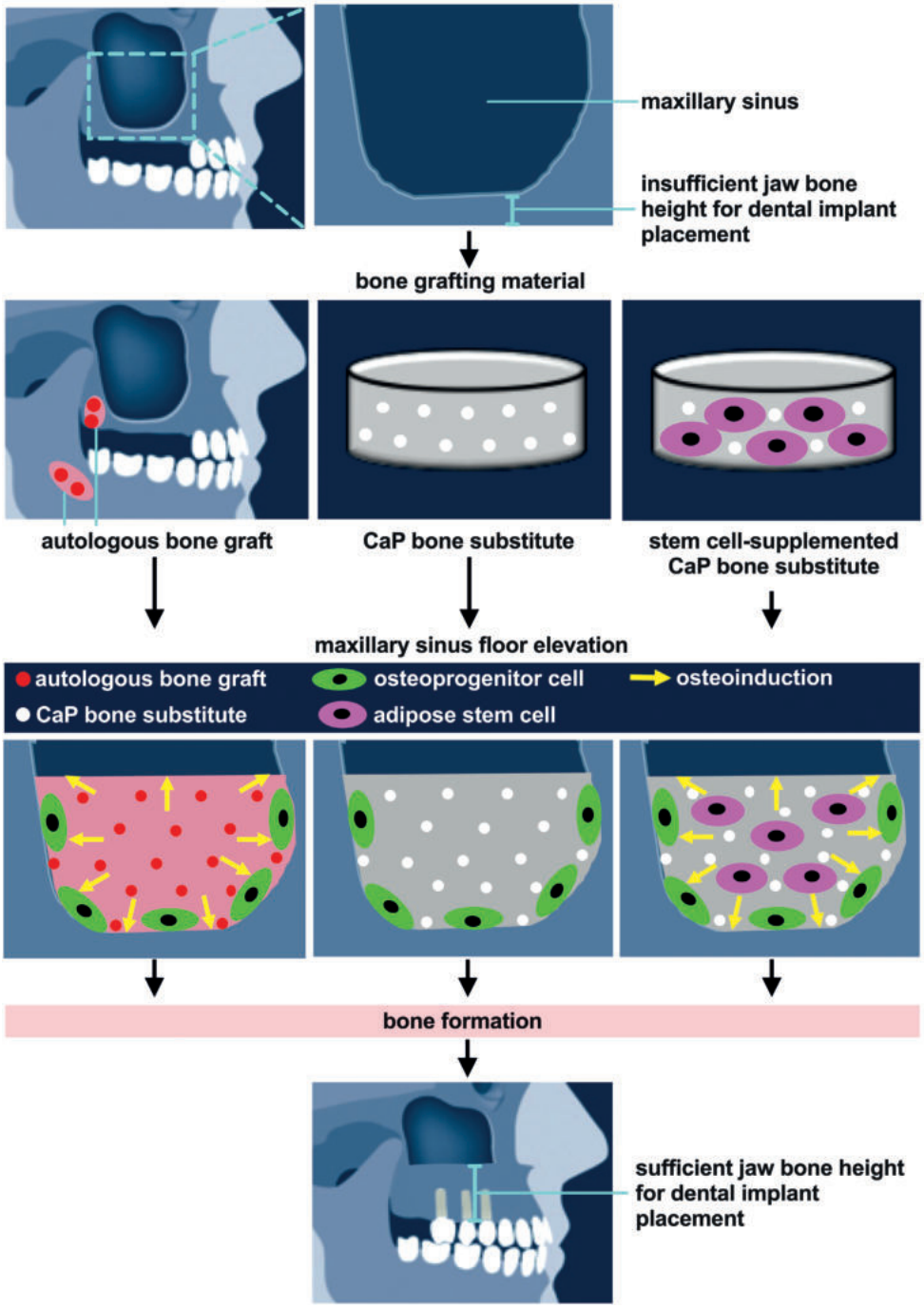
maxillary sinus
insufficient jaw bone height for dental implant placement
bone grafting material
autologous bone graft
CaP bone substitute
stem cell-supplemented CaP bone substitute
maxillary sinus floor elevation
autologous bone graft
CaP bone substitute
osteoprogenitor cell
adipose stem cell
osteoinduction
bone formation
sufficient jaw bone height for dental implant placement

GENERAL INTRODUCTION

The demand for dental implants to replace missing teeth has strongly increased over the last 30 years, and is expected to further increase in the next decade.[1] Insufficient jaw bone volume resulting from alveolar bone loss due to systemic or local causes, is a common and challenging problem for dental implant placement. Systemic causes for alveolar bone loss include congenital abnormalities,[2] general diseases,[3] and medications,[4] while local causes comprise inflammation[5] or traumatic injuries, such as accidents[6] or dental[7] and surgical treatments.[8] Maxillary sinus floor elevation (MSFE) is a commonly used pre-implant surgical procedure and is carried out to restore insufficient alveolar bone height in the lateral maxilla to allow dental implant placement (**Figure 1**). In MSFE the space created between the bottom of the maxillary sinus and the elevated trap door from the lateral sinus wall, and the lifted Schneiderian membrane, is filled with bone grafting material, *i.e.* autologous bone graft and/or bone substitute, allowing bone regeneration.[9,10] Bone regeneration remains challenging with the currently available bone grafting materials. The ideal bone regeneration material with sufficient biomimetic properties, excellent bone regeneration potential, and limited drawbacks, *e.g.* low patient morbidity, sufficient availability, low costs, has not been developed yet. In this thesis, patients underwent MSFE using autologous bone graft, calcium phosphate bone substitute only, or calcium phosphate bone substitute supplemented with stromal vascular fraction (SVF) (**Figure 1**).

▶ **Figure 1. Schematic presentation of the experimental procedure.** Maxillary sinus floor elevation (MSFE) is carried out in patients to restore insufficient bone height in the lateral maxilla to allow dental implant placement. Autologous bone graft (retromolar or tuberosity bone graft), calcium phosphate (CaP) bone substitute (β-tricalcium phosphate (β-TCP) or biphasic calcium phosphate (BCP)), or stem-cell supplemented CaP bone substitute (β-TCP + stromal vascular fraction (SVF) or BCP + SVF) can be used as bone grafting materials in MSFE. Autologous bone graft and the supplementation of adipose stem cells to the CaP bone substitute allow bone regeneration through osteoinduction and osteoconduction. CaP bone substitute allows bone regeneration through osteoconduction only. The treatment goal of MSFE is to regenerate sufficient jaw bone height for dental implant placement (illustrations were adapted from the ITI Foundation, Basel, Switzerland). CaP, calcium phosphate.

Autologous bone graft and bone substitute in jaw bone regeneration

Autologous bone graft is the gold standard for bone augmentation in MSFE, since it contains osteogenic cells and has osteoconductive as well as osteoinductive properties, and does not evoke immunogenic responses.[11,12] Various donor sites are used to harvest autologous bone, including iliac crest, calvarium, tibia, and intraoral sites (mandible, maxilla).[13–15] The choice of the donor site is based on the quantity of bone graft required, the accessibility of the donor site, the time required with regard to the harvesting procedure, and costs involved. Autologous bone graft from intraoral sites is widely used in MSFE, either applied purely or mixed with a bone substitute.[9,16] A major advantage of intraoral sites for bone harvesting compared to extraoral sites, is that the graft can be harvested under local anesthesia, while extraoral sites usually require general anesthesia.[17,18] The mandibular retromolar and maxillary tuberosity regions are favorable donor sites due to low morbidity compared to other intraoral sites.[17–19] There are multiple major clinical and biological differences between bone harvested from the retromolar area versus the tuberosity region. Bone from the retromolar region is predominantly cortical with a high mineral density, while bone from the maxillary tuberosity is mainly cancellous with a lower mineral density.[20,21] Cortical bone graft is considered to have less bone regeneration potential than cancellous bone graft, due to lack of osteogenic cells and less osteoconductive matrix surfaces.[22–24] Retromolar and tuberosity bone grafts are both widely applied autologous bone grafts. To the best of our knowledge, possible differences in bone regeneration potential and outcome between these two autologous bone grafts have never been explored.

Drawbacks of autologous bone graft, *e.g.* patient morbidity, limited availability, encourage the search for suitable alternatives with similar bioactivity. Current alternative grafting materials in MSFE are allograft, xenograft, or synthetic bone substitute.[11] Calcium phosphate bone substitute, *e.g.* hydroxyapatite (HA), β-tricalcium phosphate (β-TCP), and a combination of HA/β-TCP (biphasic calcium phosphate; BCP), are frequently used since they do not cause adverse cellular reactions.[25-28] The calcium phosphate bone substitute material is either replaced by bone or integrated into the local tissue over time, depending on the degradation properties.[25-28] However, calcium phosphate bone substitute shows low bone in-growth rates in comparison with autologous bone graft, since it only has osteoconductive properties and lack osteoinductive potential.[29,30] At present, there is no bone substitute available that has superior or even the same biological properties compared with autologous bone graft.[11,31-33] Therefore, there is a necessity to develop novel bone regeneration materials with similar bioactivity as autologous bone graft, as alternatives or adjuncts to the current bone grafting materials, in an effort to overcome the limitations of using autologous bone graft or bone substitute.

Stem cell application in jaw bone regeneration

Cellular bone tissue engineering uses bone substitute and stem cells to actively modify the patient's micro-environment towards the optimal bone regeneration niche.[29,34,35] In this approach, bone substitute (scaffold) is seeded with mesenchymal stem cells (MSCs) and/or osteoprogenitor cells to enhance their bioactivity.[34-36] The rationale behind the application of MSCs and/or osteoprogenitor cells is their key role in natural bone formation. One of the

mechanisms by which the MSCs on the scaffold orchestrate bone formation at the implant site is by differentiating into osteoblasts, that eventually will secrete osteoid and initiate mineralization.[34] In addition, MSCs can enhance bone formation indirectly at the implant site by a paracrine effect, *i.e.* secreting osteoinductive signals to recruit MSCs or activate preosteoblasts from surrounding bone to the implant site.[37,38] This might result in faster bone regeneration than when using bone substitute only. The clinically applied sources of cells in cellular bone tissue engineering in the oral and maxillofacial region are MSCs originating from bone marrow,[39,40] adipose tissue (adipose stem cells; ASC),[28] and dental tissues (dental stem cells; DSC).[41] Adult bone marrow-derived MSCs (BMSCs) are the most frequently used cells in cellular bone tissue engineering. Several successful applications of BMSCs, ASCs, and DSCs have been reported in MSFE-patients, *i.e.* increased new bone formation using BMSCs in MSFE after three to four months, ASCs after six months, and DSCs after six months, compared to using a bone substitute only.[28,39-41] BMSC-application is associated with drawbacks (*e.g.* painful harvesting procedure, cell proliferation decreases with age, costly because of the need for good manufacturing practice (GMP)-expansion),[42-44] which encourages the search for other stem cell sources. Unfortunately, the application of DSCs has the same major drawback as BMSCs, *i.e.* a low total number of stem cells. Adipose tissue is a promising source of stem cells, opening appealing new possibilities in adult stem cell therapies by overcoming the drawbacks of BMSC and DSC-application. ASCs and BMSCs show many smiliarities in surface marker profiles, multilineage potential, and growth properties.[45,46] However, in contrast to the other sources (bone marrow and dental tissue), adipose tissue has the following advantages: (a) it has a high stem cell-to-volume ratio,[45] (b) the stem cell frequency is far less sensitive to ageing, (c) harvesting can easily be upscaled according to the demand, and (d) it can be processed within a short time frame to obtain highly enriched ASC preparations (residing in the SVF).[28] Furthermore, the multipotent cells within the SVF attach very fast to the scaffold material, proliferate rapidly, and can be differentiated toward amongst others the osteogenic lineage.[47,48] SVF is a cell source with clinical feasibility due to the large quantities that can be harvested and applied in a one-step surgical procedure.[28,48]

Biophysical, biomechanical, and biochemical micro-environment (niche) for jaw bone regeneration

To develop future strategies for the application of MSCs in jaw bone regeneration, detailed knowledge of the biophysical, biomechanical, and biochemical micro-environment (niche) of bone cells at the bone regeneration site is needed. The most important bone cells involved in bone regeneration are osteoblasts, osteoclasts, and osteocytes. The physical micro-environment (niche) of bone cells consists of a dynamic set of biophysical and biomechanical stimuli, *e.g.* shear, stress, strain, pressure, acceleration, streaming potentials, and fluid flow.[49] The biochemical micro-environment (niche) of bone is a complex environment, including growth factors and cytokines, as well as collagen and other extracellular matrix proteins, enzymes, ions, and minerals, which are involved in the processes of bone formation, repair, and remodeling.[50] Bone cells are sensitive to this physical and biochemical micro-environment, and adapt their response and function accordingly.[34,51-56] Therefore, bone substitute properties

should closely match and/or actively modify the patient's bone micro-environment towards the optimal bone regeneration niche. Osteocytes which are embedded in bone matrix, may play a crucial role in the micro-environment for jaw bone regeneration.[35] Osteocytes are known as the key orchestrator of bone homeostasis, including mechanical sensing and transducing mechanical signals into chemical signals via its lacuna-canalicular fluid flow system to regulate bone formation (osteoblasts) and bone resorption (osteoclasts) during bone remodeling.[53,55,56] Mechanical loading of natural teeth keeps jaw bone mechanically strained, and the mechanosensitive osteocytes likely regulate (local) bone mass accordingly. Osteocyte morphology and orientation seem to be affected by the mechanical loading direction.[34,38,58-61] Round osteocytes are much more mechanosensitive than elongated cells.[62] It is unknown whether local osteocyte shape in jaw bone may affect local bone mass. Therefore, investigations into the relation between osteocyte shape and mechanical loading in jaw bone are much encouraged. Moreover, mechanical loading regulated crosstalk between osteocytes and MSCs are currently investigated.[63,64] When osteocytes are optimally used and stimulated by mechanical loading, the bone regeneration niche can be improved effectively and rapidly.

Vascularization in jaw bone regeneration

A major challenge in cellular bone tissue engineering is still the vascularization of the implanted graft.[65–68] Adequate vascularization is a prerequisite for successful bone regeneration. Since the amount of oxygen is limited to a diffusion distance of only ~150-200 µm from a supply blood vessel, cells lying beyond this physiological border suffer hypoxia.[69] Under this condition, osteogenic cells do not survive, since they are unable to adapt their glucose consumption, and lack the glycolytic reserves required to sustain their metabolism for more than three days.[70] Bone tissue regeneration over 200 µm exceeds the capacity of diffusion for nutrient supply and waste removal from the tissue, and thus requires an intimate supply of vascular networks.[69] Successful bone regeneration requires rapid perfusion and integration of the implanted graft with the recipient vasculature. Neovascularization by angiogenesis along with efficient vascularization is a prerequisite to this end. Therefore, optimal vascularization is needed for adequate osteogenesis in jaw bone regeneration, leading to successful placement of dental implants.

Stromal vascular fraction-supplementation in maxillary sinus floor elevation: earlier phase-I clinical trial

In a previous phase-I clinical trial, 10 patients underwent MSFE prior to dental implant placement using freshly isolated autologous, heterologous SVF seeded on either ß-TCP or BCP carriers in a one-step surgical procedure.[28] Induction of bone mass and bone formation by SVF-supplementation to calcium phosphate bone substitute, in particular in ß-TCP-treated patients, has been shown in biopsies.[28] Moreover, more bone mass seemed to correlate with blood vessel formation, and was higher in the cranial part of the SVF-supplemented biopsies, in particular in β-TCP-treated patients.[71] Based on 3-year follow-up results, feasibility, safety, and potential efficacy of SVF seeded on calcium phosphate carriers, and indicated a pro-angiogenic effect of SVF have been demonstrated. [28,71] However, no long-term results have been reported for SVF-supplementation in patients undergoing MSFE.

Stromal vascular fraction-supplementation in oral maxillofacial bone regeneration: long-term follow-up

Clinical evidence of SVF (containing ASCs)-application for bone regeneration in the oral and maxillofacial region is limited to the previously described phase-I clinical trial,[28] although the potential of SVF evokes high expectations. A few studies reported on ASC-application, *i.e.* ASCs isolated from adipose tissue, and expanded in good manufacturing practice (GMP)-facilities, in cranioplasty.[72–75] Unsatisfactory long-term clinical results of ASC-application in cranioplasty were reported.[74] During six-year follow-up of patients who underwent ASC-application in cranioplasty, four out of five patients suffered from unsatisfactory treatment outcome partially due to poor ossification, infection, or tumor recurrence, and two patients had to be re-operated due to graft resorption.[74] Stem cell-application in regenerative medicine has also raised safety concerns, *e.g.* tumorigenic potential and biodistribution.[76] Therefore, clinical studies investigating long-term safety and efficacy are essential before continuing with clinical applications using ASCs in the oral and maxillofacial region, and specifically in jaw bone regeneration.

Outline of the thesis

The overall aim of this thesis was to investigate bone formation and vascularization in jaw bone regeneration using different bone grafting materials, either or not supplemented with SVF, for dental implant placement (**Figure 1**).

In this thesis the following specific objectives/scientific questions were addressed:

1. What are the advancements in stem cell application, vascularization, and bone regeneration in the oral and maxillofacial region, with emphasis on the human jaw (**Chapter 2**)?
2. Do retromolar or tuberosity bone grafts result in different bone vitality and vascularization in patients who underwent MSFE (**Chapter 3**)?
3. Do tensile strain levels and orientation relate with osteocyte morphology and orientation in single gap versus free-ending dental implant positions in maxillary bone in patients who underwent MSFE (**Chapter 4**)?
4. Do calcium phosphate bone substitute, either or not supplemented with SVF, and autologous bone graft have similar vascularization and bone regeneration potential in patients who underwent MSFE (**Chapter 5**)?
5. Does freshly isolated autologous SVF in combination with calcium phosphate ceramic result in long-term safety, and dental implant survival based on clinical and radiological outcomes in patients who underwent MSFE (**Chapter 6**)?

Bone regeneration in MSFE remains challenging with the currently available bone regeneration materials. Stem-cell based bone tissue engineering has led to promising new treatment options. Therefore, in **Chapter 2** we presented and discussed the advancement of stem cell application, vascularization, and bone regeneration in the oral and maxillofacial region, with emphasis on the human jaw. Moreover, we proposed new strategies to improve the current techniques, which may lead to feasible clinical applications.

Autologous bone graft is currently the “gold standard” grafting material in MSFE, due to its enhanced bioactivity compared to bone substitute. Retromolar and tuberosity bone grafts are clinically widely applied autologous bone grafts. Therefore, in **Chapter 3** we investigated possible differences in bone vitality and vascularization in patients undergoing MSFE using retromolar or tuberosity bone grafts through histomorphometrical analysis of bone biopsies.

Mechanical loading and osteocytes play a crucial role in the micro-environment (niche) of the bone regeneration site. Therefore, in **Chapter 4** we investigated the relationship between the levels and orientation of tensile strain and the morphology and orientation of osteocytes in single gap versus free-ending dental implant positions in the maxillary bone through a finite element model and histomorphometrical analyses.

A major challenge in bone regeneration is still the (re)vascularization of the implanted graft. Therefore, in **Chapter 5** we investigated vascularization and bone regeneration potential of calcium phosphate bone substitute either or not SVF-supplemented versus autologous bone graft in MSFE.

Short-term results of SVF (containing ASCs)-supplementation for bone regeneration in MSFE evokes high expectations. Long-term follow-up of patients is lacking. Therefore, in **Chapter 6** we assessed the long-term safety, dental implant survival, and clinical and radiological outcomes after MSFE using freshly isolated autologous SVF-supplementation in combination with calcium phosphate ceramics.

REFERENCES

1. Elani HW, Starr JR, Da Silva JD, Gallucci GO. Trends in dental implant use in the U.S., 1999–2016, and projections to 2026. *J Dent Res.* 2018;97(13):1424–1430. doi:10.1177/0022034518792567
2. Baxter DJG, Shroff MM. Developmental maxillofacial anomalies. *Semin Ultrasound CT MR.* 2011;32(6):555–568. doi:10.1053/j.sult.2011.06.004
3. Foster BL, Ramnitz MS, Gafni RI, Burke AB, Boyce AM, Lee JS, Wright JT, Akintoye SO, Somerman MJ, Collins MT. Rare bone diseases and their dental, oral, and craniofacial manifestations. *J Dent Res.* 2014;93(7):7S-19S. doi:10.1177/0022034514529150
4. Kuroshima S, Sasaki M, Sawase T. Medication-related osteonecrosis of the jaw: A literature review. *J Oral Biosci.* 2019;61(2):99-104. doi:10.1016/j.job.2019.03.005
5. Terashima A, Takayanagi H. The role of bone cells in immune regulation during the course of infection. *Semin Immunopath.* 2019;41:619–626. doi:10.1007/s00281-019-00755-2
6. Chukwulebe S, Hogrefe C. The diagnosis and management of facial bone fractures. *Emerg Med Clin North Am.* 2019;37(1):137-151. doi:10.1016/j.emc.2018.09.012
7. Araújo MG, Lindhe J. Dimensional ridge alterations following tooth extraction. An experimental study in the dog. *J Clin Periodontol.* 2005;32(2):212–218. doi:10.1111/j.1600-051X.2005.00642.x
8. Rolski D, Kostrzewa-Janicka J, Zawadzki P, Zycińska K, Mierzwińska-Nastalska E. The management of patients after surgical treatment of maxillofacial tumors. *BioMed Res Int.* 2016:4045329. doi:10.1155/2016/4045329
9. Starch-Jensen T, Aludden H, Hallman M, Dahlin C, Christensen AE, Mordenfeld A. A systematic review and meta-analysis of long-term studies (five or more years) assessing maxillary sinus floor augmentation. *Int J Oral Maxillofac Surg.* 2018;47(1):103–116. doi:10.1016/j.ijom.2017.05.001
10. Tatum HJ. Maxillary and sinus implant reconstructions. *Dent Clin North Am.* 1986;30(2):207-229.
11. Stumbras A, Krukis MM, Januzis G, Juodzbalys G. Regenerative bone potential after sinus floor elevation using various bone graft materials: A systematic review. *Quintessence Int.* 2019;50(7):548–558. doi:10.3290/j.qi.a42482
12. Zijderveld SA, Zerbo IR, Van den Bergh JPA, Schulten EAJM, Bruggenkate CM. Maxillary sinus floor augmentation using a compared to autogenous bone grafts. *Int J Oral Maxillofac Implant.* 2005;20(3):432–440.
13. Emeka N, Neukam FW. Autogenous bone harvesting and grafting in advanced jaw resorption: Morbidity, resorption and implant survival. *Eur J Oral Implant.* 2014;7:S203-S217.
14. Klijn RJ, Meijer GJ, Bronkhorst EM, Jansen JA. Sinus floor augmentation surgery using autologous bone grafts from various donor sites: A meta-analysis of the total bone volume. *Tissue Eng Part B Rev.* 2010;16(3):295–303. doi:10.1089/ten.teb.2009.0558
15. Kalk WWI, Raghoebar GM, Jansma J, Boering G. Morbidity from lilac crest bone harvesting. *J Oral Maxillofac Surg.* 1996;54(12):1424–1429. doi:10.1016/S0278-2391(96)90257-8
16. Wallace SS, Froum SJ. Effect of maxillary sinus augmentation on the survival of endosseous dental implants. A systematic review. *Ann Periodontol.* 2003;8(1):328–343. doi:10.1902/annals.2003.8.1.328
17. Misch CM. Comparison of intraoral donor sites for onlay grafting prior to implant placement. *Int J Oral Maxillofac Implants.* 1997;12(6):767–776.
18. Raghoebar GM, Meijndert L, Kalk WWI, Vissink A. Morbidity of mandibular bone harvesting: a comparative study. *Int J Oral Maxillofac Implants.* 2007;22(3):359–365.

19. Tolstunov L. Implant zones of the jaws: implant location and related success rate. *J Oral Implant.* 2007;33(4):211–220.

20. Tolstunov L. Maxillary tuberosity block bone graft: Innovative technique and case report. *J Oral Maxillofac Surg.* 2009;67(8):1723–1729. doi:10.1016/j.joms.2009.03.043

21. Kamal M, Gremse F, Rosenhain S, Bartella AK, Hölzle F, Kessler P, Lethaus B. Comparison of bone grafts from various donor sites in human bone specimens. *J Craniofac Surg.* 2018;29(6):1661–1665. doi:10.1097/SCS.0000000000004586

22. Le Lorc'h-Bukiet I, Tulasne JF, Llorens A, Lesclous P. Parietal bone as graft material for maxillary sinus floor elevation: Structure and remodeling of the donor and of recipient sites. *Clin Oral Implants Res.* 2005;16(2):244–249. doi:10.1111/j.1600-0501.2004.01102.x

23. Blomqvist JE, Alberius P, Isaksson S, Linde A, Obrant K. Importance of bone graft quality for implant integration after maxillary sinus reconstruction. *Oral Surg Oral Med Oral Pathol Oral Radiol Endod.* 1998;86(3):268–274. doi:10.1016/S1079-2104(98)90170-6

24. Burwell RG. Studies in the transplantation of bone: VII. The fresh composite homograft-autograft of cancellous bone: An analysis of factors leading to osteogenesis in marrow transplants and in marrow-containing bone grafts. *J Bone Joint Surg Am.* 1964;46:110–140.

25. Sheikh Z, Abdallah MN, Hanafi AA, Misbahuddin S, Rashid H, Glogauer M. Mechanisms of in vivo degradation and resorption of calcium phosphate based biomaterials. *Materials (Basel).* 2015;8(11):7913–7925. doi:10.3390/ma811543

26. Kang H-J, Makkar P, Padalhin AR, Lee G-H, Im S-B, Lee B-T. Comparative study on biodegradation and biocompatibility of multichannel calcium phosphate based bone substitutes. *Mater Sci Eng C Mater Biol Appl.* 2020;110:110694. doi:10.1016/j.msec.2020.110694

27. Helder MN, Van Esterik FAS, Kwehandjaja MD, Schulten EAJM, Ten Bruggenkate CM, Klein-Nulend J. Evaluation of a new biphasic calcium phosphate for maxillary sinus floor elevation: Micro-CT and histomorphometrical analyses. *Clin Oral Implant Res.* 2018;29:488–498. doi:10.1111/clr.13146

28. Prins HJ, Schulten EAJM, Ten Bruggenkate CM, Klein-Nulend J, Helder MN. Bone regeneration using the freshly isolated autologous stromal vascular fraction of adipose tissue in combination with calcium phosphate ceramics. *Stem Cells Transl Med.* 2016;5(10):1362–1374.

29. Zijderveld SA, Zerbo IR, Van den Bergh JPA, Schulten EAJM, Ten Bruggenkate CM. Maxillary sinus floor augmentation using a beta-tricalcium phosphate (Cerasorb) alone compared to autogenous bone grafts. *Int J Oral Maxillofac Implants.* 2005;20(3):432–440.

30. Schulten EAJM, Prins HJ, Overman JR, Helder MN, Ten Bruggenkate CM, Klein-Nulend J. A novel approach revealing the effect of a collagenous membrane on osteoconduction in maxillary sinus floor elevation with β-tricalcium phosphate. *Eur Cell Mater.* 2013;25:215–228. doi:10.22203/eCM.v025a16

31. Danesh-Sani SA, Wallace SS, Movahed A, El Chaar ES, Cho SC, Khouly I, Testori T. Maxillary sinus grafting with biphasic bone ceramic or autogenous bone: Clinical, histologic, and histomorphometric results from a randomized controlled clinical trial. *Implant Dent.* 2016;25(5):588-593. doi:10.1097/ID.0000000000000474

32. Schmitt CM, Doering H, Schmidt T, Lutz R, Neukam FW, Schlegel KA. Histological results after maxillary sinus augmentation with Straumann® BoneCeramic, Bio-Oss®, Puros®, and autologous bone. A randomized controlled clinical trial. *Clin Oral Implants Res.* 2013;24(5):576–585. doi:10.1111/j.1600-0501.2012.02431.x

33. Zerbo IR, Zijderveld SA, De Boer A, Bronckers ALJJ, De Lange G, Ten Bruggenkate CM, Burger EH. Histomorphometry of human sinus floor augmentation using a porous β-tricalcium phosphate: A prospective study. *Clin Oral Implants Res.* 2004;15(6):724–732. doi:10.1111/j.1600-0501.2004.01055.x

34. Klein-Nulend J, Bacabac RG, Bakker AD. Mechanical loading and how it affects bone cells: the role of the osteocyte cytoskeleton in maintaining our skeleton. *Eur Cell Mater.* 2012;24:278–291.

35. Cao W, Helder MN, Bravenboer N, Wu G, Jin J, Ten Bruggenkate CM, Klein-Nulend J, Schulten EAJM. Is there a governing role of osteocytes in bone tissue regeneration? *Curr Osteoporos Rep.* 2020;18(5):541-550. doi:10.1007/s11914-020-00610-6

36. Robling AG, Bonewald LF. The osteocyte: New insights. *Annu Rev Physiol.* 2020;82:485–506. doi:10.1146/annurev-physiol-021119-034332

37. Klein-Nulend J, Bakker AD, Bacabac RG, Vatsa A, Weinbaum S. Mechanosensation and transduction in osteocytes. *Bone.* 2013;54(2):182–190. doi:10.1016/j.bone.2012.10.013

38. Marotti G. Osteocyte relevance orientation in human lamellar bone and its to the morphometry of periosteocytic lacunae. *Metab Bone Dis Relat Res.* 1979;1(4):325–333.

39. Rickert D, Sauerbier S, Nagursky H, Menne D, Vissink A, Raghoebar GM. Maxillary sinus floor elevation with bovine bone mineral combined with either autogenous bone or autogenous stem cells: A prospective randomized clinical trial. *Clin Oral Implant Res.* 2011;22(3):251–258. doi:10.1111/j.1600-0501.2010.01981.x

40. Kaigler D, Avila-Ortiz G, Travan S, Taut AD, Padial-Molina M, Rudek I, Wang F, Lanis A, Giannobile WV. Bone engineering of maxillary sinus bone deficiencies using enriched CD90+ stem cell therapy: A randomized clinical trial. *J Bone Miner Res.* 2015;30(7):1206–1216. doi:10.1002/jbmr.2464

41. Y Baena RR, D'Aquino R, Graziano A, Trovato, Letizia T, Aloise AC, Ceccarelli G, Cusella G, Pelegrine AA, Lupi SM. Autologous periosteum-derived micrografts and PLGA/HA enhance the bone formation in sinus lift augmentation. *Front Cell Dev Biol.* 2017;5:87. doi:10.3389/fcell.2017.00087

42. Pittenger MF, Mackay AM, Beck SC, Jaiswal RK, Douglas R, Mosca JD, Moorman MA, Simonetti DW, Craig S, Marshak DR. Multilineage potential of adult human mesenchymal stem cells. *Science.* 1999;284(5411):143–147.

43. Hernigou PH, Poignard A, Beaujean F, Rouard H. Percutaneous autologous bone-marrow grafting for nonunions: Influence of the number and concentration of progenitor cells. *J Bone Joint Surg Am.* 2005;87(7):1430–1437. doi:10.2106/JBJS.D.02215

44. Muschler GF, Nitto H, Boehm CA, Easley KA. Age- and gender-related changes in the cellularity of human bone marrow and the prevalence of osteoblastic progenitors. *J Orthop Res.* 2001;19(1):117–125. doi:10.1016/S0736-0266(00)00010-3

45. Zhu Y, Liu T, Song K, Fan X, Ma X, Cui Z. Adipose-derived stem cell: A better stem cell than BMSC. *Cell Biochem Funct.* 2008;26(6):664–675. doi:10.1002/cbf.1488

46. Jurgens WJFM, Oedayrajsingh-Varma MJ, Helder MN, Zandieh Doulabi B, Schouten, TE, Kuik DJ, Ritt MJPF, Van Milligen FJ. Effect of tissue-harvesting site on yield of stem cells derived from adipose tissue: Implications for cell-based therapies. *Cell Tissue Res.* 2008;332(3):415–426. doi:10.1007/s00441-007-0555-7

47. Jurgens WJ, Kroeze RJ, Bank RA, Ritt MJPF, Helder MN. Rapid attachment of adipose stromal cells on resorbable polymeric scaffolds facilitates the one-step surgical procedure for cartilage and bone tissue engineering purposes. *J Orthop Res.* 2011;29(6):853–860. doi:10.1002/jor.21314

48. Overman JR, Farré-Guasch E, Helder MN, Ten Bruggenkate CM, Schulten EAJM, Klein-Nulend J. Short (15 minutes) bone morphogenetic protein-2 treatment stimulates osteogenic differentiation of human adipose stem cells seeded on calcium phosphate scaffolds In vitro. *Tissue Eng Part A.* 2012;19(3–4):571–581. doi:10.1089/ten.tea.2012.0133

49. Helder MN, Knippenberg M, Klein-Nulend J, Wuisman PIJM. Stem cells from adipose tissue allow challenging new concepts for regenerative medicine. *Tissue Eng.* 2007;13(8):1799–1808. doi:10.1089/ten.2006.0165

50. Thompson WR, Clinton TR, Rubin J. Mechanical regulation of signaling pathways in bone. *Gene.* 2012;503(2):179–193. doi:10.1016/j.gene.2012.04.076.Mechanical

51. Allori AC, Sailon AM, Warren SM. Biological basis of bone formation, remodeling, and repair-part II: extracellular matrix. *Tissue Eng Part B Rev.* 2008;14(3):275-283.

52. Allori AC, Sailon AM, Warren SM. Biological basis of bone formation, remodeling, and repair-part I: Biochemical signaling molecules. *Tissue Eng Part B Rev.* 2008;14(3):259–273.

53. Klein-Nulend J, Van der Plas A, Semeins CM, Ajubi NE, Erangos JA, Nijweide PJ, Burger EH. Sensitivity of osteocytes to biomechanical stress in vitro. *FASEB J.* 1995;9(5):441–445.

54. Bonewald LF, Johnson ML. Osteocytes, mechanosensing and Wnt signaling. *Bone.* 2008;42(4):606-615.

55. Stavenschi E, Labour MN, Hoey DA. Oscillatory fluid flow induces the osteogenic lineage commitment of mesenchymal stem cells: The effect of shear stress magnitude, frequency, and duration. *J Biomech.* 2017;55:99–106. doi:10.1016/j.jbiomech.2017.02.002

56. Bacabac RG, Smit TH, Mullender MG, Dijcks SJ, Van Loon JJWA, Klein-Nulend J. Nitric oxide production by bone cells is fluid shear stress rate dependent. *Biochem Biophys Res Commun.* 2004;315(4):823–829. doi:10.1016/j.bbrc.2004.01.138

57. Bacabac RG, Smit TH, Van Loon JJWA, Zandieh Doulabi B, Helder MN, Klein-Nulend J. Bone cell responses to high-frequency vibration stress: Does the nucleus oscillate within the cytoplasm? *FASEB J.* 2006;20(7):858-864. doi:10.1096/fj.05-4966.com

58. Van Oers RFM, Wang H, Bacabac RG. Osteocyte shape and mechanical loading. *Curr Osteoporos Rep.* 2015;13(2):61–66. doi:10.1007/s11914-015-0256-1

59. Kerschnitzki M, Wagermaier W, Roschger P, Seto J, Shahar R, Duda GN, Mundlos S, Fratzl P. The organization of the osteocyte network mirrors the extracellular matrix orientation in bone. *J Struct Biol.* 2011;173(2):303–311. doi:10.1016/j.jsb.2010.11.014

60. Vatsa A, Breuls RG, Semeins CM, Salmon PL, Smit TH, Klein-Nulend J. Osteocyte morphology in fibula and calvaria - Is there a role for mechanosensing? *Bone.* 2008;43(3):452–458. doi:10.1016/j.bone.2008.01.030

61. Wang N, Butler J, Ingber D. Mechanotransduction across the cell surface and through the cytoskeleton. *Science.* 1993;260(5111):1124–1127.

62. Bacabac RG, Mizuno D, Schmidt CF, MacKintosh FC, Van Loon JJWA, Klein-Nulend J, Smit TH. Round versus flat: Bone cell morphology, elasticity, and mechanosensing. *J Biomech.* 2008;41(7):1590–1598. doi:10.1016/j.jbiomech.2008.01.031

63. Eichholz KF, Woods I, Riffault M, Johnson GP, Corrigan M, Lowry MC, Shen N, Labour MN, Wynne K, O'Driscoll L, Hoey DA. Human bone marrow stem/stromal cell osteogenesis is regulated via mechanically activated osteocyte-derived extracellular vesicles. *Stem Cells Transl Med.* 2020;9(11):1431–1447. doi:10.1002/sctm.19-0405

64. Brady RT, O'Brien FJ, Hoey DA. Mechanically stimulated bone cells secrete paracrine factors that regulate osteoprogenitor recruitment, proliferation, and differentiation. *Biochem Biophys Res Commun.* 2015;459(1):118–123. doi:10.1016/j.bbrc.2015.02.080

65. Filipowska J, Tomaszewski KA, Niedźwiedzki Ł, Walocha JA, Niedźwiedzki T. The role of vasculature in bone development, regeneration and proper systemic functioning. *Angiogenesis.* 2017;20(3):291–302. doi:10.1007/s10456-017-9541-1

66. Grayson WL, Brunnell BA, Martin E, Frazier T, Hung BP, Gimble JM. Stromal cells and stem cells in clinical bone regeneration. *Bone.* 2015;11(3):140–150. doi:10.1038/nrendo.2014.234.Stromal

67. Roux BM, Cheng M-H, Brey EM. Engineering clinically relevant volumes of vascularized bone. *J Cell Mol Med.* 2015;19(5):903–914. doi:10.1111/jcmm.12569

68. Hu K, Olsen BR. Osteoblast-derived VEGF regulates osteoblast differentiation and bone formation during bone repair. *J Clin Invest.* 2016;126(2):509–526. doi:10.1172/JCI82585

69. Colton CK. Implantable biohybrid artificial organs. *Cell Transpl.* 1995;4(4):415–436. doi:10.1177/096368979500400413

70. Moya A, Paquet J, Deschepper M, Larochette N, Oudina K, Denoeud C, Bensidhoum M, Logeart-Avramoglou D, Petit H. Human mesenchymal stem cell failure to adapt to glucose shortage and rapidly use intracellular energy reserves through glycolysis explains poor cell survival after implantation. *Stem Cells.* 2018;36(3):363–376. doi:10.1002/stem.2763

71. Farré-Guasch E, Bravenboer N, Helder MN, Schulten EAJM, Ten Bruggenkate CM, Klein-Nulend J. Blood vessel formation and bone regeneration potential of the stromal vascular fraction seeded on a calcium phosphate scaffold in the human maxillary sinus floor elevation model. *Materials (Basel).* 2018;11(1):116. doi:10.3390/ma11010161

72. Sándor GK, Tuovinen VJ, Wolff J, Patrikosk M, Jokinen J, Nieminen E, Mannerström B, Lappalainen OP, Seppänen R, Miettinen S. Adipose stem cell tissue-engineered construct used to treat large anterior mandibular defect: A case report and review of the clinical application of good manufacturing practice-level adipose stem cells for bone regeneration. *J Oral Maxillofac Surg.* 2013;71(5):938–950. doi:10.1016/j.joms.2012.11.014

73. Sándor GK, Numminen J, Wolff J, Thesleff T, Miettinen A, Tuovinen VJ, Mannerström B, Patrikoski M, Seppänen R, Miettinen S, Rautianen M, Öhman J. Adipose stem cells used to reconstruct 13 cases with cranio-maxillofacial hard-tissue defects. *Stem Cells Transl Med.* 2014;3(4):530–540.

74. Thesleff T, Lehtimäki K, Niskakangas T, Lehtimäki K, Niskakangas T, Huovinen S, Mannerström B, Miettinen S, Seppänen R, Öhman J. Cranioplasty with adipose-derived stem cells, beta-tricalcium phosphate granules and supporting mesh: Six-year clinical follow-up results. *Stem Cells Transl Med.* 2017;6:1576–1582.

75. Thesleff T, Lehtimäki K, Niskakangas T, Lehtimäki K, Niskakangas T, Mannerström B, Miettinen S, Suuronen R, Öhman J. Cranioplasty with adipose-derived stem cells and biomaterial: A novel method for cranial reconstruction. Neurosurgery. 2011;68(6):1535–1540. doi:10.1227/NEU.0b013e31820ee24e

76. Heslop JA, Hammond TG, Santeramo I, Tort Piella A, Hopp I, Zhou J, Baty R, Graziano EI, Proto Marco B, Caron A, Sköld P, Andrews PW, Baxter MA, Hay DC, Hamdam J, Sharpe ME, Patel S, Jones DR, Reinhardt J, Danen EHJ, Ben-David U, Stacey G, Björquist P, Piner J, Mills J, Rowe C, Pellegrini G, Sethu S, Antoine D, Cross MJ, Murray P, Williams DP, Kitteringham NR, Goldring CEP, Park BK. Concise review: Workshop review: Understanding and assessing the risks of stem cell-based therapies. *Stem Cells Transl Med.* 2015;4(4):389-400. doi:10.5966/sctm.2014–0110

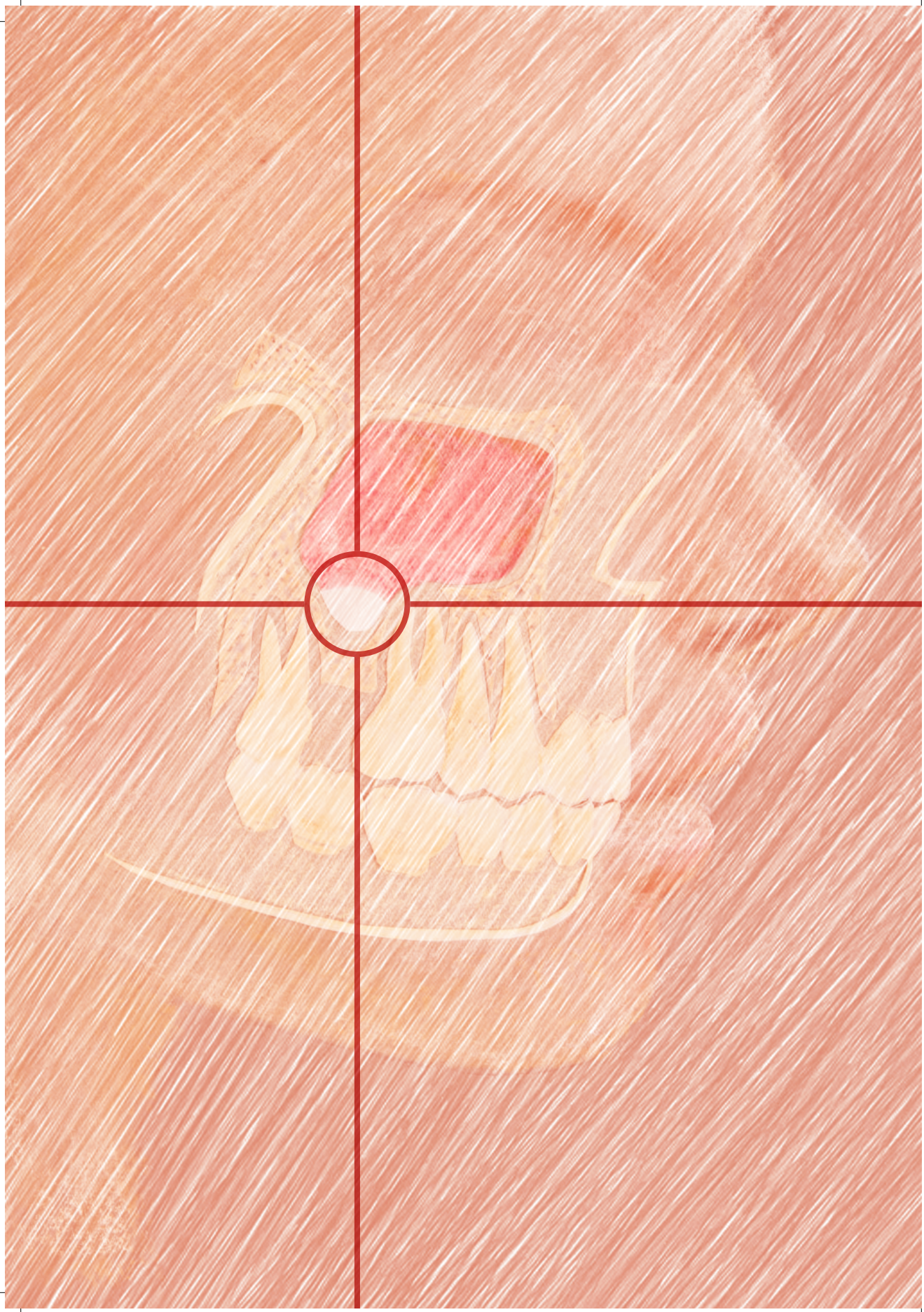

CHAPTER 2

Bone tissue regeneration in the oral and maxillofacial region: A review on the application of stem cells and new strategies to improve vascularization

Vivian Wu [1,2]
Marco N. Helder [2]
Nathalie Bravenboer [3]
Christiaan M. ten Bruggenkate [2]
Jianfeng Jin [1]
Jenneke Klein-Nulend [1]
Engelbert A.J.M. Schulten [2]

[1] Department of Oral Cell Biology, Academic Centre for Dentistry Amsterdam (ACTA), University of Amsterdam and Vrije Universiteit Amsterdam, Amsterdam Movement Sciences, Amsterdam, The Netherlands

[2] Department of Oral and Maxillofacial Surgery/Oral Pathology, Amsterdam University Medical Centers and Academic Centre for Dentistry Amsterdam (ACTA), Vrije Universiteit Amsterdam, Amsterdam Movement Sciences, Amsterdam, The Netherlands

[3] Department of Clinical Chemistry, Amsterdam University Medical Centers, Vrije Universiteit Amsterdam, Amsterdam Movement Sciences, Amsterdam, The Netherlands

Stem Cells International 2019;2019:6279721

ABSTRACT

Bone tissue engineering techniques are a promising alternative for the use of autologous bone grafts to reconstruct bone defects in the oral and maxillofacial region. However, for successful bone regeneration adequate vascularization is a prerequisite. This review presents and discusses the application of stem cells and new strategies to improve vascularization, which may lead to feasible clinical applications. Multiple sources of stem cells have been investigated for bone tissue engineering. The stromal vascular fraction (SVF) of human adipose tissue is considered a promising single-source for a heterogeneous population of essential cells with, amongst others, osteogenic and angiogenic potential. Enhanced vascularization of tissue-engineered grafts can be achieved by different mechanisms: vascular ingrowth directed from the surrounding host tissue to the implanted graft, vice versa, or concomitantly. Vascular ingrowth into the implanted graft can be enhanced by (i) optimizing the material properties of scaffolds, and (ii) their bioactivation by incorporation of growth factors or cell seeding. Vascular ingrowth directed from the implanted graft towards the host tissue can be achieved by incorporating the graft with either (i) preformed microvascular networks, or (ii) microvascular fragments (MF). The latter may have stimulating actions on both vascular ingrowth and outgrowth, since they contain angiogenic stem cells like SVF, as well as vascularized matrix fragments. Both adipose tissue-derived SVF and MF are cell sources with clinical feasibility due to their large quantities that can be harvested and applied in a one-step surgical procedure. During the past years important advancements of stem cell application and vascularization in bone tissue regeneration have been made. The development of engineered *in vitro* 3D-models mimicking the bone defect environment would facilitate new strategies in bone tissue engineering. Successful clinical application requires innovative future investigations enhancing vascularization.

INTRODUCTION

To rehabilitate patients with critical-sized bone defects surgical reconstructions are required. A critical-sized defect will not heal spontaneously or regenerate more than 10% of the lost bone during patients' lifetime.[1] These bone defects may result from systemic or local causes. Systemic conditions include congenital abnormalities,[2] general diseases,[3] and medications,[4] while local conditions comprise inflammation[5] or traumatic injuries, such as accidents[6] or dental and surgical treatments. Dental treatments, such as tooth extraction,[7] and surgical treatments, such as surgical resection of benign or malignant neoplasms,[8] may lead to substantial jaw bone defects.

Bone grafting procedures are carried out to reconstruct a bone defect.[9] In these surgical procedures autografts are still considered as the "gold standard" due to the essential combination of osteogenic, osteoinductive, and osteoconductive properties. However, autografts have some disadvantages, *e.g.* donor site morbidity and limited amount of graft tissue. In some cases bone substitutes, such as allografts, xenografts and alloplasts, are used as alternatives for autologous bone grafts, but these bone substitutes lack osteogenic, osteoinductive, and angiogenic potential.[10]

Unfortunately, the ideal bone regeneration technique and material have not yet been developed. However, recent developments in tissue engineering have led to new and better treatment options called "cellular bone tissue engineering". In this approach a scaffold with mesenchymal stem cells (MSCs) and/or osteoprogenitor cells of an external source is implanted into the bone defect site. The *ex vivo* seeded cells on the scaffold play a key role, and orchestrate the mechanism of bone formation at the target site. Multiple techniques have been investigated, applying a variety of stem cell sources and cell processing protocols.[11] Furthermore, different scaffold types are used for carrying the cells.[12]

The rationale behind the application of MSCs and/or osteoprogenitor cells is their key role in bone formation. Natural bone formation in pre- and postnatal development of the oral and maxillofacial area is performed intramembranously by recruiting mesenchymal bone marrow cells. These cells undergo osteoblastic differentiation and initiate new bone formation in the defect site. In other words, this method aims to induce bone regeneration by mimicking biologic processes that occur during embryogenesis.[13,14]

The mechanism by which MSCs promote bone regeneration can be directly by engraftment of the transplanted cells into the newly regenerated tissue, differentiating into osteoblasts that eventually will secrete osteoid and initiate mineralization.[15–17] In addition, MSCs can enhance bone regeneration indirectly by a paracrine effect, *i.e.* secretion of cytokines and growth factors such as transforming necrosis factor-α (TNF-α), platelet derived growth factor (PDGF), interleukin-1 (IL-1), and IL-6. These secreted factors may recruit resident MSCs to the regenerated site.[18,19]

In cellular bone tissue engineering MSCs are applied using two different approaches. The first approach is to directly transplant MSCs and/or osteoprogenitor cells combined with a scaffold (external scaffold) into the bone-defected site, which is a kind of an *in situ* tissue engineering.[20,21] Autogenous particulate cancellous bone and marrow are used as the source of

osteoprogenitor cells and MSCs. In this approach, the scaffold functions as a framework.[22] The second approach is to transplant MSCs that are isolated (usually from the patient), expanded *ex vivo*, seeded on adequate three-dimensional (3D)-scaffolds (internal scaffolds), and proliferated and/or predifferentiated in controlled culture conditions.[23] Such a scaffold acts as a carrier of the cells and temporary matrix while the cells produce the extracellular matrix (ECM) that is required for bone formation.[24]

A major challenge in bone tissue engineering is the vascularization of the implanted graft. Graft survival requires rapid and sufficient vascularization. Since the amount of oxygen is limited to a diffusion distance of only ~150-200 µm from a supply blood vessel, cells lying beyond this physiological border suffer from hypoxia.[25] Under this condition MSCs fail to survive, because they are not able to adapt their glucose consumption and do not possess the necessary glycolytic reserves to maintain their metabolism for more than three days.[26] New insights underline the importance of both oxygen and nutrients required for energy-related cellular metabolism, and in the end cell survival. Regenerating tissue over 200 µm exceeds the capacity of nutrient supply and waste removal from the tissue and, therefore, requires an intimate supply of vascular networks.[25] Neovascularization along with efficient supply of blood are prerequisites to this end.

The aim of this review is to present and discuss the advancement of stem cell application, vascularization and bone regeneration in the oral and maxillofacial region, with emphasis on the human jaw. Moreover, we propose new strategies to improve the current techniques, which may lead to feasible clinical applications.

SOURCES OF STEM CELLS

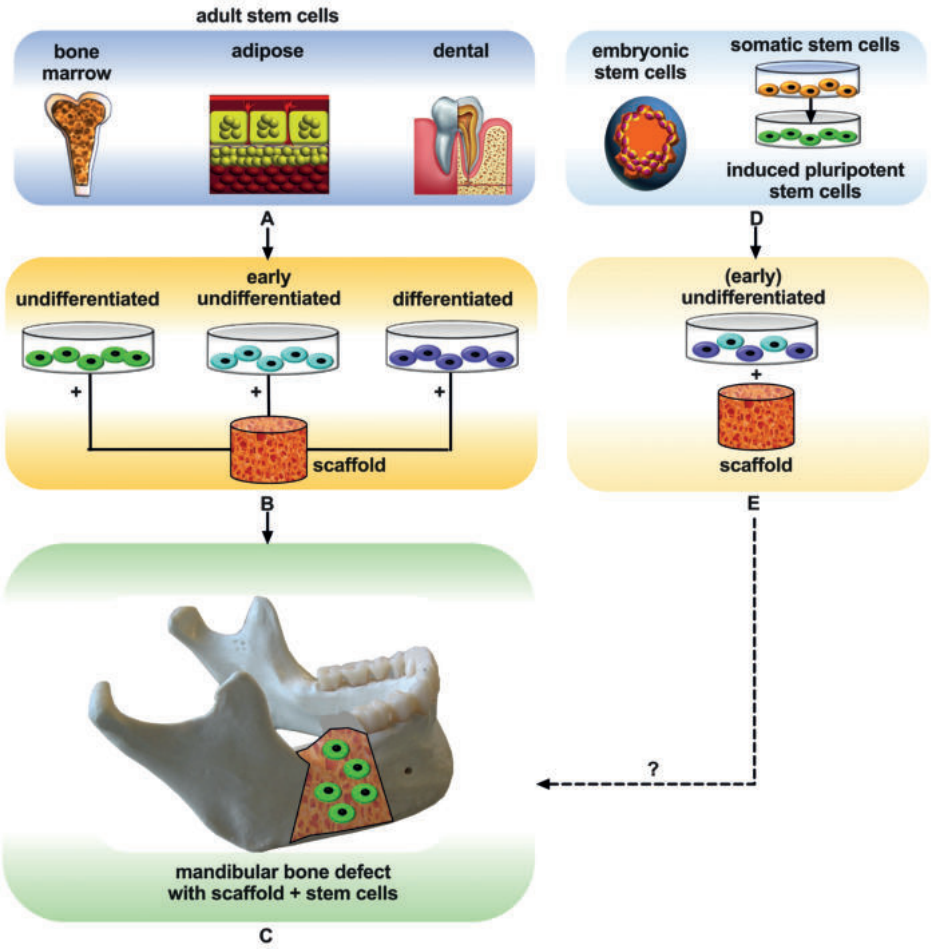

Figure 1. Overview of stem cell sources and their stage (undifferentiated, early differentiated, or differentiated) of application. Adult stem cells that are currently applied in clinical studies are retrieved from bone marrow, adipose, or dental tissue **(A)**. These cells are applied in an undifferentiated, early differentiated, or differentiated stage seeded on a scaffold **(B)**. The scaffold with the stem cells is applied in clinical trials to regenerate bone defects, such as mandibular bone defects **(C)**. Embryonic stem cells and somatic stem cells, which are first stimulated into induced pluripotent stem cells **(D)**, are applied in a (early) differentiated stage on a scaffold **(E)**. Their application in clinical trials still needs to be envisioned **(C)**. Note: In the mandibular bone defect shown **(C)** the stem cells are undifferentiated. However, the stem cells applied in such bone defects could be also early differentiated or differentiated.

Somatic stem cells, mainly mesenchymal stem cells (MSCs), that are applied in bone tissue engineering are isolated from various tissues. The clinically applied sources of stem cells in the oral and maxillofacial region originate from bone marrow, adipose tissue,[27] and dental

tissues.[28,29] *In vitro* and *in vivo* animal studies reported on the application of embryonic stem cells (ESCs)[30–32] and induced pluripotent stem cells (IPSCs)[33] in bone tissue engineering. However, these ESCs and IPSCs raise several serious ethical and safety concerns, such as teratoma formation, which continue to impede clinical implementation.[34] In Figure 1 the different sources of stem cells and their different stages of application are illustrated: undifferentiated, early differentiated or differentiated. The different stages of stem cells are categorized as follows:

- Undifferentiated: multipotent adult MSCs, pluripotent ESCs or IPSCs;
- Early differentiated: MSCs differentiated towards specific lineage, such as osteogenic lineage;
- Differentiated: specialized cell, such as osteoblast.

Clinically applicable tissue engineering involving stem cells is focused on the use of patient derived (adult) stem cells that are undifferentiated, given that terminally-differentiated cells are difficult to expand *ex vivo* relative to more highly proliferative stem/progenitor cells. The use of stem cells is also intended to achieve a complete physiological repair process that involves the MSC-mediated activation of not only bone formation but also neovascularization. Nevertheless, it is of pivotal importance to prohibit unwanted side effects such as teratoma formation which may occur by ESCs and IPSCs.

In the following an overview of the currently *in vivo* applied stem cell sources is given. Besides, Table 1 provides an overview of the recent clinical trials, published between January 1st, 2015, and November 1st, 2019, with successful application of human-derived stem cells. "A successful application" was considered as a significant outcome measurement due to the supplementation of MSCs specifically. The majority of these studies investigated bone formation as an outcome measurement based on radiography, (cone beam) computed tomography ((CB)CT), micro-computed tomography (micro-CT), or histomorphometric and/or histologic measurements. As a future direction it would be interesting to investigate the vascularization in these cases, since enhanced vascularization would be expected in relation to the enhanced osteogenetic effects observed due to the supplementation of MSCs. A complete overview of all the clinical studies applying MSCs has been described earlier.[35]

Bone marrow was the first source reported to contain MSCs.[36] Until today adult bone marrow-derived stem cells (BMSCs) are the most frequently investigated type of MSCs in bone tissue engineering. Several successful applications of BMSCs in *vivo* have been reported in the oral and maxillofacial region (Table 1). There are two different interventions in the application of BMSCs: 1) use of bone marrow aspirate (concentrated); a whole tissue fraction containing BMSCs, 2) use of *in vitro* cultivated BMSCs (expanded with or without differentiation factors) (Table 1). Concentrated bone marrow aspirate compared to non-concentrated aspirate seems to have a higher osteogenic potential *in vivo.*[37] An overview of the successful clinical trials performed with this cell source is shown in Table 1.

Table 1. Overview of clinical trials applying human-derived stem cells for bone tissue engineering applications/investigations to demonstrate *in vivo* possibilities

stem cell source	intervention	scaffold material	clinical procedure	ref
bone marrow				
posterior iliac crest	aspirate concentrated	FDBA, PRP	maxillary sinus floor elevation	141
posterior iliac crest	aspirate concentrated	DBBM	maxillary sinus floor elevation	142
posterior iliac crest	*in vitro* cultivation	β-TCP	maxillary sinus floor elevation	39
posterior iliac crest	*in vitro* cultivation	β-TCP	alveolar cleft reconstruction	42
posterior iliac crest	aspirate concentrated	COL, PRF, nano-HA	alveolar cleft reconstruction	143
posterior iliac crest	*in vitro* cultivation	HA-SI	alveolar cleft reconstruction	144
posterior iliac crest	aspirate concentrated	COL, CGF	jaw defect reconstruction (after enucleation of cyst)	145
tuberosity	*in vitro* cultivation	PLA, PRP	periodontal intrabony defect regeneration	41
adipose tissue				
abdominal	aspirate concentrated into SVF	β-TCP or BCP	maxillary sinus floor elevation	59
buccal fat pad	*in vitro* cultivation	DBBM, AB	alveolar cleft reconstruction	60
abdominal	*in vitro* cultivation	-	mandibular condylar fracture regeneration	61
dental tissue				
periosteum	mechanical disaggregation of sample tissue	PLGA, HA	maxillary sinus floor elevation	68
pulp	mechanical disaggregation of sample tissue	COL	tooth socket preservation	67
periosteum	mechanical disaggregation of sample tissue	COL	tooth socket preservation	66
pulp	mechanical disaggregation of sample tissue	COL	intrabony periodontal defects	69

Ref, reference; FDBA, freeze dried bone allografts; PRP, platelet-rich plasma; DBBM, demineralized bovine bone matrix; β-TCP, beta-tricalcium phosphate; COL, collagen sponge; PRF, platelet-rich fibrin; HA, hydroxyapatite; SI, silica; CGF, concentrated growth factor; BCP, biphasic calcium phosphate (hydroxyapatite/tricalcium phosphate); AB, autologous bone; PLGA, poly(lactic-co-glycolic acid).

Several studies showed promising results applying BMSCs in surgical procedures in the oral and maxillofacial region. Some maxillary sinus floor elevation studies presented histomorphometrical data that showed increased new bone formation after 3–4 months compared to traditional methods using bone substitutes alone.[38,39] Kaigler et al.[40] showed accelerated bone regeneration in extraction sockets of teeth when applying BMSCs or gelatin sponge compared to the controls (saline-soaked gelatin sponge). Baba et al.[41] conducted a phase I/II clinical trial involving ten patients with periodontitis, who required a surgical procedure for intrabony defects, applying bone marrow-derived stem cells with a biodegradable 3D-poly-lactic-acid-based scaffold and platelet-rich plasma. After 12 months the bone defect showed

clinically and radiographically significant improvement compared to conventional periodontal surgical procedures without application of stem cells. These results suggest successful clinical application in regenerating periodontal tissue, including bone tissue.[41] In alveolar cleft surgery, several clinical trials, mainly case reports, suggest promising results with the application of BMSCs, but complete reconstruction (bone fill) of extensive cleft defects has not been demonstrated.[42,43] In contrast, Hermund et al.[44] showed no difference in bone density and height between a control group (graft composed of a mixture of bovine bone substitute and autologous bone particles) and a test group (same scaffold, supplemented with BMSCs that were retrieved from the tuberosity and cultivated *in vitro*) after maxillary sinus floor elevation.

Unfortunately BMSC application comes with limitations: bone marrow aspiration is an invasive and painful procedure for the donor, and cell retrieval is scarce, since the frequency of BMSCs in human bone marrow is rather low (0.001%–0.01%).[45] Consequently, fresh bone marrow aspirates may result in a too low number and concentration of BMSCs to exert substantial osteogenic effects.[37] Therefore, *in vitro* culture expansion is required to obtain sufficient numbers of cells for clinical application.[46] This cell expansion, however, needs to be done in a laborious, expensive, and time-consuming good manufacturing practice (GMP) laboratory. Other limitations comprise the loss of proliferative and differentiation capacities during cell expansion,[47,48] and an increased risk for pathogen contamination and genetic transformation.[49,50] Last but not least: the number, proliferation and differentiation potential of BMSCs decline with increasing age.[51]

Adipose tissue-derived mesenchymal stem cells (ASCs) have opened appealing new possibilities in adult stem cell therapies. ASCs show many similarities with BMSCs with regard to surface marker profiles, multilineage potential, and growth properties.[52] However, in contrast to the other sources (bone marrow, dental, embryonal), adipose tissue has the following advantages: (a) it has a high stem cell-to-volume ratio,[53,54] (b) the stem cell frequency is far less sensitive to ageing,[55] (c) harvesting can easily be upscaled according to the need, and (d) it can be processed within a short time frame to obtain highly enriched ASCs preparations (residing in the stromal vascular fraction [SVF]). Furthermore, the multipotent cells within the SVF attach very fast to the scaffold material, proliferate rapidly, and can be differentiated toward amongst others the osteogenic lineage.[56,57]

Helder and colleagues formulated the concept of the one-step surgical procedure (OSP) to apply ASCs in the regeneration of bone tissues.[58] After harvesting the adipose tissue by the surgeon, the SVF-containing ASCs can be seeded onto the scaffold material without culture expansion. Then the ASC-scaffold construct can be implanted, all in the same surgical procedure. The obvious advantage of this one-step surgical procedure is not only its patient-friendliness, but also its lower costs, since a second surgical intervention and expensive *in vitro* culturing steps can be avoided.

Multiple *in vitro* studies made important advancements in the application of ASCs in bone tissue engineering.[32] Recently successful results were also obtained in clinical trials (Table 1). The results from a first clinical trial evaluating the application of ASCs showed that it is a feasible, safe, and effective treatment option in jaw bone regeneration.[59] Prins et al.[59] showed in a split-mouth design that patients undergoing maxillary sinus floor elevation for dental

implant placement benefitted from the application of ASCs. Bone and osteoid percentages were higher in study biopsies (SVF supplemented to different ceramic bone substitutes) than in control biopsies (ceramic only on contralateral side) (54). The additive effect of SVF supplementation was independent of the bone substitute β-tricalcium phosphate or biphasic calcium phosphate (hydroxyapatite/tricalcium phosphate).[59] Khojasteh et al.[60] used ASCs derived from the buccal fat pad, *in vitro* cultivated and seeded on demineralized bovine bone mineral (DBBM) and autologous bone (AB), in alveolar cleft reconstruction. Cone beam computed tomography 6 months after the treatment showed more bone formation in the test group with supplementation of ASCs. Castillo-Cardiel et al.[61] treated mandibular condylar fractures with abdominal retrieved ASCs that were *in vitro* cultivated, and injected at the fracture site. After 12 weeks of the surgical treatment, the test group with the supplemented ASCs had a 37% higher ossification rate compared to the traditional treatment (control group). A disadvantage of SVF harvesting so far is that it is performed under general anesthesia and requires (short) hospitalization. Also, postoperative care and complaints are to be regarded. However, clinical studies using local anesthesia are currently being undertaken, which may widen the applicability of this intra-operative approach.

Dental tissues provide several populations of stem cells, including the pulp of both exfoliated and adult teeth, periodontal ligament, and dental follicle.[62] Dental tissue-derived stem cells (DSCs) have generic mesenchymal stem cell-like properties such as self-renewal and multilineage differentiation into chondrogenic, osteogenic, and adipogenic cell lineages. In addition, DSCs also show neurogenic and angiogenic potential.[62] It has been demonstrated that DSCs have the ability to generate not only dental tissue such as dentine/pulp-like complexes but also bone tissue.[63,64] Stem cells from human exfoliated deciduous teeth exhibit higher proliferation rates and can be easier obtained compared to BMSCs.[65]

However, published clinical studies with successful results are scarce (Table 1). D' aquino et al.[66] used whole tissue fractions from periosteum tissue by mechanically disaggration, followed by soaking of a collagen sponge in the resulting disaggregated tissue. Calcification was enhanced in tooth socket preservation in the test group with DSCs supplemented to the collagen sponge, compared to the control group with unloaded collagen sponges. Monti et al.[67] used tissue fractions from the dental pulp, followed by soaking of a collagen sponge in a similar clinical model. Sixty days after grafting, the test site (supplemented with DSCs) showed stronger radio-opacity when compared with the control site (collagen sponge). Histological analysis showed well-differentiated bone with Haversian system formation in the test site with more bone formation. Baena et al.[68] used whole tissue fractions from periosteum tissue seeded on a poly(lactic-co-glycolic acid) (PLGA) scaffold with hydroxyapatite (HA) in maxillary sinus floor elevation surgery. They showed an increased percentage of vital mineralized tissue in the group treated with both periosteum-derived stem cells and PGLA/HA, with respect to the control group of PGLA/HA or demineralized bovine bone mineral alone, as confirmed by histological analysis and radiographic evaluations at six months after the treatment. Ferraroti et al.[69] showed clinical success after applying dental pulp stem cells on a collagen sponge in intrabony periodontal regeneration one year after treatment.

The question remains open whether in spite of the low numbers of cells, DSCs might become an attractive source of autologous SCs for bone regeneration. This source is being investigated with at least more than ten new trials underway (www.clinicaltrials.gov).

VASCULARIZATION IN BONE TISSUE REGENERATION

Successful bone tissue regeneration requires rapid perfusion and integration of the implanted graft with the recipient vasculature. Neovascularization is achieved by both vasculogenesis and angiogenesis. Vasculogenesis is originally described as *de novo* blood vessel formation by differentiation and assembly of angioblastic progenitor cells during embryogenesis.[70] However, more recently, postnatal vasculogenesis is becoming evident as a major contributor to adult neovascularization. This type of postnatal vasculogenesis is defined as the incorporation of circulating endothelial progenitor cells (EPCs) into the microvascular endothelium of newly developing microvessels.[71,72]

EPCs are mainly located within the stem cell niche in bone marrow, along with some circulating populations in the peripheral blood. When injury or tissue damage occurs, EPCs are thought to mobilize from the bone marrow into the circulation and home to tissue repair sites under the guidance of signals such as hypoxia, growth factors, chemoattractant signals, and chemokines. EPCs then invade and migrate at the same sites, and differentiate into mature endothelial cells (ECs) and/or regulate pre-existing ECs via paracrine or juxtacrine signals.[73]

Angiogenesis is defined as new blood vessel sprouting from pre-existing vessels. The first step in this process is the activation of the host microvasculature at the implantation site by angiogenic growth factors, such as vascular endothelial growth factor (VEGF) or basic fibroblast growth factor.[74] These factors may originate from different sources. They may be produced by cells of the host tissue itself due to tissue injury during the implantation procedure or in consequence of an inflammatory response to the implanted graft.

The endothelial cells, which are lining blood vessels, allow the formation of new blood capillaries by the sprouting of an existing small vessel.[75,76] Upon angiogenic activation they start to produce matrix metalloproteinases, resulting in the degradation of their basement membrane,[77] This is the prerequisite for their subsequent migration into the surrounding interstitium, which is morphologically reflected by the formation of vascular buds and sprouts. The sprouts progressively grow into the implanted tissue construct and interconnect with each other to develop new blood-perfused microvascular networks.[78] The wall of these networks is finally stabilized by the production of extracellular matrix compounds and the recruitment of smooth muscle cells or pericytes.[79]

Accordingly, successful vascularization of an implanted graft via vasculogenesis and angiogenesis is dependent on the coordinated sequence of various humoral and cellular mechanisms, and, in particular, the close interaction between the host tissue and the implanted graft. This process allows tissue growth and repair by extending and remodeling the network of blood vessels.[73,80]

VASCULARIZATION STRATEGIES IN BONE TISSUE ENGINEERING

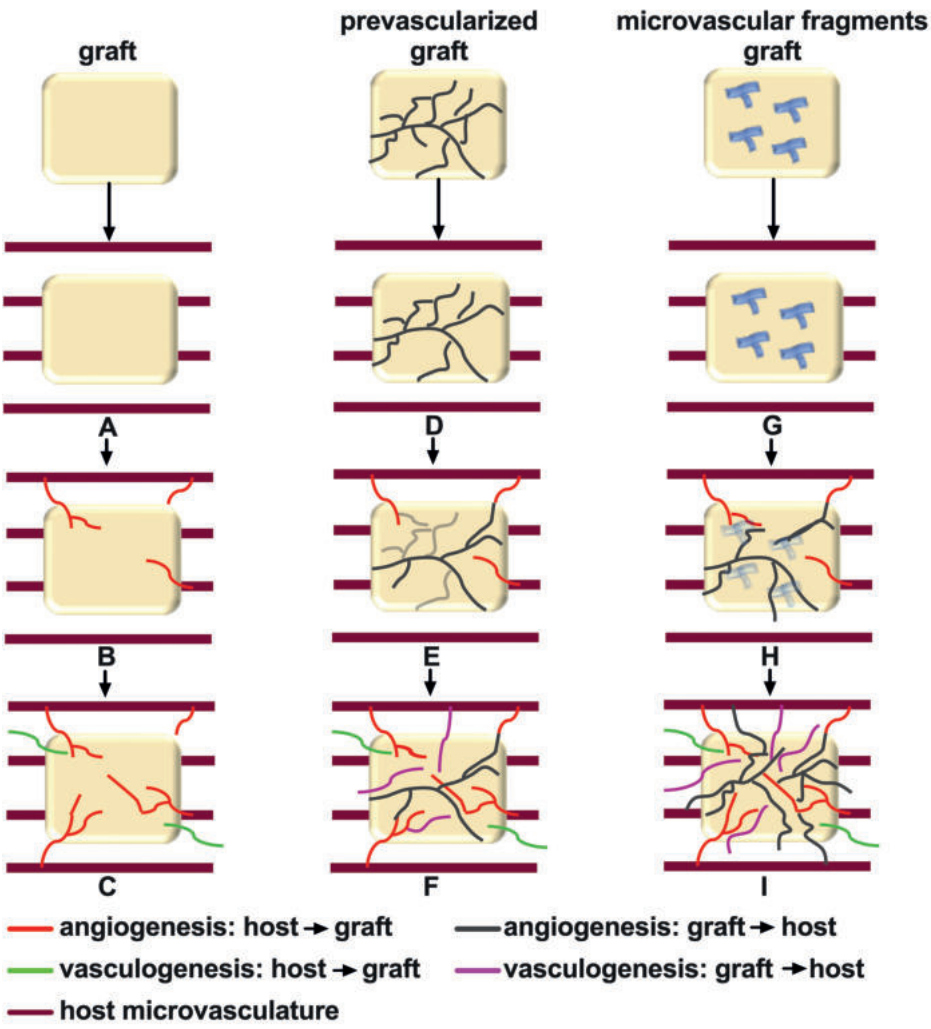

Figure 2. Overview of the three different vascularization strategies and their clinical results. First, a graft is implanted **(A)** which solely depends on the vascularization, angiogenesis and vasculogenesis, from the host towards the graft **(B)**. This results in insufficient vascularization of the graft **(C)**. Second, a prevascularized graft is implanted in the host tissue **(D)**. A high number of preformed microvessels has a suboptimal lifespan **(E)**, resulting in less microvessels for vascularization from the graft towards the host **(F)**. Third, microvascular fragments in the graft **(G)** develop rapidly into microvessels when implanted in the host tissue **(H)**. They contribute to vascularization (angiogenesis and vasculogenesis) from the graft towards the host, which results in enhanced vascularization. Vascularization starts from two directions, *i.e.* from the graft and from the host tissue **(I)**.

Several approaches to improve vascularization, through enhanced vasculogenesis and angiogenesis, of the implanted grafts are currently investigated. The classical vascularization strategies focus on the stimulation of vascular ingrowth into the implanted grafts from the surrounding host tissue by (i) optimizing the material properties of scaffolds, and (ii) their bioactivation by incorporation of growth factor delivery systems or by cell seeding. However, endothelial cell migration and physiological growth of new blood vessels has been demonstrated not to be faster than ~5 µm/h.[81] Therefore, these approaches face the problem that sufficient vascularization of the implanted graft require a prolonged time period which is associated with major tissue loss due to hypoxic conditions.

To overcome this problem, vascular ingrowth directed from the implanted graft towards the host tissue has been proposed to complement vascular ingrowth from the host tissue into the implanted graft. This can be achieved by incorporating the graft with either (i) preformed microvascular networks which can directly be perfused with blood by developing interconnections (inosculation) to the host microvasculature, or (ii) microvascular fragments which rapidly develops into microvascular networks after transfer into the host tissue (Figure 2). In the following an overview of the current possibilities and future perspectives on the above-mentioned strategies to enhance vascularization in bone tissue engineering is provided.

Material properties of scaffolds

The characteristics of the scaffold material play an important role in angiogenesis of the graft. Many different scaffold materials for bone tissue engineering have been investigated *in vivo* and *in vitro*, *e.g.* polymers, bioactive ceramics, and hybrids (composites).[12]

The chemical composition of scaffold materials has been shown to influence the angiogenic process at the implantation site. For instance, poly-L-lactide coglycolide (PLGA), hydroxyapatite (HA), and dentin scaffolds show a slight inflammatory response after implantation, inducing marked angiogenic response and a good vascularization of the grafts after 14 days.[78,82] In contrast, collagen-chitosan-hydroxyapatite hydrogel scaffolds of identical architecture induce severe inflammation, resulting in apoptotic cell death within the surrounding tissue and a complete lack of ingrowth of newly formed microvessels.[78] Polyurethane scaffolds, which exhibit an excellent *in vivo* biocompatibility, have been shown to be characterized by a poor vascularization.[83] These findings indicate that scaffold materials with slightly proinflammatory properties may stimulate the angiogenic host tissue response to the implanted scaffold material.

Combinations of biomaterials have been investigated to improve the scaffold properties. Composites consist of a combination of two or more materials with different properties, each displaying only some advantages and specific drawbacks. Polymer-ceramic composites have been successful in bone regeneration, exceeding the results obtained when these materials are used separately, showing improved mechanical and biological results.[84] The combination of PLGA (combination of poly lactide and polyglycolide) and HA or β-TCP allows to overcome the problems due to PLGA's acidic degradation products that may induce tissue necrosis and negatively affect neoangiogenesis, since HA and β-TCP neutralize the acidic degradation products of PLGA.[85]

Not only the chemical composition, but also the architecture of scaffolds is an important determinant for adequate vascularization.[86] It should contain distributed, interconnected pores and display a high porosity in order to ensure cell penetration, vascular ingrowth, nutrient diffusion, as well as waste products elimination.[87] Another key component to allow proper cell colonization (cells bound to ligands within the scaffold) is mean pore size.[88] The minimum recommended pore size for a scaffold is 100 µm[89] based on the early work of Hulbert et al.[90], but subsequent studies have shown better osteogenesis for implants with pores >300 µm.[91,92] Relatively larger pores favor direct osteogenesis, since they allow vascularization and high oxygenation, while smaller pores result in endochondral ossification, although the type of bone in growth depends on the biomaterial and the geometry of the pores. There is, however, an upper limit in porosity and pore size set by constraints associated with mechanical properties.[86,93]

Bioactivation of the scaffold by incorporation of growth factors or cell seeding

A common strategy to improve scaffold vascularization is the stimulation of the angiogenic host tissue response at the implantation site by incorporation of angiogenic growth factors. For this purpose, VEGF,[94,95] basic fibroblast growth factor,[96] platelet-derived growth factor,[97] and angiogenin[98] are the most frequently used factors. However, there are continuing concerns about the cost of multiple cytokines and delivery, potential toxicity, and suboptimal endothelial migration in large tissue grafts.

Another important aspect to consider is that many angiogenic growth factors are known to be released spontaneously by cells under stress-related conditions, including hypoxia. Due to hypoxia, bone derived-osteoblast-like cells as well as bone marrow mesenchymal stem cells (BMSCs) are known to liberate growth factors such as VEGF. Based on this cellular mechanism, an accelerated vascularization of scaffolds is also achieved by seeding the scaffolds with differentiated tissue-specific cells[99,100] or multipotent stem cells.[101,102] Although BMSCs are known to have the potential to differentiate into defined vascular cells, it has been shown that the observed acceleration of vascularization at 14 days *in vivo* more strongly depends on the liberation of VEGF by the seeded cells than the differentiation potential of the BMSCs.[99] Even though there is significant acceleration of vascularization after cell seeding, Tavossal et al.[100] showed that the majority of seeded osteoblast-like cells died within the observation period of 14 days after *in vivo* implantation of PGLA scaffolds seeded with osteoblast-like cells. This indicated that this method alone is not sufficient to accelerate the vascularization to ensure the survival of seeded cells. Qu et al.[103] showed that genetically modified cells could have a long term expression of angiogenic growth factors, independently from their state of hypoxia. They transfected BMSCs with basic fibroblast growth factor seeded on a composite scaffold in a calvarial critical-sized defect model in rats. It accelerated vascularization and bone regeneration at 4 and 8 weeks compared with the controls. However, it was also suggested that over-expression of angiogenic growth factor VEGF may cause a global reduction in bone quantity, consisting of thin trabeculae of immature matrices.[104]

Preformed microvascular networks

Different approaches to prevascularize the graft *in vitro* by seeding of vessel-forming cells onto scaffolds are being investigated. After seeding onto the scaffold, these cells rapidly assemble into immature microvessels. In contrast to the above-mentioned approaches that focus on the stimulation of vascular ingrowth into the implanted graft, prevascularization aims to generate preformed microvascular networks inside the graft prior to their implantation. After implantation, these networks can be rapidly perfused with blood by inosculation with the surrounding host microvasculature.[80]

Proangiogenic cells, such as endothelial cells, endothelial progenitor cells, and mural cells (pericytes and smooth muscle cells), are widely used as cell source. Other cell sources including adult stem cells, such as pluripotent mesenchymal stem cells from bone marrow[105,106] or adipose tissue,[106–108] and induced pluripotent stem cells[109] are also suggested as suitable sources for this purpose.

Originally, endothelial and endothelial progenitor cells were used for the formation of blood vessels, but this resulted in blood vessels with suboptimal life span.[110] Due to limited number of transplanted vascular cells surviving for a prolonged duration, neovasculature fails to recruit the obligatory perivascular cells including mural cells, and consequently does not resemble native, multilayered mature microvessels.[111] To overcome this problem, gene transfection to improve the survival and proliferation of the used vascular cells has been suggested.[110,112] However, this genetic manipulation bears an oncogenic risk.[113]

A better alternative being investigated seems to be the co-cultivation of endothelial cells with mural cells. These cells are crucial for the stabilization, maturation, and long-term survival of newly formed microvessels. Koike et al.[114] demonstrated stable microvascular networks, which survived for one year *in vivo*, through co-cultivation of human umbilical-vein endothelial cells (HUVECs) with mural precursor cells. This is in contrast to microvessels engineered with HUVECs alone, which rapidly regressed after 60 days.[110] However, limitations of cell-based prevascularization approaches are that these approaches usually need complex and time-consuming cell isolation and cultivation procedures. Besides, their safety and success is highly sensitive to the quality of the cell isolates, the applied seeding strategy, and the number of cells seeded. Multiple studies reported on a critical optimum ratio between vascular cells and tissue-specific cells within a construct.[115,116] Therefore, their clinical application is difficult to envision.

Microvascular fragments

Prevascularization methods by cell seeding using cellular isolates may result in uncertain outcomes. Moreover, the correct ratio of cells to be used is difficult to determine. This led to a novel concept exploiting the use of microvascular fragments (MF) isolated from adipose tissue by short (5–10 min) digestion.[117–119] MF is a mixture of arteriolar, capillary, and venular vessel segments.[120] Several studies successfully isolated MF from mice[117,118] and human,[119] and transplanted adipose tissue-derived MF in animals. These studies further demonstrated that these fragments rapidly develop stable, blood-perfused microvascular networks after implantation into the host tissue. In culture, MF have been shown to release the proangiogenic factors

vascular endothelial growth factor (VEGF), and basic fibroblast growth factor (bFGF).[121,122] In addition, microvascular fragments contain stem cells antigen (Sca)-1/VEGFR-2-positive endothelial progenitor cells, and mesenchymal stem cells expressing common markers, such as CD44, CD73, CD90, and CD117.[123] It has been speculated that the high vascularization potential of microvascular fragments is (partly) caused by these stem cell populations. Compared to the above described cell seeding strategies to generate *in vitro* preformed microvascular networks, the enzymatic digestion period for the isolation of microvascular fragments is much shorter (5–10 min) than of single source cells, and does not require complex and time-consuming *in vitro* incubation periods. Moreover MF can also be obtained from patients in a one-step surgical procedure with a liposuction technique under local anesthesia.[124]

However, the MF procurement does not avoid the regulatory burden of using stem cell preparations obtained by enzymatic digestion, which are considered "more than minimally manipulated" by the FDA and the European counterpart the EMA. Therefore, recently much effort was put in the development of mechanical disruption of the tissue creating microfragmented adipose tissue/nanofat ((MFAT/NFAT) (reviewed in Trivisonno et al.)[125].

Strikingly, it was found that the microfragmentation of the adipose tissue, which kept the micro-architecture (extracellular matrix with embedded mesenchymal stem cells and microvascular fragments) of the fat intact but disrupts most mature adipocytes, showed a remarkable enrichment of blood vessel-stabilizing pericytes, and release of many more growth factors and cytokines involved in tissue repair and regeneration, noticeably via angiogenesis, compared to enzymatically obtained SVF.[126] Moreover, the microfragmented adipose tissue maintained strong angiogenic and anti-inflammatory properties.[127] Autologous transplantation of such mechanically processed adipose tissue has been used with success in multiple indications, spanning a.o. cosmetics,[128,129] orthopedics,[130,131] and proctology.[132]

FUTURE DIRECTIONS

Future investigations in cellular bone tissue engineering applications should be focused on enhancing vascularization, since adequate vascularization is a prerequisite for successful clinical bone regeneration. Moreover, due to existing discrepancies in the way human MSC are harvested and whether they are either directly applied without cultivation or isolated and cultured *ex vivo*, in addition to donor-dependent variability regarding the bone forming potency, further investigations are needed to standardize the production and quality of stem cells for therapeutic applications.

A promising future direction for cellular tissue engineering in jaw bone reconstruction with feasible clinical application is the use of the stromal vascular fraction (SVF) of human adipose tissue. SVF is considered a "single-source" for cellular tissue engineering due to its heterogeneous population of essential cells, *i.e.* multipotent stem cells and progenitor cells, including endothelial cells, stroma cells, pericytes, pre-adipocytes, as well as hematopoietic cells. SVF also contains macrophages, which secrete a multitude of vascular growth factors and cytokines.[133]

The adipose stem cells (ASCs) in SVF have been shown to attach, proliferate, and osteogenically differentiate on calcium phosphate scaffolds,[134] and secrete a multitude of growth factors.[57] ASCs not only have been shown to have osteogenic potential *in vivo*,[59] but also demonstrated angiogenic potential crucial for bone tissue engineering applications in mice.[135] This is supported by *in vitro* observations that ASCs in SVF secrete a variety of angiogenic and anti-apoptotic growth factors,[136] and that SVF is highly enriched with CD34+CD45−cells. The CD34+ cells are capable of stimulating angiogenesis, and are involved in neovascularization processes that facilitate healing of ischemic tissues in mouse models.[137] Moreover, it has been demonstrated that if cultured within 3D scaffolds, the combination of endothelial cells and stromal cells derived from the SVF assemble into vascular structures, thus actively contributing to the vascularization of tissue-engineered bone grafts, and stimulating their engraftment *in vivo*.[124]

A first clinical trial confirmed that SVF/ASCs are capable to enhance bone and blood vessel formation.[59,138] The study group (bone substitute [calcium phosphate] combined with SVF/ASCs) showed a higher bone mass that positively correlated with blood vessel formation versus the control group (only bone substitute) in a maxillary sinus floor elevation model.[138] Immunohistochemical analysis of CD34, a marker of endothelial cells as well as stem cells such as endothelial progenitor stem cells and hematopoietic stem cells revealed a higher number of CD34+ blood vessels in the SVF-supplemented group (SVF+) than the bone substitutes only group (SVF-; Figure 3), indicating a pro-angiogenic effect of the SVF. In addition, the vasculogenic effect of the SVF has been indicated *in vitro*.[139]

Further investigations should also address the possibilities to enhance the osteogenic capacity of the ASCs within the treatment time of the "one-step surgery". *In vitro* results of short (minutes) incubation of ASCs with a low dose of bone morphogenetic protein-2 (BMP-2) before seeding the cells on the scaffold (β-TCP and BCP) showed promising results, *i.e.* proliferation and osteogenic differentiation were enhanced by BMP-2 pretreatment, with concomitant downregulation of adipogenic gene expression. Stimulated gene expression of the osteogenic

markers core binding factor alpha 1, collagen-1, osteonectin, and osteocalcin in the seeded ASCs were observed.[134]

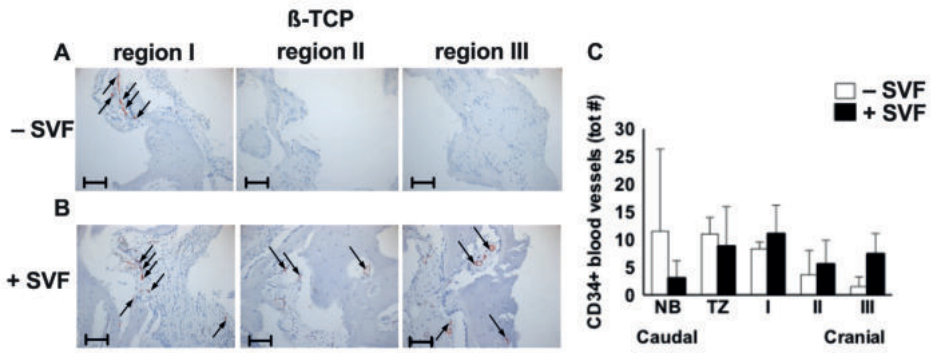

Figure 3. Immunohistochemical analysis of CD34, a marker of endothelial cells as well as stem cells such as endothelial progenitor stem cells and hematopoietic stem cells, of a maxillary bone biopsy from a patient treated with β-TCP (A–C). Magnification: 200×. The scale bar represents 100 µm. The total number of CD34+ blood vessels of selected bone biopsies taken from control sides without stem cells (white bars; n = 3), and study sides with stem cells (black bars; n=4) from patients treated with β-TCP (b). β-TCP, β-tricalcium phosphate; NB, native bone; TZ, transition zone; SVF, stromal vascular fraction; tot #, total number (adapted from Farré-Guasch et al.).[138]

Recently, several studies suggested that adipose tissue-derived microvascular fragments (MF) show higher vascularization potential than SVF.[118,126] However, further *in vitro* and *in vivo* research needs to confirm these findings. The MF and MFAT/NFAT variants of adipose tissue may spur future developments in particular for homologous applications since the regulatory burden can be avoided and the angiogenic, anti-inflammatory, and regenerative growth factor secretion properties appear at least equal but likely even higher than collagenase-digested SVF.[126,127]

The major clinical benefit of applying adipose tissue-derived SVF, MF, or MFAT/NFAT compared to other single-cell sources, is that a native mixture of essential cells can be harvested in large quantities in a one-step surgical procedure. This makes clinical application of adipose tissue-derived SVF or MF feasible, due to its lower morbidity rate and shorter treatment duration compared to the traditional treatment options, such as autologous bone harvesting, bone marrow-derived stem cells, and endothelial cells.

Appropriate *in vitro* 3D-models of bone defects to investigate cellular bone tissue engineering techniques, and specifically vascularization, are lacking. Such models would enhance the understanding of the interaction of cells with the host environment for osteogenesis and angiogenesis. Moreover, it would facilitate new possibilities for vascularization strategies. Currently exploited 2D-models and *in vivo* animal models have several limitations, including controllability, reproducibility, and flexibility of design. Recently novel strategies in 3D-models are investigated to mimic human physiology *in vitro*, including bone niche-on-a-chip and bone bioreactors.[140]

CONCLUSIONS

Important advancements have been made regarding the application of stem cells and the development of new strategies to improve vascularization in bone tissue engineering. However, adequate graft vascularization, which is a prerequisite to successful bone regeneration, is still considered a major challenge. The use of SVF of human adipose tissue seems to be a promising source for bone tissue engineering due to its heterogeneous population of essential cells for osteogenesis and angiogenesis. Besides, adipose tissue-derived MF is suggested as a promising cell source, due to its correct native cell ratios, for vascularization strategies. SVF, MF, and MFAT/NFAT are treatment options with clinical feasibility due to their large quantities that can be harvested and applied in a one-step surgical procedure. Appropriate *in vitro* models to study bone tissue engineering are lacking. Engineered *in vitro* 3D-models mimicking the bone defect environment are crucial to facilitate new bone regeneration strategies. Successful bone reconstruction in in the oral and maxillofacial region, using bone tissue engineering techniques, requires innovative future investigations focusing on the enhancement of vascularization.

REFERENCES

1. Schmitz JP, Hollinger JO. The critical size defect as an experimental model for craniomandibulofacial nonunions. *Clin Orthop Relat Res*. 1986;(205):299–308.
2. Baxter DJG, Shroff MM. Developmental maxillofacial anomalies. *Semin Ultrasound CT MR*. 2011;32(6):555–568. doi:10.1053/j.sult.2011.06.004
3. Foster BL, Ramnitz MS, Gafni RI, Burke AB, Boyce AM, Lee JS, Wright JT, Akintoye SO, Somerman MJ, Collins MT. Rare bone diseases and their dental, oral, and craniofacial manifestations. *J Dent Res*. 2014;93(7):7S–19S. doi:10.1177/0022034514529150
4. Kuroshima S, Sasaki M, Sawase T. Medication-related osteonecrosis of the jaw: A literature review. *J Oral Biosci*. 2019;61(2):99–104. doi:10.1016/j.job.2019.03.005
5. Terashima A, Takayanagi H. The role of bone cells in immune regulation during the course of infection. *Semin Immunopath*. 2019;41:619–626. doi:10.1007/s00281-019-00755-2
6. Chukwulebe S, Hogrefe C. The diagnosis and management of facial bone fractures. *Emerg Med Clin North Am*. 2019;37(1):137–151. doi:10.1016/j.emc.2018.09.012
7. Araújo MG, Lindhe J. Dimensional ridge alterations following tooth extraction. An experimental study in the dog. *J Clin Periodontol*. 2005;32(2):212–218. doi:10.1111/j.1600-051X.2005.00642.x
8. Rolski D, Kostrzewa-Janicka J, Zawadzki P, Zycińska K, Mierzwińska-Nastalska E. The management of patients after surgical treatment of maxillofacial tumors. *Biomed Res Int*. 2016:4045329. doi:10.1155/2016/4045329
9. Vorrasi JS, Kolokythas A. Controversies in traditional oral and maxillofacial reconstruction. *Oral Maxillofac Surg Clin North Am*. 2017;29(4):401–413. doi:10.1016/j.coms.2017.06.003
10. Fernandez de Grado G, Keller L, Idoux-Gillet Y, Wagner Q, Musset A, Benkirane-Jessel N, Bornert F, Offner D. Bone substitutes: A review of their characteristics, clinical use, and perspectives for large bone defects management. *J Tissue Eng*. 2018;9. doi:10.1177/2041731418776819
11. Jazayeri HE, Tahriri M, Razavi M, Khoshroo K, Fahimipour F, Dashtimoghadam E, Almeida L, Tayebi L. A current overview of materials and strategies for potential use in maxillofacial tissue regeneration. *Mater Sci Eng C*. 2017;70:913–929. doi:10.1016/j.msec.2016.08.055
12. Roseti L, Parisi V, Petretta M, Cavallo C, Desando G, Bartolotti I, Grigolo B. Scaffolds for bone tissue engineering: State of the art and new perspectives. *Mater Sci Eng C*. 2017;78:1246–1262. doi:10.1016/j.msec.2017.05.017
13. Perez JR, Kouroupis D, Li DJ, Best TM, Kaplan L, Correa D. Tissue engineering and cell-based therapies for fractures and bone defects. *Front Bioeng Biotechnol*. 2018;6:1–23. doi:10.3389/fbioe.2018.00105
14. Langhans MT, Yu S, Tuan RS. Stem cells in skeletal tissue engineering: Technologies and models. *Curr Stem Cell Res Ther*. 2015;11(6):453–474. doi:10.2174/1574888x10666151001115248
15. Kinoshita Y, Maeda H. Recent developments of functional scaffolds for craniomaxillofacial bone tissue engineering applications. *Sci World J*. 2013;2013:863157. doi:10.1155/2013/863157
16. Colter DC, Sekiya I, Prockop DJ. Identification of a subpopulation of rapidly self-renewing and multipotential adult stem cells in colonies of human marrow stromal cells. *Proc Natl Acad Sci*. 2001;98(14):7841–7845. doi:10.1073/pnas.141221698
17. Andrades JA, Santamaría JA, Nimni ME, Becerra J. Selection and amplification of a bone marrow cell population and its induction to the chondro-osteogenic lineage by rhOP-1: An in vitro and in vivo study. *Int J Dev Biol*. 2001;45(4):689–693.

18. Gerstenfeld LC, Cullinane DM, Barnes GL, Graves DT, Einhorn TA. Fracture healing as a post-natal developmental process: Molecular, spatial, and temporal aspects of its regulation. *J Cell Biochem*. 2003;88(5):87–884. doi:10.1002/jcb.10435

19. Kon T, Cho T, Aizawa T, Yamazaki M, Nooh N, Graves D, Gerstenfeld LC, Einhorn TA. Expression of osteoprotegerin, receptor activator of NF-kB ligand (osteoprotegerin ligand) and related proinflammatory cytokines during fracture healing. *J Bone Miner Res*. 2001;16(6):1004–1014.

20. Meloni SM, Jovanovic SA, Urban I, Canullo L, Pisano M, Tallarico M. Horizontal ridge augmentation using GBR with a native collagen membrane and 1:1 ratio of particulated xenograft and autologous bone: A 1-year prospective clinical study. *Clin Implant Dent Relat Res*. 2017;19(1):38–45. doi:10.1111/cid.12429

21. Urban IA, Nagursky H, Lozada JL, Nagy K. Horizontal ridge augmentation with a collagen membrane and a combination of particulated autogenous bone and anorganic bovine bone–derived mineral: A prospective case series in 25 patients. *Int J Periodontics Restorative Dent*. 2013;33(3):299–307. doi:10.11607/prd.1407

22. Yagihara K, Okabe S, Ishii J, Yagihara K, Okabe S, Ishii J, Amagasa T, Yamashiro M, Yamaguchi S, Yokoya S, Yamazaki T, Kinoshita Y.Mandibular reconstruction using a poly(l-lactide) mesh combined with autogenous particulate cancellous bone and marrow: A prospective clinical study. *Int J Oral Maxillofac Surg*. 2013;42(8):962–969. doi:10.1016/j.ijom.2013.03.010

23. Ohgushi H, Dohi Y, Yoshikawa T, Tamai S, Tabata S, Okunaga K, Shibuya T. Osteogenic differentiation of cultured marrow stromal stem cells on the surface of bioactive glass ceramics. *J Biomed Mater Res*. 1996;32(3):341-348. doi:10.1002/(SICI)1097-4636(199611)32:3<341::AID-JBM6>3.0.CO;2-S

24. Janicki P, Schmidmaier G. What should be the characteristics of the ideal bone graft substitute? Combining scaffolds with growth factors and/or stem cells. *Injury*. 2011;42(Suppl 2):S77–S81. doi:10.1016/j.injury.2011.06.014

25. Colton C. Implantable biohybrid artificial organs. *Cell Transpl*. 1995;4(4):415–436. doi:10.1088/1748-6041/1/3/001

26. Moya A, Paquet J, Deschepper M, Moya A, Paquet J, Deschepper M, Larochette N, Oudina K, Denoeud C, Bensidhoum M, Logeart-Avramoglou D, Petite H. Human mesenchymal stem cell failure to adapt to glucose shortage and rapidly use intracellular energy reserves through glycolysis explains poor cell survival after implantation. *Stem Cells*. 2018;36(3):363–376. doi:10.1002/stem.2763

27. Rodriguez AM, Elabd C, Amri EZ, Ailhaud G, Dani C. The human adipose tissue is a source of multipotent stem cells. *Biochimie*. 2005;87(1):125–128. doi:10.1016/j.biochi.2004.11.007

28. Gronthos S, Mankani M, Brahim J, Robey PG, Shi S. Postnatal human dental pulp stem cells (DPSCs) in vitro and invivo. *Proc Natl Acad Sci*. 2000;97(25):13625–13630. doi:10.1073/pnas.240309797

29. Miura M, Gronthos S, Zhao M, Lu B, Fisher LW, Robey PG, Shi S. SHED: Stem cells from human exfoliated deciduous teeth. *Proc Natl Acad Sci*. 2003;100(10):5807–5812. doi:10.1073/pnas.0937635100

30. Liu X, Wang P, Chen W, Weir MD, Bao C, Xu HHK. Human embryonic stem cells and macroporous calcium phosphate construct for bone regeneration in cranial defects in rats. *Acta Biomater*. 2014;10(10):4484–4493. doi:10.1016/j.actbio.2014.06.027

31. Bourne S, Buttery LDK, Xynos ID, Wood H, Hughes FJ, Hughes SP, Episkopou V, Polak JM. Selective differentiation of osteoblasts and in vitro bone formation from murine embryonic stem cells. *Tissue Eng*. 2001;7(1):89–99.

32. Rutledge K, Cheng Q, Pryzhkova M, Harris GM, Jabbarzadeh E. Enhanced differentiation of human embryonic stem cells on extracellular matrix-containing osteomimetic scaffolds for bone tissue engineering. *Tissue Eng Part C Methods*. 2014;20(11):865–874. doi:10.1089/ten.tec.2013.0411

33. Ardeshirylajimi A. Applied induced pluripotent stem cells in combination with biomaterials in bone tissue engineering. *J Cell Biochem*. 2017;118(10):3034–3042. doi:10.1002/jcb.25996

34. Volarevic V, Markovic BS, Gazdic M, Volarevic A, Jovicic N, Arsenijevic N, Armstrong L, Djonov V, Lako M, Stojkovic M. Ethical and safety issues of stem cell-based therapy. *Int J Med Sci*. 2018;15(1):36–45. doi:10.7150/ijms.21666

35. Shanbhag S, Suliman S, Pandis N, Stavropoulos A, Sanz M, Mustafa K. Cell therapy for orofacial bone regeneration: A systematic review and meta-analysis. *J Clin Periodontol*. 2019;46(S21):162–182. doi:10.1111/jcpe.13049

36. Friedenstein AJ, Piatetzky-Shapiro II, Petrakova K V. Osteogenesis in transplants of bone marrow cells. *J Embryol Exp Morphol*. 1966;16(3):381–390.

37. Hernigou PH, Poignard A, Beaujean F, Rouard H. Percutaneous autologous bone-marrow grafting for nonunions: Influence of the number and concentration of progenitor cells. *J Bone Joint Surg Am*. 2005;87(7):1430–1437. doi:10.2106/JBJS.D.02215

38. Rickert D, Sauerbier S, Nagursky H, Menne D, Vissink A, Raghoebar GM. Maxillary sinus floor elevation with bovine bone mineral combined with either autogenous bone or autogenous stem cells: A prospective randomized clinical trial. *Clin Oral Implant Res*. 2011;22(3):251–258. doi:10.1111/j.1600-0501.2010.01981.x

39. Kaigler D, Avila-Ortiz G, Travan S, Taut AD, Padial-Molina M, Rudek I, Wang F, Lanis A, Giannobile WV. Bone engineering of maxillary sinus bone deficiencies using enriched CD90+ stem cell therapy: A randomized clinical trial. *J Bone Miner Res*. 2015;30(7):1206–1216. doi:10.1002/jbmr.2464

40. Kaigler D, Pagni G, Park CH, Braun TM, Holman LA, Yi E, Tarle SA, Bartel RL, Giannobile WV. Stem cell therapy for craniofacial bone regeneration: A randomized, controlled feasibility trial. *Cell Transplant*. 2013;22(5):767–777. doi:10.3727/096368912X652968.Stem

41. Baba S, Yamada Y, Komuro A, Yotsui Y, Umeda M, Shimuzutani K, Nakamura S. Phase I/II trial of autologous bone marrow stem cell transplantation with a three-dimensional woven-fabric scaffold for periodontitis. *Stem Cells Int*. 2016;2016:6205910. doi:10.1155/2016/6205910

42. Bajestan MN, Rajan A, Edwards SP, Aronovich S, Cevidanes LHS, Polymeri A, Travan S, Kaigler D. Stem cell therapy for reconstruction of alveolar cleft and trauma defects in adults: A randomized controlled, clinical trial. *Clin Implant Dent Relat Res*. 2017;19(5):793–801. doi:10.1111/cid.12506

43. Behnia H, Khojasteh A, Soleimani M, Tehranchi A, Atashi A. Repair of alveolar cleft defect with mesenchymal stem cells and platelet derived growth factors: A preliminary report. *J Craniomaxillofacial Surg*. 2012;40(1):2–7. doi:10.1016/j.jcms.2011.02.003

44. Hermund NU, Stavropoulos A, Donatsky O, Nielsen H, Clausen C, Reibel J, Pakkenberg B, Holmstrup P. Reimplantation of cultivated human bone cells from the posterior maxilla for sinus floor augmentation. Histological results from a randomized controlled clinical trial. *Clin Oral Implants Res*. 2012;23(9):1031–1037. doi:10.1111/j.1600-0501.2011.02251.x

45. Pittenger MF, Mackay AM, Beck SC, Jaiswal RK, Douglas R, Mosca JD, Moorman MA, Simonetti DW, Craig S, Marshak DR. Multilineage potential of adult human mesenchymal stem cells. *Science*. 1999;284(5411):143–147.

46. Bernardo ME, Ball LM, Cometa AM, Roelofs H, Zecca M, Avanzini MA, Bertaina A, Vinti L, Lankester A, Maccario R, Ringden O, Le Blanc K, Egeler RM, Fibbe WE, Locatelli F. Co-infusion of ex vivo-expanded, parental MSCs prevents life-threatening acute GVHD, but does not reduce the risk of graft failure in pediatric patients undergoing allogeneic umbilical cord blood transplantation. *Bone Marrow Transplant*. 2011;46(2):200–207. doi:10.1038/bmt.2010.87

47. Siddappa R, Licht R, Van Blitterswijk C, De Boer J. Donor variation and loss of multipotency during in vitro expansion of human mesenchymal stem cells for bone tissue engineering. *J Orthop Res*. 2007;25(8):1029–1041. doi:10.1002/jor

48. Bruder SP, Jaiswal N, Haynesworth SE. Growth kinetics, self-renewal, and the osteogenic potential of purified human mesenchymal stem cells during extensive subcultivation and following cryopreservation. *J Cell Biochem*. 1997;64(2):278–294. doi:10.1002/(sici)1097-4644(199702)64:2<278::aid-jcb11>3.0.co;2-f

49. Rubio D, Garcia S, Paz MF, De la Cueva T, Lopez-Fernandez LA, Lloyd AC, Garcia-Castro J, Bernad A. Molecular characterization of spontaneous mesenchymal stem cell transformation. *PLoS One*. 2008;3(1). doi:10.1371/journal.pone.0001398

50. Izadpanah R, Kaushal D, Kriedt C, Tsien F, Patel B, Dufour J, Bunnell BA. Long-term in vitro expansion alters the biology of adult mesenchymal stem cells. *Cancer Res*. 2008;68(11):4229–4238. doi:10.1158/0008-5472.CAN-07-5272

51. Muschler GF, Nitto H, Boehm CA, Easley KA. Age- and gender-related changes in the cellularity of human bone marrow and the prevalence of osteoblastic progenitors. *J Orthop Res*. 2001;19(1):117–125. doi:10.1016/S0736-0266(00)00010-3

52. Jurgens WJFM, Oedayrajsingh-Varma MJ, Helder MN, Zandiehdoulabi B, Schouten TE, Kuik DJ, Ritt MJ, van Milligen FJ. Effect of tissue-harvesting site on yield of stem cells derived from adipose tissue: Implications for cell-based therapies. *Cell Tissue Res*. 2008;332(3):415–426. doi:10.1007/s00441-007-0555-7

53. Katz AJ, Tholpady A, Tholpady SS, Shang H, Ogle RC. Cell surface and transcriptional characterization of human adipose-derived adherent stromal (hADAS) cells. *Stem Cells*. 2005;23(3):412–423. doi:10.1634/stemcells.2004-0021

54. Nakagami H, Morishita R, Maeda K, Kikuchi Y, Ogihara T, Kaneda Y. Adipose tissue-derived stromal cells as a novel option for regenerative cell therapy. *J Atheroscler Thromb*. 2006;13(2):77–81. doi:10.5551/jat.13.77

55. Dufrane D. Impact of age on human adipose stem cells for bone tissue engineering. *Cell Transplant*. 2017;26(9):1496–1504. doi:10.1177/0963689717721203

56. Jurgens WJ, Kroeze RJ, Bank RA, Ritt MJPF, Helder MN. Rapid attachment of adipose stromal cells on resorbable polymeric scaffolds facilitates the one-step surgical procedure for cartilage and bone tissue engineering purposes. *J Orthop Res*. 2011;29(6):853–860. doi:10.1002/jor.21314

57. Overman JR, Helder MN, Ten Bruggenkate CM, Schulten EAJM, Klein-Nulend J, Bakker AD. Growth factor gene expression profiles of bone morphogenetic protein-2-treated human adipose stem cells seeded on calcium phosphate scaffolds in vitro. *Biochimie*. 2013;95(12):2304–2313. doi:10.1016/j.biochi.2013.08.034

58. Helder MN, Knippenberg M, Klein-Nulend J, Wuisman PIJM. Stem cells from adipose tissue allow challenging new concepts for regenerative medicine. *Tissue Eng*. 2007;13(8):1799–1808. doi:10.1089/ten.2006.0165

59. Prins HJ, Schulten EAJM, Ten Bruggenkate CM, Klein-Nulend J, Helder MN. Bone regeneration using the freshly isolated autologous stromal vascular fraction of adipose tissue in combination with calcium phosphate ceramics. *Stem Cells Transl Med*. 2016;5(10):1362–1374.

60. Khojasteh A, Kheiri L, Behnia H, Tehranchi A, Nazeman P, Nadjmi N, Soleimani M. Lateral ramus cortical bone plate in alveolar cleft osteoplasty with concomitant use of buccal fat pad derived cells and autogenous bone: Phase I clinical trial. *Biomed Res Int*. 2017;2017:6560234. doi:10.1155/2017/6560234

61. Castillo-Cardiel G, López-Echaury AC, Saucedo-Ortiz JA, Castillo-Cardiel G, López-Echaury AC, Saucedo-Ortiz JA, Fuentes-Orozco C, Michel-Espinoza LR, Irusteta-Jiménez L, Salazar-Parra M, González-Ojeda A. Bone regeneration in mandibular fractures after the application of autologous mesenchymal stem cells, a randomized clinical trial. *Dent Traumatol*. 2017;33(1):38–44. doi:10.1111/edt.12303

62. Yusof MFH, Zahari W, Hashim SNM, Osman ZF, Chandra H, Kannan TP, Noordin KBAA, Azlina A. Angiogenic and osteogenic potentials of dental stem cells in bone tissue engineering. *J Oral Biol Craniofacial Res*. 2018;8(1):48–53. doi:10.1016/j.jobcr.2017.10.003

63. Yang X, Van Der Kraan PM, Bian Z, Fan M, Walboomers XF, Jansen JA. Mineralized tissue formation by BMP2-transfected pulp stem cells. *J Dent Res*. 2009;88(11):1020–1025. doi:10.1177/0022034509346258

64. Yamada Y, Ueda M, Hibi H, Baba S. A novel approach to periodontal tissue regeneration with mesenchymal stem cells and platelet-rich plasma using tissue engineering technology: A clinical case report. *Int J Periodontics Restorative Dent*. 2006;26(4):363–369.

65. Nakamura S, Yamada Y, Katagiri W, Sugito T, Ito K, Ueda M. Stem cell proliferation pathways comparison between human exfoliated deciduous teeth and dental pulp stem cells by gene expression profile from promising dental pulp. *J Endod*. 2009;35(11):1536–1542. doi:10.1016/j.joen.2009.07.024

66. D'Aquino R, Trovato L, Graziano A, Ceccarelli G, Cusella de Angelis G, Marangini A, Nisio A, Galli M, Pasi M, Finotti M, Lupi SM, Rizzo S, Y Baena RR. Periosteum-derived micro-grafts for tissue regeneration of human maxillary bone. *J Transl Sci*. 2016;2(2):125–129. doi:10.15761/jts.1000128

67. Monti M, Graziano A, Rizzo S, Perotti C, Del Fante C, D'Aquino R, Redi CA, Y Baena RR. In vitro and in vivo differentiation of progenitor stem cells obtained after mechanical digestion of human dental pulp. *J Cell Physiol*. 2017;232(3):548–555. doi:10.1002/jcp.25452

68. Y Baena RR, D'Aquino R, Graziano A, Trovato L, Aloise AC, Gabriele Ceccarelli G, Cusella G, Pelegrine AA, Lupi SM. Autologous periosteum-derived micrografts and PLGA/HA enhance the bone formation in sinus lift augmentation. *Front Cell Dev Biol*. 2017;5:1–7. doi:10.3389/fcell.2017.00087

69. Ferrarotti F, Romano F, Gamba MN, Quirico A, Giraudi M, Audagna M, Aimetti M. Human intrabony defect regeneration with micrografts containing dental pulp stem cells: A randomized controlled clinical trial. *J Clin Periodontol*. 2018;45(7):841–850. doi:10.1111/jcpe.12931

70. Risau W, Flamme I. Vasculogenesis. *Annu Rev Cell Dev Biol*. 1995;11:73-91.

71. Asahara T, Masuda H, Takahashi T, Kalka C, Pastore C, Silver M, Kearne M, Magner M, Isner JM. Bone marrow origin of endothelial progenitor cells responsible for postnatal vasculogenesis in physiological and pathological neovascularization. *Circ Res*. 1999;85(3):221–228. doi:10.1161/01.RES.85.3.221

72. Eguchi M, Masuda H, Asahara T. Endothelial progenitor cells for postnatal vasculogenesis. *Clin Exp Nephrol*. 2007;11(1):18–25. doi:10.1007/s10157-006-0448-1

73. Balaji S, King A, Crombleholme TM, Keswani SG. The role of endothelial progenitor cells in postnatal vasculogenesis: Implications for therapeutic neovascularization and wound healing. *Adv Wound Care*. 2013;2(6):283–295. doi:10.1089/wound.2012.0398

74. Carmeliet P, Rakesh KJ. Molecular mechanisms and clinical applications of angiogenesis. *Nature*. 2011;473(7347):298–307. doi:10.1016/S0140-6736(01)91146-8

75. Logsdon EA, Finley SD, Popel AS, MacGabhann F. A systems biology view of blood vessel growth and remodelling. *J Cell Mol Med*. 2014;18(8):1491–1508. doi:10.1111/jcmm.12164

76. Ribatti D, Crivellato E. "Sprouting angiogenesis", a reappraisal. *Dev Biol*. 2012;372(2):157–165. doi:10.1016/j.ydbio.2012.09.018

77. Carmeliet P. Mechanisms of angiogenesis and lymphangiogenesis. *Nat Med*. 2000;6(3):389–395.

78. Rücker M, Laschke MW, Junker D, Carvalho C, Schramm A, Mülhaupt R, Gellrich NC, Menger MD. Angiogenic and inflammatory response to biodegradable scaffolds in dorsal skinfold chambers of mice. *Biomaterials*. 2006;27(29):5027–5038. doi:10.1016/j.biomaterials.2006.05.033

79. Anderson CR, Ponce AM, Price RJ. Immunohistochemical identification of an extracellular matrix scaffold that microguides capillary sprouting in vivo. *J Histochem Cytochem*. 2004;52(8):1063–1072. doi:10.1369/jhc.4A6250.2004

80. Laschke MW, Menger MD. Vascularization in tissue engineering: Angiogenesis versus inosculation. *Eur Surg Res*. 2012;48(2):85–92. doi:10.1159/000336876

81. Zarem HA. The microcirculatory events within full-thickness skin allografts (homografts) in mice. *Surg.* 1969; 66 392–397. 1969;66:392-397. doi:10.1007/s40610-016-0036-4

82. Rücker M, Laschke MW, Junker D, Carvalho C, Tavassol F, Mülhaupt R, Gellrich N, Menger MD. Vascularization and biocompatibility of scaffolds consisting of different calcium phosphate compounds. *J Biomed Mater Res Part A*. 2008;86(4):1002–1011. doi:10.1002/jbm.a.31722

83. Laschke MW, Strohe A, Scheuer C, Eglin D, Verrier S, Alini M, Pohlemann T, Menger MD. In vivo biocompatibility and vascularization of biodegradable porous polyurethane scaffolds for tissue engineering. *Acta Biomater.* 2009;5(6):1991–2001. doi:10.1016/j.actbio.2009.02.006

84. Victor SP, Muthu J. Polymer ceramic composite materials for orthopedic applications — Relevance and need for mechanical match and bone regeneration. *J Mechatronics*. 2014;2:1–10. doi:10.1166/jom.2014.1030

85. Zhang B, Zhang P, Wang Z, Lyu Z, Wu H. Tissue-engineered composite scaffold of poly(lactide-co-glycolide) and hydroxyapatite nanoparticles seeded with autologous mesenchymal stem cells for bone regeneration. *J Zhejiang Univ Sci B*. 2017;18(11):963–976. doi:10.1631/jzus.B1600412

86. Karageorgiou V, Kaplan D. Porosity of 3D biomaterial scaffolds and osteogenesis. *Biomaterials*. 2005;26(27):5474–5491. doi:10.1016/j.biomaterials.2005.02.002

87. Kuboki Y, Takita H, Kobayashi D, Tsuruga E, Inoue M, Murata M, Nagai N, Dohi Y, Ohgushi H. BMP-induced osteogenesis on the surface of hydroxyapatite with geometrically feasible and nonfeasible structures: Topology of osteogenesis. *J Biomed Mater Res*. 1998;39(2):190–199. doi:10.1002/(SICI)1097-4636(199802)39:2<190::AID-JBM4>3.0.CO;2-K

88. Bružauskaitė I, Bironaitė D, Bagdonas E, Bernotienė E. Scaffolds and cells for tissue regeneration: different scaffold pore sizes—different cell effects. *Cytotechnology*. 2016;68(3):355–369. doi:10.1007/s10616-015-9895-4

89. Jones AC, Arns CH, Sheppard AP, Hutmacher DW, Milthorpe BK, Knackstedt MA. Assessment of bone ingrowth into porous biomaterials using micro-CT. *Biomaterials*. 2007;28(15):2491–2504. doi:10.1016/j.biomaterials.2007.01.046

90. Hulbert SF, Young FA, Mathews RS, Klawitter JJ, Talbert CD, Stelling FH. Potential of ceramic materials as permanently implantable skeletal prostheses. *J Biomed Mater Res*. 1970;4(3):433–456. doi:10.1002/jbm.820040309

91. Kuboki Y, Jin Q, Takita H. Geometry of carriers controlling phenotypic expression in BMP-induced osteogenesis and chondrogenesis. *J Bone Joint Surg Am*. 2001;83–A(Suppl 1 (Pt II)):S1–S105.

92. Tsuruga E, Takita H, Itoh H, Wakisaka Y, Kuboki Y. Pore size of porous hydroxyapatite as the cell-substratum controls BMP-induced osteogenesis. *J Biochem*. 1997;121(2):317–324. doi:10.1093/oxfordjournals.jbchem.a021589

93. Druecke D, Langer S, Lamme E, Pieper J, Ugarkovic M, Steinau HU. Neovascularization of poly(ether ester) block-copolymer scaffolds in vivo: Long-term investigations using intravital fluorescent microscopy. *J Biomed Mater Res - Part A*. 2004;68(1):10–18. doi:10.1002/jbm.a.20016

94. Kaigler D, Wang Z, Horger K, Mooney DJ, Krebsbach PH. VEGF scaffolds enhance angiogenesis and bone regeneration in irradiated osseous defects. *J Bone Miner Res*. 2006;21(5):735–744. doi:10.1359/jbmr.060120

95. Chen L, He Z, Chen B, Yang M, Zhao Y, Sun W, Xiao Z, Zhang J, Dai J. Loading of VEGF to the heparin cross-linked demineralized bone matrix improves vascularization of the scaffold. *J Mater Sci Mater Med*. 2010;21(1):309–317. doi:10.1007/s10856-009-3827-9

96. Li X, Guo B, Xiao Y, Yuan T, Fan Y, Zhang X. Influences of the steam sterilization on the properties of calcium phosphate porous bioceramics. *J Mater Sci Mater Med*. 2016;27(1):5. doi:10.1007/s10856-015-5617-x

97. Li B, Davidson JM, Guelcher SA. The effect of the local delivery of platelet-derived growth factor from reactive two-component polyurethane scaffolds on the healing in rat skin excisional wounds. *Biomaterials*. 2009;30(20):3486–3494. doi:10.1016/j.biomaterials.2009.03.008

98. Shi H, Han C, Mao Z, Ma L, Gao C. Enhanced angiogenesis in porous collagen-chitosan scaffolds loaded with angiogenin. *Tissue Eng Part A*. 2008;14(11):1775–1785. doi:10.1089/ten.tea.2007.0007

99. Schumann P, Tavassol F, Lindhorst D, Stuehmer C, Bormann KH, Kampmann A, Mülhaupt R, Laschke MW, Menger MD, Gellrich NC, Rücker M. Consequences of seeded cell type on vascularization of tissue engineering constructs in vivo. *Microvasc Res*. 2009;78(2):180–190. doi:10.1016/j.mvr.2009.06.003

100. Tavassol F, Schumann P, Lindhorst D, Sinikovic B, Voss A, von See C, Kampmann A, Bormann KH, Carvalho C, Mülhaupt R, Harder Y, Laschke MW, Menger MD, Gellrich NC, Rücker M. Accelerated angiogenic host tissue response to poly(L-Lactide-co-Glycolide) scaffolds by vitalization with osteoblast-like cells. *Tissue Eng Part A*. 2010;16(7):2265–2279. doi:10.1089/ten.tea.2008.0457

101. Moioli EK, Clark PA, Chen M, Dennis JE, Erickson HP, Gerson SL, Mao JJ. Synergistic actions of hematopoietic and mesenchymal stem/progenitor cells in vascularizing bioengineered tissues. *PLoS One*. 2008;3(12). doi:10.1371/journal.pone.0003922

102. Liu S, Zhang H, Zhang X, Wei L, Huang X, Xie H, Zhou J, Wang W, Zhang Y, Liu Y, Deng Z, Jin Y. Synergistic angiogenesis promoting effects of extracellular matrix scaffolds and adipose-derived stem cells during wound repair. *Tissue Eng Part A*. 2011;17(5-6):725–739. doi:10.1089/ten.tea.2010.0331

103. Qu D, Li J, Li Y, Gao Y, Zuo Y, Hsu Y, Hu J. Angiogenesis and osteogenesis enhanced by bFGF ex vivo gene therapy for bone tissue engineering in reconstruction of calvarial defects. *J Biomed Mater Res Part A*. 2011;96 A(3):543–551. doi:10.1002/jbm.a.33009

104. Helmrich U, Di Maggio N, Güven S, Groppa E, Melly L, Largo RD, Heberer M, Martin I, Scherberich A, Banfi A. Osteogenic graft vascularization and bone resorption by VEGF-expressing human mesenchymal progenitors. *Biomaterials*. 2013;34(21):5025–5035. doi:10.1016/j.biomaterials.2013.03.040

105. Liu J, Liu C, Sun B, Shi C, Qiao C, Ke X, Liu S, Liu X, Sun H. Differentiation of rabbit bone mesenchymal stem cells into endothelial cells in vitro and promotion of defective bone regeneration In vivo. *Cell Biochem Biophys*. 2014;68(3):479–487. doi:10.1007/s12013-013-9726-1

106. Pill K, Hofmann S, Redl H, Holnthoner W. Vascularization mediated by mesenchymal stem cells from bone marrow and adipose tissue: A comparison. *Cell Regen*. 2015;4:8. doi:10.1186/s13619-015-0025-8

107. Klar AS, Güven S, Biedermann T, Luginbühl J, Böttcher-Haberzeth S, Meuli-Simmen C, Meuli M, Martin I, Scherberich A, Reichmann E. Tissue-engineered dermo-epidermal skin grafts prevascularized with adipose-derived cells. *Biomaterials*. 2014;35(19):50655078. doi:10.1016/j.biomaterials.2014.02.049

108. Miranville A, Heeschen C, Sengenès C, Curat CA, Busse R, Bouloumié A. Improvement of postnatal neovascularization by human adipose tissue-derived stem cells. *Circulation*. 2004;110(3):349–355. doi:10.1161/01.CIR.0000135466.16823.D0

109. Clayton ZE, Sadeghipour S, Patel S. Generating induced pluripotent stem cell derived endothelial cells and induced endothelial cells for cardiovascular disease modelling and therapeutic angiogenesis. *Int J Cardiol*. 2015;197:116–122. doi:10.1016/j.ijcard.2015.06.038

110. Schechner JS, Nath AK, Zheng L, Kluger MS, Hughes CC, Sierra-Honigmann MR, Lorber MI, Tellides G, Kashgarian M, Bothwell AL, Pober JS. In vivo formation of complex microvessels lined by human endothelial cells in an immunodeficient mouse. *Proc Natl Acad Sci U S A*. 2000;97(16):9191–9196. doi:10.1073/pnas.150242297

111. Sweeney M, Foldes G. It takes two: Endothelial-perivascular cell cross-talk in vascular development and disease. *Front Cardiovasc Med*. 2018;5(October):1–14. doi:10.3389/fcvm.2018.00154

112. Yang J, Nagavarapu U, Relloma K, Sjaastad MD, Moss WC, Passaniti A, Herron GS. Telomerized human microvasculature is functional in vivo. *Nat Biotechnol*. 2001;19(3):219–224. doi:10.1038/85655

113. Clément F, Grockowiak E, Zylbersztejn F, Fossard G, Gobert S, Maguer-Satta V. Stem cell manipulation, gene therapy and the risk of cancer stem cell emergence. *Stem Cell Investig*. 2017;4(7):1–15. doi:10.21037/sci.2017.07.03

114. Koike N, Fukumura D, Gralla O, Au P, Schechner JS, Jain RK. Tissue engineering: Creation of long-lasting blood vessels. 2004;428(6979):138–139. doi:10.1080/15555270601041821

115. Paik KJ, Zielins ER, Atashroo DA, Maan ZN, Duscher D, Luan A, Walmsley GG, Momeni A, Vistnes S, Gurtner GC, Longaker MT, Wan DC. Studies in fat grafting: Part V. Cell-assisted lipotransfer to enhance fat graft retention is dose dependent. *Plast Reconstr Surg*. 2015;136(1):67–75. doi:10.1016/j.physbeh.2017.03.040

116. Verseijden F, Posthumus-Van Sluijs SJ, Farrell E, Van Neck JW, Hovius SE, Hofer SO, Van Osch GJ. Prevascular structures promote vascularization in engineered human adipose tissue constructs upon implantation. *Cell Transplant*. 2010;19(8):1007–1020. doi:10.3727/096368910X492571

117. Frueh FS, Später T, Scheuer C, Menger MD, Laschke MW. Isolation of murine adipose tissue-derived microvascular fragments as vascularization units for tissue engineering. *J Vis Exp*. 2017;2017(122):1–7. doi:10.3791/55721

118. Später T, Frueh FS, Nickels RM, Menger MD, Laschke MW. Prevascularization of collagen-glycosaminoglycan scaffolds: Stromal vascular fraction versus adipose tissue-derived microvascular fragments. *J Biol Eng*. 2018;12(1):1–13. doi:10.1186/s13036-018-0118-3

119. Shepherd BR, Chen HYS, Smith CM, Gruionu G, Williams SK, Hoying JB. Rapid perfusion and network remodeling in a microvascular construct after implantation. *Arter Thromb Vasc Biol*. 2004;24(5):898–904. doi:10.1161/01.ATV.0000124103.86943.1e

120. Hoying JB, Boswell CA, Williams SK. Angiogenic potential of microvessel fragments established in three-dimensional collagen gels. *In Vitro Cell Dev Biol Anim*. 1996;32(7):409–419. doi:10.1007/BF02723003

121. Laschke MW, Kleer S, Scheuer C, Schuler S, Garcia P, Eglin D, Alini M, Menger MD. Vascularisation of porous scaffolds is improved by incorporation of adipose tissue-derived microvascular fragments. *Eur Cells Mater*. 2012;24:266–277. doi:10.22203/eCM.v024a19

122. Pilia M, McDaniel JS, Guda T, Chen XK, Rhoads RP, Allen RE, Corona BT, Rathbone CR. Transplantation and perfusion of microvascular fragments in a rodent model of volumetric muscle loss injury. *Eur Cells Mater*. 2014;28(210):11–24. doi:10.22203/eCM.v028a02

123. McDaniel JS, Pilia M, Ward CL, Pollot BE, Rathbone CR. Characterization and multilineage potential of cells derived from isolated microvascular fragments. *J Surg Res*. 2014;192(1):214–222. doi:10.1016/j.jss.2014.05.047

124. Koduru S V., Leberfinger AN, Pasic D, Forghani A, Lince S, Hayes DJ, Ozbolat IT, Ravnic DJ. Cellular based strategies for microvascular engineering. *Stem Cell Rev Reports*. 2019;15(2):218–240. doi:10.1007/s12015-019-09877-4

125. Trivisonno A, Alexander RW, Baldari S, Cohen SR, Di Rocco G, Gentile P, Magalon G, Magalon J, Miller RB, Womack H,Toietta G. Concise review: Intraoperative strategies for minimal manipulation of autologous adipose tissue for cell- and tissue-based therapies. *Stem Cells Transl Med*. 2019; 8(12):1265–1271. doi:10.1002/sctm.19-0166

126. Vezzani B, Shaw I, Lesme H, Yong L, Khan N, Tremolada C, Péault B. Higher pericyte content and secretory activity of microfragmented human adipose tissue compared to enzymatically derived stromal vascular fraction. *Stem Cells Transl Med*. 2018;7(12):876–886. doi:10.1002/sctm.18-0051

127. Ceserani V, Ferri A, Berenzi A, Benetti A, Ciusani E, Pascucci L,Bazzucchi C, Coccè V, Bonomi A, Pessina A, Ghezzi E, Zeira O , Ceccarelli P, Versari S, Tremolada C, Alessandri G. Angiogenic and anti-inflammatory properties of micro-fragmented fat tissue and its derived mesenchymal stromal cells. *Vasc Cell*. 2016;8(1):1–12. doi:10.1186/s13221-016-0037-3

128. Van Dongen JA, Stevens HP, Parvizi M, Van der Lei B, Harmsen MC. The fractionation of adipose tissue procedure to obtain stromal vascular fractions for regenerative purposes. *Wound Repair Regen*. 2016;24(6):994–1003. doi:10.1111/wrr.12482

129. Gentile P, Scioli MG, Bielli A, Orlandi A, Cervelli V. Comparing different nanofat procedures on scars: Role of the stromal vascular fraction and its clinical implications. *Regen Med*. 2017;12(8):939–952. doi:10.2217/rme-2017-0076

130. Desando G, Bartolotti I, Martini L, Giavaresi G, Aldini NN, Fini M, Roffi A, Perdisa F, Filardo G, Kon E, Grigolo B. Regenerative features of adipose tissue for osteoarthritis treatment in a rabbit model: Enzymatic digestion versus mechanical disruption. *Int J Mol Sci*. 2019;20(11):1–16. doi:10.3390/ijms20112636

131. Cattaneo G, De Caro A, Napoli F, Chiapale D, Trada P, Camera A. Micro-fragmented adipose tissue injection associated with arthroscopic procedures in patients with symptomatic knee osteoarthritis. *BMC Musculoskelet Disord*. 2018;19(1):1–7. doi:10.1186/s12891-018-2105-8

132. Naldini G, Sturiale A, Fabiani B, Giani I, Menconi C. Micro-fragmented adipose tissue injection for the treatment of complex anal fistula: a pilot study accessing safety and feasibility. *Tech Coloproctol*. 2018;22(2):107–113. doi:10.1007/s10151-018-1755-8

133. Cho CH, Koh YJ, Han J, Sung HK, Jong Lee H, Morisada T, Schwendener RA, Brekken RA, Kang G, Oike Y, Choi TS, Suda T, Yoo OJ, Koh GY. Angiogenic role of LYVE-1-positive macrophages in adipose tissue. *Circ Res*. 2007;100(4). doi:10.1161/01.RES.0000259564.92792.93

134. Overman JR, Farré-Guasch E, Helder MN, Ten Bruggenkate CM, Schulten EAJM, Klein-Nulend J. Short (15 minutes) bone morphogenetic protein-2 treatment stimulates osteogenic differentiation of human adipose stem cells seeded on calcium phosphate scaffolds in vitro. *Tissue Eng Part A*. 2012;19(3–4):571–581. doi:10.1089/ten.tea.2012.0133

135. Kim A, Kim DH, Song HR, Kang WH, Kim HJ, Lim HC, Cho DW, Bae JH. Repair of rabbit ulna segmental bone defect using freshly isolated adipose-derived stromal vascular fraction. *Cytotherapy*. 2012;14(3):296–305. doi:10.3109/14653249.2011.627915

136. Rubina K, Kalinina N, Efimenko A, Lopatina T, Melikhova V, Tsokolaeva Z, Sysoeva V, Tkachuk V, Parfyonova Y. Adipose stromal cells stimulate angiogenesis via promoting progenitor cell differentiation, secretion of angiogenic factors, and enhancing vessel maturation. *Tissue Eng Part A*. 2009;15(8):2039–2050. doi:10.1089/ten.tea.2008.0359

137. Madonna R, De Caterina R. In vitro neovasculogenic potential of resident adipose tissue precursors. *Am J Physiol Cell Physiol*. 2008;295(5):1271–1280. doi:10.1152/ajpcell.00186.2008

138. Farré-Guasch E, Bravenboer N, Helder MN, Schulten EAJM, Ten Bruggenkate CM, Klein-Nulend J. Blood vessel formation and bone regeneration potential of the stromal vascular fraction seeded on a calcium phosphate scaffold in the human maxillary sinus floor elevation model. *Materials (Basel)*. 2018;11(1):116. doi:10.3390/ma11010161

139. Zakhari JS, Zabonick J, Gettler B, Williams SK. Vasculogenic and angiogenic potential of adipose stromal vascular fraction cell populations in vitro. *In Vitro Cell Dev Biol Anim*. 2018;54(1):32–40. doi:10.1007/s11626-017-0213-7

140. Scheinpflug J, Pfeiffenberger M, Damerau A, Schwarz F, Textor M, Lang A, Schulze F. Journey into bone models: A review. *Genes (Basel)*. 2018;9(5). doi:10.3390/genes9050247

141. Bertolai R, Catelani C, Aversa A, Rossi A, Giannini D, Bani D. Bone graft and mesenchimal stem cells: Clinical observations and histological analysis. *Clin Cases Miner Bone Metab.* 2015;12(2):183–187. doi:10.11138/ccmbm/2015.12.2.183

142. Pasquali PJ, Teixeira ML, Oliveira TA, De Macedo LGS, Aloise AC, Pelegrine AA, Maxillary sinus augmentation combining bio-oss with the bone marrow aspirate concentrate: A histomorphometric study in humans. *Int J Biomater.* 2015;2015:12128. doi:10.1155/2015/121286

143. Al-Ahmady HH, Abdelazeem AF, Bellah Ahmed NE, Shawkat WM, Elmasry M, Abdelrahman MA, Abderazik MA. Combining autologous bone marrow mononuclear cells seeded on collagen sponge with nano hydroxyapatite, and platelet-rich fibrin: reporting a novel strategy for alveolar cleft bone regeneration. *J Craniomaxillofac Surg.* 2018;46(9):1593–1600. doi:10.1016/j.jcms.2018.05.049.

144. Khalifa ME, Gomaa NE. Dental arch expansion after alveolar cleft repair using autogenous bone marrow derived mesenchymal stem cells versus autogenous chin bone graft. *J Dent Treatment Oral Care.* 2017; 2(1):1–10.

145. Talaat WM, Ghoneim MM, Salah O, Adly OA. Autologous bone marrow concentrates and concentrated growth factors accelerate bone regeneration after enucleation of mandibular pathologic lesions. *J Craniofac Surg.* 2018;29(4):992–997. doi:10.1097/SCS.0000000000004371

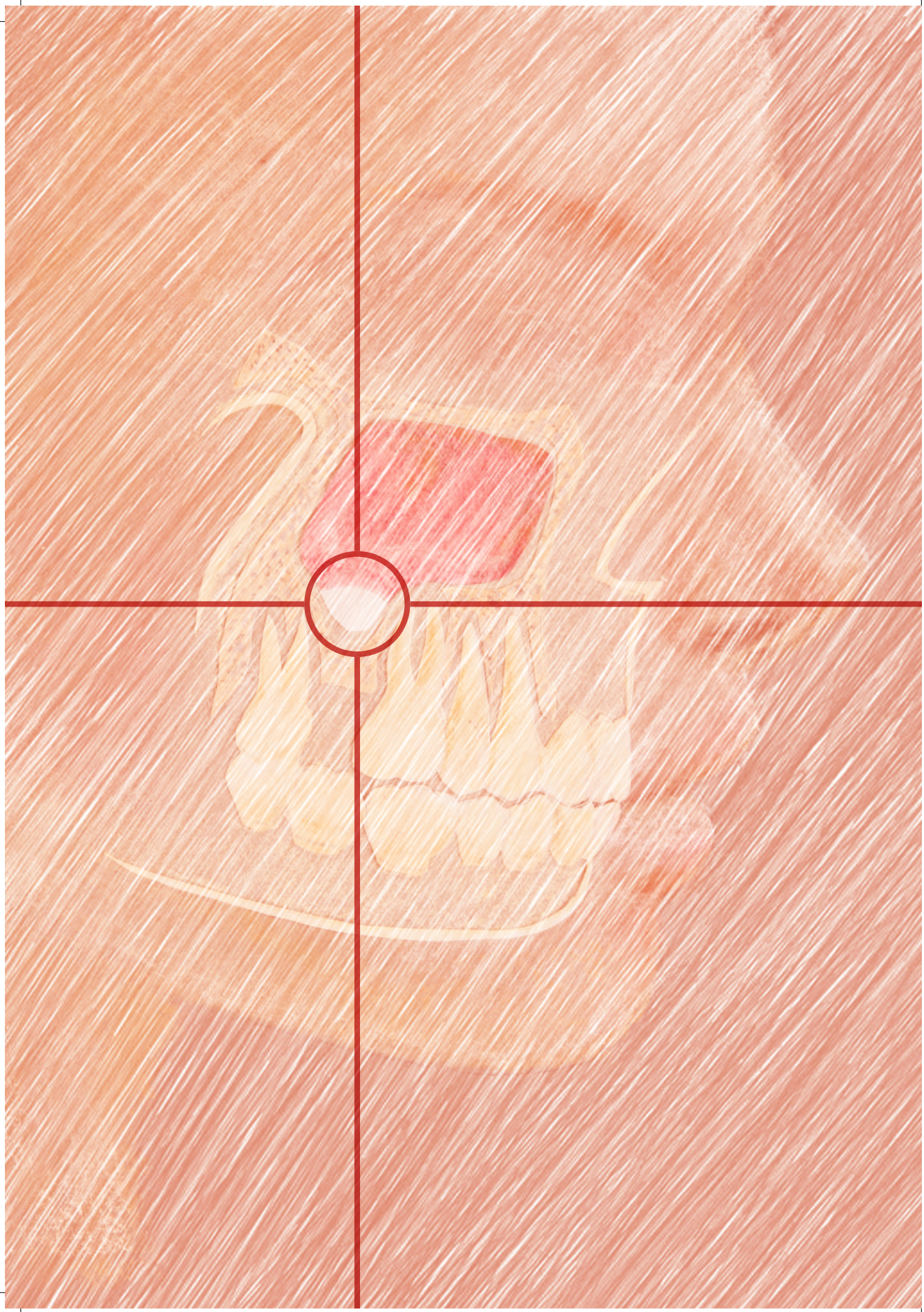

CHAPTER 3

Bone vitality and vascularization of mandibular and maxillary bone grafts in maxillary sinus floor elevation: A retrospective cohort study

Vivian Wu [1,2]
Engelbert A.J.M. Schulten [2]
Marco N. Helder [2]
Christiaan M. ten Bruggenkate [2]
Nathalie Bravenboer [3]
Jenneke Klein-Nulend [1]

[1] *Department of Oral Cell Biology, Academic Centre for Dentistry Amsterdam (ACTA), University of Amsterdam and Vrije Universiteit Amsterdam, Amsterdam Movement Sciences, Amsterdam, The Netherlands*

[2] *Department of Oral and Maxillofacial Surgery/Oral Pathology, Amsterdam University Medical Centers and Academic Centre for Dentistry Amsterdam (ACTA), Vrije Universiteit Amsterdam, Amsterdam Movement Sciences, Amsterdam, The Netherlands*

[3] *Department of Clinical Chemistry, Amsterdam University Medical Centers, Vrije Universiteit Amsterdam, Amsterdam Movement Sciences, Amsterdam, The Netherlands*

Clinical Implant Dentistry and Related Research 2023;25(1):141–151

ABSTRACT

Mandibular retromolar (predominantly cortical) and maxillary tuberosity (predominantly cancellous) bone grafts are used in patients undergoing maxillary sinus floor elevation (MSFE) for dental implant placement. The aim of this retrospective cohort study was to investigate whether differences exist in bone formation and vascularization after grafting with either bone source in patients undergoing MSFE. Fifteen patients undergoing MSFE were treated with retromolar (n=9) or tuberosity (n=6) bone grafts. Biopsies were taken 4-months postoperatively prior to dental implant placement, and histomorphometrically analyzed to quantify bone and osteoid area, number of total, apoptotic, and RANKL-positive osteocytes, small and large-sized blood vessels, and osteoclasts. The grafted area was divided in three regions (caudal-cranial): RI, RII, RIII. Bone volume was 40% (RII, RIII) higher and osteoid volume 10% (RII) lower in retromolar compared to tuberosity-grafted areas. Total osteocyte number and number of RANKL-positive osteocytes were 23% (RII) and 90% (RI, RII) lower, but osteoclast number was higher (retromolar: 12, tuberosity: 0) in retromolar-grafted areas. Total number of blood vessels was 80% (RI) to 60% (RIII) lower, while the percentage of large-sized blood-vessels was 86% (RI) to 25% (RIII) higher in retromolar-grafted areas. Number of osteocyte lacunae and apoptotic osteocytes were similar in both bone grafts used. Compared to retromolar bone, tuberosity bone showed increased bone vitality and vascularization in patients undergoing MSFE, likely due to faster bone remodeling or earlier start of new bone formation. Therefore, tuberosity bone grafts might perform better in enhancing bone regeneration.

INTRODUCTION

Maxillary sinus floor elevation (MSFE) is a frequently performed surgical procedure to restore insufficient bone height in the posterior maxilla allowing dental implant placement.[1–4] In MSFE, the space created between the maxillary alveolar process, the elevated Schneiderian membrane, and the inwardly rotated lateral sinus wall is filled with graft material. Autologous bone is considered as the gold standard grafting material in MSFE,[5,6] due to its osteoconductive as well as osteoinductive properties. Moreover, it contains osteogenic cells, and does not evoke immunogenic responses. Histologically, autologous bone grafts in MSFE result in predominantly a mature, lamellar type regenerated bone with higher mineralized bone volumes compared to bone substitutes which result in regenerated bone with lower mineralized bone volumes with a more immature, woven type of bone.[7–9] Therefore, autologous bone demonstrates increased bone regenerative potential compared to other grafting materials, such as synthetic, xenograft, or allograft bone substitutes with only osteoconductive properties.[5]

Various donor sites are available to harvest autologous bone, including iliac crest, calvarium, tibia, and intraoral sites (mandible, maxilla).[10–13] The choice of the donor site is based on the type and quantity of bone graft required, the ease of access to the donor site, and the time required with regard to the harvesting procedure and costs involved.[3, 12–15] Autologous bone grafts from intraoral sources are widely used in MSFE, either applied purely or mixed with a bone substitute.[3] A major advantage of intraoral sites for bone harvesting compared to extraoral sites, is that the graft can be harvested under local anesthesia.[13,14] The mandibular retromolar and maxillary tuberosity regions are favorable donor sites due to low morbidity compared to other intraoral sites.[13,14,16] There are multiple clinical and biological differences between bone harvested from the retromolar versus the tuberosity region. Bone from the retromolar region is predominantly cortical with a high mineral density, while bone from the tuberosity is more cancellous with a lower mineral density.[16,17]

Cortical bone grafts are considered to have less bone regeneration potential than cancellous bone grafts, due to the lack of osteogenic bone marrow cells and less osteoconductive matrix surface.[18–20] Cortical bone grafts show delayed vascularization due to their lack of porosity and consequent inhibition of vascular ingrowth, resulting in reduced diffusion of oxygen and nutrients through the cortical matrix. Therefore, cells in cortical grafts, compared to cancellous grafts, are less likely to survive grafting procedures. It has been suggested that primitive osteogenic cells surviving transplantation and forming mature osteoblasts are crucial for the formation of new bone.[20–22] Moreover, cortical bone grafts contain fewer osteoprogenitors than cancellous bone. Finally, the remodeling period of cortical bone graft takes longer, due to longer resorption time preceding osteogenic new bone formation.[21,22]

The majority of histologic and histomorphometric studies evaluating different sites and methods of autologous bone grafting in MSFE investigated bone grafts from the iliac crest and chin.[12] Only four studies investigated purely retromolar bone graft in MSFE.[8,23–25] No studies investigated purely tuberosity bone graft in MSFE. Comparison of the bone regeneration potential of retromolar bone grafts with tuberosity bone grafts in MSFE by means of histological and histomorphometrical analysis has not been performed so far.

Therefore, this study aimed to investigate possible differences in bone vitality and vascularization in patients undergoing MSFE using retromolar or tuberosity bone grafts through histomorphometrical analysis of bone biopsies. Four months post-MSFE we evaluated the biopsies prior to dental implant placement. It was hypothesized that tuberosity compared to retromolar bone graft will show enhanced new bone formation in patients undergoing MSFE. In this study, we report the first comparison of retromolar and tuberosity bone grafts for bone vitality and vascularization in patients undergoing MSFE.

MATERIALS AND METHODS

Study approval

The protocol was approved by the medical ethics committee (IRB) of the VU University Medical Center in Amsterdam (#2016.105). All patients signed a written informed consent before participation in the study. The study was performed according to the STROBE guidelines.[26]

Patient selection

Fifteen patients (4 females and 11 males), who were partially edentulous in the posterior maxilla and required dental implants for prosthetic rehabilitation between 2003 and 2012 were selected consecutively for this study (Table 1). All patients required an MSFE due to insufficient vertical bone height (≤3 mm) in at least one of the planned dental implant positions. Since some biopsies of these locations broke apart and could not be reconstructed properly, we sometimes had to switch to adjacent biopsies instead.

Table 1. Patient data

Donor site	Gender (♂,♀)	Age (years)	Residual bone height (mm)	Dental implant position	Biopsy location
Retromolar	♀	44	3	16	Single gap
Retromolar	♂	49	1	27	Multiple gap
Retromolar	♂	54	11	24	Free-ending
Retromolar	♂	55	4	16	Free-ending
Retromolar	♂	62	7	25	Free-ending
Retromolar	♂	67	1	16	Free-ending
Retromolar	♂	67	6	14	Free-ending
Retromolar	♂	60	6	16	Free-ending
Retromolar	♂	53	5	26	Free-ending
Tuberosity	♂	67	1	25	Multiple gap
Tuberosity	♀	50	10	24†	Free-ending
Tuberosity	♀	50	9	25†	Free-ending
Tuberosity	♀	35	6	17	Free-ending
Tuberosity	♂	65	8	25	Free-ending
Tuberosity	♀	58	9	26	Free-ending
Tuberosity	♂	61	7	15‡	Free-ending
Tuberosity	♂	61	5	16‡	Free-ending

Gender, age, residual bone height, dental implant position, biopsy location in patients undergoing MSFE treated with mandibular retromolar or maxillary tuberosity bone grafts. †same patient, ‡same patient.

The average age of the patients was 56±2 years (mean±SEM). Nine patients undergoing MSFE received mandibular retromolar bone graft, and six patients received a maxillary tuberosity bone graft. The average residual bone height was 6±1 mm (mean±SEM), with an average

residual bone height in patients grafted with retromolar bone of 5±1 mm (mean±SEM) and with tuberosity bone of 7±1 mm (mean±SEM). Patient demographics are summarized in Table 1.

The patients included in this study had a healthy periodontium and were non-smokers or moderate smokers (<10 cigarettes/day). Patients who required horizontal bone augmentation, and patients with specific conditions, *e.g.* systemic diseases, drug abuse, heavy smokers, other semi-invasive dental treatments, and/or pregnancy, were not included in this study. One oral and maxillofacial surgeon performed all surgical procedures both in the Alrijne Hospital, Leiderdorp, and in Amsterdam UMC, location VUmc, Amsterdam, The Netherlands.

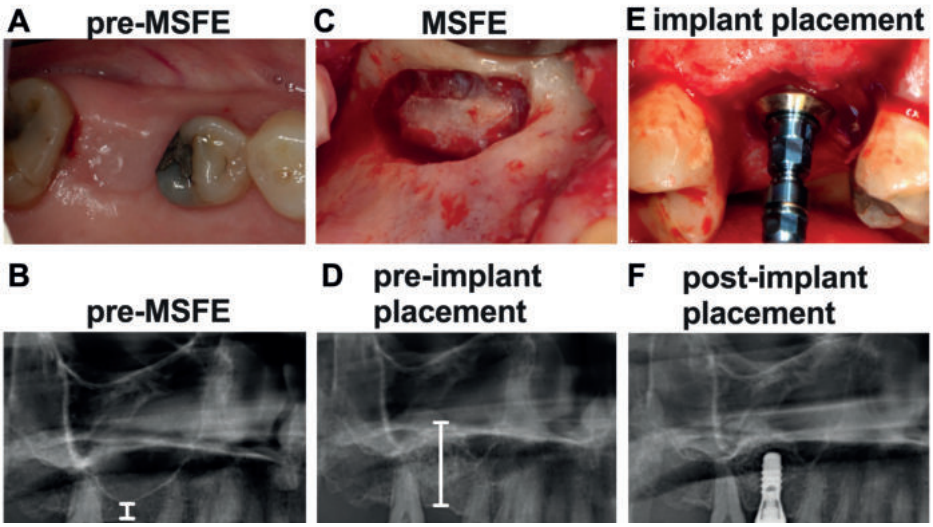

Figure 1. Clinical photographs of MSFE via a lateral approach allowing dental implant placement, and their corresponding radiographs to evaluate maxillary sinus and alveolar bone height. (A) Pre-operative photograph of the clinical situation. **(B)** Preoperative radiograph of the maxillary sinus. White line: residual native bone height. **(C)** Photograph of the lateral window during MSFE. **(D)** Radiograph of the maxillary sinus 4-months post-MSFE prior to implant placement. White line: total bone height. **(E)** Photograph of implant placement at 4-months post-MSFE. **(F)** Radiograph of the maxillary sinus directly after implant placement.

Maxillary sinus floor elevation

All fifteen patients underwent MSFE as previously described.[2] A preoperative clinical photograph (Figure 1A) and a radiograph (Figure 1B) were taken, and a lateral bony window was prepared and turned inward and upward leaving the lifted Schneiderian membrane intact (Figure 1C). The generated cavity within the maxillary sinus was filled with pure autologous bone harvested from either the retromolar or tuberosity region. Wound closure was performed with Gore-Tex sutures (W.L. Gore and Associates, Newark, DE, USA), which were removed after 10–14 days. All patients received antibiotic prophylaxis, consisting of 500 mg amoxicillin, 3 times daily starting 1 day preoperatively and continuing 7 days postoperatively. After a healing period of 4-months (post-

MSFE), prior to dental implant placement, a panoramic radiograph was made to determine the increase in vertical tissue height at the planned dental implant positions (Figure 1D).

Autologous bone graft harvesting technique

The retromolar bone grafts were harvested in half-cylinder shape with explantation trephines (inner diameter 4.2 mm; Institute Straumann AG, Basel, Switzerland), with a drilling speed of 500 rpm with minimal pressure and using sterile saline for copious irrigation, from the external oblique ridge of the mandible. The harvested half-cylinder bone cores were used as a cylinder to fill the recipient site. The half-cylinders were not milled but placed as such in the maxillary sinus bottom. The maxillary tuberosity bone grafts were harvested with hammer and osteotome. The harvested bone pieces were cut with a bone rongeur into smaller pieces to fill the recipient site. Wound closure was performed with resorbable sutures.

Dental implant surgery

Four months after MSFE, dental implant surgery was performed under local anesthesia (Figure 1E). A crestal incision was made with mesial and distal buccal vertical release incisions. A full thickness mucoperiosteal flap was raised to expose the underlying alveolar ridge, which was inspected visually for sufficient bone volume for the intended dental implant placement. Bone biopsies were obtained during dental implant surgery, using trephine drills with a length of 40.5 mm, and with an external diameter of 3.5 mm matching the outer core diameter of the dental implants and an inner diameter of 2.5 mm (Institute Straumann AG, Basel, Switzerland), with a drilling speed of 500 rpm and using sterile saline for copious irrigation, prior to dental implant insertion. Immediately after dental implant placement, a panoramic radiograph was made to check dental implant positions (Figure 1F). Panoramic radiographs taken pre-MSFE, as well as before dental implant placement, were used for morphometric measurements to determine the increase in vertical tissue height at the planned dental implant positions, using digital software. Calculations were performed with the use of a conversion factor (1.25x) that adjusted for magnification of the panoramic radiograph. After 3-months osseointegration of the dental implants the superstructures were fabricated and placed by the patient's dentist.

Bone biopsies

The bone biopsies taken during dental implant surgery with a trephine drill were fixated in 4% phosphate-buffered formaldehyde solution (Klinipath BV, Duiven, The Netherlands) for at least 24 hours. The bone biopsies were carefully removed from the trephine burr by cutting the burr, and opening it. There after the bone biopsies were transferred to 70% ethanol, and stored until use for histomorphometrical analysis, as described below under 'Histology and histomorphometry'. The caudal side of the bone biopsy had a sharp cutting edge in contrast to a dome shaped, crumbled cranial side (Figure 2A, B). These histologic features were used to identify the apicocoronal orientation of the biopsy. Subsequently, the whole research team verified whether the apicocoronal orientation of the biopsy corresponded with the histological appearance. Consensus was reached for all specimens.

Seventeen biopsies from gap, multiple gap and free-ending locations were evaluated (Table 1). The following biopsy location definitions were used: 1) single gap location: a natural tooth is present at both sides of the dental implant location; 2) multiple gap location: a natural tooth is present on either side of at least two dental implants next to each other; multiple bone biopsies can be retrieved in this type of gap; and 3) free-ending location: there is only one natural tooth present at the mesial side of the dental implant location(s); multiple bone biopsies can be retrieved in this situation.

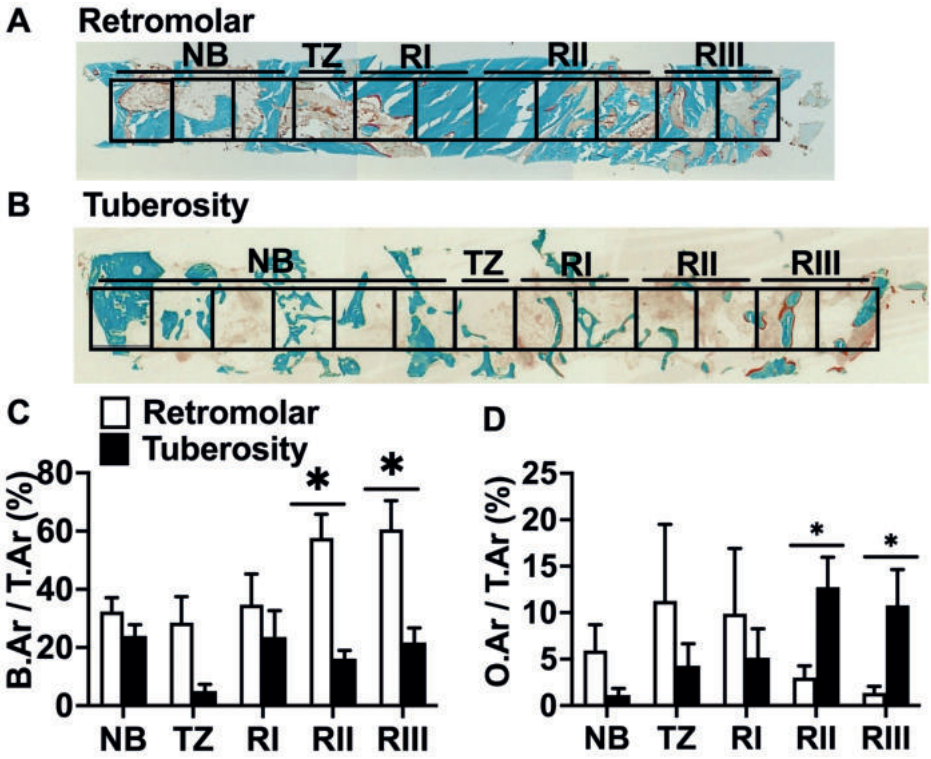

Figure 2. Histomorphometric analysis of biopsies taken after MSFE with retromolar or tuberosity bone graft. (A) Representative biopsy from one patient after MSFE with retromolar bone graft. **(B)** Representative biopsy from one patient after MSFE with tuberosity bone graft. Midsagittal histological sections of each biopsy were stained with Goldner's trichome method, to distinct mineralized bone tissue (green) and unmineralized osteoid (red). Biopsies were divided in consecutive 1 mm^2 regions of interest (ROIs). The transition zone (TZ) indicated the first ROI where graft material was observed. The images illustrated more bone and less osteoid in retromolar than in tuberosity bone biopsies (RII and RIII regions). Original magnification: 100×. **(C)** Bone volume (bone area over total area (B.Ar/T.Ar %)), and **(D)** Osteoid volume (osteoid area over total area (O.Ar/T.Ar %)) as assessed by histomorphometrical analysis. B.Ar/T.Ar and O.Ar/T.Ar were assessed for NB, TZ, Rl, Rll, and Rlll. Values are mean±SEM (n=3–9). *Significantly different between retromolar and tuberosity bone graft, $p<0.05$. B.Ar, bone area; T.Ar, total area; O.Ar, osteoid area; NB, native bone, TZ, transition zone, RI, region I; RII, region II; RIII, region III.

Histology and histomorphometry

After dehydration in descending alcohol series, the bone specimens were embedded without prior decalcification in low temperature polymerizing methylmethacrylate (MMA, Merck Schuchardt OHG, Hohenbrunn, Germany). Longitudinal sections of 5 µm thickness were prepared using a Jung K (R. Jung, Heidelberg, Germany) or Polycut 2500 S microtome (Leica, Wetzlar, Germany). Midsagittal histological sections of each biopsy were stained with Goldner's Trichome method,[27] to distinguish mineralized bone tissue (green) and unmineralized osteoid (red). The histological sections were divided into multiple regions of interest (ROI) of 1 mm^2 for blinded histomorphometrical analysis, as previously described.[28] Depending on the length of the biopsy, the number of ROIs ranged from 5-15. Vertical tissue height measurements of the residual native bone and graft at the planned dental implant position on the panoramic radiograph were made pre-MSFE, as well as prior to dental implant placement (Figure 1D). The vertical tissue height of the residual native bone on the radiographs resembled the height of the residual native bone in the biopsy. The vertical tissue height of the graft on the radiographs resembled the height of the graft in the biopsy. The whole research team verified whether the radiographically determined transition zone corresponded with the histological appearance, including parameters such as occurrence of apoptotic osteocytes and empty osteocyte lacunae to identify grafted material. Consensus was reached for all specimens. The transition zone (TZ) indicates the first ROI where graft material was observed when analyzing from the caudal to the cranial side of the biopsy. Since the biopsies analyzed had different lengths, we decided to define them in three regions after the transition zone (TZ). The first two ROIs on the right of the transition zone were defined as region I (RI), the two or three ROIs in the center (even or odd numbers) as region II (RII), and the two most cranial ROIs as region III (RIII). The digital images of the scanned biopsies were analyzed, starting from the caudal side of the biopsy, and continuing towards the cranial side. This previously described method allowed to compare similar regions for all biopsies with respect to the bone regeneration and blood vessel formation in the augmented maxillary sinus.[28-30]

For each separate area of interest, the histomorphometrical measurements were performed with a computer using an electronic stage table and a Leica DC 200 digital camera (Leica, Wetzlar, Germany). The computer software used was Leica QWin© (Leica Microsystems Image Solutions, Rijswijk, The Netherlands) or NIS-Elements AR 4.10.01 (Nikon GmbH, Düsseldorf, Germany) at 40x magnification according to the ASBMR nomenclature[31] to acquire digital images. Bone volume (bone area over total tissue area; B.Ar/T.Ar %) and osteoid volume (osteoid area over bone area; O.Ar/B.Ar %) were calculated as previously described.[32] The total number of lacunae over bone area (N.Tt.Lac/B.Ar $n.mm^{-2}$) and the total number of osteocytes over total number of lacunae (N.Ot/N.Tt.Lac %) were calculated. Only sharp and clearly displayed lacunae with and without osteocytes were included for analysis.

Blood vessel numbers, taking into account the blood vessel size, were determined as mean value of two separate blinded counts. Blood vessel size was calculated as the total blood vessel area expressed in $µm^2$. According to their diameter, blood vessels were divided into small (0–400 $µm^2$) or large vessels (>400 $µm^2$).

Tartrate-resistant acid phosphatase (TRAcP) staining was used to visualize bone resorbing multinuclear cells (osteoclasts) and was performed on a subset of biopsies (n=6) These sections were selected adjacent to biopsy sections that were stained with Goldner's trichrome method. TRAcP staining was performed according to a standardized protocol.[33] Quantitative analysis of the number of TRAcP-positive osteoclasts was carried out at 200x magnification throughout the biopsies according to the previously described ROIs, overlapping with the optical areas in the Goldner's trichrome-stained sections as closely as possible, using the same computer software and microscope used for quantification of the other histomorphometric parameters in the Goldner trichrome-stained sections. Within each area, the total number of TRAcP-positive osteoclasts over bone area (N.Ocl/B.Ar) was calculated.

Immunohistochemistry

A previously described protocol for immunostaining was used.[28,29,34] To visualize and calculate the number of apoptotic osteocytes, immunohistochemical staining for Cleaved Caspase-3 was carried out on a subset of biopsies (n=6). Receptor activator of nuclear factor-κB ligand (RANKL) expression by osteocytes was also detected by immunohistochemistry on a subset of biopsies (n=6). Bone sections embedded in MMA (see "histology and histomorphometry") were treated with xylene/chloroform (Merck, Darmstadt, Germany) to remove MMA. Sections were rehydrated and endogenous peroxidase quenched with 3% H_2O_2 in phosphate-buffered saline (PBS) containing 40% methanol. Antigen retrieval was performed by incubation with 0.5% saponin (Sigma, St. Louis, MO) in PBS for 30 min, followed by incubation with 3.5 µg/mL DNAse II (Sigma) in a mixture of 25 mM Tris with 10 mM $MgSO_4$ for 10 min at room temperature. Then sections were incubated with 3% H_2O_2 in PBS containing 40% methanol to block endogenous peroxidase. Non-specific binding of immunoglobulin G was blocked by incubation with 5% normal goat serum in PBS containing 0.05% Tween. Incubation with primary antibody was performed overnight at 4°C with 1/1000 rabbit-antiCleaved Caspase-3 antibody (Cell Signaling Technology, Beverly, MA), or rabbit-antiRANKL antibody (Cell Signaling Technology, Beverly, MA) in PBS containing 0.05% Tween. Sections were then incubated for 1 h with 1/200 biotin-labeled goat-anti-rabbit immunoglobulin G (Vector Labs, Burlingame, CA) in PBS containing 0.05% Tween, and for 10 min with a Biotin XX Tyramide SuperBoost™ Kit (Thermo Fisher Scientific). For color development, sections were incubated with DAB-nickel substrate. Sections with Cleaved Caspase-3 antibody were counterstained with 0.2% toluidine blue in H_2O, and sections with RANKL antibody with hematoxylin-eosin. Negative controls were performed without primary antibodies. Total number of Cleaved Caspase-3-positive osteocytes over bone area (N.Casp+/B.Ar n.mm^{-2}) and total number of Cleaved Caspase-3-positive osteocytes over total number of vital osteocytes (N.Casp+/N.Ot %), and total number of RANKL-positive osteocytes over bone area (N.RANKL+/B.Ar n.mm^{-2}) were calculated.

Statistical analysis

Data are presented as mean±standard error of the mean (SEM). Data analysis and statistical analysis were performed using GraphPad Prism 5 software (GraphPad Software, La Jolla, CA, USA) and IBM SPSS 23 statistical software (CircleCI, San Francisco, CA, USA). The number

of cases in this study (8–10 cases per group) was based on our own studies and previously published studies[35-37] that presented histological evaluation of bone biopsies. We could not carry out a power analysis, since we did not choose one specific parameter to compare the groups. Also, a direct comparison between the two graft types was not done before, so we decided to perform a multi-parameter evaluation to identify potential differences in an unbiased manner. This study observed multiple parameters in the biopsies of the two bone graft types. Biopsies from all treated patients were compared between the retromolar and tuberosity bone groups. An unpaired two-tailed Student's t-test was performed to test differences in age and residual bone height between patients with retromolar and tuberosity bone grafts. No statistical differences were observed.

An unpaired nonparametric Mann Whitney U and Pearson's Chi-squared test was performed to test differences between retromolar and tuberosity bone biopsies per region of interest. A paired Wilcoxon signed rank and McNemar test was performed to assess to test the different parameters between the different regions of interests within each bone group. Statistical significance was considered, if p-values were <0.05.

RESULTS

In retromolar bone biopsies, compared to tuberosity bone biopsies, a higher bone volume (B.Ar/T.Ar %; mean±SEM) in the center (RII: retromolar: 58%±8%; tuberosity: 16%±3%) and at the cranial side (RIII: retromolar: 60%±10%; tuberosity: 22%±5%) of the grafted area was observed (p<0.05; Figure 2A, B, C). The other regions showed no significant differences in bone volume between biopsies with retromolar (native bone (NB): 32%±5%; transition zone (TZ): 28%±9%; RI: 45%±8%) and tuberosity (NB: 24%±4%; TZ: 5%±2%; RI: 23%±9%) bone grafts (Figure 2C). There was a trend towards higher bone volume in regions towards the cranial side in retromolar bone grafts (p=0.06; Figure 2C). There was no difference between the three regions (RI–RIII) in tuberosity bone grafts.

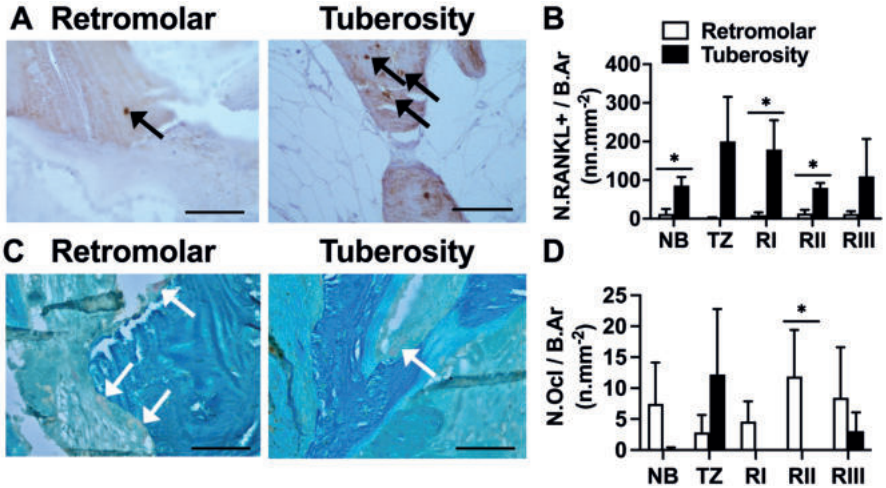

Figure 3. Total number of RANKL-positive osteocytes, and TRAcP-positive osteoclasts in biopsies taken after MSFE with retromolar or tuberosity bone graft. (A) To visualize and calculate the number of RANKL-positive osteocytes within the biopsies, consecutive sections were receptor activator of nuclear factor kappa-B ligand (RANKL)-stained (brown) in biopsies taken after MSFE with retromolar or tuberosity bone graft. Images illustrate less RANKL-positive osteocytes in retromolar than in tuberosity bone biopsies (RI region). Black arrows: RANKL-positive cells. **(B)** Total number of RANKL-positive osteocytes over bone area (N.RANKL+/B.Ar n.mm^{-2}) was assessed for NB, TZ, RI, RII, and RIII. **(C)** To visualize and calculate the number of osteoclasts within the biopsies, consecutive sections were tartrate-resistant acid phosphatase (TRAcP)-stained (red) in biopsies taken after MSFE with retromolar or tuberosity bone graft. Images illustrate more TRAcP-positive osteoclasts in retromolar than in tuberosity bone biopsies (RIII region). White arrows: TRAcP-positive osteoclasts. **(D)** Number of TRAcP-positive osteoclasts over bone area (N.Ocl/B.Ar n.mm^{-2}) was assessed for NB, TZ, RI, RII, and RIII. Values are mean±SEM (n=3). *Significantly different between retromolar and tuberosity bone graft, p<0.05. NB, native bone, TZ, transition zone, RI, region I; RII, region II; RIII, region III. Magnification: 200x. Scale bar: 100 µm.

In retromolar bone biopsies, compared to tuberosity bone biopsies, less osteoid volume (O.Ar/B.Ar %; mean±SEM) in the center (RII: retromolar: 3%±1%; tuberosity: 13%±3%) and at the cranial side (RIII: retromolar: 1%±1%; tuberosity: 11%±4%) was found (p<0.05; Figure 2A,

B, D). The other regions showed no differences in osteoid volume between retromolar (NB: 6%±3%; TZ: 11%±8%; RI: 10%±7%) and tuberosity (NB: 1%±1%; TZ: 4%±2%; RI: 5%±3%) bone grafts (Figure 2D). Osteoid volume tended to increase towards the cranial side of the biopsies within tuberosity bone grafts (p=0.06*),* but was similar in the biopsies with retromolar grafts (Figure 2D).

In retromolar bone biopsies, compared to tuberosity bone biopsies, a lower total number of RANKL-positive osteocytes per bone area (N.RANKL+/B.Ar n.mm^{-2}; mean±SEM) in residual native bone (NB: retromolar: 13±13; tuberosity: 86±23), at the caudal side (RI: retromolar: 9±8; tuberosity: 179±76) and in the center (RII: retromolar: 14±9; tuberosity: 80±12) of the grafted area (p<0.05) was found, but values seemed different (not statistically significant) for the other regions (retromolar: TZ: 2±2; RIII: 13±7; tuberosity: TZ: 200±115; RIII: 110±97; Figure 3A, B). Moreover, no significant differences in total number of RANKL-positive osteocytes per bone area were found between the regions per bone graft (Figure 3B).

In retromolar bone biopsies, compared to tuberosity bone biopsies, a higher total number of TRAcP-positive osteoclasts per bone area (N.Ocl/B.Ar n.mm^{-2}; mean±SEM) in the center (RII: retromolar: 12±8; tuberosity: 0) of the grafted area was found (p<0.05; Figure 3C,D), but the total number of TRAcP-positive osteoclasts per bone area was similar for the other regions (retromolar: NB: 7±7; TZ: 3±3; RI: 5±3; RIII: 8±8; tuberosity: NB: 0; TZ: 12±11; RI: 0; RIII: 3±3; Figure 3D). Moreover, no significant differences in total number of TRAcP-positive osteoclasts per bone area were found between the regions per bone graft (Figure 3D).
The total number of osteocyte lacunae per bone area (N.Tt.Lac/B.Ar n.mm^{-2}; mean±SEM) was similar between biopsies with retromolar (NB: 324±50; TZ: 323±52; RI: 225±43; RII: 1002±954; RIII: 472±215) and tuberosity bone grafts (NB: 433±70; TZ: 254±113; RI: 1386±960; RII: 533±51; RIII: 521±72; Figure 4A, B). The total number of lacunae was also similar between the different regions per bone graft (Figure 4B).

In retromolar bone biopsies, compared to tuberosity bone biopsies, a lower total number of osteocytes per total number of osteocyte lacunae (N.Ot/N.Tt.Lac %; mean±SEM) was observed in the center (RII: retromolar: 46±9%; tuberosity: 69±6%) of the grafted area (p<0.05). The total number of osteocytes was similar in the other regions (retromolar: NB: 66%±11%; TZ: 80%±4%; RI: 52%±9%; RIII: 50%±9%; tuberosity: NB: 66%±5%; 49%±25%; TZ: 76%±4%; RI: 76%±4%; RIII: 60%±9%; Figure 4A, C). In retromolar bone biopsies, a lower total number of osteocytes in the grafted area (RI, RII, RIII) was observed than in NB (p*<0.05*; Figure 4C). Also, a lower total number of osteocytes was seen in the center (RII) and cranial side (RIII) of the grafted area than in the transition zone (TZ; p<0.05; Figure 4C. There were no significant differences in total number of osteocytes between the different regions in biopsies with tuberosity bone grafts.

Immunohistochemical staining of Cleaved Caspase-3, a marker for cells that are undergoing apoptosis, showed a similar total number of apoptotic osteocytes per bone area (N.Casp+/B.Ar n. mm^{-2}; mean±SEM) in both retromolar and tuberosity bone biopsies (retromolar: NB: 44±33; TZ: 33±2; RI: 39±17; RII: 14±6; RIII: 9±7; tuberosity: NB: 13±7; TZ: 0±0; RI: 8±5; RII: 63±60; RIII: 17±17; Figure 4D, E). Total number of apoptotic osteocytes was also similar in the different regions per bone graft (Figure 4D, E). In retromolar and tuberosity bone a similar percentage of osteocytes was apoptotic (N.Casp+/N.Ot %, mean±SEM*)* (retromolar: NB: 40%±30%; TZ: 28%±21%;

RI: 31%±6%; RII: 17%±5%; RIII: 13%±2%; tuberosity: NB: 6%±2%; TZ: 0%±0%; RI: 7%±5%; RII: 20%±19%; RIII: 8%±8%; Figure 4D, F). There were no significant differences in percentage apoptotic osteocytes in the different regions per bone graft (Figure 4F).

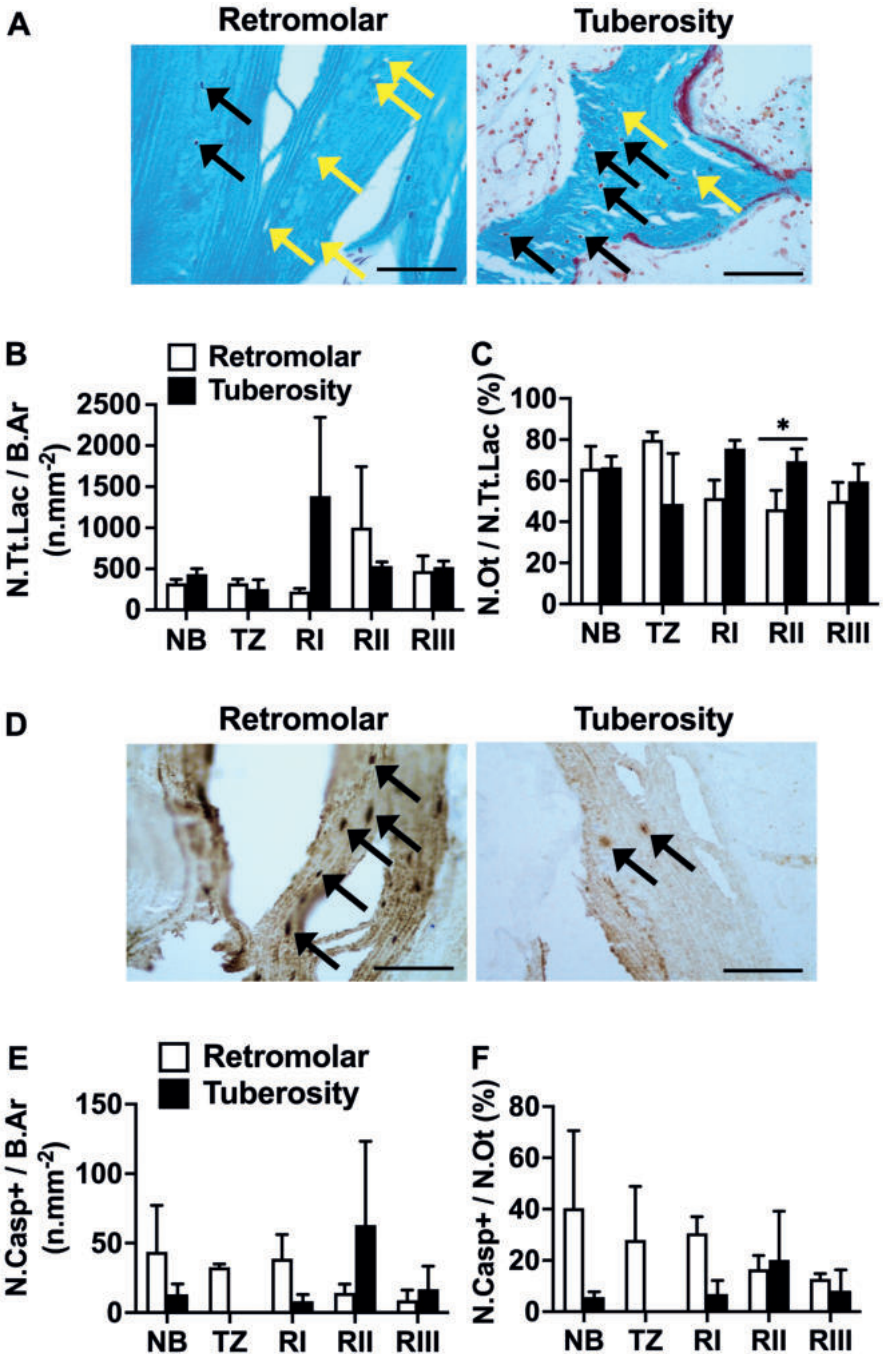

▶ Figure 4. Total number of osteocytes, lacunae and apoptotic osteocytes in biopsies taken after MSFE with retromolar or tuberosity bone graft. (A) Number of osteocytes (black arrows) and empty osteocyte lacunae (yellow arrows) were calculated in biopsies stained with Goldner's trichome taken after MSFE with retromolar and tuberosity bone graft. Images illustrate less osteocytes and more empty osteocyte lacunae in retromolar than in tuberosity bone biopsies (RII region). **(B)** Total number of lacunae over bone area (N.Tt.Lac /B.Ar n.mm^{-2}), and **(C)** Total number of osteocytes over total number of lacunae (N.Ot/N.Tt.Lac %) were assessed for NB, TZ, RI, RII, and RIII. **(D)** To visualize and calculate apoptotic osteocytes within the biopsies, consecutive sections were stained with Cleaved Caspase-3 (black) in biopsies taken after MSFE with retromolar or tuberosity bone graft. Black arrows: Cleaved Caspase-3 positive apoptotic osteocytes. Images illustrate more Caspase-3-positive apoptotic osteocytes in retromolar than in tuberosity bone biopsies (RI region). **(E)** Total number Cleaved Caspase-3-positive osteocytes over bone area (N.Casp+/B.Ar n.mm^{-2}), and **(F)** Total number of Cleaved Caspase-3-positive osteocytes over total number of osteocytes (N.Casp+/N.Ot %) were assessed for NB, TZ, RI, RII, and RIII. Values are mean±SEM (n=3–9). *Significantly different between retromolar and tuberosity bone graft, $p<0.05$. N.Ot, number of osteocytes; B.Ar, bone area; N.Casp+, number of Cleaved Caspase-3-positive osteocytes; N.Tt.Lac, total number of lacunae; NB, native bone, TZ, transition zone, RI, region I; RII, region II; RIII, region III. Magnification: 200x. Scale bar: 100 µm.

In retromolar bone biopsies, compared to tuberosity bone biopsies, a lower total number of blood vessels (N.bloodves; mean±SEM) in residual native bone (retromolar: NB: 8±1; tuberosity: NB: 21±6) and in the grafted area (retromolar: RI: 5±2; RII: 5±1; RIII: 4±1; tuberosity: RI: 21±6; RII: 25±10; RIII: 10±3) was observed ($p<0.05$; Figure 5A, B), but was similar for the transition zone (retromolar: TZ: 8±1; tuberosity: TZ: 38±15; Figure 4B). In retromolar bone biopsies, the total number of blood vessels was positively correlated with osteoid volume in the grafted area (RI–RIII; $r=0.43$, $p<0.05$). In retromolar bone biopsies, compared to tuberosity bone biopsies, a higher percentage of large sized blood vessels in native bone (NB: retromolar: 52%; tuberosity: 33%), transition zone (TZ: retromolar: 71%; tuberosity: 38%), at the caudal side (RI: retromolar: 67%; tuberosity: 36%), and in the center (RII: retromolar: 69%; tuberosity: 55%) of the grafted area was observed ($p<0.05$), but values were similar at the cranial side of the grafted area (RIII: retromolar: 63%; tuberosity: 65%; Figure 5C). In retromolar bone biopsies a higher percentage of large sized blood vessels, and a lower percentage of small sized blood vessels was shown in the transition zone and grafted area (large sized blood vessels: TZ: 71%; RI: 67%; RII: 69%; RIII: 63%) than in the residual native bone area (NB: 52%; $p<0.05$; Figure 5C). Moreover, in RII (69%) compared to RIII (63%) there was a higher percentage of large sized blood vessels, and a lower percentage of small sized blood vessels ($p<0.05$; Figure 5C). In tuberosity bone biopsies, a higher percentage of large sized blood vessels, and a lower percentage of small sized blood vessels was found in the grafted area (large sized blood vessels: RII: 55%; RIII: 65%) than in the residual native bone area (NB: 33%; $p<0.05$; Figure 5C). Moreover, in tuberosity bone biopsies, the percentage of large sized blood vessels was increasing, and the percentage of small sized blood vessels was decreasing, in the grafted area from the caudal towards the cranial side of the biopsy (large sized blood vessels: RI: 36%; RII: 55%; RIII: 65%; small sized blood vessels: RI: 64%; RII: 45%; RIII: 35%; $p<0.05$; Figure 5C).

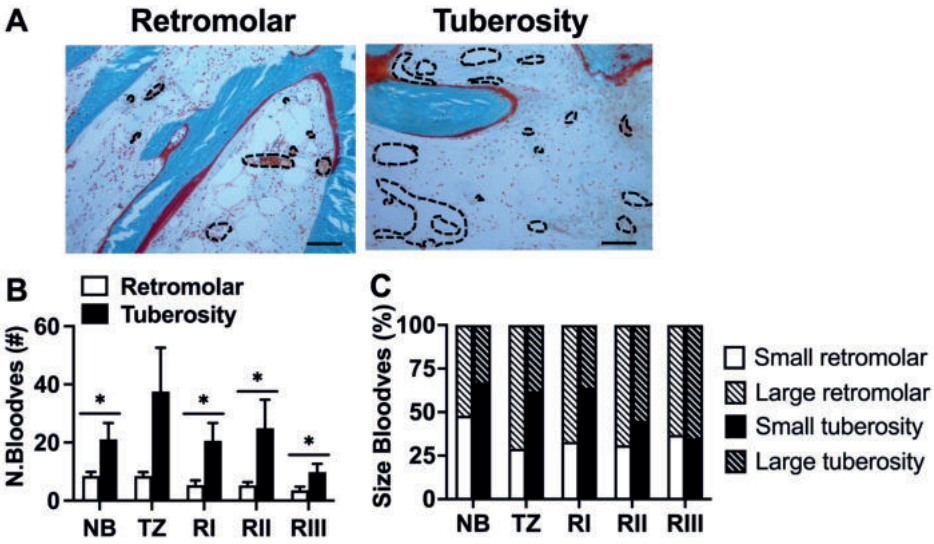

Figure 5. Total number of large sized and small sized blood vessels in biopsies taken after MSFE with retromolar or tuberosity bone graft. (A) Blood vessel number was calculated in biopsies stained with Goldner's trichome taken after MSFE with retromolar or tuberosity bone graft. Images illustrate less blood vessels in retromolar than in tuberosity bone biopsies (RII region). Black dotted circumferential line: blood vessel. **(B)** Total number of blood vessels (N.Bloodves), and **(C)** Percentage of large sized and small sized blood vessels was assessed for NB, TZ, Rl, Rll, and Rlll. Values are mean±SEM (n=3–9). *Significantly different between retromolar and tuberosity bone graft, $p<0.05$. N.Bloodves, number of blood vessels; NB, native bone, TZ, transition zone, RI, region I; RII, region II; RIII, region III. Magnification: 100x. Scale bar: 100 µm.

DISCUSSION

Four months post-MSFE, differences in bone vitality and vascularization were observed between retromolar and tuberosity bone graft. Compared to tuberosity bone biopsies, retromolar bone biopsies showed: (i) 40% higher bone volume (B.Ar/T.Ar %) in the grafted RII and RIII regions; (ii) 10% lower osteoid volume (O.Ar/B.Ar %) in these two regions; (iii) 90% lower total number of RANKL-positive osteocytes in the grafted area (caudal side (RI) and center (RII)); (iv) higher total number of osteoclasts in region RII of the grafted area; (v) 23% lower total number of osteocytes per total number of osteocyte lacunae (N.Ot/N.Tt.Lac %) in region RII; (vi) 80% to 25% lower total number of blood vessels in the grafted area from RI to RIII; (vii) 31% (RI) and 14% (RII) higher number of large sized blood vessels in the grafted area; and (viii) similar total number of osteocytes, and total number of apoptotic osteocytes.

Since our results showed more osteoid formation and a higher number of blood vessels in the grafted areas of patients who underwent MSFE with tuberosity bone grafts compared to patients with retromolar bone grafts, we postulate that tuberosity bone grafts might result in faster bone regeneration than retromolar bone grafts in MSFE.

Moreover, retromolar bone biopsies showed higher bone volume in the grafted area than tuberosity bone biopsies. These findings may be explained by a higher mineralization degree of the original graft, as retromolar bone grafts are predominantly composed of cortical bone, and tuberosity bone grafts of cancellous bone.[21,38] A slower bone remodeling process of cortical bone versus cancellous bone is expected.[21,38] Therefore, our observation that significant differences in mineralized bone area are present in our biopsies, likely results from the original composition of the bone graft and not yet from new bone formation. Since the bone biopsies in the present study were retrieved 4-months post-MSFE, differences in mineralized bone area due to bone remodeling between the two graft materials may be leveled in the long term, if graft remodeling has occurred to a high degree. Apoptotic osteocytes and empty lacunae were observed in both types of bone grafts, and therefore bone remodeling will likely continue after the biopsy retrieval (4-month time point). This is in line with findings by others showing that the bone mineralization degree in cortical bone grafts (chin and retromolar area), but not in corticocancellous bone grafts, decreases during 6-months post-MSFE period.[25,38] However, 6-months post-MSFE the bone mineralization degree is still higher in cortical than corticocancellous bone grafts, indicating that both graft origin and remodeling rate influence the mineralization degree.[25,38]

In this study, lower osteoid volume at the cranial and center of the retromolar bone-grafted areas, compared to tuberosity bone-grafted areas, was found. The reason for this observation is currently unexplained. Interestingly, osteoid volume increased towards the cranial side of the grafted area, which may have resulted from active bone formation starting from the cranial side of the biopsy. This is in line with earlier observations that bone formation may start not only from the maxillary native bone, but from the cranial side as well.[29,35] Moreover, it has been shown that the Schneiderian membrane of the maxillary sinus, which is lifted during MSFE to insert the graft material, contains a cell population with potential for osteogenic differentiation.[40]

We found similar total numbers of lacunae and apoptotic osteocytes in biopsies from retromolar and tuberosity bone-grafted areas. Remarkably, we observed a 90% lower total number of RANKL-positive osteocytes at the caudal side and in the center of the grafted area, and a higher number of TRAcP-positive osteoclasts in the center of the grafted area of retromolar vs. tuberosity bone biopsies. Osteocytes embedded in bone have been postulated to orchestrate bone homeostasis by regulating both bone-forming osteoblasts and bone-resorbing osteoclasts.[41,42] RANKL expression by osteocytes is an important signal to recruit osteoclasts.[43,44] RANKL, a transmembrane protein from the tumor necrosis factor (TNF) superfamily, is known to play a central role in osteoclastogenesis.[45] Therefore, the lower number of RANKL-positive osteocytes observed in retromolar bone biopsies in our study, may indicate less active bone remodeling in retromolar than in tuberosity bone grafts.

Bone is highly vascularized, and vascular development needs to be induced prior to osteogenesis. Our results showed that the total number of blood vessels in the grafted area was lower in retromolar versus tuberosity bone biopsies, which was accompanied by a lower percentage of osteoid volume. In contrast, the higher percentage of small sized blood vessels and the lower percentage of large sized blood vessels as we observed in the tuberosity bone-grafted areas indicates higher angiogenic activity in tuberosity bone graft. This is in agreement with earlier studies showing that bone formation is related to increased blood vessel formation.[29,39] The lower total number of osteocytes in the center of the grafted area of the retromolar grafts may consequently be the result of reduced diffusion of oxygen and nutrients due to delayed vascularization in these grafts. This confirms findings in earlier studies, *i.e.* that cortical bone grafts, compared to cancellous bone grafts, show delayed vascularization due to lack of porosity and consequent inhibition of vascular ingrowth.[21]

The study was conducted retrospectively resulting in several limitations. A limitation of the present study was that we compared two different autologous bone grafts in patients undergoing unilateral MSFE. To exclude inter-patient variation, a bilateral sinus floor elevation model would be more appropriate to compare two different grafting materials. Another limitation of this study was that we only analyzed biopsies at one time point, preventing to assess the dynamics of the remodeling process in both types of bone grafts. Therefore, we can only deduce that retromolar grafts displayed a slower bone remodeling rate, but cannot rule out that remodeling might reach similar levels at a later time point. Another limitation of this study was the use of two bone harvestings techniques. However, the bone harvestings techniques were unlikely to affect the results of our study in terms of bone vitality of the graft, since the harvesting techniques were as "atraumatic" as possible. This appears to be histologically confirmed since we did not observe necrotic bone tissue. A limitation of this study was also that no follow-up data of the patients could be obtained. However, no complaints regarding all dental implants have been reported thus far.

In summary, we found that the use of tuberosity bone graft in human MSFE resulted in a 10% higher osteoid volume in the center and at the cranial side of the grafted area, and 150–300% higher total number of blood vessels in the total grafted area compared to retromolar bone grafts. We conclude that tuberosity bone grafts showed enhanced bone vitality and vascularization in patients undergoing MSFE in comparison with retromolar bone grafts, either due

to a faster bone remodeling rate or due to an earlier start of bone remodeling in tuberosity bone graft-treated patients. Based on our histological data, it appears that tuberosity bone might perform better as an autologous graft material in MSFE than retromolar bone, since more osteoid was deposited, more blood vessels were formed, and a more active remodeling process was initiated. A shorter healing period before dental implant placement and loading might be feasible, if tuberosity bone grafts are used.

ACKNOWLEDGEMENTS

This work was granted by Health-Holland (project no. LSHM19016, “BB”). The authors thank H.W. van Essen and M.A. van Duin for assistance in histological processing and histomorphometrical analysis.

REFERENCES

1. Boyne PJ, James RA. Grafting of the maxillary sinus floor with autogenous marrow and bone. *J Oral Surg.* 1980;38(8):613–6.
2. Tatum HJ. Maxillary and sinus implant reconstructions. *Dent Clin North Am* 1986;30(2):207–229.
3. Wallace SS, Froum SJ. Effect of maxillary sinus augmentation on the survival of endosseous dental implants. A systematic review. *Ann Periodontol.* 2003;8(1):328–343. doi:10.1902/annals.2003.8.1.328
4. Zijderveld SA, Schulten EAJM, Aartman IHA, Ten Bruggenkate CM. Long-term changes in graft height after maxillary sinus floor elevation with different grafting materials: Radiographic evaluation with a minimum follow-up of 4.5 years. *Clin Oral Implants Res*. 2009;20(7):691–700. doi:10.1111/j.1600-0501.2008.01697.x
5. Stumbras A, Krukis MM, Januzis G, Juodzbalys G. Regenerative bone potential after sinus floor elevation using various bone graft materials: A systematic review. *Quintessence Int.* 2019;50(7):548–558. doi:10.3290/j.qi.a42482
6. Zijderveld SA, Zerbo IR, Van den Bergh JPA, Schulten EAJM, Ten Bruggenkate CM. Maxillary sinus floor augmentation using a beta-tricalcium phosphate (Cerasorb) alone compared to autogenous bone grafts. *Int J Oral Maxillofac Implants.* 2005;20(3):432–440.
7. Danesh-Sani SA, Wallace SS, Movahed A, El Chaar ES, Cho SC, Khouly I, Testori T. Maxillary sinus grafting with biphasic bone ceramic or autogenous bone: Clinical, histologic, and histomorphometric results from a randomized controlled clinical trial. *Implant Dent.* 2016;25(5):588–593. doi:10.1097/ID.0000000000000474
8. Schmitt CM, Doering H, Schmidt T, Lutz R, Neukam FW, Schlegel KA. Histological results after maxillary sinus augmentation with Straumann® BoneCeramic, Bio-Oss®, Puros®, and autologous bone. A randomized controlled clinical trial. *Clin Oral Implants Res.* 2013;24(5):576–585. doi:10.1111/j.1600-0501.2012.02431.x
9. Zerbo IR, Zijderveld SA, De Boer A, Bronckers AL, De Lange G, Ten Bruggenkate CM, Burger EH. Histomorphometry of human sinus floor augmentation using a porous β-tricalcium phosphate: A prospective study. *Clin Oral Implants Res.* 2004;15(6):724–732. doi:10.1111/j.1600-0501.2004.01055.x
10. Emeka N, Neukam FW. Autogenous bone harvesting and grafting in advanced jaw resorption: Morbidity, resorption and implant survival. *Eur J Oral Implantol.* 2014;7:S203–S217.
11. Kalk WWI, Raghoebar GM, Jansma J, Boering G. Morbidity from iliac crest bone harvesting. *J Oral Maxillofac Surg.* 1996;54(12):1424–1429. doi:10.1016/S0278-2391(96)90257-8
12. Klijn RJ, Meijer GJ, Bronkhorst EM, Jansen JA. Sinus floor augmentation surgery using autologous bone grafts from various donor sites: A meta-analysis of the total bone volume. *Tissue Eng Part B Rev.* 2010;16(3):295–303. doi:10.1089/ten.teb.2009.0558
13. Misch CM. Comparison of intraoral donor sites for onlay grafting prior to implant placement. *Int J Oral Maxillofac Implants.* 1997;12(6):767–776.
14. Raghoebar GM, Meijndert L, Kalk WWI, Vissink A. Morbidity of mandibular bone harvesting: a comparative study. *Int J Oral Maxillofac Implants.* 2007;22(3):359–365.
15. Tolstunov L. Implant zones of the jaws: Implant location and related success rate. *J Oral Implantol.* 2007;33(4):211–220.
16. Tolstunov L. Maxillary tuberosity block bone graft: Innovative technique and case report. *J Oral Maxillofac Surg.* 2009;67(8):1723–1729. doi:10.1016/j.joms.2009.03.043

17. Kamal M, Gremse F, Rosenhain S, Bartella AK, Hölzle F, Kessler P, Lethaus B. Comparison of bone grafts from various donor sites in human bone specimens. *J Craniofac Surg.* 2018;29(6):1661–1665. doi:10.1097/SCS.0000000000004586

18. Le Lorc'h-Bukiet I, Tulasne JF, Llorens A, Lesclous P. Parietal bone as graft material for maxillary sinus floor elevation: Structure and remodeling of the donor and of recipient sites. *Clin Oral Implants Res.* 2005;16(2):244–249.

19. Blomqvist JE, Alberius P, Isaksson S, Linde A, Obrant K. Importance of bone graft quality for implant integration after maxillary sinus reconstruction. *Oral Surg Oral Med Oral Pathol Oral Radiol Endod.* 1998;86(3):268–274. doi:10.1016/S1079-2104(98)90170-6

20. Burwell RG. Studies in the transplantation of bone: VII. The fresh composite homograft-autograft of cancellous bone: An analysis of factors leading to osteogenesis in marrow transplants and in marrow-containing bone grafts. *J Bone Joint Surg.* 1964;46:110–140.

21. Fleming JE, Cornell CN, Muschler GF. Bone cells and matrices in orthopedic tissue engineering. *Orthop Clin North Am.* 2000;31(3):357–374. doi:10.1016/S0030-5898(05)70156-5

22. Gerressen M, Hermanns-Sachweh B, Riediger D, Hilgers RD, Spiekermann H, Ghassemi A. Purely cancellous vs. corticocancellous bone in sinus floor augmentation with autogenous iliac crest: A prospective clinical trial. *Clin Oral Implants Res.* 2009; 20(2):109–115. doi:10.1111/j.1600-0501.2008.01619.x

23. Crespi R, Mariani E, Benasciutti E, Capparè P, Cenci S, Gherlone, E. Magnesium-enriched hydroxyapatite versus autologous bone in maxillary sinus grafting: Combining histomorphometry with osteoblast gene expression profiles ex vivo. *J Periodontol.* 2009;80(4):586–593. doi:10.1902/jop.2009.080466

24. Lundgren S, Moy P, Johansson C, Nilsson H. Augmentation of the maxillary sinus floor with particulated mandible: A histologic and histomorphometric study. *Int J Oral Maxillofac Implants.* 1996;11(6):760–766.

25. Thorwarth M, Srour S, Felszeghy E, Kessler P, Schultze-Mosgau S, Schlegel KA. Stability of autogenous bone grafts after sinus lift procedures: A comparative study between anterior and posterior aspects of the iliac crest and an intraoral donor site. *Oral Surg Oral Med Oral Path Oral Radiol Endod.* 2005;100(3):278–284. doi:10.1016/j.tripleo.2004.12.017

26. Von Elm E, Altman DG, Egger M, Pocock SJ, Gøtzsche PC, Vandenbroucke JP. The strengthening the reporting of observational studies in epidemiology (STROBE) statement: Guidelines for reporting observational studies. *J Clin Epidemiol.* 2008;61(4):344-349. doi:10.1016/j.jclinepi.2007.11.008

27. Plenk HJ. The microscopic evaluation of hard tissue implants. In Williams DF, Ed. *Techniques of biocompatibility testing*. CRC Press Inc; 1986:35–81.

28. Helder MN, Van Esterik FAS, Kwehandjaja MD, Prins HJ, Ten Bruggenkate CM, Klein-Nulend J, Schulten EAJM. Evaluation of a new biphasic calcium phosphate for maxillary sinus floor elevation: Micro-CT and histomorphometrical analyses, *Clin Oral Implants Res.* 2018;29(5):488–498. doi:10.1111/clr.13146

29. Farré-Guasch E, Bravenboer N, Helder MN, Schulten EAJM, Ten Bruggenkate CM, Klein-Nulend J. Blood vessel formation and bone regeneration potential of the stromal vascular fraction seeded on a calcium phosphate scaffold in the human maxillary sinus floor elevation model. *Materials.* 2018;11(1),116. doi:10.3390/ma11010161

30. Schulten EAJM, Prins HJ, Overman JR, Helder MN, Ten Bruggenkate CM, Klein-Nulend J. A novel approach revealing the effect of a collagenous membrane on osteoconduction in maxillary sinus floor elevation with β -tricalcium phosphate. *Eur Cells Mater.* 2013;25:215–228. doi:org/10.22203/eCM.v025a16

31. Dempster DW, Compston JE, Drezner MK, Glorieux FH, Kanis JA, Malluche H, Meunier PJ, Ott SM, Recker RR, Parfitt AM. Standardized nomenclature, symbols, and units for bone histomorphometry: A 2012 update of the report of the ASBMR histomorphometry nomenclature committee. *J Bone Miner Res.* 2013;28(1):2–17. doi:10.1002/jbmr.1805

32. Parfitt AM. Bone histomorphometry: Standardization of nomenclature, symbols and units (summary of proposed system). *Bone.* 1988;9(1):67–69. doi:10.1016/8756-3282(88)90029-4

33. Van de Wijngaert F, Burger H. Demonstration of tartrate-resistant acid phosphatase in un-decalcified, glycolmethacrylate-embedded mouse bone: A possible marker for (pre)osteoclast identification. *J Histochem Cytochem.* 1986;34:1317–1323. doi:10.1177/34.10.3745910

34. Dekker H, Schulten EAJM, Lichters I, Lichters I, Van Ruijven L, Van Essen HW, Blom G, Bloemena E, Ten Bruggenkate CM, Kullaa AM, Bravenboer N. Osteocyte apoptosis, bone marrow adiposity, and fibrosis in the irradiated human mandible. *Adv Radiat Oncol.* 2022;7(4):100951. doi: 10.1016/j.adro.2022.10095

35. Aladmawy MA, Natto ZS, Kreitzer M, Ogata Y, Hur Y. Histological and histomorphometric evaluation of alveolar ridge preservation using an allograft and nonresorbable membrane with and without primary closure: A pilot randomized controlled clinical trial. *Medicine (Baltimore).* 2022;101(26):e29769. doi: 10.1097/MD.0000000000029769

36. Tsugawa AJ, Arzi B, Vapniarsky N, Verstraete FJM. A retrospective study on mandibular reconstruction following excision of canine acanthomatous ameloblastoma. *Front Vet Sci.* 2022;9:900031. doi: 10.3389/fvets.2022.900031

37. Mandelli F, Traini T, Ghensi P. Customized-3D zirconia barriers for guided bone regeneration (GBR): Clinical and histological findings from a proof-of-concept case series. *J Dent.* 2021;114:103780. doi: 10.1016/j.jdent.2021.103780

38. Schlegel KA, Schultze-Mosgau S, Wiltfang J, Neukam FW, Rupprecht S, Thorwarth M. Changes of mineralization of free autogenous bone grafts used for sinus floor elevation. *Clin Oral Implants Res.* 2006;17(6):673–678. doi:10.1111/j.1600-0501.2006.01186.x

39. Prins HJ, Schulten EAJM, Ten Bruggenkate CM, Klein-Nulend J, Helder MN. Bone regeneration using the freshly isolated autologous stromal vascular fraction of adipose tissue in combination with calcium phosphate ceramics. *Stem Cells Transl Med.* 2016;5(10):1362–1374. doi:10.5966/sctm.2015-0369

40. Berbéri A, Al-Nemer F, Hamade E, Noujeim Z, Badran B, Zibara, K. Mesenchymal stem cells with osteogenic potential in human maxillary sinus membrane: an in vitro study. *Clin Oral Investig.* 2017;21(5):1599–1609. doi:10.1007/s00784-016-1945-6

41. Bonewald LF. The amazing osteocyte. *J Bone Miner Res.* 2011;2:229-238. doi:10.1002/jbmr.320

42. Burger EH, Klein-Nulend J. Mechanotransduction in bone--role of the lacuno-canalicular network. *FASEB J.* 1999;13:Suppl:S101-S112.

43. Nakashima T, Hayashi M, Fukunaga T, Kurata K, Oh-Hora M, Feng JQ, Bonewald LF, Kodama T, Wutz A, Wagner EF, Penninger JM, Takayanagi H. Evidence for osteocyte regulation of bone homeostasis through RANKL expression. *Nat Med.* 2011;17(10):1231–1234. doi:10.1038/nm.2452

44. Zhao S, Kato Y, Zhang Y, Harris S, Ahuja SS, Bonewald LF. MLO-Y4 osteocyte-like cells support osteoclast formation and activation. *J Bone Miner Res.* 2002;17:2068–2079. doi:10.1359/jbmr.2002.17.11.2068

45. Kong YY, Yoshida H, Sarosi I, Tan HL, Timms E, Capparelli C, Morony S, Oliveira-dos-Santos AJ, Van G, Itie A, Khoo W, Wakeham A, Dunstan CR, Lacey DL, Mak TW, Boyle WJ, Penninger JM. OPGL is a key regulator of osteoclastogenesis, lymphocyte development and lymph-node organogenesis. *Nature.* 1999;397(6717):315–323. doi:10.1038/16852

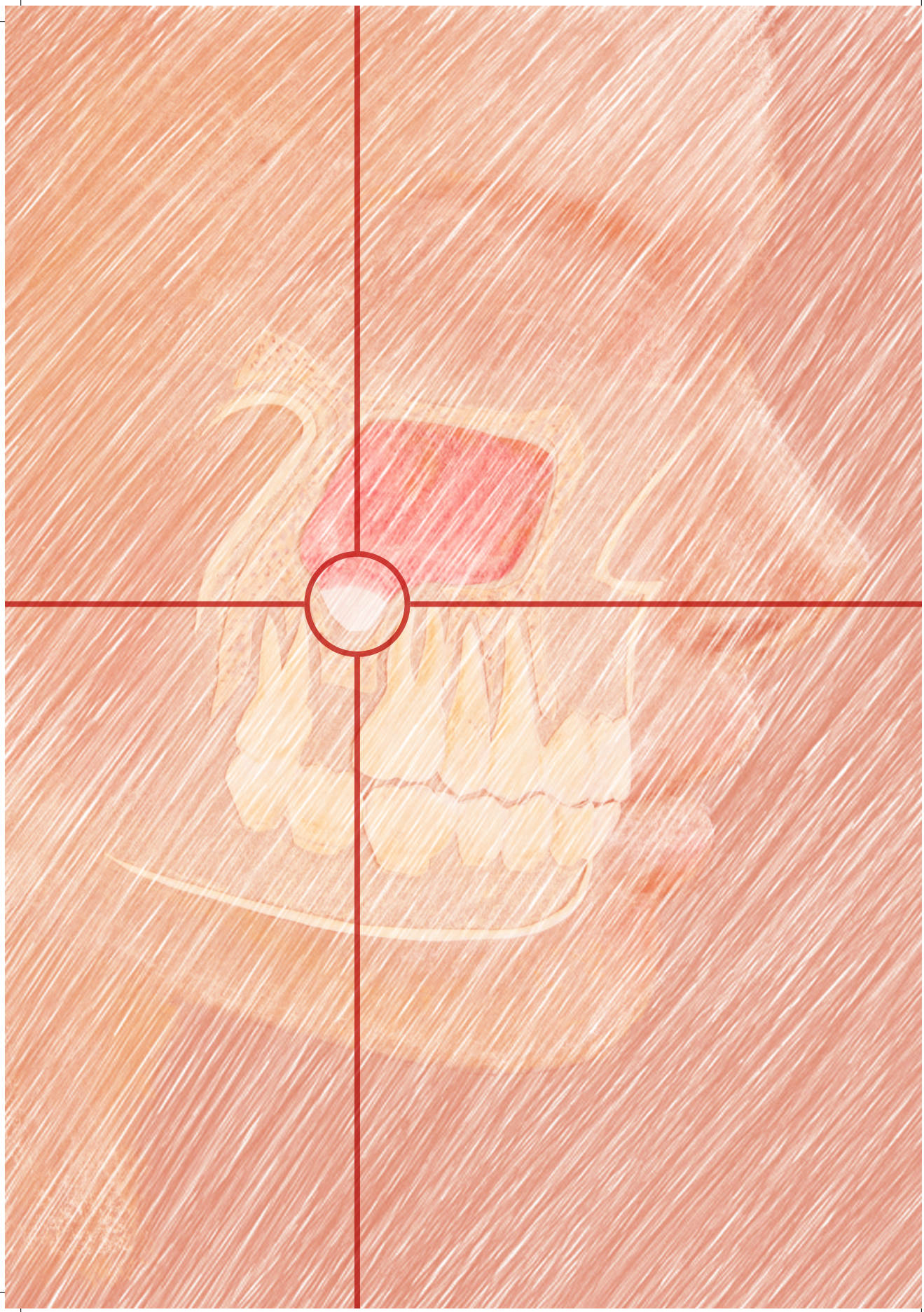

CHAPTER 4

Osteocyte morphology and orientation in relation to strain in jaw bone

Vivian Wu [1,2]
René F.M. van Oers [1,3]
Engelbert A.J.M. Schulten [2]
Marco N. Helder [2]
Rommel G. Bacabac [4]
Jenneke Klein-Nulend [1]

[1] *Department of Oral Cell Biology, Academic Centre for Dentistry Amsterdam (ACTA), University of Amsterdam and Vrije Universiteit Amsterdam, Amsterdam Movement Sciences, Amsterdam, The Netherlands*

[2] *Department of Oral and Maxillofacial Surgery/Oral Pathology, Amsterdam University Medical Centers and Academic Centre for Dentistry Amsterdam (ACTA), Vrije Universiteit Amsterdam, Amsterdam Movement Sciences, Amsterdam, The Netherlands*

[3] *Department of Dental Materials Science, Academic Centre for Dentistry Amsterdam (ACTA), University of Amsterdam and Vrije Universiteit Amsterdam, Amsterdam Movement Sciences, Amsterdam, The Netherlands*

[4] *Department of Physics, Medical Biophysics Group, University of San Carlos, Cebu City, Philippines*

International Journal of Oral Science 2018;10(1):2

ABSTRACT

Bone mass is important for dental implant success, and is regulated by mechanoresponsive osteocytes. We aimed to investigate the relation between levels and orientation of tensile strain and morphology and orientation of osteocytes in different dental implant positions in maxillary bone. Bone biopsies were retrieved from eight patients, who underwent maxillary sinus-floor elevation with β-tricalcium phosphate, prior to implant placement. Gap versus free-ending locations were compared by using 1) three-dimensional finite element model of the maxilla to predict tensile strain magnitude and direction, and 2) histology and histomorphometric analyses. The finite element model predicted larger, differently directed tensile strains in gap versus free-ending locations. Mean percentage of mineralized residual native-tissue volume, osteocyte number (mean±SD: 97±40/region-of-interest), and osteocyte shape (~90% elongated, ~10% round) were similar for both locations. However, osteocyte surface area was 1.5-times larger in gap than in free-ending locations, and elongated osteocytes in these locations were more cranially-caudally oriented. In conclusion, significant differences in osteocyte surface area and orientation seem to exist locally in maxillary bone, that may be related to tensile strain magnitude and orientation. This might reflect local differences in osteocyte mechanosensitivity and bone quality, suggesting differences in dental implant success based on location in the maxilla.

INTRODUCTION

Bone quality at the patient's implant site is an important local factor for the success of dental implants.[1,2] It influences dental implant stability at the time of surgery,[3,4] and osseointegration at a second stage.[5,6] Implant success rates are different at various implant sites in the jaw, with highest failure rates occurring in the maxillary posterior region.[7] Bone quality is determined by mechanical properties, bone mineral density, bone architecture, and extracellular matrix composition.[1,8]

Bone structure is continuously remodeled by bone-resorbing osteoclasts and bone-forming osteoblasts, regulated by osteocytes.[9] Osteocytes act as mechanosensors of bone producing signaling molecules affecting osteoblastic and/or osteoclastic activities. A prominent theory is that mechanosensing by osteocytes occurs via strain-induced fluid flow through the lacuno-canalicular network.[10]

Osteocyte morphology varies in different types of bone. Elongated osteocytes are found in load-bearing long bones that are predominantly loaded parallel to their longitudinal direction. On the other hand, round osteocytes are found in flat bones such as calvariae, loaded with much lower amplitudes radially and/or tangentially due to intracranial pressure and/or mastication.[11] Osteocyte morphology and orientation thus seem to be affected by the mechanical loading direction. Osteocyte lacunae have been shown to be aligned to the collagen fiber orientation,[12,13] which may correspond to the orientation of tensile strains in the bone.[14] External mechanical forces on cells are known to affect cytoskeletal structure and thus cell morphology.[9,15] Moreover, round osteocytes are much more mechanosensitive than elongated cells.[16] Round osteocytes in calvaria bone experience much lower mechanical loads than long bone, which might indicate that their morphology can maintain their physiological functions even in the presence of low mechanical loads and hence are more mechanosensitive than elongated osteocytes in long bones which are exposed to higher mechanical loads.[11] Therefore osteocyte morphology at the implant location may predict the success of dental implants.

Bone quality has been assessed by bone density in bone biopsies using histomorphometry and densitometry, but cellular parameters for bone quality have not been determined.[17] To date not much is known about osteocyte morphology and orientation in human jaw bone.

In this study, it is hypothesized that 1) tensile strains in maxillary bone are larger and more uniformly directed in single gap compared to free-ending locations; and 2) osteocytes are larger, more elongated, and more uniformly oriented in single gap versus free-ending locations. Therefore, this study aimed to investigate the relation between the levels and orientation of tensile strain, and morphology and orientation of osteocytes in single gap versus free-ending dental implant positions in maxillary bone through a finite element (FE) model and histomorphometric analysis.

MATERIALS AND METHODS

Patient selection

Eight patients, six men and two women, who were partially edentulous in the posterior maxilla, were selected. All patients required a maxillary sinus floor elevation (MSFE) due to insufficient maxillary bone height; the vertical bone height before MSFE was 4–10 mm.

The mean age of the patients was 58 years (range: 40–73 years). All patients were non-smokers or smoked <10 cigarettes per day. Patients with systemic diseases, drug abuse, and/or pregnancy were excluded from participation, as well as patients requiring horizontal bone augmentation.

The study was performed in accordance with the principles of the Declaration of Helsinki. Since the study involved CE-marked calcium phosphates being used for their intended purpose (carrier material for bone augmentation in MSFE procedures), no specific regulatory approval from a medical ethical committee was required. Patients provided written informed consent before inclusion in the study.

Clinical bone quality classification

Bone quality was pre-operatively assessed, and classified based on the amount of cortical bone versus cancellous bone.[18]

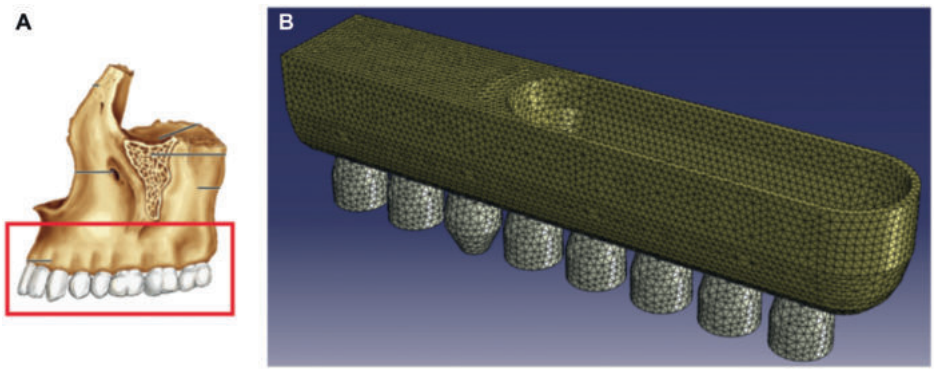

Figure 1. Translation of the maxillary dental arch into an FE model. (A) Anatomical image of maxillary bone showing one side of the superior dental arch (adapted from Marieb and Hoehn)[21]. **(B)** The FE model showing the maxillary dental arch with the sinus cavity. Individual teeth can be removed from this model to simulate patient-specific cases.

Maxillary sinus floor elevation surgery

A preoperative panoramic radiograph was made from each patient to calculate the alveolar bone height at each planned implant position. The MSFE procedure was performed with Ceros® β-tricalcium phosphate (β-TCP) granules with 60% porosity/0.7–1.4 mm grain size (Thommen Medical AG, Grenchen, Switzerland) as previously described.[19] The oral mucoperiosteal flap was closed using Gore-Tex sutures (W.L. Gore and Associates, Newark, DE, USA), which were

removed 10–14 days post-operatively. All patients received antibiotic prophylaxis, consisting of 500 mg amoxicillin 4-times daily, starting one day preoperatively and continuing a week postoperatively. After a healing period of 6-months, prior to the dental implant placement, a panoramic radiograph was made in order to measure the available tissue height for dental implant placement. Dental implants were placed as previously described.[20]

Biopsy retrieval

Bone biopsies were collected using a trephine burr (outer and inner diameter 3.5 mm and 2.5 mm, respectively), and fixed in 4% phosphate-buffered formaldehyde (Klinipath BV, Duiven, The Netherlands). Subsequently, biopsies were transferred to 70% ethanol, and stored until used for histomorphometry. One midsagittal section per biopsy was evaluated as described below.

Seventeen biopsies from gap or free-ending locations were evaluated. The following dental implant location definitions were used: 1) single gap location: a natural tooth is present at both sides of the implant location; 2) multiple gap location: a natural tooth is present on either side of at least two implant locations next to each other; multiple bone biopsies can be retrieved in this gap; 3) free-ending location: there is only one natural tooth present at one side (mesially) of the implant location(s); multiple bone biopsies can be retrieved in this situation.

Finite element model

A three-dimensional model of the maxillary sinus floor (Figure 1) was designed with the Finite Element (FE) software Abaqus/CAE (version 6.12, Dassault Systemes Simulia, Providence, RI, USA) to predict tensile strain in the maxillary bone. Individual teeth could be removed from this model to simulate patient-specific cases. While the dimensions of the model approximate the anatomical dimensions, the dental arch was straightened, to simplify visualization and comparison with dental radiographs.

All material behavior was assumed to be linear-elastic and isotropic. The maxillary bone was modelled with a Young's modulus of 10 GPa and Poisson's ratio of 0.3. Cortical and cancellous bone was not distinguished, since demarcation between these two bone types would vary greatly in the MSFE patients. Teeth were given a Young's modulus of 24 GPa, based on the stiffness of dentin. The focus was on strains at the implant positions rather than within the remaining teeth, and therefore enamel and pulp were not modeled as separate materials.

Teeth were loaded with an occlusal (vertical) load of 100 N, comparable to the human bite force.[22] As a boundary condition, the bone section was fixed in mesio-distal direction at its mesial surface, and fixed in all directions at its cranial surface.

Histology and histomorphometrical analysis

After dehydration in an ascending alcohol series, the bone specimens were embedded without prior decalcification in low temperature polymerizing methylmethacrylate (MMA, Merck Schuchardt OHG, Hohenbrunn, Germany) as previously described.[23] Longitudinal sections of 5 µm thickness were prepared, and midsagittal sections were stained with Goldner's Trichome, in order to distinguish mineralized bone tissue (green) and unmineralized osteoid (red).[24]

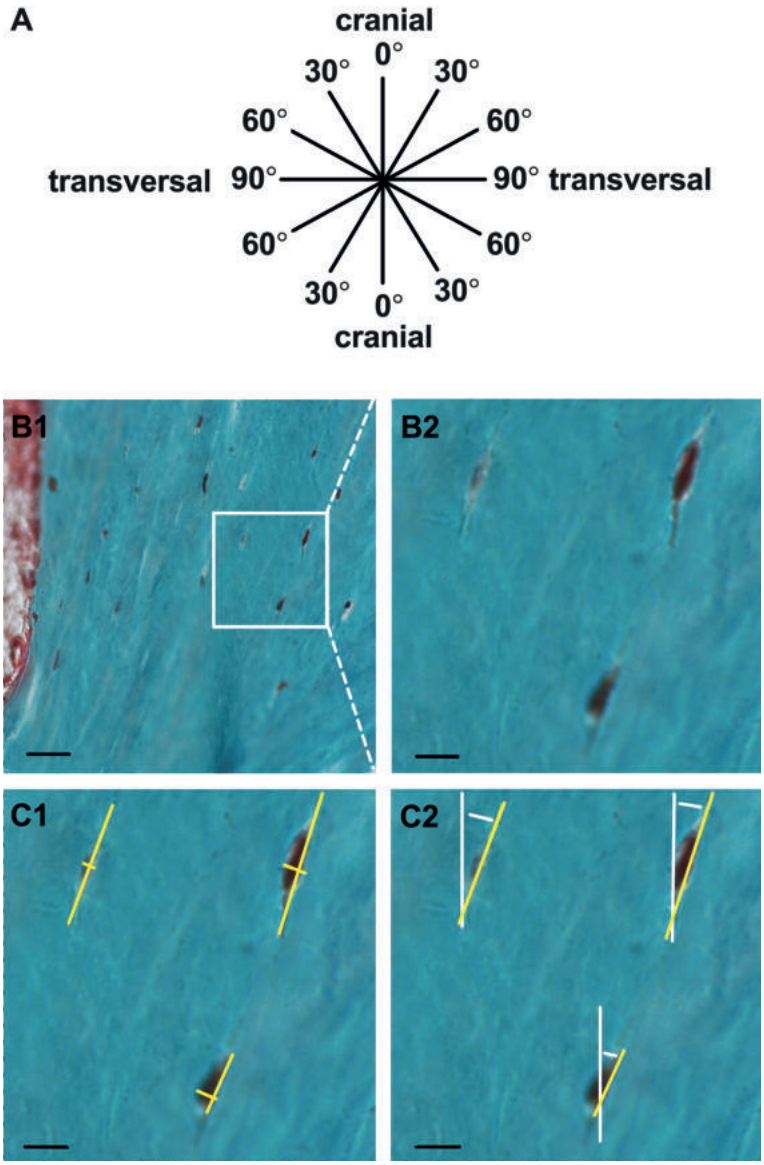

Figure 2. Histomorphometrical analysis for osteocyte surface area and orientation in biopsies from the maxillary bone. (A) Schematic diagram showing the osteocyte orientation in the maxillary bone described by an angle from 0°–90° measured from the cranial-caudal axis. **(B1)** Digital image showing an overview of a random bone area in a ROI at 400x magnification: osteocytes with lacunae (brown), mineralized bone tissue (green), and unmineralized osteoid (red). Scale bar, 25 µm. **(B2)** Digital image showing 1322x magnification of the area indicated in B1. Scale bar, 7.5 µm. **(C1)** The yellow lines on the osteocyte represent the measured length and width of the osteocyte. The length was determined as the longest distance (length axis) of the cell, and the width (width axis) as the longest distance that meets the length axis at a right angle. The osteocyte surface area was computed by the ellipse formula "π x ½ length x ½ width" for square measure. The osteocyte morphology was determined by the formula "width/length";

"<0.8" indicating elongated, and "≥0.8" indicating round. Scale bar, 7.5 µm. **(C2)** The orientation of the osteocyte was measured by the angle between the length axis of the osteocyte (yellow line) and the cranial-caudal axis of the biopsy (white line). The white dotted line shows the angle measured between the two axes. Scale bar, 7.5 µm. ROI, region of interest.

Histological sections were divided in regions of interest (ROI) of 1 mm^2. Each ROI was analyzed separately using a Leica DC 200 digital camera and Leica QWin© software (Leica Microsystems Image Solutions, Rijswijk, The Netherlands), as well as ImageJ (US National Institutes of Health, Bethesda, MD, 1997–2014). A demarcation line indicated the transition from the "residual native bone" (RNB) floor to the regenerated "grafted maxillary sinus floor" (GMSF) bone.

The mineralized bone tissue was calculated as mean percentage of mineralized volume in each ROI, as previously described.[19,25]

Osteocyte morphology and orientation

Osteocyte morphology and orientation were analyzed in each ROI (Figure 2). In a random bone area in each ROI a digital image was acquired at 400x magnification (Figure 2B1). Only sharp and clearly displayed lacunae with live osteocytes were analyzed. Osteocyte number, surface area, morphology, and orientation were determined "blind" by two researchers.

For osteocyte surface area calculation, the ellipse formula "**π** x ½ length x ½ width" was used (Figure 2C1). Osteocyte morphology was defined with the formula "width/length"; "<0.8" distinguishing elongated, and "≥0.8" distinguishing round (Figure 2C1). Osteocyte orientation was described by an angle from 0–90° measured from the caudal-cranial axis. The cranial-caudal axis side was labeled 0°, the transversal axis 90°. Osteocyte orientation was measured by the angle between the length axis of the osteocyte (Figure 2C2: yellow line) and the cranial-caudal axis (Figure 2C2: white line).

Statistical analysis

Data are presented as mean±standard deviation (SD). Statistical analysis was performed using SPSS version 20 software. The Mann-Whitney test and the Pearson Chi-square test were performed to compare results obtained from the different volumes of interest between the biopsies in a gap and free-ending implant position. Statistical significance was considered when $p<0.05$.

RESULTS

Table 1. Maxillary bone biopsy details and histomorphometrical analysis of residual native bone (RNB)

Pt. #	Biopsy location	Dental implant position	Time (months)	Bone class	N	R (%)	Area mean ± SD (µm²)	Osteocyte orientation (%)		
								0°-30°	30°-60°	60°-90°
1	Single gap	26	8	II	15	8.8	78.5 ± 31.1	54.8	21.5	23.7
2	Single gap	26	9	II	70	8.3	56.0 ± 25.8	40.0	30.8	29.2
3	Multiple gap	16	>36	III	58	7.4	25.6 ± 12.2*	37.0	31.5	31.5
		17	13	III	71	13.2	65.2 ± 28.7	47.6	33.3	19.1
4	Multiple Gap	24	11	II	83	7.8	45.8 ± 25.6*	41.6	49.3	9.1
		25	11	II	67	3.5	43.6 ± 20.4*	35.9	35.9	28.2
		26	9	II	121	4.3	35.1 ± 22.0*	16.4	38.8	44.8 *
5	Free-ending	25	>36	III	151	11.6	46.4 ± 32.0*	47.8	25.4	26.8
		26	10	III	78	12.0	57.9 ± 23.4*	22.5	29.6	47.9 *
		27	6	III	108	11.1	47.6 ± 26.6*	33.3	37.5	29.2
6	Free-ending	23	3	III	108	6.5	57.5 ± 34.8*	57.4	23.8	18.8
		25	>24	III	119	19.0	59.5 ± 30.2*	55.0	30.0	15.0
		26	9	III	34	9.5	31.2 ± 13.1*	35.7	32.1	32.1
7	Free-ending	24	12	III	226*	8.0	53.3 ± 21.8*	50.0	32.5	16.7
		26	12	III	146	22.6	69.5 ± 35.6	43.0	34.4	22.6
8	Free-ending	25	>24	III	184	7.5	72.3 ± 32.7	30.7	29.7	39.6 *
		26	10	III	51	13.5	87.9 ± 54.4	28.9	37.8	33.3 *

Osteocyte number, morphology (round versus elongated), surface area and orientation were assessed.
*Significantly different from the average of patient #1 and #2, $p<0.05$
Pt. #, patient number; Time (months), time of biopsy retrieval after tooth extraction; Bone class, clinical bone quality classification (Lekholm and Zarb 1985); N, number of osteocytes per region of interest; R (%), percentage of round osteocytes; Area (µm²), osteocyte surface area.

Maxillary bone biopsy details and histomorphometrical analysis of residual native bone (RNB) data of the eight patients are shown in Table 1. The evaluation of two patients, a single gap location (Patient #1) and free-ending locations (Patient #5) are shown in detail in Figure 3 and 4.

Patients

The period between the tooth extraction and the biopsy retrieval at the single gap location was eight to nine months (Table 1: Patient #1 and #2). While this period at the multiple gap locations varied from nine to >36 months (Table 1: Patient #3 and #4), this period spanned three to >36 months in the free ending locations (Table 1: Patient #5–#8).

Preoperatively clinical bone quality was classified as type II in all the single gap locations, and as type III in all the free-ending locations (Table 1: Bone class).[18] Clinical bone quality does not seem to be directly correlated with the period between the tooth extraction and the biopsy retrieval. No clinical signs of inflammation were observed during biopsy retrieval.

Radiological evaluation

Panoramic radiographs were made preoperatively (not shown) and six months after MSFE prior to biopsy retrieval. A single gap location in patient #1 (Figure 3A) and free-ending locations in patient #5 (Figure 3C) are shown. The mean height gain of the maxillary sinus floor at the biopsy positions was similar for all patients (mean±SD: 7.5±1.7 mm).

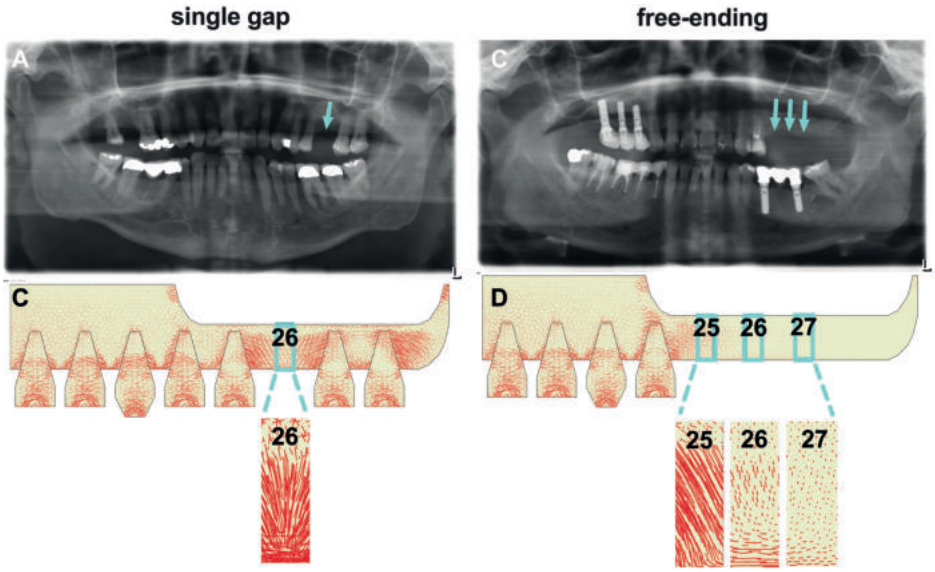

Figure 3. Panoramic radiograph and finite element model representing the single gap and free-ending locations in the maxillary bone prior to biopsy retrieval. (A) Radiograph showing the single gap location prior to biopsy retrieval (26), directly between two neighbouring natural teeth. **(B)** FE model predicting the large tensile strain in the single gap location (26). A ×7.5 magnification of the tensile strain shows the tensile strain directed from the natural tooth to the single gap location. **(C)** Radiograph showing the free-ending locations prior to biopsy retrieval (25, 26, 27). There are no natural teeth distal from the biopsy locations present. **(D)** FE model showing a decreasing tensile strain magnitude with the distance from the natural tooth; the location (27) experienced the smallest tensile strain compared to the other locations (25, 26). A ×7.5 magnification of the tensile strain showing the tensile strain oriented from the mesial neighbouring natural tooth to the free-ending locations (25, 26, 27). The red lines indicate the tensile strain in the maxillary bone; the direction and length of the red lines indicate, respectively, the direction and magnitude of the tensile strain in the maxillary bone.

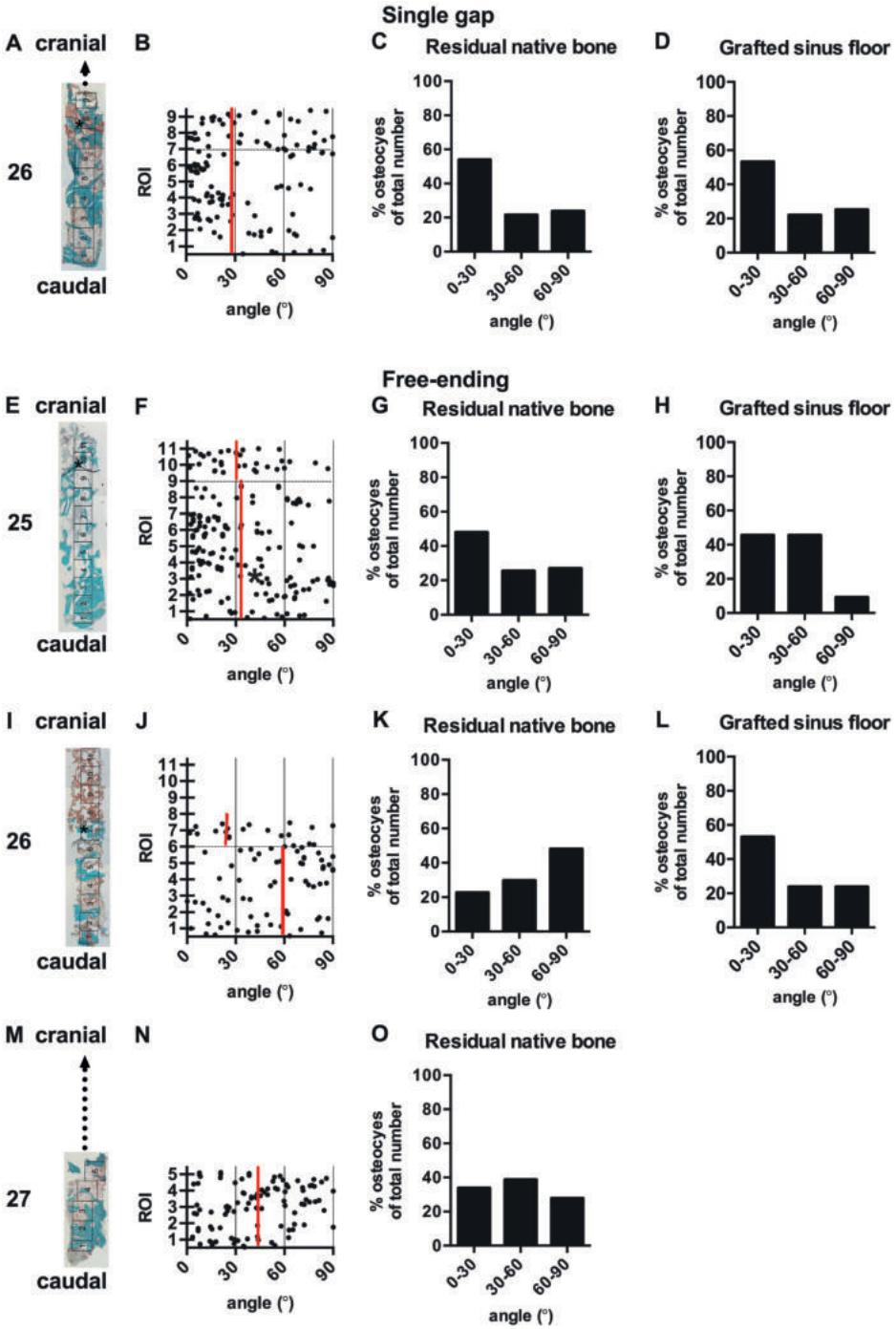
Single gap
A cranial
26
caudal
B
ROI
angle (°)
C
Residual native bone
% osteocyes of total number
0-30
30-60
60-90
angle (°)
D
Grafted sinus floor
Free-ending
E cranial
25
caudal
F
G
Residual native bone
H
Grafted sinus floor
I cranial
26
caudal
J
K
Residual native bone
L
Grafted sinus floor
M cranial
27
caudal
N
O
Residual native bone

Figure 4. Histology and osteocyte orientation in the maxillary bone. (A) Single gap location (26). Overview of a mid-sagittal section of the whole biopsy stained with Goldner's Trichome. For histomorphometrical analysis, the biopsy was divided in consecutive ROI of 1 mm^2. The maxillary sinus floor indicates the border between the residual native bone (RNB) and the grafted maxillary sinus floor (GMSF) (*). Mineralized bone tissue (green) and unmineralized osteoid (red) were both observed in RNB and GMSF. Some part of the biopsy was broken and excluded from the histomorphometric analysis (dotted lines). **(B)** Schematic overview of the osteocyte orientation per ROI in the biopsy. Every dot in the diagram represents a measured osteocyte. The vertical red line indicates the median of the osteocyte orientation. The horizontal black dotted line represents the border between the ROIs from the RNB and GMSF. **(C)** Evaluation of osteocyte orientation in the RNB at the single gap location (26). 54.8% of the osteocytes had a cranial-caudal orientation (angle 0°–30°), 23.7% a transversal orientation (angle 60°–90°), and 21.5% an orientation between these axes (angle 30°–60°). **(D)** Evaluation of osteocyte orientation in the GMSF at the single gap location (26). 53.1% of the osteocytes had a cranial-caudal orientation (angle 0°–30°), 25% a transversal orientation (angle 60°–90°), and 21.9% an orientation between these axes (angle 30°–60°). **(E)** Free-ending location (25). Mineralized bone tissue (green) and unmineralized osteoid (red) were both observed in RNB and GMSF. **(F)** See as described for (B). **(G)** Evaluation of osteocyte orientation in the RNB at the free-ending location (25). 47.8% of the osteocytes had a cranial-caudal orientation (angle 0°–30°), 26.8% a transversal orientation (angle 60°–90°) and 25.4% an orientation between these axes (angle 30°–60°). **(H)** Evaluation of osteocyte orientation in the GMSF at the free-ending location (25). 45.5% of the osteocytes had a cranial-caudal orientation (angle 0°–30°), 9.0% a transversal orientation (angle 60°–90°), and 45.5% an orientation between these axes (angle 30°–60°). **(I)** Free-ending location (26). Mineralized bone tissue (green) was only observed in RNB and unmineralized osteoid (red) in RNB and GMSF. **(J)** See as described for (B). **(K)** Evaluation of osteocyte orientation in the RNB at the free-ending location (26). 22.5% of the osteocytes had a cranial-caudal orientation (angle 0°–30°), 47.9% a transversal orientation (angle 60°–90°), and 29.6% an orientation between these axes (angle 30°–60°). **(L)** Evaluation of osteocyte orientation in the GMSF at the free-ending location (26). 52.9% of the osteocytes had a cranial-caudal orientation (angle 0°–30°), 23.6% a transversal orientation (angle 60°–90°), and 23.5% an orientation between these axes (angle 30°–60°). **(M)** Free-ending location (27). Mineralized bone tissue (green) and unmineralized osteoid (red) were both observed in RNB. Some part of the biopsy was broken and excluded from the histomorphometric analysis (dotted lines). **(N)** See as described for (B). **(O)** Evaluation of osteocyte orientation in the RNB at the free-ending location (26). 33.3% of the osteocytes had a cranial-caudal orientation (angle 0°–30°), 29.2% a transversal orientation (angle 60°–90°), and 37.5% an orientation between these axes (angle 30°–60°).

FE model

The FE model predicted that tensile strains were largest close to the natural tooth and decreased in magnitude with increasing distance from the tooth. This strain profile was caused by bending of the sinus floor between the mesial and distal teeth. To better understand the strain profile, it should be kept in mind that the respective figures show a 2D section from a 3D model (Figure 1). In the 3D model, the maxillary sinus floor was also supported by the buccal and lingual sides of the sinus cavity.

Tensile strain magnitude and direction were different in single gap and free-ending implant locations. In the single gap locations the tensile strain was large and uniformly directed in cranial-caudal direction (Figure 3B). In the free-ending locations the tensile strain magnitude decreased >2-fold by one tooth distance from the natural tooth (Figure 3D). The tensile strain was less uniformly oriented than in the single gap locations.

Histology

All intact biopsies, and a few broken but well evaluable biopsies were included in the study. Newly formed mineralised bone tissue, containing lacunae with live osteocytes, unmineralized osteoid areas, and connective tissue were observed around the β-TCP particles cranial to the native residual bone in the biopsies. Approximately 10% of the observed lacunae were empty in all regions. Bone ingrowth was determined, from the border between the RNB and the GMSF towards the cranial side. Newly formed bone was in close contact with the bone substitute granules (Figure 4A, E, I, M). Some biopsies showed no newly formed mineralised bone tissue, but only unmineralized osteoid areas and connective tissue in the most cranially located ROIs (Figure 4I).

Histomorphometrical evaluation of mineralized residual native bone tissue

No differences were observed for mean percentage of mineralized native residual bone tissue volume between single gap and free-ending implant locations (mean±SD (%); single gap: 33.4±14.1; free-ending: 32.8±20.4, 27.3±13.9, 37.4±19.7).

Osteocyte number and morphology in residual native bone

Single gap, multiple gap and free-ending implant locations showed similar numbers of osteocytes per ROI (mean±SD: 97±40; Table 1). In all locations, most osteocytes (~90%) were elongated, while only ~10% of the cells were round (Table 1). One free-ending location (24) had significantly more round cells than other locations (Table 1; Patient #7). In a single gap location (26) the osteocyte surface area was about 1.5 times larger than in multiple gap and free-ending locations (Table 1; Patient #1–6; $p<0.05$).

Osteocyte orientation

Osteocyte orientation in single gap locations of two patients were similar (Table 1: Patient #1 and #2). As a reference value the average osteocyte orientation of patient #1 and #2 was taken for the other multiple gap and free-ending locations. The osteocyte orientation of a single gap location patient #1 and a free-ending location patient #5 are shown in detail (Figure 4).

Osteocyte orientation was similar in single gap (26; patient #1) RNB (median: 27.4°) and GMSF (median: 27.4°; Figure 4B). In the RNB, 54.8% of the osteocytes had a cranial-caudal orientation (Figure 4), and in the GMSF 53.1% (Figure 4D).

Osteocyte orientation was similar in free-ending (25; patient #5) RNB (median: 32.9°) and GMSF (median: 30.3°; Figure 4F). 47.8% of the osteocytes in the RNB had a cranial-caudal orientation (Figure 4G), and 45.5% in the GMSF (Figure 4H). Moreover, osteocyte orientation was different in free-ending location (26) between RNB (median 58.0°) and GMSF (median: 25.8°) (Figure 4J; $p<0.05$). 22.5% of the osteocytes in the RNB had a cranial-caudal orientation (Figure 4K), and 52.9% in the GMSF (Figure 4L) Osteocyte orientation in free-ending location (27) was only measured in RNB (median 43.2), since GMSF was lacking (Figure 4N). 33.3% of the osteocytes had a cranial-caudal orientation (Figure 4O). Osteocyte orientation in RNB in free-ending location (26) was different from the single gap reference value (Table 1: Patient #5; $p<0.05$).

Moreover, the osteocyte orientation in in free-ending (25; patient #8) and (26; patient #8) RNB was significantly different from the reference value of patient #1 and #2.

DISCUSSION

The aim of this study was to investigate the relation between tensile strain and osteocyte morphology and orientation in human maxillary bone. FE analysis and histological and histomorphometrical data were used to predict possible differences in maxillary bone quality between single gap versus free-ending locations. The FE model predicted larger and differently oriented tensile strains in single gap compared to free-ending implant locations. Histomorphometrically, no differences were observed for mineralized RNB volume, and number and morphology of osteocytes between the single gap and free-ending locations. Osteocytes in single gap locations had a more cranial-caudal orientation and larger surface area than in free-ending locations. These results suggest possible differences in dental implant success related to osteocyte mechanosensitivity in single gap and free-ending implant positions in the maxilla.

Although FE modeling has been used extensively to predict biomechanical stress directions in dental implants and its surrounding bone in relation to implant success,[26] it has never been used in relation to osteocyte morphology and orientation. The presence of remaining teeth near the implant position keeps bone mechanically strained. The tensile strains were directed from the natural tooth to the biopsy location(s), resulting in a difference in tensile strain orientation between single gap and free-ending locations.

In the FE model individual teeth could be removed to simulate patient-specific cases. Whereas the biopsies showed a heterogeneous patchwork of cortical bone, trabecular bone, β-TCP granules, and connective tissue, the sinus floor was modeled as a homogeneous tissue of intermediate stiffness. This was for two reasons: (i) there were not sufficient 3D data present for each patient to model the actual heterogeneity of the whole sinus floor, and (ii) the focus was on the broad stress trajectories resulting from the remaining dentition, which was best investigated by leaving other factors equal.

Even though the time of extraction appears comparable (8–13 months) for most of the retrieved biopsies, there is a clinical difference in bone quality between single gap versus free-ending locations: class II in most of the gap locations and class III in the free-ending locations. This suggests a higher amount of cortical bone and a lower amount of cancellous bone in single gap than in free-ending locations. However, no differences were observed between mineralized bone tissue volumes between the different locations suggesting no changes in bone formation at the time of biopsy retrieval. Since osteocytes fulfil a role as mechanosensors of bone, it is plausible that bone formation will be affected differently in single gap than in free-ending implant positions in the long term, due to differences in tensile strain magnitude and orientation.

Nearly all osteocytes were elongated in both single gap and free-ending locations, implying a dominant loading direction in these bone regions. Osteocytes in gap locations showed significantly larger surface areas than those in free-ending locations, suggesting differences in osteocyte mechanosensitivity. Since the osteocyte cell body likely plays a role in direct mechanosensing of matrix stiffness, this might relate to differences in bone architecture.[16,27] Moreover, it has been shown in vitro that different mechanical stimuli cause different cellular

deformation.[28] This would suggest that differences in tensile strain result in changes in the osteocyte cytoskeleton and different morphology.[9] Since differences in osteocyte morphology were not observed, differences in tensile strain might have been too small to cause substantial cytoskeletal changes.

Osteocytes in single gap locations and in free-ending locations directly neighbouring a natural tooth on one side had a cranial-caudal orientation, resulting from large and uniformly directed tensile strain. Osteocytes in the various free-ending locations of one patient had different orientations from each other and the single gap location, resulting from a decrease in tensile strain magnitude from the natural tooth to the most distal free-ending location. These data are in line with previous observations showing elongated osteocytes aligned in the principal loading direction and osteocytes aligned to the collagen fiber orientation[12,13] which corresponds to the orientation of tensile strain in the bone.[14]

A limitation of our study is that we only had two-dimensional sections to analyse the orientation of three-dimensional osteocytes. However, this does not affect our conclusion regarding any possible differences in morphology between the different implant locations, since histomorphometry is based on the principle that statistical information of three-dimensional structures can be obtained from two-dimensional cross-sections, if a sufficient number of cross sections is measured. Information about surfaces can be obtained from cross-sections of these surfaces, *i.e.* lines. Another limitation of this study might be the small number of patients.

In conclusion, these data show significant differences in surface area and orientation of osteocytes, in particular in areas of maxillary bone that are related to the tensile strain magnitude and orientation. The exact implication of osteocyte orientation on dental implant success, however, is complex and deserves further study. This exploratory study gives, for the first time, a view on the relation of tensile strain with osteocyte morphology and orientation in the maxillary bone, which might contribute to a better understanding of the cellular processes that lead to different bone quality in various dental implant positions and eventually to the success of dental implants in the maxilla.

ACKNOWLEDGEMENTS

The work of René F.M. van Oers was supported by a grant from the University of Amsterdam for the stimulation of a research priority area Oral Regenerative Medicine. Rommel G. Bacabac received logistic support from the Research Office of the University of San Carlos, Cebu City. We thank Marion A. van Duin, Jan Harm Koolstra, and Noortje de Boer for technical support and advice.

REFERENCES

1. Lindh C, Obrant K, Petersson A. Maxillary bone mineral density and its relationship to the bone mineral density of the lumbar spine and hip. *Oral Surg Oral Med Oral Pathol Oral Radiol.* 2004;98(1):102–109. doi:10.1016/s1079-2104(03)00460-8
2. Drage NA, Palmer RM, Blake G, Wilson R, Crane F, Fogelman I. A comparison of bone mineral density in the spine, hip and jaws of edentulous subjects. *Clin Oral Implants Res.* 2007;18(4):496–500. doi:10.1111/j.1600-0501.2007.01379.x
3. Ozan O, Turkyilmaz I, Yilmaz B. A preliminary report of patients treated with early loaded implants using computerized tomography-guided surgical stents: flapless versus conventional flapped surgery. *J Oral Rehabil.* 2007;34(11):835–840. doi:10.1111/j.1365-2842.2007.01772.x
4. Schenk RK, Buser D. Osseointegration: A reality. *Periodontol* 2000. 1998;17(1):22–35. doi:10.1111/j.1600-0757.1998.tb00120.x
5. Lioubavina-Hack N, Lang NP, Karring T. Significance of primary stability for osseointegration of dental implants. *Clin Oral Implants Res.* 2006;17(3):244–250. doi:10.1111/j.1600-0501.2005.01201.x.
6. Fuh LJ, Huang HL, Chen CS, Fu KL, Shen YW, Tu MG, Shen WC, Hsu JT. Variations in bone density at dental implant sites in different regions of the jawbone. *J Oral Rehabil.* 2010;37(5):346–351. doi:10.1111/j.1365-2842.2010.02061.x
7. Becker W, Becker BE, Alsuwyed A, Al-Mubarak S. Long-term evaluation of 282 implants in maxillary and mandibular molar positions: A prospective study. *J Periodontol.* 1999;70(8):896901. doi:10.1902/jop.1999.70.8.896
8. Hohlweg-Majert B, Metzger MC, Kummer T, Schulze D. Morphometric analysis - Cone beam computed tomography to predict bone quality and quantity. *J Craniomaxillofac Surg.* 2011;39(5):330–334. doi:10.1016/j.jcms.2010.10.002
9. Klein-Nulend J, Bacabac RG, Bakker AD. Mechanical loading and how it affects bone cells: The role of the osteocyte cytoskeleton in maintaining our skeleton. *Eur Cell Mater.* 2012;24:278–291. doi:10.22203/ecm.v024a20
10. Klein-Nulend J, Bakker AD, Bacabac RG, Vatsa A, Weinbaum S. Mechanosensation and transduction in osteocytes. *Bone.* 2013;54(2):182–190. doi: 10.1016/j.bone.2012.10.013
11. Vatsa A, Breuls RG, Semeins CM, Salmon PL, Smit TH, Klein-Nulend J. Osteocyte morphology in fibula and calvaria – Is there a role for mechanosensing? *Bone.* 2008;43(3):452–458. doi:10.1016/j.bone.2008.01.030
12. Marotti G. Osteocyte orientation in human lamellar bone and its relevance to the morphometry of periosteocytic lacunae. *Metab Bone Dis Relat Res.* 1979;1(4):325–333.
13. Kerschnitzki M, Wagermaier W, Roschger P, Seto J, Shahar R, Duda GN, Mundlos S, Fratzl P. The organization of the osteocyte network mirrors the extracellular matrix orientation in bone. *J Struct Biol.* 2011;173(2):303–311. doi:10.1016/j.jsb.2010.11.014
14. Van Oers RF, Wang H, Bacabac RG. Osteocyte shape and mechanical loading. *Curr Osteoporos Rep.* 2015;13(2):61–66. doi:10.1007/s11914-015-0256-1
15. Wang N, Butler JP, Ingber DE. Mechanotransduction across the cell surface and through the cytoskeleton. *Science.* 1993;260(5111):1124–1127. doi:10.1126/science.7684161
16. Bacabac RG, Mizuno D, Schmidt CF, MacKintosh FC, Van Loon JJWA, Klein-Nulend J, Smit TH. Round versus flat: Bone cell morphology, elasticity, and mechanosensing. *J Biomech.* 2008;41(7):1590–1598. doi:10.1016/j.jbiomech.2008.01.031

17. Thomsen JS, Ebbesen EN, Mosekilde LI. Relationships between static histomorphometry and bone strength measurements in human iliac crest bone biopsies. *Bone.* 1998; 22(2):153–163. doi:10.1016/s8756-3282(97)00235-4

18. Lekholm U, Zarb GA. Patient selection and preparation. In: Brånemark PI, Zarb GA, Albrektsson T, eds. *Tissue integrated prostheses.* Chicago: Quintessance, 1985:199–209.

19. Schulten EA, Prins HJ, Overman JR, Helder MN, Ten Bruggenkate CM, Klein-Nulend J. A novel approach revealing the effect of a collagenous membrane on osteoconduction in maxillary sinus floor elevation with β-tricalcium phosphate. *Eur Cell Mater.* 2013;25(25):215–228. doi: 10.22203/ecm.v025a16

20. Frenken JW, Bouwman WF, Bravenboer N, Zijderveld SA, Schulten EAJM, Ten Bruggenkate CM. The use of Straumann Bone Ceramic in a maxillary sinus floor elevation procedure: A clinical, radiological, histological and histomorphometric evaluation with a 6-month healing period. *Clin Oral Implants Res.* 2010;21(2):201–208. doi:10.1111/j.1600-0501.2009.01821.x

21. Marieb E, Hoehn K. *Human anatomy.* 7th ed. New York City: Pearson, 2014.

22. Van Eijden TM. Three-dimensional analyses of human bite-force magnitude and moment. *Arch Oral Biol.* 1991;36(7):535–539.doi:10.1016/0003-9969(91)90148-n

23. Zerbo IR, Zijderveld SA, de Boer A. Histomorphometry of human sinus floor augmentation using a porous beta-tricalcium phosphate: a prospective study. *Clin Oral Implants Res.* 2004;15(6):724–732.

24. Plenk H Jr. The microscopic evaluation of hard tissue implants. In: Williams DF, eds. *Techniques of biocompatibility testing.* Boca Raton: CRC Press Inc, 1986:35–81.

25. Parfitt AM, Drezner MK, Glorieux FH Glorieux FH, Kanis JA, Malluche H, Meunier PJ, Ott SM, Recker RR, Parfitt AM. Bone histomorphometry: Standarization of nomenclature, symbols, and units. Report of the ASBMR histomorphometry nomenclature committee. *J Bone Miner Res.* 1987;2(6):5950610. doi:10.1002/jbmr.5650020617

26. Geng JP, Tan KB, Liu GR. Application of finite element analysis in implant dentistry: A review of the literature. *J Prosthet Dent.* 2001;85(6):585–598. doi:10.1067/mpr.2001.115251

27. Van Hove RP, Nolte PA, Vatsa A, Semeins CM, Salmon PL, Smit TH, Klein-Nulend J. Osteocyte morphology in human tibiae of different bone pathologies with different bone mineral density--Is there a role for mechanosensing? *Bone.* 2009;45:321–329. doi:10.1016/j.bone.2009.04.238

28. McGarry JG, Klein-Nulend J, Mullender MG, Prendergast PJ. A comparison of strain and fluid shear stress in stimulating bone cell responses – A computational and experimental study. *FASEB J.* 2005;19(3):482–484. doi:10.1096/fj.04-2210fje

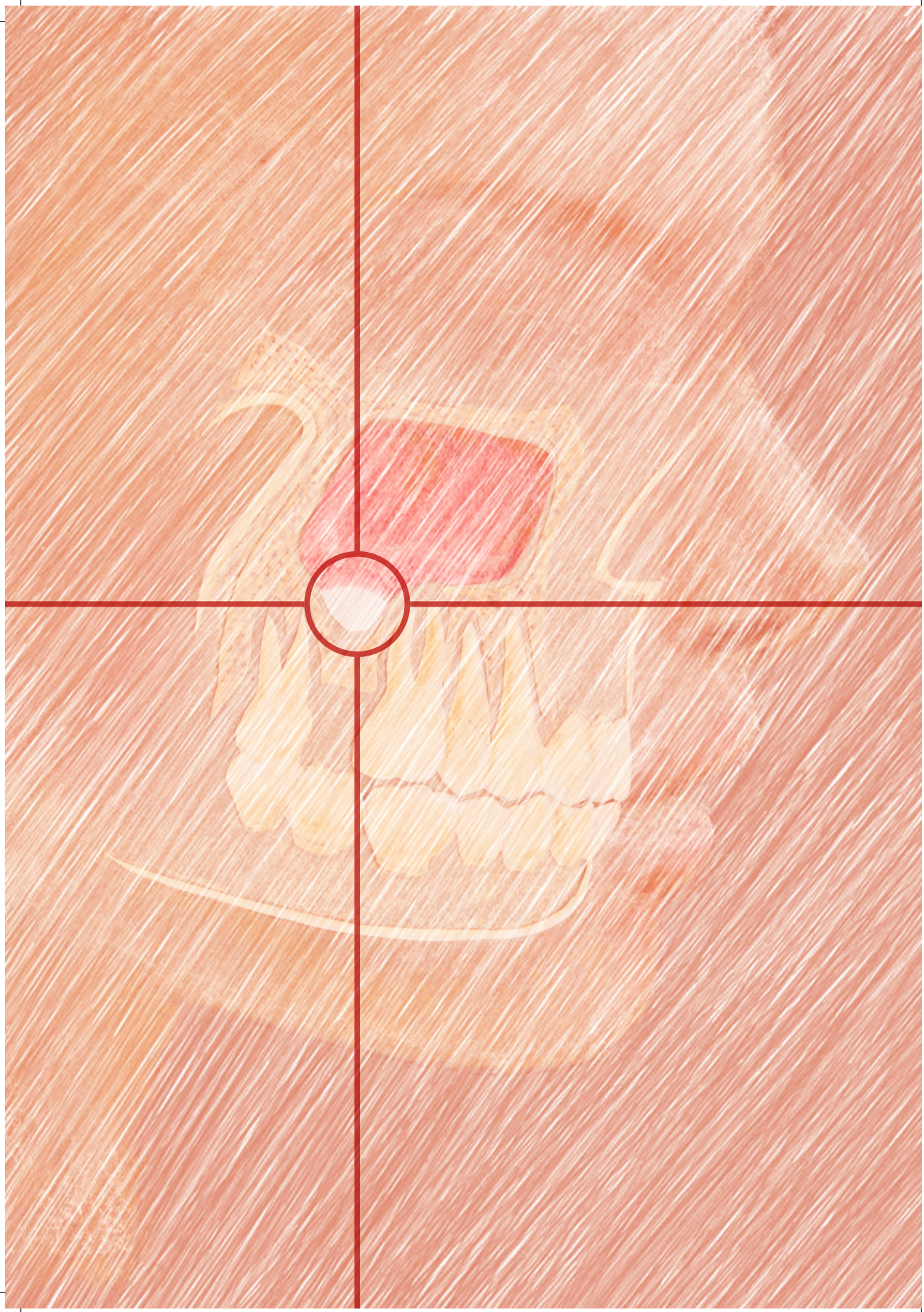

CHAPTER 5

Vascularization and bone regeneration potential of calcium phosphate bone substitutes either or not adipose stem cell-supplemented versus autologous bone grafts in maxillary sinus floor elevation: A retrospective cohort study

Vivian Wu [1,2]
Marco N. Helder [2]
Engelbert A.J.M. Schulten [2]
Christiaan M. ten Bruggenkate [2]
Jenneke Klein-Nulend [1]
Nathalie Bravenboer [3]

[1] *Department of Oral Cell Biology, Academic Centre for Dentistry Amsterdam (ACTA), University of Amsterdam and Vrije Universiteit Amsterdam, Amsterdam Movement Sciences, Amsterdam, The Netherlands*

[2] *Department of Oral and Maxillofacial Surgery/Oral Pathology, Amsterdam University Medical Centers and Academic Centre for Dentistry Amsterdam (ACTA), Vrije Universiteit Amsterdam, Amsterdam Movement Sciences, Amsterdam, The Netherlands*

[3] *Department of Clinical Chemistry, Amsterdam University Medical Centers, Vrije Universiteit Amsterdam, Amsterdam Movement Sciences, Amsterdam, The Netherlands*

Manuscript in preparation for submission

ABSTRACT

Bone substitutes are used as alternatives for autologous bone grafts in maxillary sinus floor elevation (MSFE) for dental implant placement. The freshly isolated autologous stromal vascular fraction (SVF), highly enriched with adipose stem cells, adds osteogenic and angiogenic properties to bone substitutes. This retrospective cohort study aimed to investigate vascularization and bone regeneration potential of calcium phosphate (CaP) bone substitutes either or not SVF-supplemented versus autologous bone grafts in MSFE.

Patients undergoing MSFE were treated with retromolar bone (n=8), tuberosity bone (n=6), ß-tricalcium phosphate (ß-TCP; n=3), biphasic calcium phosphate (BCP; n=13), ß-TCP plus SVF (n=5) or BCP plus SVF (n=5). Biopsies were taken 4–6 months postoperatively, and bone formation and blood vessel number assessed.

Blood vessel number, bone and osteoid volume were lower in CaP than autologous bone biopsies in the cranial area. Blood vessel number and osteoid volume were similar in SVF-supplemented CaP and retromolar, but lower than in tuberosity bone biopsies. Bone volume was similar in SVF-supplemented CaP as in tuberosity, but lower than in retromolar bone biopsies.

In conclusion, SVF-supplemented CaP bone substitutes seemed to have similar vascularization potential as retromolar, but not tuberosity bone grafts in MSFE. Therefore, SVF-supplemented CaP substitutes might be promising to enhance bone regeneration. Future studies with more patients and higher SVF-dosages might further improve efficacy of SVF-supplementation in MSFE.

INTRODUCTION

Maxillary sinus floor elevation (MSFE) is carried out to restore insufficient alveolar bone height in the lateral maxilla to allow dental implant placement. In MSFE the space created between the maxillary alveolar process, the elevated Schneiderian membrane, and the inwardly rotated lateral sinus wall, is filled with graft material, *i.e.* autologous bone and/or bone substitutes, allowing bone regeneration.[1,2] A major challenge in bone regeneration is the vascularization of the implanted graft.[3,4] Bone is highly vascularized, and vascular development needs to be induced prior to osteogenesis.[5] Since the amount of oxygen is limited to a diffusion distance of only ~150-200 µm from a supply blood vessel, hypoxia affects cells lying beyond this physiological border.[6] Under this condition, osteogenic cells fail to survive, since they are not able to adapt their glucose consumption and lack the necessary glycolytic reserves to sustain their metabolism for more than three days.[7] Tissue regeneration over 200 µm exceeds the capacity diffusion for nutrient supply and waste removal from the tissue, requiring an intimate supply of vascular networks.[6] Successful bone regeneration requires rapid perfusion and integration of the implanted graft with the recipient vasculature. Neovascularization is achieved by both vasculogenesis, *i.e.* the incorporation of circulating endothelial progenitor cells (EPCs) into the microvascular endothelium of newly developing microvessels, and angiogenesis, *i.e.* new blood vessel sprouting from preexisting vessels. Improved understanding and new approaches to enhance vascularization are needed, since optimal vascularization is a prerequisite for jaw bone regeneration, leading to successful placement of dental implants.

Bone formation has been related to angiogenesis in MSFE with different grafting materials.[8–11] Autologous bone is still considered the 'gold standard' grafting material in MSFE, due to the essential combination of osteogenic, osteoinductive, and osteoconductive properties as well as prevention of immunogenic responses.[12] The mandibular retromolar and maxillary tuberosity regions are favorable intra-oral donor sites due to low morbidity compared to other intraoral sites. Current research has shown that tuberosity bone grafts enhance bone vitality and vascularization in MSFE compared to retromolar bone grafts[10]. Tuberosity bone grafts result in more osteoid deposition, vascularization, and active bone remodeling, indicating that tuberosity bone might perform better as autologous graft in MSFE than retromolar bone. However, morbidity caused by the harvesting procedure and limited availability of autologous bone, encourages the search for suitable alternatives with similar bioactivity.

Calcium phosphate (CaP) bone substitutes, e.g. hydroxyapatite (HA), β-tricalcium phosphate (β-TCP), and a combination of HA/β-TCP, are frequently used because they do not evoke adverse cellular reactions and, in time, the material is either replaced by bone or integrated into the body, depending on the degradation properties. However, CaP bone substitutes show low bone in-growth rates compared to autologous bone grafts since they only have osteoconductive properties and lack osteoinductive potential.[13,14] Cell-based bone tissue engineering is a promising strategy to enhance vascular ingrowth directed from the host tissue towards the bone substitute and/or vice versa.[4] Moreover, to improve bone formation, osteogenic cells that secrete osteoinductive signals to recruit cells from surrounding bone are provided.[15,16] This might shorten the time needed to obtain sufficient vascularization and bone regeneration than is required when using bone substitute only.

During the past decades, multiple sources of stem cells have been investigated for cell-based bone tissue engineering in the oral and maxillofacial region.[4] The stromal vascular fraction (SVF) of human adipose tissue is considered a promising single source for a heterogeneous population of essential cells, with osteogenic and angiogenic potential.[4,9,17] Moreover, SVF is a cell source with clinical feasibility due to the large quantities that can be harvested and applied in a one-step surgical procedure.[17,18] In a previous phase-I clinical trial, 10 patients underwent MSFE prior to dental implant placement using freshly isolated autologous, heterologous SVF seeded on either ß-TCP (n=5) or biphasic calcium phosphate (BCP; n=5) carriers in a one-step surgical procedure.[17] Induction of bone mass and bone formation by SVF-supplementation to CaP bone substitutes, in particular in ß-TCP-treated patients, has been shown in biopsies.[17] However, histologic and histomorphometric evidence of adipose stem cell(ASC)-application for bone regeneration in the oral and maxillofacial region is limited, although the potential of ASCs evokes high expectations.[9,17]

The majority of studies in MSFE have focused on new bone formation around different graft materials. A few studies compared vascularization in different graft materials in MSFE.[8,9,19,20] Enhanced microvessel density, *i.e.* number of microvessels per square millimeter, has been observed in autologous bone graft (iliac crest) compared to bone substitute (bovine-derived) 3-months post-MSFE.[20] Similar microvessel density has been observed in autologous bone graft (chin) and bone substitute (HA, CaP, equine-derived) mixed with autologous bone graft (chin) 8–10months post-MSFE.[8,19] Higher blood vessel number in SVF-supplemented ß-TCP and BCP-treated patients than in ß-TCP and BCP-treated patients 6-months post-MSFE has been observed.[9] Moreover, bone mass seemed to correlate with blood vessel formation, and were higher in the cranial part of the SVF-supplemented biopsies, in particular in β-TCP-treated patients.[9] A pro-angiogenic effect of SVF has been indicated.[9,17] To the best of our knowledge, comparison of vascularization and bone regeneration potential of CaP bone substitutes either or not SVF-supplemented with autologous bone grafting ('gold standard') in MSFE has not been performed so far.

This study aimed to investigate vascularization and bone regeneration potential of calcium phosphate (CaP) bone substitutes either or not SVF-supplemented versus autologous bone grafts in MSFE. We evaluated ß-TCP and BCP bone substitute with and without SVF-supplementation, and retromolar and tuberosity bone biopsies 4–6 months post-MSFE prior to dental implant placement. It was hypothesized that CaP bone substitutes show lower, and SVF-supplemented CaP bone substitute biopsies similar vascularization and bone regeneration potential, as autologous bone grafts in MSFE. In this study, we report the first comparison of SVF-supplemented CaP bone substitutes and autologous bone grafts for vascularization and bone regeneration potential in patients undergoing MSFE.

MATERIALS AND METHODS

Study design

This study included 40 patients, who were also enrolled in earlier studies.[10,17,21] All patients were partially edentulous in the posterior maxilla and required dental implants for prosthetic rehabilitation between 2003 and 2012. All patients required an MSFE due to insufficient vertical bone height (≤3 mm) in at least one of the planned dental implant positions. In all patients MSFE was carried out according to the "top hinge trap door" procedure[2], prior to dental implant placement.

Eight patients undergoing MSFE received mandibular retromolar bone graft, and six patients received a maxillary tuberosity bone graft (Table 1).[10] The detailed surgical procedures have been previously described.[10] In short, the retromolar bone grafts were harvested in half-cylinder shape with explantation trephines (inner diameter 4.2 mm; Institute Straumann AG, Basel, Switzerland) from the external oblique ridge of the mandible. The harvested half-cylinder bone cores were used to fill the maxillary sinus cavity. The maxillary tuberosity bone grafts were harvested with hammer and osteotome. The harvested bone pieces were cut with a bone rongeur into smaller pieces to fill the maxillary sinus cavity. Bone biopsies were taken 4-months post-MSFE during dental implant surgery with a hollow Straumann® trephine drill (inner diameter 2.5 mm; Institute Straumann AG, Basel, Switzerland).

Ten patients undergoing MSFE received a porous BCP scaffold consisting of 60% HA and 40% β-TCP (Straumann® Bone Ceramic; Institute Straumann AG, Basel, Switzerland; Table 1).[21] The detailed surgical procedures have been previously described.[21] Bone biopsies were taken 6-months post-MSFE during dental implant surgery with a hollow Straumann® trephine drill (inner diameter 2.5 mm; Institute Straumann AG, Basel, Switzerland).

Ten patients undergoing MSFE received freshly isolated autologous, heterologous SVF seeded on either porous ß-TCP (Ceros®, Thommen Medical, Grenchen, Switzerland; n=5) or BCP (Straumann® Bone Ceramic, Institut Straumann AG, Basel, Switzerland; n=5) carriers in a one-step surgical procedure (Table 1).[17] Patients received either ß-TCP (n=5) or BCP (n=5) with SVF-supplementation on one side (study side), whereas bilaterally-treated patients (6 of 10) received calcium phosphate without SVF-supplementation on the opposite side (control side). Detailed description of the surgical procedure has been described[17]. In short, surgery started by collecting >125 mL of adipose tissue by lipoaspiration. This tissue was processed with a CE marked Celution device (Cytori Therapeutics, Inc., San Diego, CA, USA) to obtain SVF. For implantation cells were seeded at 10^7 nucleated SVF-cells (~2×10^5 ASC-like cells)/g ß-TCP or BCP carrier. Bone biopsies were taken 6-months post-MSFE during dental implant surgery with a hollow Straumann® trephine drill (inner diameter 2.5 mm; Institute Straumann AG, Basel, Switzerland).

The average age of the patients treated with retromolar bone graft was 56±7 years (mean±SD), tuberosity bone graft 56±12 years, ß-TCP bone substitutes 58±12 years, BCP bone substitutes 54±12 years, SVF-supplemented ß-TCP bone substitutes 59±9 years, and SVF-supplemented BCP bone substitutes 53±3 years. Patient demographics are summarized in Table 1.

Table 1. Patient demographics (as published earlier)[10,17,21]

Autologous bone									
Retromolar					Tuberosity				
Pt#	Gender (♂,♀),	age (years)	Unilateral/ bilateral case	Dental implant positions	Pt#	Gender (♂,♀),	age (years)	Unilateral/ bilateral case	Dental implant positions
1	♀	44	Unilateral	**16**	9	♂	67	Unilateral	**25**
2	♂	49	Unilateral	25, 26, **27**	10	♀	50	Unilateral	**24, 25**
3	♂	54	Unilateral	**24**, 26	11	♀	35	Unilateral	**17**
4	♂	55	Unilateral	**16**	12	♂	65	Unilateral	**25**
5	♂	62	Unilateral	**25**, 26	13	♀	58	Unilateral	**26**
6	♂	67	Unilateral	**14**, 15, **16**	14	♂	61	Unilateral	**15, 16**
7	♂	60	Unilateral	**16**					
8	♂	53	Unilateral	**26**					
CaP bone substitutes									
ß-TCP					BCP				
Pt#	Gender (♂,♀),	age (years)	Unilateral/ bilateral case	Dental implant positions	Pt#	Gender (♂,♀),	age (years)	Unilateral/ bilateral case	Dental implant positions
15	♀	58	Bilateral	14, 15, **16**	18	♀	24	Unilateral	**16**
16	♀	46	Bilateral	24, 25, **26**	19	♀	68	Unilateral	**25**
17	♂	69	Bilateral	14, 15, **16**	20	♀	58	Unilateral	**26**
					21	♀	67	Unilateral	**16**
					22	♂	57	Unilateral	**16**
					23	♂	59	Unilateral	**26**
					24	♂	45	Unilateral	**26**
					25	♂	55	Unilateral	**15**
					26	♂	39	Unilateral	**16**
					27	♂	66	Unilateral	**15**
					28	♀	57	Bilateral	24, **26**
					29	♂	56	Bilateral	25, **26**, 27
					30	♀	51	Bilateral	25, **26**
CaP bone substitutes with stem cells									
ß-TCP+SVF					BCP+SVF				
Pt#	Gender (♂,♀),	age (years)	Unilateral/ bilateral case	Dental implant positions	Pt#	Gender (♂,♀),	age (years)	Unilateral/ bilateral case	Dental implant positions
31	♀	58	Bilateral	24, 25, **26**	36	♀	57	Bilateral	14, 15, **16**
32	♀	46	Bilateral	14, **15**, 16	37	♂	56	Bilateral	15, 16, **17**
33	♂	69	Bilateral	25, 26, **27**	38	♀	51	Bilateral	15, **16**
34	♀	59	Unilateral	24, 25, **26**	39	♀	52	Unilateral	14, **15**, 16
35	♂	64	Unilateral	15, **16**	40	♂	51	Unilateral	23, 25, **26**

▶ Gender and age (years), whether the patients were treated unilaterally or bilaterally ("split-mouth design"), type of graft material used to augment bone of the maxillary sinus floor, *i.e.* autologous bone or CaP bone substitutes with and without SVF-supplementation, and the dental implant positions (Fédération Dentaire Internationale system) are given. Selected biopsies are displayed in bold. Pt #, patient number; CaP, calcium phosphate; β-TCP, β-tricalcium phosphate; BCP, biphasic calcium phosphate consisting of 60% hydroxyapatite and 40% β-tricalcium phosphate; SVF, stromal vascular fraction.

The present study was conducted according to the guidelines of the Declaration of Helsinki, and approved by the medical ethical committee (IRB) of the VU University Medical Center in Amsterdam (Dossier number: 2020.344: ABR NL71857.029.20; #2016.105). All patients signed a written informed consent before participation in the study.

Biopsy processing and evaluation

All biopsies were fixed in 4% phosphate-buffered formaldehyde solution (Klinipath BV, Duiven, the Netherlands) at 4°C for at least 24 h, removed from the drill. The bone biopsies were carefully removed from the trephine burr by cutting the burr, and opening it. Thereafter the bone biopsies were transferred to 70% ethanol, and stored until use for histomorphometrical analysis, as described below under "Histology and histomorphometry". The caudal side of the bone biopsy had a sharp cutting edge in contrast to a dome-shaped, crumbled cranial side. These histologic features were used to identify the apical-coronal orientation of the autologous bone biopsies. The whole research team verified whether the apical-coronal orientation of the biopsy corresponded to the histological appearance. Consensus was reached for all biopsy specimens.

Histology and histomorphometry

After dehydration in descending alcohol series, the bone specimens were embedded without prior decalcification in low temperature polymerizing methylmethacrylate (MMA, Merck Schuchardt OHG, Hohenbrunn, Germany). Longitudinal sections of 5 µm thickness were prepared using a Jung K microtome (R. Jung, Heidelberg, Germany). Midsagittal histological sections of each biopsy were stained with Goldner's Trichome method[22] in order to distinguish mineralized bone tissue (green) and unmineralized osteoid (red). The histological sections were divided into regions of interest (ROI) of 1 mm^2 for blinded histomorphometrical analysis, as previously described.[21] Depending on the length of the biopsy, the number of ROIs ranged from 5–15. For patients treated with autologous bone grafts, vertical tissue height measurements of the residual native bone and graft at the planned dental implant position on the panoramic radiograph were made pre-MSFE, as well as prior to dental implant placement. The vertical tissue height of the residual native bone on the radiographs resembled the height of the residual native bone in the biopsy. The vertical tissue height of the graft on the radiographs resembled the height of the graft in the biopsy. The whole research team verified whether the radiographically determined transition zone corresponded with the histological appearance, including parameters such as the occurrence of apoptotic osteocytes and empty osteocyte lacunae to identify grafted material. The consensus was reached for all specimens.

The transition zone (TZ) indicates the first ROI where graft material was observed when analyzing from the caudal to the cranial side of the biopsy. Since the biopsies analyzed had different lengths, we decided to define them in three regions after the transition zone (TZ).

The first two ROIs on the right of the transition zone were defined as Region I (RI), the two or three ROIs in the center (even or odd numbers) as Region II (RII), and the two most cranial ROIs as Region III (RIII). The digital images of the scanned biopsies were analyzed, starting from the caudal side of the biopsy, and continuing towards the cranial side. This previously described method allowed us to compare similar regions for all biopsies with respect to the bone regeneration and vascularization in the augmented maxillary sinus.[9,10,13,21]

For each separate area of interest, the histomorphometrical measurements were performed using an electronic stage table and a Leica DC 200 digital camera (Leica, Wetzlar, Germany). The computer software used was Leica QWin© (Leica Microsystems Image Solutions, Rijswijk, The Netherlands) or NIS-Elements AR 4.10.01 (Nikon GmbH, Düsseldorf, Germany) at 40x magnification according to the ASBMR nomenclature to analyze digital images.[23] Bone volume (bone area over total tissue area; B.Ar/T.Ar%) and osteoid volume (osteoid area over bone area; O.Ar/B.Ar%) were calculated according to the international standardization.[23]

Blood vessel numbers were determined as mean value of two separate blinded counts. Blood vessel size was calculated as the total blood vessel area expressed in μm^2. According to their area, blood vessels were divided into small (0–400 μm^2) or large vessels (>400 μm^2).[9]

Immunohistochemistry

Immunohistochemical staining for CD34, a marker for endothelial cells, as well as stem cells, such as endothelial progenitor stem cells and hematopoietic stem cells, was performed to quantify microvessel density according to previously described procedures.[24,25] Immunohistochemical staining for smooth muscle actin (SMA), marker for smooth muscle cells as well as pericytes was performed to detect vascular maturity.[25,26] A previously described protocol for immunostaining was used on retromolar bone (n=4), β-TCP bone substitute (n=3), BCP bone substitute (n=3), SVF-supplemented β-TCP bone substitute (n=4), and SVF-supplemented BCP bone substitute biopsies (n=4).[9] The following primary antibodies were used for CD34, CD34 Monoclonal Mouse Anti-Human CD34 Class II Clone QBEnd-10 1:20, Dako, Carpinteria, MI, USA, and for SMA, SMA Monoclonal Mouse Anti-Human Smooth Muscle Actin Clone 1A4 1:50, Dako, Carpinteria, MI, USA.

Statistical analysis

Data are presented as mean ± standard deviation (SD). Statistical analysis was performed using GraphPad Prism 9 software (GraphPad Software, La Jolla, CA, USA). One-way analysis of variance (ANOVA) was performed to test possible age, and biopsy harvesting time points differences and between patients treated with retromolar bone, tuberosity bone, ß-TCP, BCP, SVF-supplemented ß-TCP, and SVF-supplemented BCP. No statistical differences in age, and biopsy harvesting time points were observed. An unpaired nonparametric Mann–Whitney U-test was performed to investigate differences between autologous bone biopsies and CaP bone substitutes with or without SVF-supplementation biopsies per region of interest. Statistical significance was considered, if p-values were <0.05.

RESULTS

Quantitative histomorphometric evaluation

Number of blood vessels, bone volume, and osteoid volume

Number of blood vessels (N.Bloodves) was lower at the cranial side of ß-TCP biopsies (RIII) compared to retromolar bone biopsies (p<0.05), but was similar at the other regions throughout the grafted area in CaP bone substitutes and retromolar bone biopsies (Figure 1A, C, D, G). Number of blood vessels was lower at the center of the grafted area (RII) in CaP bone biopsies compared to tuberosity bone biopsies (p<0.05), but was similar at the other regions throughout the grafted area (RI, RIII) in CaP bone substitutes and tuberosity bone biopsies (Figure 1B, C, D, H). Number of blood vessels decreased towards the cranial side in CaP bone substitutes as well as retromolar and tuberosity bone biopsies. Number of blood vessels was similar in the grafted area (RI–RIII) in SVF-supplemented CaP bone substitutes compared to retromolar bone biopsies (Figure 1A, E, F, I). Number of blood vessels increased towards the cranial side of the grafted area in SVF-supplemented CaP bone substitutes biopsies, in contrast to retromolar and tuberosity bone biopsies where a decrease was observed. Number of blood vessels was lower at the center of the grafted area (RII) in SVF-supplemented CaP bone substitutes biopsies compared to tuberosity bone biopsies (p<0.05; Figure B, E, F, J), but was similar at the other regions throughout the grafted area (RI, RIII).

Bone volume (B.Ar/T.Ar%) was lower at the center and cranial side of the grafted area (RII, RIII) in CaP bone substitutes biopsies compared to retromolar and tuberosity bone biopsies (p<0.05; Figure 1A, B, K, L). Bone volume decreased towards the cranial side of the grafted area in CaP bone substitutes biopsies, whereas in retromolar and tuberosity bone biopsies bone volume increased towards the cranial side of the grafted area (Figure 1A–D). No bone was observed in the most cranial area (region III) in ß-TCP biopsies (Figure 1C). In contrast to CaP bone substitutes biopsies, SVF-supplemented CaP bone substitutes biopsies showed increased bone volume towards the cranial side of the biopsy (Figure 1E, F, M, N). Bone volume was lower at the center and cranial side of the grafted area (RII, RIII) in SVF-supplemented CaP bone substitutes biopsies compared to retromolar bone (p<0.05; Figure 1M). Bone volume was also lower at the center of the grafted area (RII; p<0.05), but was similar at the cranial side of the grafted area (RIII) compared to tuberosity bone (Figure 1N).

Osteoid volume (O.Ar/T.Ar%) was lower at the cranial side of the grafted area (RIII) in CaP bone substitutes biopsies compared to retromolar and tuberosity bone biopsies (p<0.05; Figure 1O, P). Osteoid volume decreased towards the cranial side of the grafted area (RIII) in CaP bone substitutes as well as retromolar bone biopsies. No osteoid formation was observed in the most cranial area in ß-TCP biopsies (RIII). Osteoid volume in the grafted area of SVF-supplemented CaP bone substitutes biopsies increased towards the cranial side, and was similar as in retromolar bone biopsies (RI–RIII; Figure 1Q). However, osteoid volume at the center and cranial side of the grafted area (RII, RIII) in SVF-supplemented CaP bone substitutes biopsies was still lower than in tuberosity bone biopsies (p<0.05; Figure 1R).

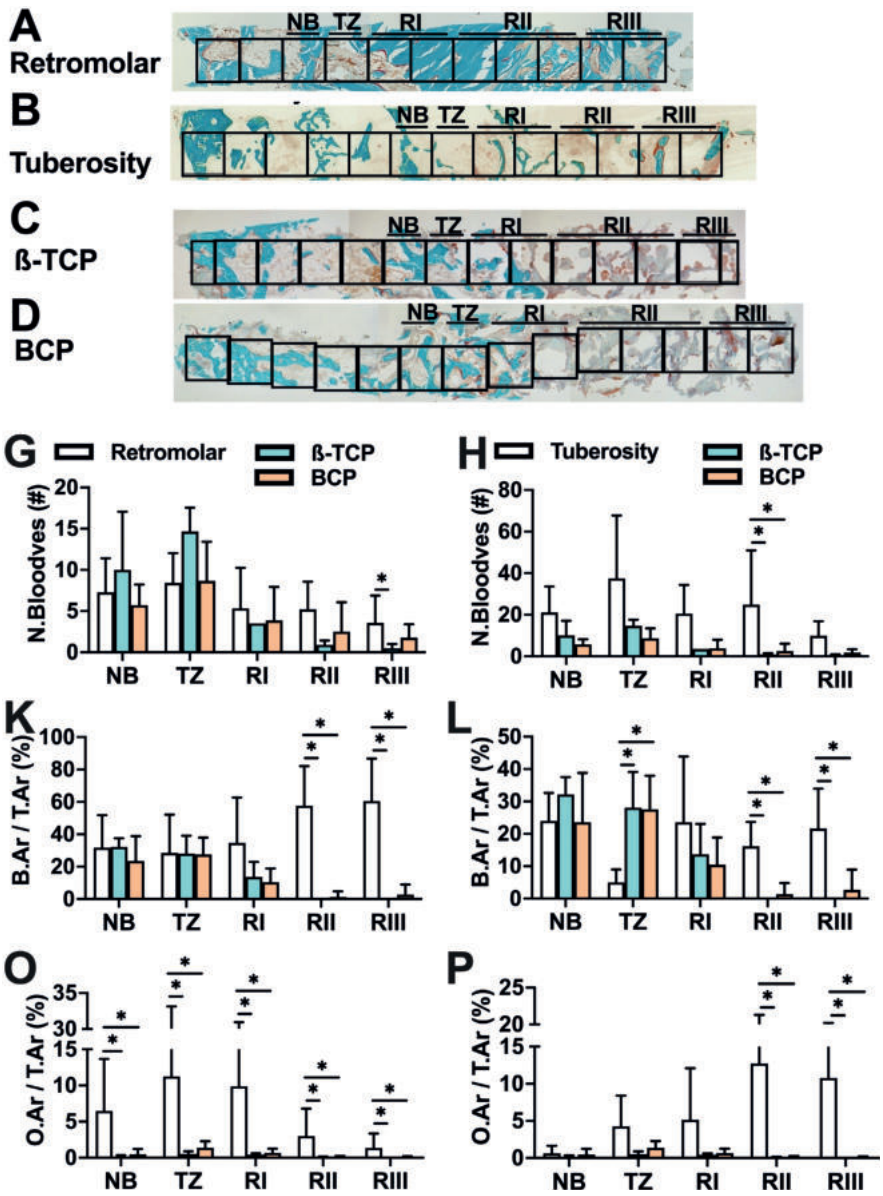

Figure 1. Histomorphometrical analysis of bone biopsies from patients after maxillary sinus floor elevation: number of blood vessels, bone volume (B.Ar/T.Ar %), osteoid volume (O.Ar/T.Ar %). Patients undergoing maxillary sinus floor elevation (MSFE) were grafted with autologous bone (retromolar or tuberosity bone), CaP bone substitutes (β-TCP or BCP), or CaP bone substitutes with stem cells (β-TCP+SVF or BCP+SVF). Representative biopsy from one patient after MSFE with retromolar bone **(A)**, tuberosity bone **(B)**, β-TCP **(C)**, BCP **(D)**, β-TCP+SVF **(E)**, and BCP+SVF **(F)**. Midsagittal histological sections of each biopsy were stained with Goldner's trichome method, to distinct mineralized bone tissue (green) and unmineralized osteoid (red). Biopsies were divided in consecutive 1 mm^2 regions of interest (ROIs). The transition zone (TZ) indicated the first ROI where graft material was observed. The images illustrated less bone and less osteoid volume in BCP and β-TCP biopsies compared to retromolar and tuberosity bone

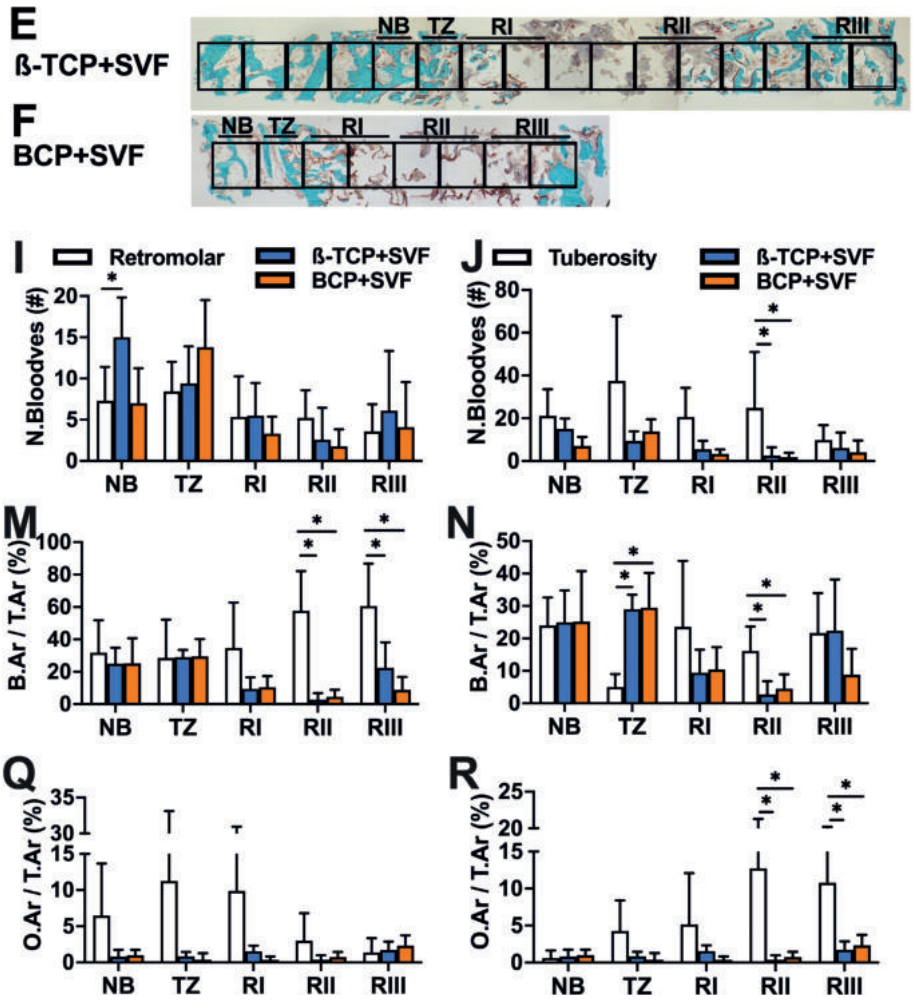

biopsies at the center and the cranial side of the grafted area (RII, RIII). Moreover, the images illustrated less bone and similar osteoid volume in BCP+SVF and β-TCP+SVF biopsies compared to retromolar bone biopsies at the center and cranial side of the grafted area (RII, RIII). The images illustrated similar bone and less osteoid volume in BCP+SVF and β-TCP+SVF biopsies compared to tuberosity bone biopsies at the cranial side of the grafted area (RIII). Original magnification: 100x. Total number of blood vessels (N.Bloodves) in biopsies taken after MSFE with retromolar bone versus β-TCP or BCP **(G)**, tuberosity bone versus β-TCP or BCP **(H)**, retromolar bone versus β-TCP+SVF or BCP+SVF **(I)**, tuberosity bone versus β-TCP+SVF or BCP+SVF **(J)**. Bone volume (bone area over total area (B.Ar/T.Ar %)) in biopsies taken after MSFE with retromolar bone versus β-TCP or BCP **(K)**, tuberosity bone versus β-TCP or BCP **(L)**, retromolar bone versus β-TCP+SVF or BCP+SVF **(M)**, tuberosity bone versus β-TCP+SVF or BCP+SVF **(N)**. Osteoid volume (osteoid area over total area (O.Ar/T.Ar %)) in biopsies taken after MSFE with retromolar bone versus β-TCP or BCP **(O)**, tuberosity bone versus β-TCP or BCP **(P)**, retromolar bone versus β-TCP+SVF or BCP+SVF **(Q)**, tuberosity bone versus β-TCP+SVF or BCP+SVF **(R)**. Values are mean±SD (n=3–12). *Significantly different from retromolar bone graft, $p<0.05$. B.Ar, bone area; T.Ar, total area; O.Ar, osteoid area; NB, native bone, TZ, transition zone, RI, region I; RII, region II; RIII, region III. β-TCP, β-tricalcium phosphate; BCP, biphasic calcium phosphate consisting of 60% hydroxyapatite and 40% β-tricalcium phosphate; SVF, stromal vascular fraction.

Small and large sized blood vessels

When analyzing the relative percentages of small and large sized blood vessels in the different regions of the grafted area, we found in retromolar bone biopsies a similar percentage of small and large blood vessels (38%) in region I, which both decreased gradually from caudal towards cranial to ~20% in region III (Table 2). A different pattern of blood vessel distribution was observed in tuberosity bone biopsies, *i.e.* in region I and III equal small and large vessel percentages (~30% with an approximate 1:1 ratio between small and large vessels) and even an increase in region II (~47% with an approximate 1:1 ratio between small and large vessels) of blood vessels was observed.

Blood vessel distribution in CaP bone substitutes showed a similar pattern as in retromolar bone biopsies, *i.e.* a steady decrease in relative number of blood vessels towards the cranial side (Table 2). We observed high small and large vessel percentages (~60% with an approximate 1:1 ratio between small and large vessels) in region I, and low small and large vessel percentages (~15% with an approximate 1:1 ratio between small and large vessels) in region III.

Table 2. Distribution of small and large sized blood vessels in the grafted area in biopsies obtained from patients after maxillary sinus floor elevation by histomorphometrical analysis.

		Blood vessels, % of total									
Graft	Size of blood vessel	RI	RII	RIII	Total	Graft	Size of blood vessel	RI	RII	RIII	Total
Retromolar	Small	38	34	28	100						
	Large	38	47	15	100						
Tuberosity	Small	34	46	20	100						
	Large	26	47	27	100						
ß-TCP	Small	68	26	6	100	ß-TCP+SVF	Small	40	13	47	100
	Large	69	20	11	100		Large	47	10	43	100
BCP	Small	52	26	22	100	BCP+SVF	Small	29	43	28	100
	Large	55	25	19	100		Large	59	7	34	100

Patients undergoing maxillary sinus floor elevation were treated with autologous bone graft (retromolar or tuberosity bone graft), calcium phosphate bone substitutes (β-tricalcium phosphate (β-TCP) or biphasic calcium phosphate (BCP)), or calcium phosphate bone substitutes with stem cells (β-TCP + stromal vascular fraction (SVF) or BCP + SVF). The grafted area was divided in three regions (caudal-cranial): region I (RI), region II (RII), and region III (RIII). N=3–12. RI, region I; RII, region II; RIII, region III; β-TCP, β-tricalcium phosphate; BCP, biphasic calcium phosphate consisting of 60% hydroxyapatite and 40% β-tricalcium phosphate; SVF, stromal vascular fraction. Total: RI+RII+RIII.

Blood vessel distribution in the SVF-supplemented CaP bone substitutes biopsies showed a different pattern than in CaP bone substitutes biopsies without SVF-supplementation (Table 2). In SVF-supplemented ß-TCP bone substitute biopsies blood vessels showed a biphasic pattern, *i.e.* high small and large vessel percentages (~40% with an approximate 1:1 ratio between small and large vessels) in region I, four-fold lower small and large percentages in region II, and another ~40% and 1:1 ratio in region III. Blood vessel distribution in the SVF-supplemented BCP bone substitute biopsies showed another pattern, *i.e.* small vessels were comparable in

region I and III, with a rise in region II, whereas large vessel counts were highest number in region I, lowest in region II, and intermediate in region III. The small sized blood vessels in the SVF-supplemented BCP bone substitute bone biopsies showed a similar pattern of distribution over the grafted area as the blood vessels in tuberosity bone biopsies.

Immunohistochemical was performed on retromolar bone graft biopsies (Figure S1). The total number of CD34+ and SMA+ blood vessels was similar in CaP bone substitutes with or without SVF-supplementation biopsies compared to retromolar bone biopsies.

DISCUSSION

Four to six months after MSFE, differences in vascularization and bone regeneration potential were observed between CaP bone substitutes either or not SVF-supplemented versus autologous bone grafts in MSFE. CaP bone substitutes compared to autologous bone biopsies, showed lower blood vessel number, bone and osteoid volume in the grafted area. SVF-supplemented CaP bone substitutes biopsies, showed similar blood vessel number and osteoid volume as retromolar, but lower than in tuberosity bone biopsies. SVF-supplemented CaP bone substitutes showed similar bone volume as tuberosity, but lower than in retromolar bone biopsies. These results support our hypothesis that SVF-supplemented CaP bone substitutes biopsies may show similar vascularization and bone regeneration potential as retromolar, but not tuberosity bone grafts in MSFE.

SVF-supplementation in CaP bone substitutes biopsies enhanced blood vessel number and osteoid formation to a similar level as in retromolar bone biopsies. It is likely that the osteogenic capacities of SVF indirectly enhance blood vessel formation by (pre)osteoblasts. (Pre) osteoblasts are a major source of VEGF, *i.e.* one of the most important regulators in vasculogenesis and angiogenesis. Our observations of significantly increased blood vessel number in SVF-supplemented CaP bone substitutes biopsies compared to CaP bone substitutes, were in line with observations of others.[9,27–29] Increased small as well as large blood vessel percentage at the cranial side of SVF-supplemented CaP bone substitutes biopsies were observed. Increased percentage of small blood vessels may indicate increased formation of new blood capillaries by the sprouting of an existing small vessel, *i.e.* angiogenesis. Large blood vessels are considered to be more mature vessels. SVF-supplementation likely has a strong pro-angiogenic effect. Since only one dosage of SVF (ASCs) was used in these patients, the encouraging initial efficacy data and complete absence of adverse effects certainly warrant further studies to evaluate whether higher ASC dosages may show more effective blood vessel and osteoid formation without additional side effects.

Retromolar bone biopsies showed the highest bone volume in the grafted area. These findings may be explained by a higher mineralization degree of the original graft, as retromolar bone grafts are predominantly composed of cortical bone, and tuberosity bone grafts of cancellous bone.[30,31] We observed the lowest bone and osteoid volume, and blood vessel formation in CaP bone substitutes biopsies, which is in line with observations by others showing delayed bone formation with CaP bone substitutes in MSFE compared to autologous bone[32–34]. This lower bone volume in CaP bone substitutes biopsies is likely the result of a lower bone formation rate by osteoconduction than osteogenesis. SVF-supplementation significantly increased bone and osteoid volume in CaP bone substitutes biopsies, likely as result of a pro-osteogenic effect of SVF.[17]

More active bone formation at the cranial side of SVF-supplemented CaP bone substitutes and tuberosity bone biopsies was observed. This is in line with earlier observations that bone formation may start not only from the maxillary native bone, but from the cranial side as well.[9] It has been shown that the Schneiderian membrane of the maxillary sinus, which is lifted during MSFE to insert the graft material, contains a cell population with potential for osteogenic differ-

entiation.[35] The additive value of SVF-supplementation in bone formation at the cranial side of the grafted area, may be the result of ASCs transdifferentiating toward bone-forming cells or increased ASC paracrine factor secretion that regulate progenitor cell recruitment from the original lateral bony window and/or the Schneiderian membrane of the maxillary sinus. Moreover, our observations of increased bone as well as vascularization in MSFE, were in line with observations of others.[8,9,19]

This study was conducted retrospectively resulting in several limitations. One limitation of the present study was that the autologous bone grafts were used in patients undergoing unilateral MSFE. To exclude inter-patient variation, a bilateral maxillary sinus floor elevation model would be more appropriate to compare two different grafting materials. Another limitation of this study was that we only analyzed biopsies at one time point per grafting material, preventing to assess the dynamics of the remodeling process in the different types of bone grafts. Although statistical analysis revealed no difference between the outcome measurements related to different biopsy harvesting time points between autologous bone (4-months post-MSFE) and CaP bone substitutes either or not SVF-supplemented (6-months post-MSFE), this may be considered another limitation of the study. Therefore, we can only deduce that SVF-supplemented CaP bone substitutes showed lower vascularization than tuberosity bone graft, but we cannot rule out that the blood vessel numbers might reach similar levels at a later time point.

In summary, we found that the use of SVF-supplemented CaP bone substitutes in human MSFE resulted in similar blood vessel number and osteoid volume as retromolar, but not tuberosity bone 4–6 months post-MSFE prior to dental implant placement. We conclude that SVF-supplemented CaP bone substitutes showed similar vascularization and bone regeneration potential as retromolar, but not tuberosity bone grafts in patients undergoing MSFE, due to a potential vasculogenic, angiogenic, and osteogenic effect of SVF-supplementation. Based on our histological data, it appears that SVF-supplemented CaP bone substitutes might perform similarly as retromolar bone graft in MSFE, since comparable blood vessel number and osteoid were observed. Therefore, SVF-supplemented CaP bone substitutes might be promising to replace autologous bone for enhanced bone regeneration. Future studies with more patients and higher SVF-dosages are welcomed to further improve efficacy of SVF-supplementation in MSFE.

ACKNOWLEDGEMENTS

This work was granted by Health-Holland (project no. LSHM19016, “BB”).The authors thank H.W. van Essen and M.A. van Duin for assistance in histological processing and histomorphometrical analysis.

REFERENCES

1. Starch-Jensen T, Aludden H, Hallman M, Dahlin C, Christensen AE, Mordenfeld A. A systematic review and meta-analysis of long-term studies (five or more years) assessing maxillary sinus floor augmentation. *Int J Oral Maxillofac Surg.* 2018;47(1):103–116. doi:10.1016/j.ijom.2017.05.001
2. Tatum HJ. Maxillary and sinus implant reconstructions. *Dent Clin North Am.* 1986;30(2):207–229.
3. Filipowska J, Tomaszewski KA, Niedźwiedzki Ł, Walocha JA, Niedźwiedzki T. The role of vasculature in bone development, regeneration and proper systemic functioning. *Angiogenesis.* 2017;20(3):291–302. doi:10.1007/s10456-017-9541-1
4. Wu V, Helder MN, Bravenboer N, Ten Bruggenkate CM, Jin J, Klein-Nulend J, Schulten EAJM. Bone tissue regeneration in the oral and maxillofacial region: A review on the application of stem cells and new strategies to improve vascularization. *Stem Cells Int.* 2019:6279721. doi:10.1155/2019/6279721
5. Hu K, Olsen BR. Osteoblast-derived VEGF regulates osteoblast differentiation and bone formation during bone repair. *J Clin Invest.* 2016;126(2):509–526. doi:10.1172/JCI82585
6. Colton C. Implantable biohybrid artificial organs. *Cell Transpl.* 1995;4(4):415–436. doi:10.1088/1748-6041/1/3/001
7. Moya A, Paquet J, Deschepper M, Larochette N, Oudina K, Denoeud C, Bensidhoum M, Logeart-Avramoglou D, Petite H. Human mesenchymal stem cell failure to adapt to glucose shortage and rapidly use intracellular energy reserves through glycolysis explains poor cell survival after implantation. *Stem Cells.* 2018;36(3):363–376. doi:10.1002/stem.2763
8. Boëck-Neto RJ, Artese L, Piattelli A, Shibli JA, Perrotti V, Piccirilli M, Marcantonio E Jr. VEGF and MVD expression in sinus augmentation with autologous bone and several graft materials. *Oral Dis.* 2009;15:148–154. doi:10.1111/j.1601-0825.2008.01502.x
9. Farré-Guasch E, Bravenboer N, Helder MN, Schulten EAJM, Ten Bruggenkate CM, Klein-Nulend J. Blood vessel formation and bone regeneration potential of the stromal vascular fraction seeded on a calcium phosphate scaffold in the human maxillary sinus floor elevation model. *Materials (Basel).* 2018;11(1):116. doi:10.3390/ma11010161
10. Wu V, Schulten EAJM, Helder MN, Ten Bruggenkate CM, Bravenboer N, Klein-Nulend J. Bone vitality and vascularization of mandibular and maxillary bone grafts in maxillary sinus floor elevation: A retrospective cohort study. *Clin Implant Dent Relat Res.* 2022:1–11. doi:10.1111/cid.13142
11. Kamolratanakul P, Mattheos N, Yodsanga S, Pornchai J. The impact of deproteinized bovine bone particle size on histological and clinical bone healing outcomes in the augmented sinus: A randomized controlled clinical trial. *Clin Implant Dent Relat Res.* 2022;24:361–371. doi:10.1111/cid.13083
12. Stumbras A, Krukis MM, Januzis G, Juodzbalys G. Regenerative bone potential after sinus floor elevation using various bone graft materials: A systematic review. *Quintessence Int.* 2019;50(7):548–558. doi:10.3290/j.qi.a42482
13. Schulten EAJM, Prins HJ, Overman JR, Helder MN, Ten Bruggenkate CM, Klein-Nulend J. A novel approach revealing the effect of a collagenous membrane on osteoconduction in maxillary sinus floor elevation with β-tricalcium phosphate. *Eur Cell Mater.* 2013;25:215–228. doi:10.22203/eCM.v025a16
14. Zijderveld SA, Zerbo IR, Van den Bergh JPA, Schulten EAJM, Ten Bruggenkate CM. Maxillary sinus floor augmentation using a beta-tricalcium phosphate (Cerasorb) alone compared to autogenous bone grafts. *Int J Oral Maxillofac Implants.* 2005;20(3):432–440.

15. Grayson WL, Bunnell BA, Martin E, Frazier T, Hung BP, Gimble JM. Stromal cells and stem cells in clinical bone regeneration. *Nat Rev Endocrinol.* 2015;11(3):140–150. doi:10.1038/nrendo.2014.234

16. Gimble JM, Bunnell BA, Guilak F. Human adipose-derived cells: An update on the transition to clinical translation. *Regen Med.* 2012;7(2):225–235. doi:10.2217/rme.11.119

17. Prins HJ, Schulten EAJM, Ten Bruggenkate CM, Klein-Nulend J, Helder MN. Bone regeneration using the freshly isolated autologous stromal vascular fraction of adipose tissue in combination with calcium phosphate ceramics. *Stem Cells Transl Med.* 2016;5(10):1362–1374.

18. Helder MN, Knippenberg M, Klein-Nulend J, Wuisman PIJM. Stem cells from adipose tissue allow challenging new concepts for regenerative medicine. *Tissue Eng.* 2007;13(8):1799–1808. doi:10.1089/ten.2006.0165

19. Artese L, Piattelli A, Stefano DA, Piccirilli M, Pagnutti S, D'Alimonte E, Perrotti V. Sinus lift with autologous bone alone or in addition to equine bone : An immunohistochemical study in man. *Implant Dent.* 2011;20(5):383–388. doi:10.1097/ID.0b013e3182310b3d

20. Degidi M, Artese L, Rubini C, Perrotti V, Iezzi G, Piattelli A. Microvessel density in sinus augmentation procedures using anorganic bovine bone and autologous bone: 3 months results. *Implant Dent.* 2007;16(3):317–325. doi:10.1097/ID.0b013e3180de4c5f

21. Helder MN, Van Esterik FAS, Kwehandjaja MD, Ten Bruggenkate CM, Klein-Nulend J, Schulten EAJM. Evaluation of a new biphasic calcium phosphate for maxillary sinus floor elevation: Micro-CT and histomorphometrical analyses. *Clin Oral Implant Res.* 2018;29:488–498. doi:10.1111/clr.13146

22. Plenk Jr H. The microscopic evaluation of hard tissue implants. In: William DF, ed. *Techniques of Biocompatibility Testing.* Boca Raton, Florida: CRC Press Inc; 1986.

23. Dempster DW, Compston JE, Drezner MK, Glorieux FH, Kanis JA, Malluche H, Meunier PJ, Ott SM, Recker RR, Parfitt AM. Standardized nomenclature, symbols, and units for bone histomorphometry: A 2012 update of the report of the ASBMR histomorphometry nomenclature committee. *J Bone Miner Res.* 2013;28:1–16. doi:10.1002/jbmr.1805

24. Chen Y, Wang J, Zhu XD, Tang ZR, Yang X, Tan YF, Fan YJ, Zhang XD. Enhanced effect of β-tricalcium phosphate phase on neovascularization of porous calcium phosphate ceramics: In vitro and in vivo evidence. *Acta Biomater.* 2015;11(1):435–448. doi:10.1016/j.actbio.2014.09.028

25. Pusztaszeri MP, Seelentag W, Bosman FT. Immunohistochemical expression of endothelial markers CD31, CD34, von Willebrand factor, and Fli-1 in normal human tissues. *J Histochem Cytochem.* 2006;54(4):385–395. doi:10.1369/jhc.4A6514.2005

26. Brey EM, McIntire L V, Johnston CM, Reece GP, Patrick CW. Three-dimensional, quantitative analysis of desmin and smooth muscle alpha actin expression during angiogenesis. *Ann Biomed Eng.* 2004;32(8):1100–1107. doi:10.1114/B:ABME.0000036646.17362.c4

27. Kim A, Kim DH, Song HR, Kang WH, Kim HJ, Lim HC, Cho DW, Bae JH. Repair of rabbit ulna segmental bone defect using freshly isolated adipose-derived stromal vascular fraction. *Cytotherapy.* 2012;14(3):296–305. doi:10.3109/14653249.2011.627915

28. Madonna R, De Caterina R. In vitro neovasculogenic potential of resident adipose tissue precursors. *Am J Physiol Cell Physiol.* 2008;295(5):1271–1280. doi:10.1152/ajpcell.00186.2008

29. Vergroesen PP, Kroeze RJ, Helder MN, Smit TH. The use poly(L-lactide-co-caprolactone) as a scaffold for adipose stem cells in bone tissue engineering: Application in a spinal fusion model. *Macromol Biosci.* 2011;14:722–730.

30. Fleming JE, Cornell CN, Muschler GF. Bone cells and matrices in orthopedic tissue engineering. *Orthop Clin North Am.* 2000;31(3):357–374. doi:10.1016/S0030-5898(05)70156-5

31. Schlegel KA, Schultze-Mosgau S, Wiltfang J, Neukam FW, Rupprecht S, Thorwarth M. Changes of mineralization of free autogenous bone grafts used for sinus floor elevation. *Clin Oral Implants Res.* 2006;17(6):673–678. doi:10.1111/j.1600-0501.2006.01186.x

31. Danesh-Sani SA, Wallace SS, Movahed A, El Chaar ES, Cho SC, Khouly I, Testori T. Maxillary sinus grafting with biphasic bone ceramic or autogenous bone: Clinical, histologic, and histomorphometric results from a randomized controlled clinical trial. *Implant Dent.* 2016;25(5):588–593. doi:10.1097/ID.0000000000000474

32. Schmitt CM, Doering H, Schmidt T, Lutz R, Neukam FW, Schlegel KA. Histological results after maxillary sinus augmentation with Straumann® BoneCeramic, Bio-Oss®, Puros®, and autologous bone. A randomized controlled clinical trial. *Clin Oral Implants Res.* 2013;24(5):576–585. doi:10.1111/j.1600-0501.2012.02431.x

33. Zerbo I, Zijderveld S, de Boer A, Bronckers AL, De Lange G, Ten Bruggenkate CM, Burger EH. Histomorphometry of human sinus floor augmentation using a porous beta-tricalcium phosphate: A prospective study. *Clin Oral Implant Res.* 2004;15(6):724–732.

34. Berbéri A, Al-Nemer F, Hamade E, Noujeim Z, Badran B, Zibara K. Mesenchymal stem cells with osteogenic potential in human maxillary sinus membrane: An in vitro study. *Clin Oral Investig.* 2017;21(5):1599–1609. doi:10.1007/s00784-016-1945-6

SUPPLEMENTARY MATERIAL

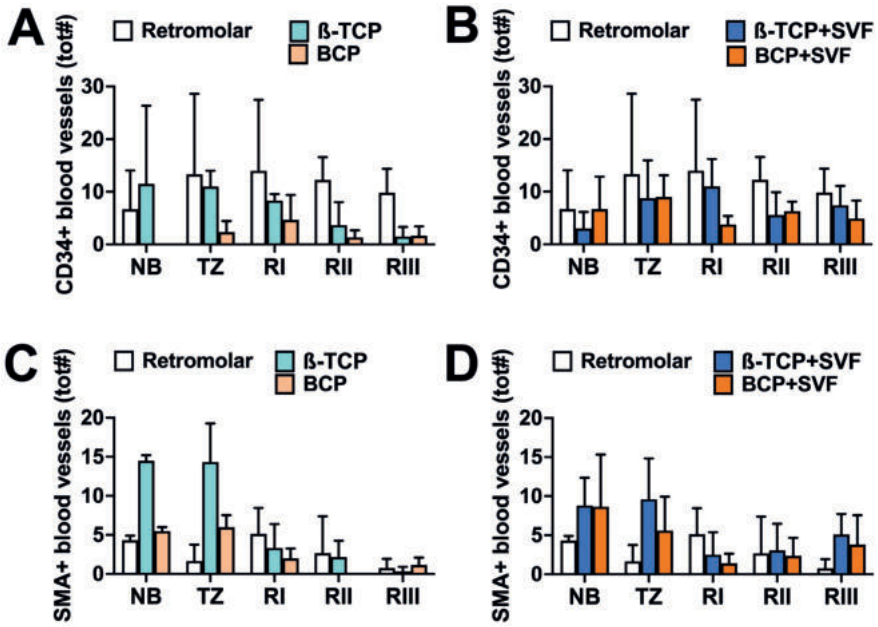

Figure S1. Immunohistochemical analysis of CD34 and of α-smooth muscle actin (SMA) of bone biopsies from patients after MSFE grafted with retromolar bone, CaP bone substitutes (β-TCP or BCP) or CaP bone substitutes with stem cells (β-TCP+SVF or BCP+SVF). CD34 is a marker of endothelial cells as well as stem cells such as endothelial progenitor stem cells and hematopoietic stem cells. SMA is a marker of pericytes, as well as smooth muscle cells present in the blood vessel walls. **(A)** Number of CD34+ blood vessels in biopsies taken after MSFE with retromolar bone versus β-TCP or BCP. **(B)** Number of CD34+ blood vessels in biopsies taken after MSFE with retromolar bone versus β-TCP + SVF or BCP + SVF. **(C)** Number of SMA+ blood vessels in biopsies taken after MSFE with retromolar bone versus β-TCP or BCP. **(D)** Number of SMA+ blood vessels in biopsies taken after MSFE with retromolar bone versus β-TCP + SVF or BCP + SVF. Values are mean±SD (n=3–4). NB, native bone, TZ, transition zone, RI, region I; RII, region II; RIII, region III. β-TCP, β-tricalcium phosphate; BCP, biphasic calcium phosphate consisting of 60% hydroxyapatite and 40% β-tricalcium phosphate; SVF, stromal vascular fraction.

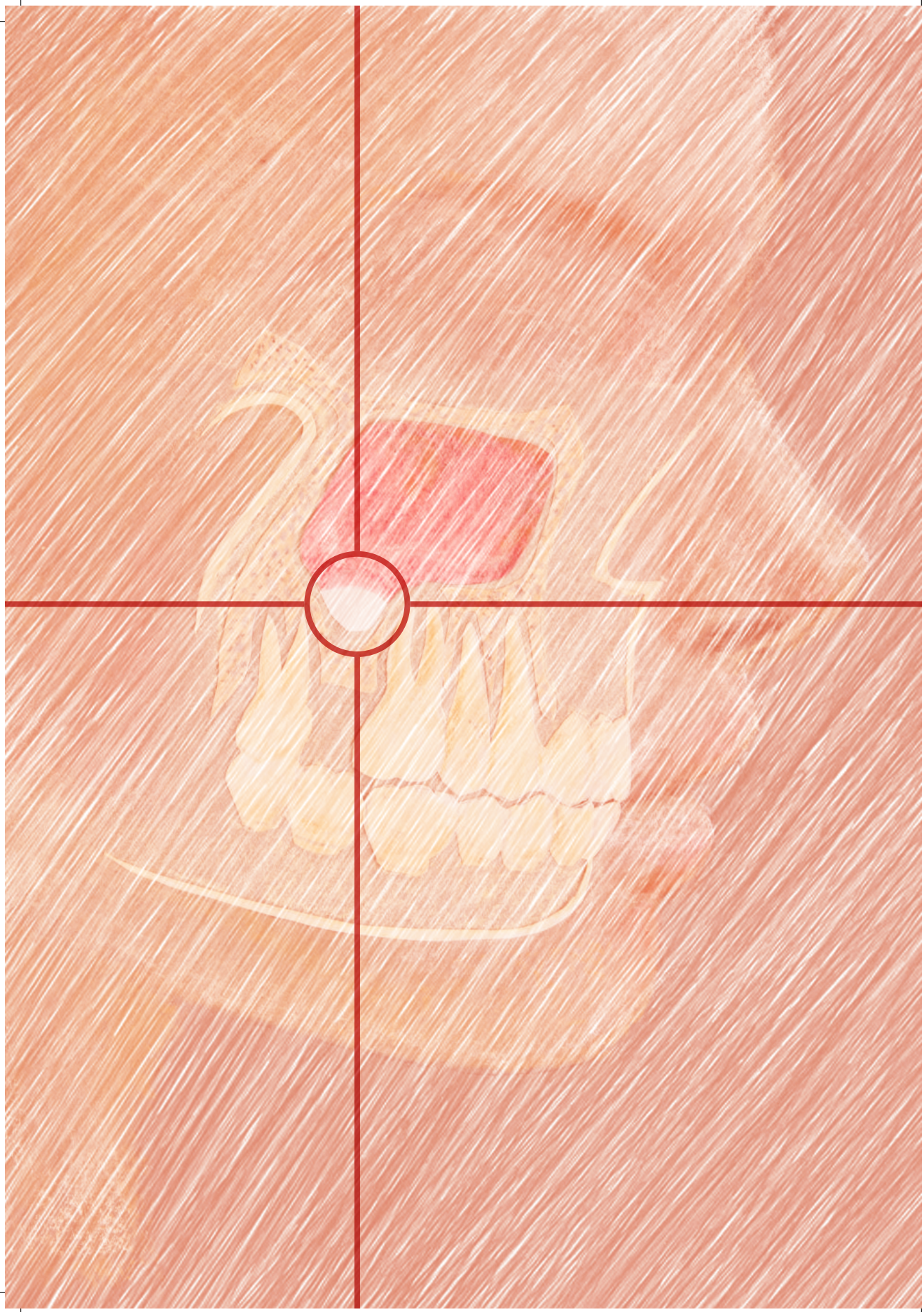

CHAPTER 6

Long-term safety of bone regeneration using autologous stromal vascular fraction and calcium phosphate ceramics: A 10-year prospective cohort study

Vivian Wu [1,2]
Jenneke Klein-Nulend [1]
Nathalie Bravenboer [3]
Christiaan M. ten Bruggenkate [2]
Marco N. Helder [2]
Engelbert A.J.M. Schulten [2]

[1] Department of Oral Cell Biology, Academic Centre for Dentistry Amsterdam (ACTA), University of Amsterdam and Vrije Universiteit Amsterdam, Amsterdam Movement Sciences, Amsterdam, The Netherlands

[2] Department of Oral and Maxillofacial Surgery/Oral Pathology, Amsterdam University Medical Centers and Academic Centre for Dentistry Amsterdam (ACTA), Vrije Universiteit Amsterdam, Amsterdam Movement Sciences, Amsterdam, The Netherlands

[3] Department of Clinical Chemistry, Amsterdam University Medical Centers, Vrije Universiteit Amsterdam, Amsterdam Movement Sciences, Amsterdam, The Netherlands

Stem Cells Translational Medicine 2023;szad045

ABSTRACT

This prospective cohort study aimed to assess long-term safety, dental implant survival, and clinical and radiological outcomes after maxillary sinus floor elevation (MSFE; lateral window technique) using freshly isolated autologous stromal vascular fraction (SVF) combined with calcium phosphate ceramics. All 10 patients previously participating in a phase-I trial were included in this 10-year follow-up. They received either ß-tricalcium phosphate (ß-TCP; n=5) or biphasic calcium phosphate (BCP; n=5) with SVF-supplementation on one side (study). Bilaterally-treated patients (6 of 10; 3 ß-TCP, 3 BCP) received only calcium phosphate on the opposite side (control). Clinical and radiological assessments were performed on 44 dental implants at 1-month pre-MSFE, and 0.5–10-year post-MSFE. Implants were placed 6-months post-MSFE. No adverse events or pathology were reported during 10-year follow-up**.** Forty-three dental implants (98%) remained functional. Control and study sides showed similar peri-implant soft tissue quality, sulcus bleeding index, probing depth, plaque index, keratinized mucosa width, as well as marginal bone loss (0–6 mm), graft height loss (0–6 mm), and graft volume reduction. Peri-implantitis was observed around six implants (control: 4; study: 2) in three patients. This study is the first to demonstrate the 10-year safety of SVF-supplementation in MSFE for jawbone reconstruction. SVF-supplementation showed enhanced bone regeneration in the short-term (previous study), and led to no abnormalities clinically and radiologically in the long-term.

INTRODUCTION

Bone regeneration to restore bone defects in the oral and maxillofacial region remains challenging. Patients with insufficient alveolar bone height in the lateral maxilla for dental implant placement are currently treated with maxillary sinus floor elevation (MSFE), using autologous bone and/or bone substitute.[1] Autologous bone is considered the gold standard grafting material in MSFE, due to the essential combination of osteogenic, osteoinductive, and osteoconductive properties as well as prevention of immunogenic responses.[2] However, morbidity caused by the harvesting procedure and limited availability of autologous bone encourage the search for suitable alternatives with similar bioactivity.

Calcium phosphate ceramics show low bone in-growth rates in comparison with autologous bone grafts since they only have osteoconductive properties and lack osteoinductive potential.[3] Many studies have actively been conducted to improve the bioactivity of calcium phosphate ceramics in bone regeneration (for a review, see: Jeong et al.).[4] Cell-based bone tissue engineering is a promising strategy to improve bone formation by providing osteogenic cells that secrete osteoinductive signals to recruit cells from surrounding bone.[5–8] This might shorten the time needed to obtain sufficient bone regeneration than is required when using bone substitute only.

During the past decades, multiple sources of stem cells have been investigated for bone tissue engineering in the oral and maxillofacial region.[8] Adipose tissue-derived mesenchymal stem cells (ASCs) have opened new possibilities in adult stem cell therapies, since the use of ASCs has eliminated drawbacks associated with adult bone marrow-derived mesenchymal stem cells (*e.g.* costly and time-consuming Good Manufacturing Practice (GMP)-expansion necessary, painful harvesting procedure), which are still the most frequently used cells in cell-based bone tissue engineering.[8] The stromal vascular fraction (SVF) of human adipose tissue is considered a promising source for essential cells with osteogenic and angiogenic potential.[7–11] Moreover, SVF is a cell source with clinical feasibility due to the large quantities that can be harvested and applied in a one-step surgical procedure.[7,12] A disadvantage of SVF harvesting so far is that liposuction of adipose tissue is performed under general anesthesia and requires (short) hospitalization.

Clinical evidence of ASC-application for bone regeneration is limited, although the potential of ASCs evokes high expectations.[7,13–15] To the best of our knowledge, only one study reported unsatisfactory clinical results of ASC-application in cranioplasty during six-year follow-up; four out of five patients suffered from unsatisfactory treatment outcome partially due to poor ossification, infection, or tumor recurrence, and two patients had to be re-operated due to graft resorption.[16] Stem cell-application in regenerative medicine has also raised safety concerns, *e.g.* tumorigenic potential and biodistribution.[17] Therefore, clinical studies investigating long-term safety and efficacy are essential before continuing with clinical applications using (adipose) stem cells.

In a previous phase-I clinical trial, 10 patients underwent MSFE prior to dental implant placement using freshly isolated autologous SVF seeded on either ß-tricalcium phosphate (ß-TCP) or biphasic calcium phosphate (BCP) carriers in a one-step surgical procedure.[7] No

serious adverse events were reported during the procedure and 3-year follow-up. In addition, biopsies showed more induction of bone mass and bone formation by SVF-supplementation compared to the calcium phosphate carriers, in particular in ß-TCP-treated patients.[7] Paired analysis of the 6 bilaterally-treated patients revealed markedly higher bone volume and bone formation, demonstrating an additive effect of SVF, independent of the bone substitute.[7] Moreover, more bone mass seemed to correlate with blood vessel formation, and was higher in the cranial part of the study biopsies, in particular in β-TCP-treated patients.[9] Based on short-term results (~3 years), we demonstrated for the first time the feasibility, safety, and potential efficacy of SVF seeded on calcium phosphate carriers, and indicated a pro-angiogenic effect of SVF.[7,9]

The present prospective cohort study was designed as a 10-year follow-up of patients previously enrolled in our phase-I clinical trial.[7] We aimed to assess long-term safety, dental implant survival, and clinical and radiological outcomes after MSFE (lateral window technique) using calcium phosphate ceramics (ß-TCP or BCP) with and without freshly isolated autologous SVF-supplementation.

MATERIALS AND METHODS

Study design and patient selection

This prospective cohort study was designed as a 10-year follow-up of patients previously enrolled in a phase-I clinical trial investigating safety and potential additive effect of SVF in MSFE using lateral window technique on bone regeneration.[7] Ten patients who required dental implants for prosthetic rehabilitation in the partially edentulous posterior maxilla were included. All patients had an adequate alveolar bone height of at least 4 mm, but not more than 8 mm at the lateral maxilla. Detailed patient inclusion and exclusion criteria have been previously described.[7] Firstly, four patients with unilateral MSFE-indication, and six patients with bilateral MSFE-indication were selected by consecutive sampling.[7] Secondly, two equal treatment groups were created by random treatment allocation, *i.e.* ß-TCP (5 patients: 2 unilateral, 3 bilateral) or BCP-treatment (5 patients: 2 unilateral, 3 bilateral) group. All unilateral MSFE-patients received calcium phosphate with SVF. All bilateral MSFE-patients (split-mouth) received pure calcium phosphate on one side (control), and calcium phosphate with SVF on the other side of the maxilla (study). Control and study sides were randomly assigned to prevent bias. The surgical procedures have been previously described.[7] In short, adipose tissue was processed with a CE-marked Celution device (Cytori Therapeutics, Inc., San Diego, CA, USA) to obtain SVF. For implantation, scaffolds were seeded with 10^7 nucleated SVF-cells (~2×10^5 ASC-like cells)/g calcium phosphate carrier (Ceros® ß-TCP (Thommen Medical, Grenchen, Switzerland) or Straumann® Bone Ceramic consisting of 60% hydroxyapatite (HA) and 40% β-TCP (Straumann AG, Basel, Switzerland)). Implants were placed 6-months post-MSFE in a single-stage procedure under local anesthesia. Extensive cell characterizations were performed, as described previously.[7] In short, the SVF surface marker expression profiles as determined with fluorescence-activated cell sorting were consistent with previous reports, including the CD34 positivity reported for ASCs.[18–20] Radiologically, all implants showed absence of bone loss beyond marginal bone level changes resulting from initial bone remodeling at 3-months after implant placement. All implants showed peri-implant health (absence of erythema, heavy bleeding on probing, swelling, suppuration, and probing depth <6 mm) during short-term follow-up (~3 years). All patients received dental implant maintenance in regular Dutch oral health care system, *i.e.* one to four visits to the dentist and/or oral hygienist per year.

The present study was conducted according to the guidelines of the Declaration of Helsinki, and approved by the medical ethical committee (IRB) of the VU University Medical Center in Amsterdam (Dossier number: 2020.344: ABR NL71857.029.20). All patients signed a written informed consent before participation in the study. The study was performed according to the STROBE guidelines.[21]

One experienced surgeon (VW) performed anamnesis, as well as all clinical (intra-oral) and quantitative radiological assessments. Three experienced surgeons (VW, CMB, EAJMS) carried out qualitative radiological assessments. Intra and inter-examiner calibration was done before the start of the study. Intra-examiner calibration included identification of clinical and radiological reference points, and associated radiological linear measurements. Inter-examiner calibration included identification of pathology and abnormalities. Discrepancies between

examiners were resolved through discussion. Treatment groups remained concealed for examiners. Panoramic radiographs and CBCT-scans were taken at different time points during the previous phase-I study[7] and at 10-year follow-up (Table S1). To control for enlargement of the anatomical structures as a result of panoramic radiography, dental implant length was used as a reference.

Primary outcome measure

Safety

Safety outcomes related to the product or procedure were assessed. General health changes and (serious) adverse events were patient-reported through a health questionnaire. Maxillary sinus-related problems such as sinusitis were patient-reported through anamnesis. Clinical (intra-oral) and radiological assessments (panoramic radiographs and cone beam computerized tomography (CBCT) scans) were carried out to detect any pathology and abnormalities.

Secondary outcome measures

Implant survival

Number of implants *in situ* was counted.

Peri-implant condition

Soft tissue physical appearance was scored per dental implant site as no abnormalities or swollen. Soft tissue color was scored as white-necrotic, pink or red, and soft tissue surface morphology at the buccal aspect of each implant as smooth or stippled.

Sulcus bleeding index (SBI), and probing depth (PD; in mm) were scored at four locations (mesial, buccal, distal, palatal) around the implant. SBI was scored as: Score 0: no bleeding when passing a periodontal probe along the gingival margin adjacent to the implant; Score 1: isolated bleeding spot; Score 2: confluent red line of blood on margin; Score 3: heavy or profuse bleeding.[22] Probing depth was registered using a manual probe and light force (~0.25 N). The highest values of SBI and PD were used for statistical analyses at the patient and implant level.

Marginal bone loss (in mm) was assessed on panoramic radiographs. Marginal bone loss was defined as the perpendicular distance from the implant-abutment interface to the radiographic bone level at the mesial and distal aspects of each implant, since the implants were placed "flush" (at the same height) to the alveolar ridge. Mean values of marginal bone loss at the mesial and distal aspect of each implant were calculated, and the highest value per patient and per implant site was used for statistical analysis.

Since baseline radiographic and probing data were absent, the following case definitions of peri-implant health and disease, *i.e.* peri-implant mucositis and peri-implantitis, were applied at 10-year follow-up: Peri-implant health: absence of erythema, bleeding on probing, swelling, and suppuration; Peri-implant mucositis: bleeding on gentle probing <0.25 N, absence of bone loss >2 mm; Peri-implantitis: ≥3 mm marginal bone loss combined with ≥6 mm PD with bleeding and/or suppuration.[23]

Peri-implant disease risk factors

Patient-reported smoking and diabetes were obtained through a health questionnaire. Patient-reported dental implant maintenance, and dental implant-related biological complications were obtained through anamnesis. Full-mouth periodontal condition screening was carried out according to the Dutch Periodic Periodontal Screening-index (PPS) by one examiner.[24] Probing depth was scored at four locations (mesial, buccal, distal, palatal) around every tooth. Then the highest PPS-score for each quadrant was determined: Score 1: probing depth: 0–3 mm; Score 2: probing depth 4–5mm; Score 3: probing depth >6 mm. Plaque index (PI) was scored by one examiner at four locations (mesial, buccal, distal, palatal), as: Score 0: no plaque; Score 1: plaque only recognized by running a probe across the smooth marginal implant surface; Score 2: plaque was seen by the naked eye; Score 3: soft matter abundance.[22] The width of keratinized mucosa (KM; in mm) was scored at one location (buccal) around the dental implant. The highest PI values, and the lowest KM values were used for statistical analysis at the patient and implant level. Furthermore, overcontouring (emergence angle and convexity) of the abutment-prosthesis complex was assessed clinically and radiologically.

Technical complications

Patient-reported longevity of the restorations were obtained through anamnesis. Implant, connection, or suprastructure-related technical complications were assessed clinically and radiologically (panoramic radiograph).

Graft and residual maxillary sinus characteristics

Pathology, *e.g.* Schneiderian mucosal hypertrophy (>1 mm), mucosal cysts, polyps, bone lesions, neoplasms, and antroliths were assessed on panoramic radiographs and CBCT-scans. Irregularities of graft or residual maxillary sinus area, and recognizable demarcation of the original maxillary sinus floor and radiopaque graft were assessed on CBCT-scans. Graft structure was scored as homogenous or non-homogenous, and as bone-like or non-bone-like. Any radiopacities or radiolucencies in the grafted area, and/or graft scalloping were documented. The residual maxillary sinus area was characterized as air-filled or non-air-filled.

Tissue height, and graft height loss

Tissue height (in mm) was assessed on panoramic radiographs. Tissue height was defined as the perpendicular distance from the implant-abutment interface (dental implant mid axis) to the cranial border of the graft. Graft height loss (in mm) was calculated by subtracting tissue height at 10-year follow-up from tissue height at dental implant placement. Mean values of tissue height, and graft height loss were calculated for study and control sides, and used for statistical analysis on patient level.

Statistical analysis

Data are presented as mean±standard deviation (SD). Statistical analysis was performed with GraphPad Prism 9 software (GraphPad, La Jolla, CA, USA; http://www.graphpad.com/). Mann Whitney U-test was used to test differences in clinical (SBI, PD, PI, KM) and radiological

outcomes (marginal bone and graft height loss) between ß-TCP or BCP study (with SVF) and control sides (without SVF), at the patient and/or implant level. Study and control sides were assumed independent variables in bilaterally-treated patients. The Mann Whitney U-test showed no statistical differences between data from ß-TCP and BCP-control sides. Therefore, data of ß-TCP and BCP-treated patients were pooled, and a (paired) Wilcoxon signed rank test was used to test differences between study and control sides. To investigate a possible relationship between different clinical and radiological outcomes, Spearman correlation-test were conducted. Kruskal Wallis Test was performed to test differences in (baseline) alveolar bone height between ß-TCP, ß-TCP+SVF, BCP, and BCP+SVF-treated sides. Statistical significance was considered if $P<0.05$.

RESULTS

Patients enrolled

All 10 patients who had participated in the previous phase-I clinical trial were included in the 10-year follow-up (Table 1). The average patient age at 10-year follow-up was 66±7 years (range: 56–79 years). A total of 44 dental implants were included for analysis.

Table 1. Patient data

Pt#	Gender (♂,♀), age (years)	Unilateral/ bilateral case	Control/study side	Graft material	Dental implant positions
1	♀, 69	Bilateral	Control Study	ß-TCP ß-TCP	*14*, 15, 16 *24*, 25, 26
2	♀, 56	Bilateral	Control Study	ß-TCP ß-TCP	*24*, 25, 26 14, 15, 16
3	♂, 79	Bilateral	Control Study	ß-TCP ß-TCP	*14*, 15, 16 25, 26, 27
4	♀, 69	Unilateral	Study	ß-TCP	*24*, 25, 26
5	♂, 74	Unilateral	Study	ß-TCP	15, 16
6	♀, 66	Bilateral	Control Study	BCP BCP	24, 26 *14*, 15, 16
7	♂, 65	Bilateral	Control Study	BCP BCP	25, 26, 27 *15*, 16, 17
8	♀, 61	Unilateral	Study	BCP	14, 15, 16
9	♂, 62	Unilateral	Study	BCP	*23*, 25, 26
10	♀, 62	Bilateral	Control Study	BCP BCP	25, 26 15, 16

Gender and age at time of 10-year follow-up, whether the patients were treated unilaterally or bilaterally ("split-mouth design"), bone substitute used to augment bone of the maxillary sinus floor, and the dental implant positions (Fédération Dentaire Internationale system) are given. Italicalized numbers, biopsies completely positioned in residual native bone. Pt#, patient number; ß-TCP, ß-tricalcium phosphate; BCP, biphasic calcium phosphate.

Primary outcome measure

Safety

No general health changes, (serious) adverse events, pathology or abnormalities related to the product or procedure were observed. The 10-year follow-up was uneventful for 7 out of 10 patients. Patient #3 was diagnosed with coronary artery disease, hypertension, and diabetes mellitus type II. Patient #5 was diagnosed with heart arrhythmias, hypertension, and a cerebral vascular accident. Patient #10 was diagnosed with heart arrhythmias. None of these events were related to the product or procedure. No patient reported any complications related to dental implant treatment and/or MSFE.

Secondary outcome measures

Implant survival

One implant, completely positioned in alveolar bone, was replaced due to failure within 6-months after initial dental implant placement (patient #1, study side, ß-TCP, implant site 24). Implant survival rate at 10-year follow-up was 92.9% (13 out of 14) for study sides, and 100% (9 out of 9) for control sides in ß-TCP-treated patients, as well as for study sides (14 out of 14) and control sides (7 out of 7) in BCP-treated patients.

Peri-implant condition

Physical soft tissue appearance with no abnormalities, *i.e.* pink color and stippled surface morphology, was observed (buccal) at dental implants from study and control sides of ß-TCP and BCP-treated patients (Fig. 1).

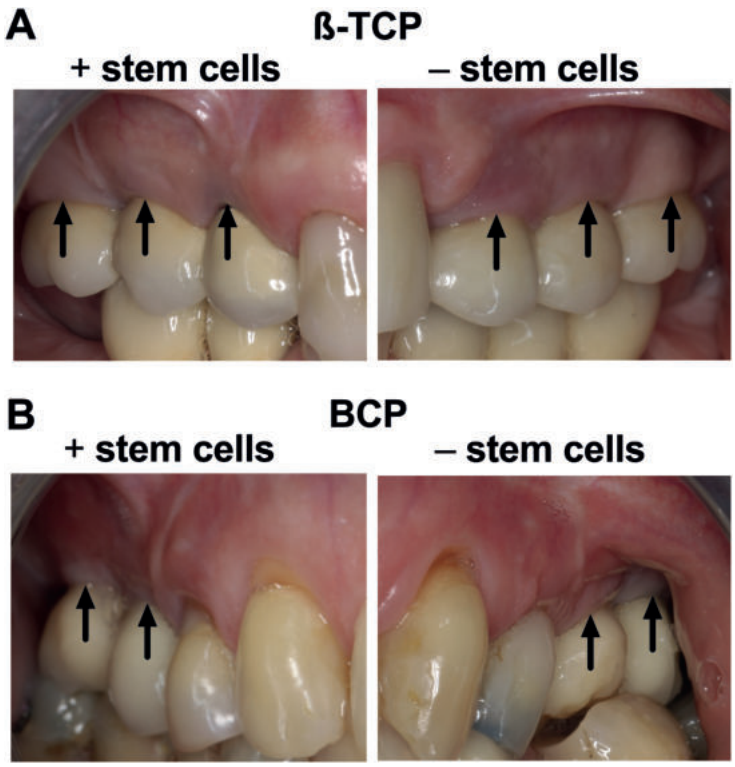

Figure 1. Representative intra-oral photographs of β-TCP-treated and BCP-treated patients with and without stem cells at 10-years after implant placement. (A) Intra-oral photographs of bilaterally-treated patients with β-TCP plus stem cells and β-TCP only, **(B)** BCP plus stem cells and BCP only. Soft tissue soft tissue around the dental implants showed a physical appearance with no abnormalities, *i.e.* pink coloured, firm tissue quality, stippled surface morphology, and ≥2 mm width of keratinized mucosa. Black arrows: implant positions.

Table 2. Clinical (sulcus bleeding index, probing depth, plaque index, width of keratinized mucosa) and radiological (marginal bone loss) outcomes of ß-TCP and BCP with and without SVF-supplementation at the patient level at 10-year follow-up

	Patient level (#sides)								
	ß-TCP			BCP			ß-TCP or BCP		
	Unilateral (2 patients) Bilateral (3 patients)			Unilateral (2 patients) Bilateral (3 patients)			Bilateral (6 patients)		
	Control side - stem cells (n=3)	Study side + stem cells (n=5)	P	Control side - stem cells (n=3)	Study side + stem cells (n=5)	P	Control side - stem cells (n=6)	Study side + stem cells (n=6)	P
Sulcus bleeding index (SBI)									
0	0	0		0	0		0	0	
1	1	3	0.892	1	3	0.357	2	3	0.500
2	2	1		1	2		3	3	
3	0	1		1	0		1	0	
Probing depth (PD; mm)									
0 – 3	0	0		0	0		0	0	
4 – 5	1	3	0.357	1	4	0.375	2	4	0.125
6 – 7	1	2		1	1		2	2	
8 – 9	1	0		1	0		2	0	
Plaque index (PI)									
0	3	4		1	2		4	4	
1	0	1	>0.999	2	2	>0.999	2	1	>0.999
2	0	0		0	1		0	1	
3	0	0		0	0		0	0	
Width keratinized mucosa (KM; mm)									
≥ 2	3	4	>0.999	2	3	>0.999	5	3	0.500
0 – 1	0	1		1	2		1	3	
Marginal bone loss (mm)									
0 – 2	1	3		2	4		3	5	
3 – 4	2	2	>0.999	0	1	0.732	2	1	0.250
5 – 6	0	0		1	0		1	0	

For each patient the highest value of sulcus bleeding index, probing depth, plaque index, and marginal bone loss was scored, as well as the lowest value of width of keratinized mucosa. *Study side significantly different from control side, $P<0.05$. ß-TCP, ß-tricalcium phosphate; BCP, biphasic calcium phosphates; n, number of patients.

At the patient level, SBI was similar between study and control sides in ß-TCP-treated ($P=0.892$) and BCP-treated patients ($P=0.357$; Table 2). SBI was similar between study and control sides in bilaterally-treated patients ($P=0.500$; Table 2). PD was similar between study and control sides in ß-TCP-treated ($P=0.357$) and BCP-treated patients ($P=0.357$; Table 2). PD was similar between study and control sides in bilaterally-treated patients ($P=0.125$; Table 2). Marginal bone loss was similar between study and control sides in ß-TCP-treated ($P>0.999$)

and BCP-treated patients (P=0.732; Table 2). Marginal bone loss was similar between study and control sides in bilaterally-treated patients (*P*=0.250; Table 2). Clinical and radiological outcomes of SVF-supplementation at the site level are summarized in Table S2, S4.

At the implant level, SBI was similar between study and control sides in ß-TCP-treated (*P*=0.405) and BCP-treated patients (*P*=0.092; Table 3). SBI was similar between study and control sides in bilaterally-treated patients (*P*>0.999; Table 3). PD was also similar between study and control sides in ß-TCP-treated (*P*=0.250) and BCP-treated patients (*P*=0.677; Table 3). PD was similar between study and control sides in bilaterally-treated patients (*P*=0.343; Table 3). Marginal bone loss was similar between study and control sides in ß-TCP-treated (*P*=0.162) and in BCP-treated patients (*P*=0.767; Table 3). Marginal bone loss was similar between study and control sides in bilaterally-treated patients (*P*=0.188; Table 3).

Peri-implant health was observed around two dental implants at the control side of one ß-TCP-treated patient (pt#3), as well as around one dental implant at the study side of one BCP-treated patient (pt#9; Table S5). At the control side, peri-implantitis was observed around three dental implants of one ß-TCP-treated patient (pt#1), and around one implant of one BCP-treated patient (pt#7; Table S5). At the study side, peri-implantitis was observed around one dental implant of one ß-TCP-treated patient (pt#4), and around one implant of one BCP-treated patient (pt#7; Table S5). Peri-mucositis was observed around all other implants at control and study sides (Table S5).

Peri-implant disease risk factors

All patients were nonsmokers. Patient #3 was diagnosed with diabetes mellitus type II. Regular dental implant maintenance program (1–4 times/year) was carried out in 9 out of 10 patients by the dentist and/or oral hygienist. Patient #7 reported no dental implant maintenance program for 2 years. No patient-reported biological complications were registered. Periodontal condition screening revealed a PPS-score of 1 (0–3 mm) or 2 (4–5 mm) in all patients.

At the patient level, PI at dental implant sites was similar between study and control sides in ß-TCP-treated (*P*>0.999) and BCP-treated patients (*P*>0.999; Table 2). PI was similar between study and control sides in bilaterally-treated patients (*P*>0.999; Table 2). KM was similar in study and control sides in ß-TCP-treated (*P*>0.999) and BCP-treated patients (*P*>0.999; Table 2). KM was similar between study and control sides in bilaterally-treated patients (*P*=0.500; Table 2). Clinical and radiological outcomes of SVF-supplementation at the site level are summarized in Table S2, S4.

At the implant level, PI was similar between study and control sides in ß-TCP-treated (*P*=0.240), and BCP-treated patients (*P*=0.898; Table 3). PI was similar between study and control sides in bilaterally-treated patients (*P*>0.999; Table 3). KM was similar in study and control sides in ß-TCP-treated (*P*>0.999) and BCP-treated patients (*P*>0.999; Table 3). KM was similar between study and control sides in bilaterally-treated patients (*P*=0.218; Table 3).

Technical complications

All initially placed suprastructures were still in function (~10 years). No implant, connection, or suprastructure-related technical complications were observed.

Table 3. Clinical (sulcus bleeding index, probing depth, plaque index, width of keratinized mucosa) and radiological (marginal bone loss) outcomes of SVF-supplementation at the implant level at 10-year follow-up

	Implant level (#dental implants)								
	ß-TCP			BCP			ß-TCP or BCP		
	Unilateral (2 patients) Bilateral (3 patients)			Unilateral (2 patients) Bilateral (3 patients)			Bilateral (6 patients)		
	Control side - stem cells (n=9)	Study side + stem cells (n=14)	P	Control side - stem cells (n=7)	Study side + stem cells (n=14)	P	Control side - stem cells (n=16)	Study side + stem cells (n=17)	P
Sulcus bleeding index (SBI)									
0	2	1		0	2		2	1	
1	1	9	0.405	4	10	0.092	5	13	0.146
2	6	3		2	2		8	3	
3	0	1		1	0		1	0	
Probing depth (PD; mm)									
0 – 3	0	1		1	0		1	1	
4 – 5	5	10	0.250	4	12	0.677	9	13	0.343
6 – 7	4	3		1	2		5	3	
8 – 9	0	0		1	0		1	0	
Plaque index (PI)									
0	9	11		4	7		13	13	
1	0	3	0.240	3	6	0.898	3	3	>0.999
2	0	0		0	1		0	1	
3	0	0		0	0		0	0	
Width keratinized mucosa (KM; mm)									
≥ 2	9	13	>0.999	6	11	>0.999	15	12	0.218
0 – 1	0	1		1	3		1	5	
Marginal bone loss (mm)									
0 – 2	5	12		6	13		11	16	
3 – 4	4	2	0.162	0	1	0.767	4	1	0.188
5 – 6	0	0		1	0		1	0	

For each implant the highest value of sulcus bleeding index, probing depth, plaque index, marginal bone loss was scored, as well as the lowest value of width of keratinized mucosa. *Study side significantly different from control side, $P<0.05$. ß-TCP, ß-tricalcium phosphate; BCP, biphasic calcium phosphate; n, number of implants.

Graft and residual maxillary sinus characteristics

Schneiderian mucosal hypertrophy was observed at 10-year follow-up in the study side of one ß-TCP-treated patient (pt#4), and in study and control sides of four BCP-treated patients (pt#6: study and control sides; pt#7: control side; pt#8: study side; pt#10: study side; Fig. 2; Table S4). Schneiderian mucosal hypertrophy was similar on radiographs pre-MSFE in all patients.

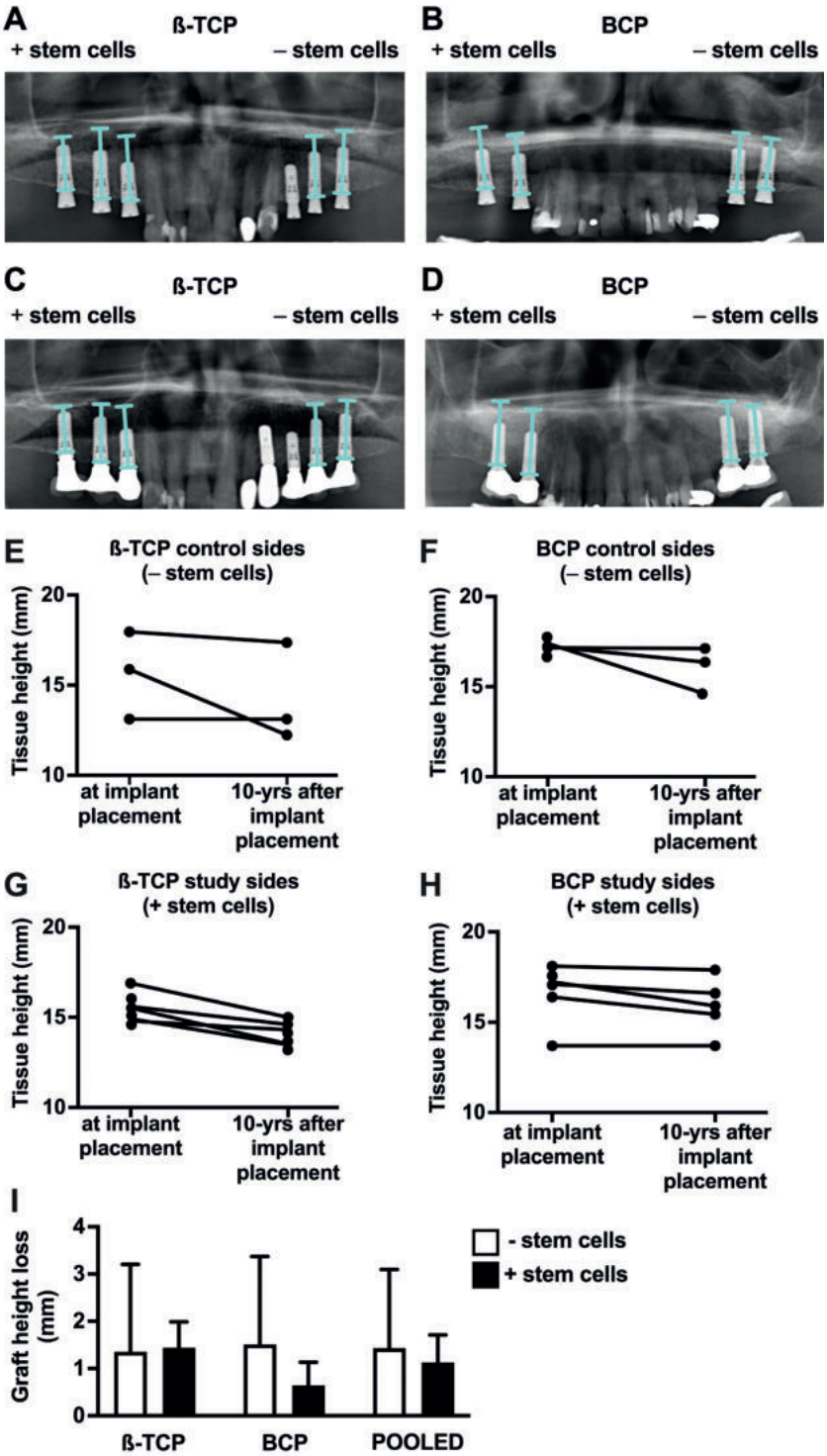
A
ß-TCP
+ stem cells
– stem cells
B
BCP
+ stem cells
– stem cells
C
ß-TCP
+ stem cells
– stem cells
D
BCP
+ stem cells
– stem cells
E
ß-TCP control sides
(– stem cells)
Tissue height (mm)
20
15
10
at implant placement
10-yrs after implant placement
F
BCP control sides
(– stem cells)
Tissue height (mm)
20
15
10
at implant placement
10-yrs after implant placement
G
ß-TCP study sides
(+ stem cells)
Tissue height (mm)
20
15
10
at implant placement
10-yrs after implant placement
H
BCP study sides
(+ stem cells)
Tissue height (mm)
20
15
10
at implant placement
10-yrs after implant placement
I
Graft height loss (mm)
4
3
2
1
0
- stem cells
+ stem cells
ß-TCP
BCP
POOLED

▶ **Figure 2. Tissue height, and graft height loss at the implant position at implant placement, and at 10-years after implant placement in β-TCP and BCP-treated patients with and without stem cells.** Representative panoramic radiographs: **(A)** Immediately after dental implant placement in a patient treated with β-TCP only and β-TCP plus stem cells. **(B)** Immediately after dental implant placement in a patient treated with BCP only and BCP plus stem cells. **(C)** 10-years after implant placement in a patient treated with β-TCP only and β-TCP plus stem cells. **(D)** 10-years after implant placement in a patient treated with BCP only and BCP plus stem cells. Blue line: Tissue height at implant position. Tissue height at implant placement, and 10-years after implant placement in patients-treated with **(E)** β-TCP only (n=3), **(F)** BCP only (n=3), **(G)** β-TCP plus stem cells (n=5), **(H)** BCP plus stem cells (n=5). **(I)** Graft height loss at 10-years after implant placement in β-TCP only (n=3), β-TCP plus stem cells (n=5), BCP only (n=3), BCP plus stem cells (n=5), pooled β-TCP and BCP only (bilaterally-treated; n=6), pooled β-TCP and BCP plus stem cells (bilaterally-treated; n=6), n, number of patients.

No other pathologies were observed. Graft volume reduction was observed in all study and control sides in ß-TCP-treated and BCP-treated patients at 10-year follow-up, compared with 5-months post-MSFE (Fig. 3). Recognizable demarcation of the original maxillary sinus floor and homogenous graft structure was seen (Fig. 3 A, B, D). Bone-like structured graft was observed in study and control sides in all ß-TCP-treated patients (pt#1–pt#5), but only in study and control side in one out of five BCP-treated patients (pt#7; Fig. 3). A recognizable demarcation of radiopaque graft was observed in study sides in three ß-TCP-treated patients (pt#3–pt#5), and in study and control sides in all BCP-treated patients (pt#6–pt#10; Fig. 3). No radiopacities or radiolucencies were seen in the graft material (Fig. 3). Radiologically air-filled maxillary sinus was observed in study and control sides in all patients. Qualitative radiological outcomes of SVF-supplementation are summarized in Table S3.

Tissue height, and graft height loss

Tissue height between dental implant placement and 10-year follow-up was reduced (reduction range: 5.2–14.1%) in study and control sides in all patients (Fig. 2A–H). Graft height loss between dental implant placement and 10-year follow-up was similar between study and control sides in ß-TCP-treated (study: 1.35±0.55 mm; control: 1.44±1.88 mm; Fig. 2I), as well as in BCP-treated patients (study: 0.64±0.49 mm; control: 1.51±1.86 mm; Fig. 2J). Graft height loss between dental implant placement and 10-year follow-up was similar between study and control sides in bilaterally-treated patients (study: 1.13±0.58 mm; control: 1.43±1.66 mm; Fig. 2K). Radiological outcomes of SVF-supplementation at the site level are summarized in Table S2.

Correlations between different clinical and radiological outcomes

In control sides of ß-TCP-treated patients, the following significant correlations were observed: SBI and PD (mm; r=0.634), SBI and marginal bone loss (mm; r=0.592), PD (mm) and marginal bone loss (mm; r=0.738), KM (mm) and marginal bone loss (mm; r=-0.471; Table 4; P<0.05). In study sides of ß-TCP-treated patients, the only statistically significant correlation observed was between SBI and PD (mm; r=0.525; Table 4; P<0.05).

In control sides of BCP-treated patients, the following significant correlations were observed: SBI and PD (mm; r=0.729), SBI and marginal bone loss (mm; r=0.607), PD (mm) and marginal bone loss (mm; r=0.853; Table 4; P<0.05). In study sides of BCP-treated patients, statis-

tically significant correlation observed was observed between SBI and PD (mm; r=0.405), PD (mm) and marginal bone loss (mm; r=0.526; Table 4; P<0.05).

There was no statistical difference in (baseline) alveolar bone height between ß-TCP, ß-TCP+SVF, BCP, and BCP+SVF-treated sides. Moreover, no correlation between baseline alveolar bone height and graft height loss was found.

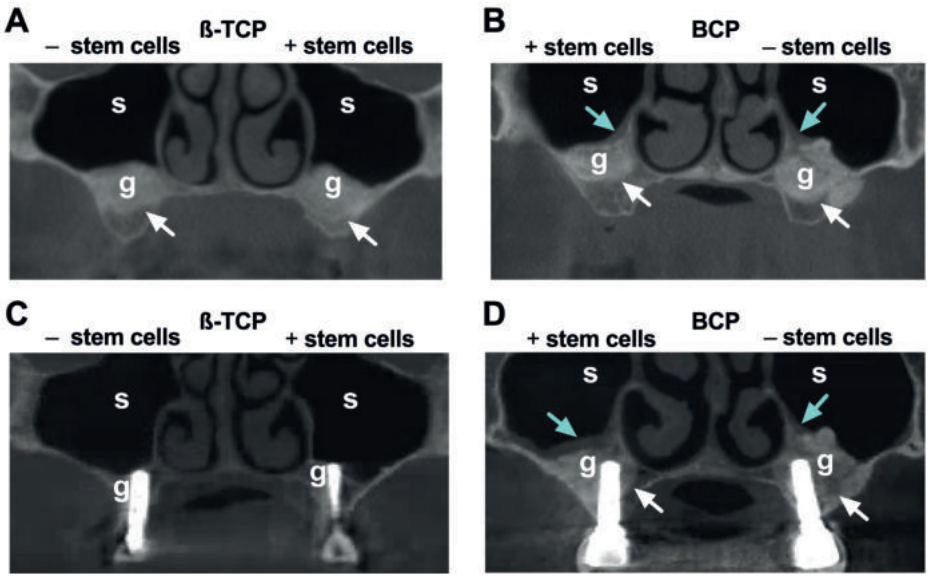

Figure 3. Cone beam computerized tomography (CBCT)-scans of β-TCP-treated and BCP-treated patients with and without stem cells at 5-months post-MSFE and at 10-years after implant placement. CBCT-scans of bilaterally-treated patients with: (A) β-TCP only and β-TCP plus stem cells, and **(B)** BCP plus stem cells and BCP only, at 5-months post-MSFE. In (A, B) homogenous radiopaque graft with a demarcation between residual native bone and the graft, and an air-filled residual maxillary sinus is visible. CBCT-scans of bilaterally-treated patients with: **(C)** β-TCP only and β-TCP plus stem cells, and **(D)** BCP plus stem cells and BCP only, at 10-years after implant placement. In (C, D) homogenous radiopaque graft, reduced graft volume, and an air-filled residual maxillary sinus is visible. g, graft; s, residual maxillary sinus; White arrows: demarcation original sinus floor; Blue arrows: Schneiderian mucosal hypertrophy.

Table 4. Correlation coefficient matrix of measured clinical (plaque index, sulcus bleeding index, probing depth, width of keratinized mucosa) and radiological outcomes (marginal bone loss) of SVF-supplementation at 10-year follow-up

		Control (- stem cells)				Study (+ stem cells)			
		Plaque index (PI)	Sulcus bleeding index (SBI)	Probing depth (PB; mm)	Width keratinized mucosa (KM; mm)	Plaque index (PI)	Sulcus bleeding index (SBI)	Probing depth (PD; mm)	Width keratinized mucosa (KM; mm)
ß-TCP	Plaque index (PI)	-	-	-	-	-	-	-	-
	Sulcus bleeding index (SBI)	0.000	-	-	-	0.000	-	-	-
	Probing depth (PD; mm)	0.000	**0.634**	-	-	0.000	**0.525**	-	-
	Width keratinized mucosa (KM; mm)	0.000	- 0.278	- 0.012	-	0.000	- 0.165	- 0.107	-
	Marginal bone loss (mm)	0.000	**0.592**	**0.738**	**- 0.471**	0.000	- 0.237	0.178	0.338
BCP	Plaque index (PI)	-	-	-	-	-	-	-	-
	Sulcus bleeding index (SBI)	0.000	-	-	-	0.000	-	-	-
	Probing depth (PD; mm)	0.000	**0.729**	-	-	0.000	**0.405**	-	-
	Width keratinized mucosa (KM; mm)	0.000	0.792	0.042	-	0.000	0.213	0.187	-
	Marginal bone loss (mm)	0.000	**0.607**	**0.853**	0.415	0.000	0.331	**0.526**	- 0.081

SVF, stromal vascular fraction; ß-TCP, ß-tricalcium phosphate; BCP, biphasic calcium phosphates. Bold values: significant at the 0.05 level.

DISCUSSION

In this 10-year prospective cohort study, SVF-supplementation in combination with calcium phosphate ceramics proofed to be safe for all patients undergoing MSFE. No adverse effects and pathology were found based on general health, clinical, and radiological assessments. A 100% implant survival rate was found in control sides of ß-TCP-treated patients, and study and control sides of BCP-treated patients. A 92.9% implant survival rate (100% after 6-months follow-up) was found in study sides of ß-TCP-treated patients, as a result of the loss of one implant. The failure was likely the result of premature loading by the temporary prosthesis.[7] Since this implant was completely positioned in residual native bone, the cause of failure was unlikely related to SVF-supplementation.

Stem cell-based therapies are associated with certain risks (*e.g.* tumor, biodistribution, etc.).[17] However, in our study no indications for safety concerns were found regarding SVF (containing ASCs)-application for MSFE. Similar clinical and radiological outcomes of dental implant success were observed in study and control sides of both ß-TCP-treated and BCP-treated patients. Moreover, graft-related problems resulting from the application of autologous ASCs in cranioplasty, *i.e.* graft resorption and late infection, have raised concerns about the long-term results of ASC-application in bone regeneration.[16] Regardless of stem cell-application, it should be noted that cranioplasty shows a 13-times higher complication rate requiring reoperation than MSFE using the lateral window technique due to the different nature of the surgical site, *i.e.* large critical sized, tumorigenic defect.[16,25] In our study, no patients reported any graft-related problems after MSFE, and showed 92.9–100% implant survival rate (100% following 6-months follow-up), which confirmed the successful long-term clinical outcomes after SVF-supplementation in jawbone reconstruction.

This study investigated peri-implantitis, which is a biofilm-associated pathological condition occurring in the tissues around an osseointegrated implant, characterized by bleeding on probing and/or suppuration and progressive loss of supporting bone.[26] We observed peri-implantitis in three out of ten patients (30% prevalence), which agrees with prevalence rates (15–34%) reported by others.[27–29] None of the established peri-implant disease risk factors (*i.e.* poor oral hygiene, prosthesis overcontouring, history of periodontitis, diabetes, and smoking)[30,31] were observed in these three peri-implantitis patients. One peri-implantitis patient did not receive implant maintenance for the last two years. Lack of implant maintenance may elevate the risk for peri-implantitis.[32] Implant maintenance therapy of peri-implant mucositis may prevent peri-implantitis onset.[33] Whether there is an association between keratinized mucosa and peri-implantitis is unclear.[32] In our study, we did not find a correlation between inadequate width of keratinized mucosa (<2 mm) and increased marginal bone loss. There was no difference in peri-implantitis prevalence between study and control sides. Therefore, SVF-supplementation did not affect peri-implantitis prevalence at 10-year follow-up.

Our results showed no correlation between baseline alveolar bone height varying from 4 to 8 mm and implant survival or graft height loss at 10-year follow-up. Others have also shown that alveolar bone height of more than 4 mm does not affect implant survival after MSFE using the

lateral window technique.[34] Long-term graft height stability after MSFE is an important factor for implant success.[35] We observed similar graft height loss in ß-TCP (14%) and BCP-treated (12%) patients at 10-year follow-up. The graft height loss in ß-TCP-treated patients was less compared to other reported studies at 5-year follow-up (28–39%).[36,37] The difference in graft height loss could be related to the heterogeneity in our relatively small study population. The graft height loss in BCP-treated patients did agree with other reported studies (9–24%) using BCP with different HA/β-TCP ratio, *i.e.* 20/80 (BCP20/80), 60/40 (BCP60/40), or 70/30 (BCP70/30), at 5-year[36] or 6-year follow-up.[38] A higher HA/ß-TCP ratio seems to decrease graft height loss.[36,38] SVF-supplementation seemed to inhibit (not significant) graft-height loss in study sides of BCP-treated patients but future studies with more patients are needed for verification.

We observed Schneiderian mucosal hypertrophy (>1 mm) pre-operatively in five patients (prevalence rate: 50%), which is in line with a prevalence rate (55%) reported by others[39]. The extent of pre-existing Schneiderian mucosal hypertrophy did not increase after MSFE during 10-year follow-up in all patients. Schneiderian membrane hypertrophy is characteristic of maxillary sinusitis, but also common in asymptomatic patients.[39] Moreover, no abnormalities (*i.e.* mucosal cysts, polyps, bone lesions, neoplasms, antroliths) in the maxillary sinus were observed after MSFE with SVF-supplementation. This indicates that SVF-supplementation did not induce abnormalities in the maxillary sinus, suggesting that no pathologic condition had developed, and that SVF-supplementation can be safely used in MSFE.

An expected moderate to strong correlation (r=0.5–1) between sulcus bleeding and marginal bone loss was found at control sides, but not study sides, of ß-TCP-treated patients. The absence of this correlation in the study sides might suggest a positive effect of SVF-supplementation on the peri-implant condition, since sulcus bleeding and marginal bone loss are symptoms of peri-implant tissue inflammation. Future studies with more patients are needed to reveal a possible effect of SVF-supplementation on peri-implant condition.

The study design resulted in potential observer bias, which is a limitation. The surgeons were not blinded for the type of graft during MSFE, and had prior knowledge of the research aims. Data collection and analysis at 10-year follow-up were performed blinded, thereby excluding observer bias. A limitation of our study was that no baseline radiographic and probing data after the first year of implant loading were recorded. Therefore, onset and progression of peri-implant disease could not be determined.

Our study used enzymatic preparation of ASCs, which is still the most frequently used method to isolate ASCs from adipose tissue.[40] However, in most countries this method is considered as "more than minimal manipulation" of stem cells.[40] The extensive use and manipulation of stem cells within a clinical setting has been hindered by the GMP regulations regarding "cell manufacturing". These regulations are not applicable to "minimally manipulated" stem cells according to the European Parliament and Council (EC regulation no. 1394/2007). Enzymatic preparation of ASCs, therefore, falls within the definition of an advanced therapy medicinal product according to the European Parliament and Council. Enzymatic preparation of ASC was considered a limitation of our study, based on European legislation. As an alternative method, mechanical disaggregation of the adipose tissue into small fat particles, so-called micro-fragmented fat (MFAT), has been investigated to decrease regulatory burden, and shorten

the translation into the clinical setting.[41–43] Intact microarchitecture of MFAT preserves a similar or even higher number of regenerative cells than the enzymatically derived SVF.[44–46]

Our previous phase-I study used general anesthesia to avoid complications during adipose tissue procurement and MSFE surgery.[7] Clinical studies using local anesthesia for liposuction are currently being undertaken.[47,48] This may broaden the applicability of SVF-supplementation to calcium phosphate ceramics by decreasing the treatment burden for patients, and improving the cost-effectiveness of the treatment.

Although the potential of ASCs evokes high expectations for the application of cellular bone tissue engineering,[8] clinical evidence of abdominal derived-ASC-application for oral and maxillofacial bone regeneration is limited to a few successful short-term outcomes (≤3-year follow-up).[7,13,49] To the best of our knowledge, no long-term results have been reported. Stem cell-application in regenerative medicine has raised safety concerns, *e.g.* tumorigenic potential and biodistribution.[17] This can only manifest itself in the long term. Therefore, clinical studies investigating long-term safety and efficacy are crucial before continuing with clinical application of (adipose) stem cells.

The primary objectives of the previous phase-I clinical study were feasibility and safety of SVF in combination with calcium phosphate ceramics in MSFE.[7] A power analysis could not be carried out, since there was no specific parameter to compare the groups. Also, a direct comparison between the four graft types, *i.e.* ß-TCP, ß-TCP+SVF, BCP, and BCP+SVF, was not done earlier, and therefore a multi-parameter evaluation was performed to identify potential differences in treatment outcome in an unbiased manner. A sample size of ten patients is commonly accepted for a (pilot) phase-I clinical study. Regardless of this low number of patients, the encouraging finding that SVF-supplementation is safe in both short and long-term certainly warrants further studies to evaluate whether *e.g.* using higher dosages of SVF, altered scaffold properties, or application of other adipose tissue processing methods may enhance bone formation without increasing side effects.

This study demonstrated for the first time the long-term safety of SVF-supplementation in combination with calcium phosphate ceramics in MSFE using the lateral window technique for jawbone reconstruction. SVF-supplementation enhanced bone regeneration in the short-term, as shown in our previous study,[7] and led to no abnormalities, clinically and radiologically, in the long-term. Future studies with more patients and higher SVF-dosages might further improve efficacy and open new possibilities for a variety of cell-based bone tissue engineering applications.

ACKNOWLEDGEMENTS

This work was granted by Health-Holland (project no. LSHM19016, “BB”) and ZonMW, the Netherlands organization for health research and development (project no. 116001009).

REFERENCES

1. Starch-Jensen T, Aludden H, Hallman M, Dahlin C, Christensen AE, Mordenfeld A. A systematic review and meta-analysis of long-term studies (five or more years) assessing maxillary sinus floor augmentation. *Int J Oral Maxillofac Surg.* 2018;47(1):103–116. doi:10.1016/j.ijom.2017.05.001
2. Stumbras A, Krukis MM, Januzis G, Juodzbalys G. Regenerative bone potential after sinus floor elevation using various bone graft materials: A systematic review. *Quintessence Int.* 2019;50(7):548–558. doi:10.3290/j.qi.a42482
3. Zijderveld SA, Zerbo IR, Van den Bergh JPA, Schulten EAJM, Ten Bruggenkate CM. Maxillary sinus floor augmentation using a β-tricalcium phosphate (Cerasorb) alone compared to autogenous bone grafts. *Int J Oral Maxillofac Implants.* 2005;20(3):432–440.
4. Jeong J, Kim JH, Shim JH, Hwang NS, Heo CY. Bioactive calcium phosphate materials and applications in bone regeneration. *Biomater Res.* 2019;23(1):4. doi:10.1186/s40824-018-0149-3
5. Gimble JM, Bunnell BA, Guilak F. Human adipose-derived cells: An update on the transition to clinical translation. *Regen Med.* 2012;7(2):225–235. doi:10.2217/rme.11.119
6. Grayson WL, Bunnell BA, Martin E, Frazier T, Hung BP, Gimble JM. Stromal cells and stem cells in clinical bone regeneration. *Nat Rev Endocrinol.* 2015;11(3):140–150. doi:10.1038/nrendo.2014.234
7. Prins HJ, Schulten EAJM, Ten Bruggenkate CM, Klein-Nulend J, Helder MN. Bone regeneration using the freshly isolated autologous stromal vascular fraction of adipose tissue in combination with calcium phosphate ceramics. *Stem Cells Transl Med.* 2016;5(10):1362–1374.
8. Wu V, Helder MN, Bravenboer N, Ten Bruggenkate CM, Jin J, Klein-Nulend J, Schulten EAJM. Bone tissue regeneration in the oral and maxillofacial region: A review on the application of stem cells and new strategies to improve vascularization. *Stem Cells Int.* 2019:6279721. doi:10.1155/2019/6279721
9. Farré-Guasch E, Bravenboer N, Helder MN, Schulten EAJM, Ten Bruggenkate CM, Klein-Nulend J. Blood vessel formation and bone regeneration potential of the stromal vascular fraction seeded on a calcium phosphate scaffold in the human maxillary sinus floor elevation model. *Materials (Basel).* 2018;11(1):116. doi:10.3390/ma11010161
10. Ferroni L, De Francesco F, Pinton P, Gardin C, Zavan B. Methods to isolate adipose tissue-derived stem cells. *Methods Cell Biol.* 2022;171:215-228. doi:10.1016/bs.mcb.2022.04.011
11. De Francesco F, Ricci G, D'Andrea F, Nicoletti GF, Ferraro GA. Human adipose stem cells: From bench to bedside. *Tissue Eng Part B Rev. 2015;21(6):572-584. doi:10.1089/ten.TEB.2014.0608*
12. Helder MN, Knippenberg M, Klein-Nulend J, Wuisman PIJM. Stem cells from adipose tissue allow challenging new concepts for regenerative medicine. *Tissue Eng.* 2007;13(8):1799–1808. doi:10.1089/ten.2006.0165
13. Sándor GK, Tuovinen VJ, Wolff J, Patrikoski M, Jokinen J, Nieminen E, Mannerström B, Lappalainen O, Seppänen R, Miettinen S. Adipose stem cell tissue-engineered construct used to treat large anterior mandibular defect: A case report and review of the clinical application of good manufacturing practice-level adipose stem cells for bone regeneration. *J Oral Maxillofac Surg.* 2013;71(5):938–950. doi:10.1016/j.joms.2012.11.014
14. Sándor GK, Numminen J, Wolff J, Thesleff T, Miettinen A, Tuovinen VJ, Mannerström B, Patrikoski M, Seppänen R, Miettinen S, Rautiainen M, Öhman J. Adipose stem cells used to reconstruct 13 cases with cranio-maxillofacial hard-tissue defects. *Stem Cells Transl Med.* 2014;3(4):530–540.

15. Thesleff T, Lehtimäki K, Niskakangas T, Mannerström B, Miettinen S, Suuronen R, Öhman J. Cranioplasty with adipose-derived stem cells and biomaterial: A novel method for cranial reconstruction. *Neurosurgery.* 2011;68(6):1535–1540. doi:10.1227/NEU.0b013e31820ee24e

16. Thesleff T, Lehtimäki K, Niskakangas T, Huovinen S, Mannerström B, Miettinen S, Seppänen-Kaijansinkko R, Öhman J. Cranioplasty with adipose-derived stem cells, beta-tricalcium phosphate granules and supporting mesh: Six-year clinical follow-up results. *Stem Cells Transl Med.* 2017;6:1576–1582.

17. Heslop JA, Hammond TG, Santeramo I, Tort Piella A, Hopp I, Zhou J, Baty R, Graziano EI, Proto Marco B, Caron A, Sköld P, Andrews PW, Baxter MA, Hay DC, Hamdam J, Sharpe ME, Patel S, Jones DR, Reinhardt J, Danen EH, Ben-David U, Stacey G, Björquist P, Piner J, Mills J, Rowe C, Pellegrini G, Sethu S, Antoine DJ, Cross MJ, Murray P, Williams DP, Kitteringham NR, Goldring CE, Park BK. Concise review: Workshop review: Understanding and assessing the risks of stem cell-based therapies. *Stem Cells Transl Med.* 2015;4(4):389–400. doi:10.5966/sctm.2014-0110

18. Bourin P, Bunnell BA, Casteilla L, Dominici M, Katz AJ, March KL, Redl H, Rubin JP, Yoshimura K, Gimble JM. Stromal cells from the adipose tissue-derived stromal vascular fraction and culture expanded adipose tissue-derived stromal/stem cells: A joint statement of the international federation for adipose therapeutics and science (IFATS) and the international society for cellular therapy (ISCT). *Cytotherapy.* 2013;15(6):641–648. doi:10.1016/j.jcyt.2013.02.006

19. Naaijkens BA, Niessen HWM, Prins HJ, Krijnen PA, Kokhuis TJ, de Jong N, van Hinsbergh VW, Kamp O, Helder MN, Musters RJ, van Dijk A, Juffermans LJ. Human platelet lysate as a fetal bovine serum substitute improves human adipose-derived stromal cell culture for future cardiac repair applications. *Cell Tissue Res.* 2012;348(1):119–130. doi:10.1007/s00441-012-1360-5

20. Varma MJO, Breuls RGM, Schouten TE, Jurgens WJ, Bontkes HJ, Schuurhuis GJ, van Ham SM, van Milligen FJ. Phenotypical and functional characterization of freshly isolated adipose tissue-derived stem cells. *Stem Cells Dev.* 2007;16(1):91–104. doi:10.1089/scd.2006.0026

21. Von Elm E, Altman DG, Egger M, Pocock SJ, Gøtzsche PC, Vandenbroucke JP. The strengthening the reporting of observational studies in epidemiology (STROBE) statement: Guidelines for reporting observational studies. *Int J Surg.* 2014;12(12):1495–1499. doi:10.1016/j.ijsu.2014.07.013

22. Mombelli A, Van Oosten MA, Schurch Jr E, Land NP. The microbiota associated with successful or failing osseointegrated titanium implants. *Oral Microbiol Immunol.* 1987;2(4):145–151. doi:10.1111/j.1399-302x.1987.tb00298.x

23. Berglundh T, Armitage G, Araujo MG, Avila-Ortiz G, Blanco J, Camargo PM, Chen S, Cochran D, Derks J, Figuero E, Hämmerle CHF, Heitz-Mayfield LJA, Huynh-Ba G, Iacono V, Koo KT, Lambert F, McCauley L, Quirynen M, Renvert S, Salvi GE, Schwarz F, Tarnow D, Tomasi C, Wang HL, Zitzmann N. Peri-implant diseases and conditions: Consensus report of workgroup 4 of the 2017 world workshop on the classification of periodontal and peri-Implant diseases and conditions. *J Clin Periodontol.* 2018;45(Suppl 20):S286–S291. doi:10.1111/jcpe.12957

24. Van Strydonck DAC, Katsamakis S, Van der Weijden GA. Parodontale screening, diagnostiek en behandeling in de algemene praktijk. https://congressus-nvvp.s3-eu-west-1.amazonaws.com/files/76fda55ce78a4385aca3ff5322b7471d.pdf?Signature= JxjETpttxBNS9Cts5cqYThWkrXo%3D&-Expires=1674232659&AWSAccessKeyId=AKIAIUTTQ23AZYZKILZQ&response-content-disposition=inline%3Bfilename%3D2._MC_Richtlijn_Parodontale_Screening_met_PDF.pdf. Published 2020.

25. Pjetursson BE, Tan WC, Zwahlen M, Lang NP. A systematic review of the success of sinus floor elevation and survival of implants inserted in combination with sinus floor elevation: Part I: Lateral approach. *J Clin Periodontol.* 2008;35(Suppl 8):216–240. doi:10.1111/j.1600-051X.2008.01272.x

26. Schwarz F, Derks J, Monje A, Wang H. Peri-implantitis. *J Periodontol.* 2018;89(Suppl 1):S267–S290. doi:10.1002/JPER.16-0350

27. Derks J, Schaller D, Håkansson J, Wennström JL, Tomasi C, Berglundh T. Peri-implantitis - Onset and pattern of progression. *J Clin Periodontol.* 2016;43(4):383–388. doi:10.1111/jcpe.12535

28. Kordbacheh Changi K, Finkelstein J, Papapanou PN. Peri-implantitis prevalence, incidence rate, and risk factors: A study of electronic health records at a U.S. dental school. Clin Oral Implants Res. 2019;30(4):306–314. doi:10.1111/clr.13416

29. Renvert S, Lindahl C, Persson GR. Occurrence of cases with peri-implant mucositis or peri-implantitis in a 21-26 years follow-up study. *J Clin Periodontol.* 2018;45(2):233–240. doi:10.1111/jcpe.12822

30. Lindhe J, Meyle J. Peri-implant diseases: Consensus report of the sixth European workshop on periodontology. *J Clin Periodontol.* 2008;35(Suppl 8):282–285. doi:10.1111/j.1600-051X.2008.01283.x

31. Schwarz F, Alcoforado G, Guerrero A, Jönsson D, Klinge B, Lang N, Mattheos N, Mertens B, Pitta J, Ramanauskaite A, Sayardoust S, Sanz-Martin I, Stavropoulos A, Heitz-Mayfield L. Peri-implantitis: Summary and consensus statements of group 3. The 6th EAO Consensus Conference 2021. *Clin Oral Implants Res.* 2021;32(Suppl 21):245–253. doi:10.1111/clr.13827

32. Rodrigo D, Sanz-Sánchez I, Figuero E, Llodrá JC, Bravo M, Caffesse RG, Vallcorba N, Guerrero A, Herrera D. Prevalence and risk indicators of peri-implant diseases in Spain. *J Clin Periodontol.* 2018;45(12):1510–1520. doi:10.1111/jcpe.13017

33. Salvi G, Zitzmann N. The effects of anti-infective preventive measures on the occurrence of biologic implant complications and implant loss: A systematic review. *Int J Oral Maxillofac Implants.* 2014;29(Suppl):292–307. doi:10.11607/jomi.2014suppl.g5.1

34. Chao Y, Chen H, Mei C, Tu Y, Lu H. Meta-regression analysis of the initial bone height for predicting implant survival rates of two sinus elevation procedures. *J Clin Periodontol.* 2010;37(5):456–465. doi:10.1111/j.1600-051X.2010.01555.x

35. Hatano N, Shimizu Y, Ooya K. A clinical long-term radiographic evaluation of graft height changes after maxillary sinus floor augmentation with a 2:1 autogenous bone/xenograft mixture and simultaneous placement of dental implants. *Clin Oral Implants Res.* 2004;15(3):339–345. doi:doi: 10.1111/j.1600-0501.2004.00996.x

36. Bouwman WF, Bravenboer N, Ten Bruggenkate CM, Eijsackers FA, Stringa N, Schulten EAJM. Tissue level changes after maxillary sinus floor elevation with three types of calcium phosphate ceramics: A radiological study with a 5-year follow-up. *Materials (Basel).* 2021;14(6):1471. doi:10.3390/ma14061471

37. Zijderveld SA, Schulten EAJM, Aartman IHA, ten Bruggenkate CM. Long-term changes in graft height after maxillary sinus floor elevation with different grafting materials: radiographic evaluation with a minimum follow-up of 4.5 years. *Clin Oral Implants Res.* 2009:691–700. doi:10.1111/j.1600-0501.2008.01697.x

38. Cha J, Kim C, Pae H, Lee J, Jung U, Choi S. Maxillary sinus augmentation using biphasic calcium phosphate: Dimensional stability results after 3–6 years. *J Periodontal Implant Sci.* 2019;49(1):47–57. doi:10.5051/jpis.2019.49.1.47

39. Lana JP, Carneiro PMR, Machado V de C, De Souza PEA, Manzi FR, Horta MC. Anatomic variations and lesions of the maxillary sinus detected in cone beam computed tomography for dental implants. *Clin Oral Implants Res.* 2012;23(12):1398–1403. doi:10.1111/j.1600-0501.2011.02321.x

40. Trivisonno A, Alexander RW, Baldari S, Cohen SR, Rocco GD, Genitle P, Magalon G, Magalon J, Miller R, Womack H, Toietta G. Concise review: Intraoperative strategies for minimal manipulation of autologous adipose tissue for cell- and tissue-based therapies. *Stem Cells Transl Med.* 2019; 8(12):1265-1271. doi:10.1002/sctm.19-0166

41. Busato A, De Francesco F, Biswas R, Mannuci S, Conti G, Fracasso G, Conti A, Riccio V, Riccio M, Sbarbati A. Simple and rapid non-enzymatic procedure allows the isolation of structurally preserved connective tissue micro-fragments enriched with SVF. *Cells.* 2020;10(1):36. doi:10.3390/cells10010036

42. Senesi L, De Francesco F, Marchesini A, Pangrazi PP, Bertolini M, Riccio V, Riccio M. Efficacy of adipose-derived mesenchymal stem cells and stromal vascular fraction alone and combined to biomaterials in tendinopathy or tendon injury: Systematic review of current concepts. *Medicina (Kaunas).* 2023;59(2):273. doi:10.3390/medicina59020273

43. Sesé B, Sanmartín JM, Ortega B, Matas-Palau A, Llull R. Nanofat cell aggregates: A nearly constitutive stromal cell inoculum for regenerative site-specific therapies. *Plast Reconstr Surg.* 2019;144(5):1079-1088. doi:10.1097/PRS.0000000000006155

44. Vezzani B, Shaw I, Lesme H, Yong L, Khan N, Tremolada C, Péault B. Higher pericyte content and secretory activity of microfragmented human adipose tissue compared to enzymatically derived stromal vascular fraction. *Stem Cells Transl Med.* 2018;7(12):876-886. doi:10.1002/sctm.18-0051

45. Senesi L, De Francesco F, Farinelli L, Manzotti S, Gagliardi G, Papalia GF, Riccio M, Gigante A. Mechanical and enzymatic procedures to isolate the stromal vascular fraction from adipose tissue: Preliminary results. *Front Cell Dev Biol.* 2019;7:88. doi:10.3389/fcell.2019.00088

46. De Francesco F, Mannucci S, Conti G, Prè ED, Sbarbati A, Riccio M. A non-enzymatic method to obtain a fat tissue derivative highly enriched in adipose stem cells (ASCs) from human lipoaspirates: Preliminary results. *Int J Mol Sci.* 2018;19(7):2061. doi:10.3390/ijms19072061

47. Boeni R, Waechter-Gniadek P V. Safety of tumescent liposuction under local anesthesia in 9,002 consecutive patients. *Dermatol Surg.* 2021;47(5):e184–e187. doi:10.1097/DSS.0000000000002987

48. Goldman JJ, Wang WZ, Fang XH, Williams SJ, Baynosa RC. Tumescent liposuction without lidocaine. *Plast Reconstr Surg Glob Open.* 2016;4(8):e829. doi:10.1097/GOX.0000000000000830

49. Castillo-Cardiel G, López-Echaury AC, Saucedo-Ortiz JA, Fuentes-Orozco C, Michel-Espinoza LR, Irusteta-Jiménez L, Salazar-Parra M, González-Ojeda A. Bone regeneration in mandibular fractures after the application of autologous mesenchymal stem cells, a randomized clinical trial. *Dent Traumatol.* 2017;33(1):38-44. doi:10.1111/edt.12303

SUPPLEMENTARY MATERIALS

Table S1. Radiological data per patient

	Panoramic radiograph								CBCT-scan				
Pt#	T=0	T=1	T=2	T=3	T=4	T=5	T=6	T=7	T=0	T=2	T=5	T=6	T=7
1	x	x	x	x	x	x		x	x	x			x
2	x	x	x	x	x	x	x	x	x	x		x	x
3	x	x	x	x	x		x	x	x	x	x	x	x
4	x	x	x	x	x	x	x	x	x	x			x
5	x	x	x	x	x	x		x	x	x	x		x
6	x	x	x	x	x	x	x	x	x	x	x	x	x
7	x	x	x	x	x			x	x	x			x
8	x	x	x	x	x			x	x	x			x
9	x	x	x	x	x			x	x	x			x
10	x	x	x	x	x	x	x	x	x	x		x	x

Panoramic radiograph and cone beam-computerized tomography (CBCT)-scan taken per patient per visit. T0=intake; T1=directly after maxillary sinus floor elevation (MSFE); T2=5-months post-MSFE (ridgemapping visit); T3=6-months post-MSFE(directly after implant placement); T4=9-months post-MSFE(osseointegration check visit); T5=18-months post-MSFE (1-year after implant placement); T6=36-months post-MSFE (2.5-years after implant placement); T7=126-months post-MSFE (10-years after implant placement).

Table S2. Radiological outcomes of SVF-supplementation at the site level at 10-years follow-up.

		Marginal bone loss (mm)						Tissue height (mm) at implant position			
		Control (- stem cells)			Study (+ stem cells)			Control (- stem cells)		Study (+ stem cells)	
Pt#	Graft	Imp	M	D	Imp	M	D	Imp		Imp	
1	ß-TCP	14	3	3	24	0	0	14	n.a.	24	n.a.
	ß-TCP	15	4	4	25	1	2	15	12	25	14
	ß-TCP	16	3	4	26	1	0	16	12	26	13
2	ß-TCP	24	2	1	14	0	1	24	n.a.	14	16
	ß-TCP	25	1	0	15	0	0	25	18	15	16
	ß-TCP	26	0	0	16	1	1	26	17	16	13
3	ß-TCP	14	1	3	25	0	1	14	n.a.	25	16
	ß-TCP	15	1	1	26	1	1	15	14	26	14
	ß-TCP	16	0	0	27	1	1	16	12	27	13
4	ß-TCP				24	3	3			24	n.a.
	ß-TCP				25	0	1			25	17
	ß-TCP				26	0	0			26	12
5	ß-TCP				15	0	3			15	15
	ß-TCP				16	0	0			16	12
6	BCP	24	0	0	14	0	0	24	17	14	n.a.
	BCP	26	0	0	15	0	0	26	17	15	16
	BCP				16	0	0			16	15
7	BCP	25	0	0	15	0	0	25	16	15	n.a.
	BCP	26	0	0	16	0	2	26	15	16	16
	BCP	27	5	6	17	3	2	27	13	17	16
8	BCP				14	0	0			14	18
	BCP				15	0	0			15	16
	BCP				16	0	0			16	16
9	BCP				23	1	1			23	n.a.
	BCP				25	1	1			25	14
	BCP				26	1	1			26	13
10	BCP	25	0	0	15	0	0	25	22	15	18
	BCP	26	0	0	16	0	0	26	19	16	18

For each implant the marginal bone loss (mm) was determined at the mesial and distal implant surface, and the tissue height (mm) and graft height loss (mm) at the implant mid-axis and at inter-implant (distal) position on the panoramic radiograph. SVF, stromal vascular fraction, Pt#, patient number; Imp, implant position; M, mesial; D, distal; ß-TCP, ß-tricalcium phosphate; BCP, biphasic calcium phosphates.

	Graft height loss (mm) at implant position				Tissue height (mm) at inter-implant (distal) position				Graft height loss (mm) at inter-implant (distal) position			
	Control (- stem cells)		Study (+ stem cells)		Control (- stem cells)		Study (+ stem cells)		Control (- stem cells)		Study (+ stem cells)	
	Imp		Imp		Imp		Imp		Imp		Imp	
	14	n.a.	24	n.a.	14	13	24	17	14	2	24	0
	15	4	25	2	15	14	25	13	15	2	25	1
	16	4	26	1	16	11	26	10	16	7	26	2
	24	n.a.	14	1	24	16	14	15	24	3	14	2
	25	0	15	2	25	16	15	14	25	0	15	4
	26	1	16	4	26	15	16	13	26	1	16	1
	14	n.a.	25	0	14	15	25	17	14	2	25	0
	15	0	26	2	15	12	26	17	15	0	26	2
	16	0	27	0	16	12	27	16	16	3	27	1
			24	n.a.			24	20			24	0
			25	2			25	13			25	2
			26	0			26	9			26	0
			15	2			15	13			15	1
			16	2			16	14			16	0
	24	0	14	n.a.	24	18	14	16	24	1	14	0
	26	0	15	1	26	17	15	13	26	0	15	2
			16	1			16	13			16	2
	25	1	15	n.a.	25	15	15	15	25	1	15	0
	26	1	16	1	26	17	16	16	26	0	16	1
	27	6	17	1	27	14	17	15	27	6	17	1
			14	0			14	17			14	1
			15	1			15	16			15	0
			16	0			16	17			16	0
			23	n.a.			23	n.a.			23	n.a.
			25	0			25	14			25	1
			26	0			26	12			26	1
	25	0	15	0	25	17	15	18	25	0	15	0
	26	2	16	0	26	17	16	18	26	1	16	0

Table S3. Qualitative radiological outcomes of SVF-supplementation at 10-years follow-up on panoramic radiograph and cone beam computerized tomography (CBCT)-scan.

	Pt#1				Pt#2					Pt#3					Pt#4		Pt#5	
	Control - stem cells		Study + stem cells		Control - stem cells		Study + stem cells			Control - stem cells		Study + stem cells			Study + stem cells		Study + stem cells	
	Imp		Imp		Imp		Imp			Imp		Imp			Imp		Imp	
	15	16	25	26	25	26	14	15	16	15	16	25	26	27	25	26	15	16
Panoramic radiograph																		
Irregularities sinus floor																		
Recognizable demarcation original sinusfloor	x	x	x	x	x	x	x	x	x	x	x	x	x	x	x	x	x	x
Homogenous graft structure	x	x	x	x	x	x	x	x	x	x	x	x	x	x	x	x	x	x
Recognizable demarcation radio-opaque graft															x	x	x	x
Bone-like structured graft	x	x	x	x	x	x	x	x	x	x	x	x	x	x				
Radiopacities in the graft																		
Radiolucencies in the graft																		
Scalloping of the graft												x	x	x		x		
Air-filled residual maxillary sinus	x	x	x	x	x	x	x	x	x	x	x	x	x	x	x	x	x	x
Schneiderian mucosal hypertrophy															x	x		
Pathology																		
β-TCP																		
CBCT-scan																		
Irregularities sinus floor																		
Recognizable demarcation original trapdoor								x			x			x				
Recognizable demarcation original sinusfloor																		x
Homogenous graft structure	x	x	x	x	x	x	x	x	x	x	x	x	x		x	x	x	x
Recognizable demarcation radio-opaque graft														x				
Bone-like structured graft	x	x	x	x	x	x	x	x	x	x	x	x	x		x	x	x	x
Radiopacities in the graft																		
Radiolucencies in the graft																		
Scalloping of the graft (buc-pal)		x		x												x		
Air-filled residual maxillary sinus	x	x	x	x	x	x	x	x	x	x	x	x	x	x	x	x	x	x
Schneiderian mucosal hypertrophy															x	x		
Pathology																		

		Pt#6				Pt#7					Pt#8			Pt#9		Pt#10			
		Control - stem cells		Study + stem cells		Control - stem cells			Study + stem cells		Study + stem cells			Study + stem cells		Control - stem cells		Study + stem cells	
		Imp		Imp		Imp			Imp		Imp			Imp		Imp		Imp	
		24	26	15	16	25	26		16	17	14	15	16	25	26	25	26	14	15
BCP	Panoramic radiograph																		
	Irregularities sinus floor													x	x	x	x		
	Recognizable demarcation original sinusfloor	x	x	x	x	x	x	x	x	x	x	x	x	x	x	x	x	x	x
	Homogenous graft structure	x	x	x	x	x	x	x	x	x	x	x	x	x	x	x	x	x	x
	Recognizable demarcation radio-opaque graft	x	x	x	x	x	x	x	x	x	x	x	x	x	x	x	x	x	x
	Bone-like structured graft																		
	Radiopacities in the graft																		
	Radiolucencies in the graft																		
	Scalloping of the graft																		
	Air-filled residual maxillary sinus	x	x	x	x	x	x	x	x	x	x	x	x	x	x	x	x	x	x
	Schneiderian mucosal hypertrophy	x	x	x	x						x	x	x						
	Pathology																		
	CBCT-scan																		
	Irregularities sinus floor													x	x		x		
	Recognizable demarcation original trapdoor	x	x	x	x														
	Recognizable demarcation original sinusfloor										x	x		x	x	x	x	x	x
	Homogenous graft structure	x	x	x		x	x	x	x	x	x	x	x					x	x
	Recognizable demarcation radiopaque graft	x	x	x	x											x	x	x	x
	Bone-like structured graft					x	x	x	x	x									
	Radiopacities in the graft																		
	Radiolucencies in the graft																		
	Scalloping of the graft (buc-pal)					x	x	x	x	x		x	x						
	Air-filled residual maxillary sinus	x	x	x	x	x	x	x	x	x	x	x	x	x	x	x	x	x	x
	Schneiderian mucosal hypertrophy	x	x	x	x	x	x	x			x					x			
	Pathology																		

SVF, stromal vascular fraction; β-TCP, ß-tricalcium phosphate; BCP, biphasic calcium phosphate; CBCT, cone beam computerized tomography.

Table S4. Clinical outcomes of SVF-supplementation at the site level at 10-years follow-up

		Plaque Index										Probing Depth (mm)										Sulcus Bleeding Index									
		Control (– stem cells)					Study (+ stem cells)					Control (– stem cells)					Study (+ stem cells)					Control (– stem cells)					Study (+ stem cells)				
Pt#	Graft	Imp	M	B	D	P	Imp	M	B	D	P	Imp	M	B	D	P	Imp	M	B	D	P	Imp	M	B	D	P	Imp	M	B	D	P
1	ß-TCP	14	0	0	0	0	24	0	0	0	0	14	7	5	7	4	24	5	3	3	3	14	1	2	2	1	24	1	1	0	1
	ß-TCP	15	0	0	0	0	25	0	0	0	0	15	4	6	8	6	25	5	3	4	4	15	2	2	2	2	25	1	1	1	1
	ß-TCP	16	0	0	0	0	26	0	0	0	0	16	7	4	7	6	26	5	3	5	4	16	2	2	2	2	26	2	1	1	2
2	ß-TCP	24	0	0	0	0	14	0	0	0	0	24	6	4	5	5	14	2	2	4	2	24	2	2	2	2	14	0	0	1	0
	ß-TCP	25	0	0	0	0	15	0	0	0	0	25	5	4	5	5	15	2	2	4	2	25	1	0	0	2	15	0	0	1	0
	ß-TCP	26	0	0	0	0	16	0	0	0	0	26	3	3	3	4	16	2	3	2	3	26	2	0	0	2	16	0	1	0	0
3	ß-TCP	14	0	0	0	0	25	0	0	0	0	14	5	2	5	3	25	7	2	4	2	14	1	0	0	0	25	1	0	0	0
	ß-TCP	15	0	0	0	0	26	0	0	0	0	15	4	2	4	2	26	4	3	4	4	15	0	0	0	0	26	1	0	1	1
	ß-TCP	16	0	0	0	0	27	0	0	0	0	16	4	2	4	2	27	4	2	3	5	16	0	0	0	0	27	1	0	0	1
4	ß-TCP						24	0	0	0	0						24	7	3	6	6						24	0	1	0	3
	ß-TCP						25	0	0	0	0						25	4	2	6	3						25	0	0	0	1
	ß-TCP						26	0	0	0	0						26	4	2	4	4						26	1	0	2	1
5	ß-TCP						15	1	0	0	0						15	5	3	3	2						15	0	1	0	0
	ß-TCP						16	0	1	0	0						16	5	3	5	3						16	2	1	1	1
6	BCP	24	0	0	0	0	14	0	0	0	0	24	3	2	2	3	14	5	2	3	3	24	0	1	0	1	14	1	0	0	1
	BCP	26	0	0	0	0	15	0	0	0	0	26	4	2	4	3	15	5	3	4	3	26	0	0	1	1	15	1	0	0	1
	BCP						16	0	0	0	0						16	4	3	3	2						16	0	0	0	0
7	BCP	25	0	0	1	0	15	2	1	0	0	25	5	3	5	4	15	4	2	3	3	25	2	0	0	1	15	0	0	1	0
	BCP	26	1	0	1	0	16	0	0	1	0	26	5	3	5	5	16	5	2	6	3	26	2	0	0	1	16	1	0	1	0
	BCP	27	0	0	0	0	17	0	0	0	0	27	9	8	9	7	17	7	3	5	4	27	2	3	3	3	17	2	1	1	0
8	BCP						14	0	0	0	0						14	5	3	3	3						14	0	1	0	0
	BCP						15	0	0	0	0						15	5	3	3	3						15	0	0	0	1
	BCP						16	0	0	0	0						16	5	5	3	4						16	1	1	0	1
9	BCP						23	0	0	1	0						23	3	3	4	2						23	0	0	0	0
	BCP						25	0	0	1	0						25	5	2	3	2						25	1	0	1	0
	BCP						26	0	0	1	0						26	4	2	4	5						26	1	0	0	0
10	BCP	25	0	0	0	0	15	0	1	0	0	25	6	3	3	3	15	5	3	3	4	25	1	1	0	0	15	1	1	0	2
	BCP	26	0	1	0	0	16	0	1	0	0	26	3	2	4	5	16	3	2	4	3	26	1	1	0	2	16	1	1	1	1

For each implant the highest value of plaque index, sulcus bleeding index, and probing depth were scored. Plaque index was determined at the mesial, buccal, distal, and palatal implant surface: score 0: no plaque detected; score 1: plaque only recognized by running a probe across the smooth marginal implant surface; Score 2: plaque was seen by the naked eye; score 3: abundance of soft matter. Probing depth (mm) was determined at the mesial, buccal, distal, and palatal implant surface. Sulcus bleeding index was determined at the mesial, buccal, distal, and palatal implant surface: score 0: no bleeding when a periodontal probe was passed along the gingival margin adjacent to the implant; score 1: isolated bleeding spot visible; score 2: blood formed a confluent red line on margin; score 3: heavy or profuse bleeding. P-value: is based on Mann-Whitney U-test. SVF, stromal vascular fraction; ß-TCP, ß-tricalcium phosphate; BCP, biphasic calcium phosphates; Control, control side; Study, study side; n, total number of implants.

Table S5. Peri-implant health, peri-implantitis, and peri-mucositis around dental implants in ß-TCP and BCP-treated patients with and without SVF-supplementation at 10-year follow-up.

Pt#	Control/study side	Graft material	Dental implant positions
1	Control	ß-TCP	**14, 15, 16**
	Study	ß-TCP	*24, 25, 26*
2	Control	ß-TCP	*24, 25, 26*
	Study	ß-TCP	*14, 15, 16*
3	Control	ß-TCP	*14,* 15, 16
	Study	ß-TCP	*25, 26, 27*
4	Study	ß-TCP	**24,** *25, 26*
5	Study	ß-TCP	*15, 16*
6	Control	BCP	*24, 26*
	Study	BCP	*14, 15, 16*
7	Control	BCP	*25, 26,* **27**
	Study	BCP	*15, 16,* **17**
8	Study	BCP	*14, 15, 16*
9	Study	BCP	23, *25, 26*
10	Control	BCP	*25, 26*
	Study	BCP	*15, 16*

Peri-implant health, peri-implantitis, and peri-mucositis at 10-year follow-up. The control side was treated with only a calcium phosphate bone substitute, and the study wide was treated with a calcium phosphate bone substitute with SVF-supplementation. The dental implant positions are given according to the Fédération Dentaire Internationale system. Peri-implant health, underline; Peri-implantitis, bold; Peri-mucositis, italics. Pt#, patient number; ß-TCP, ß-tricalcium phosphate; BCP, biphasic calcium phosphate.

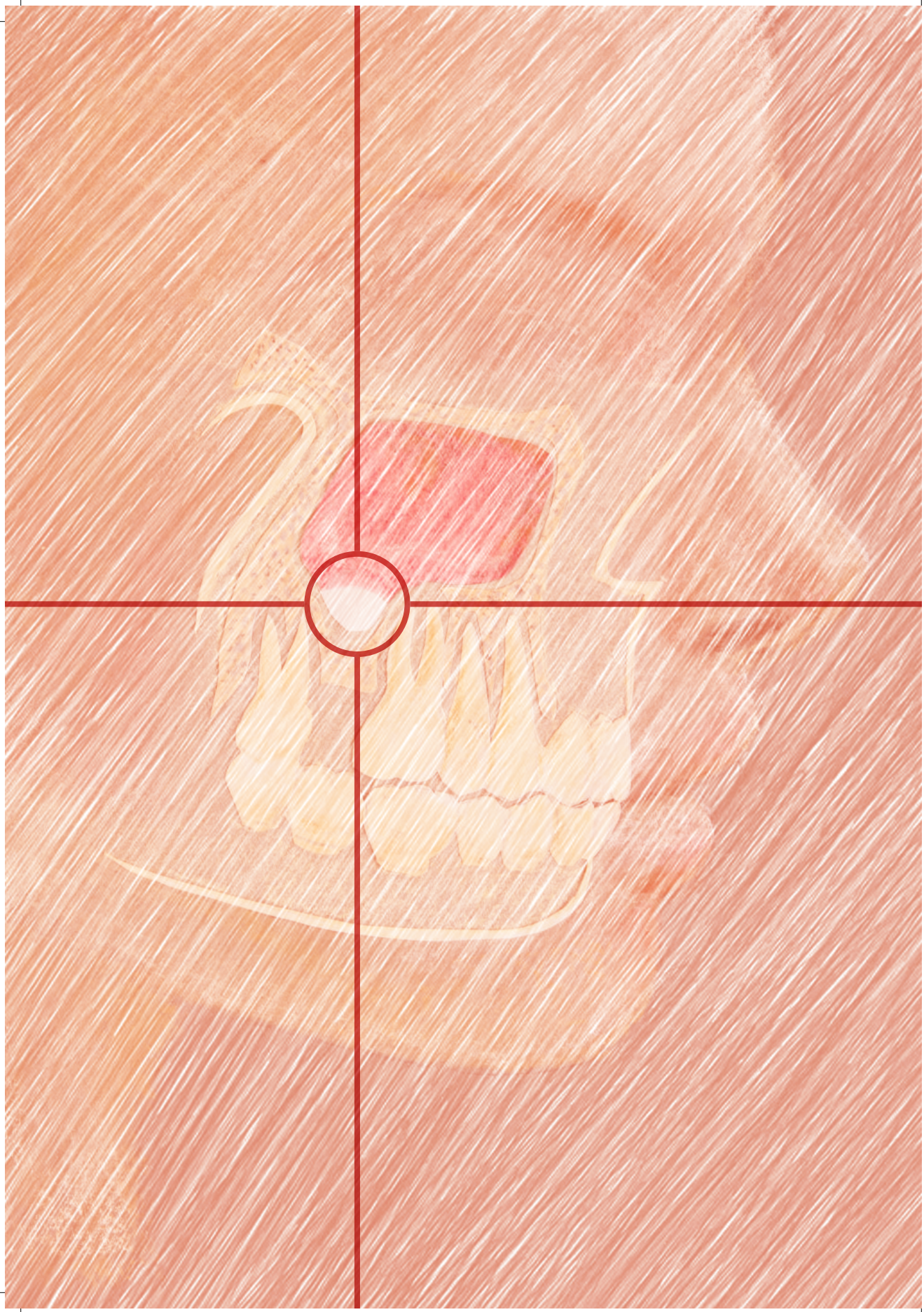

CHAPTER 7

General discussion

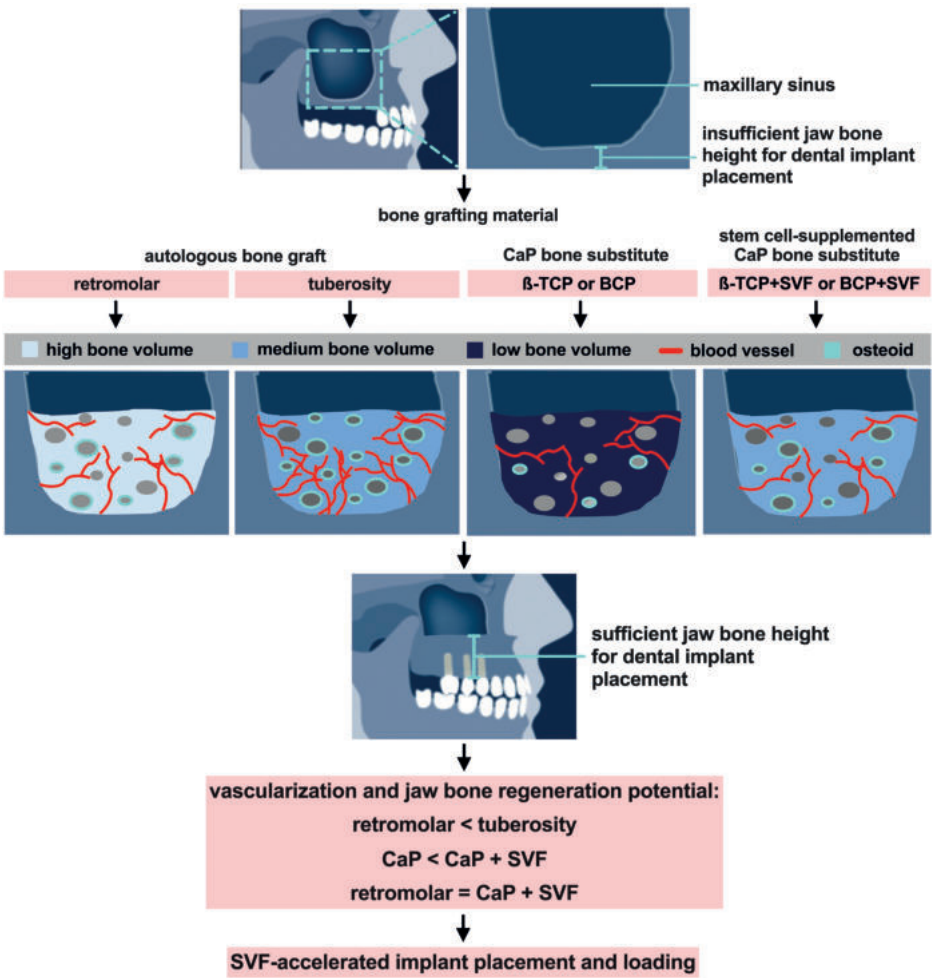

Figure 1. Schematic presentation of bone regeneration and vascularization potential of different bone grafting materials in maxillary sinus floor elevation (MSFE). Insufficient bone height in the lateral maxilla to allow dental implant placement. Autologous bone graft (retromolar or tuberosity bone graft), calcium phosphate (CaP) bone substitute (β-tricalcium phosphate (β-TCP) or biphasic CaP (BCP)), or stem-cell supplemented CaP bone substitute (β-TCP + stromal vascular fraction (SVF) or BCP + SVF) were used as bone grafting material in MSFE. Highest bone volume was observed in retromolar bone graft, and lowest in CaP bone substitute. Similar bone volume was observed in tuberosity bone graft and CaP bone substitute + SVF. Highest vascularization was observed in tuberosity bone graft, and lowest in CaP bone substitute. Similar vascularization was observed in retromolar bone graft and CaP bone substitute + SVF. Highest osteoid volume was observed in tuberosity bone graft, and lowest in CaP bone substitute. Similar osteoid volume was observed in retromolar bone graft and CaP bone substitute + SVF. SVF-supplementation increased vascularization and osteoid volume in CaP bone substitute to a similar level of using retromolar bone graft in patients who had undergone MSFE. Therefore, SVF-supplementation might accelerate dental implant placement and loading (illustrations were adapted from the ITI Foundation, Basel, Switzerland). BCP, biphasic calcium phosphate; β-TCP, β-tricalcium phosphate; CaP, calcium phosphate; SVF, stromal vascular fraction.

GENERAL DISCUSSION

The overall aim of this thesis was to investigate bone formation and vascularization in jaw bone regeneration using different bone grafting materials, either or not supplemented with stromal vascular fraction (SVF), for dental implant placement.

In this thesis (**Chapters 3–6**), we used the maxillary sinus floor elevation (MSFE) as a human experimental model for the application and evaluation of different bone grafting materials **(Figure 1)**. Moreover, we used MSFE as a human "split-mouth" model for the application of a calcium phosphate bone substitute supplemented with SVF in jaw bone regeneration (**Chapters 5 and 6**). The MSFE model allows histological examination of biopsies that have been collected prior to dental implant placement without interfering with the clinical routine, as well as intra-patient treatment comparison when using a "split-mouth" design. MSFE is a suitable model to investigate bone regeneration without comorbidities of the surgical technique itself, since it has a low graft-failure rate (1.9%).[1] The maxillary sinus model provides a non-pathologic osteogenic chamber to assess the additive value of cellular bone tissue engineering for bone regeneration.

At present, there is no bone substitute available that has similar or superior biological properties compared with autologous bone graft, which is still considered the 'gold standard' graft material in MSFE. However, it is widely overlooked that even autologous bone may have varying efficacies depending on the harvesting site. This issue was addressed in **Chapter 3**, where we compared the mandibular retromolar and maxillary tuberosity regions which are common autologous bone donor sites due to low morbidity compared to other intraoral sites.[2–4] Using histological and histomorphometrical analysis, we evaluated the bone regeneration potential and vascularization (number of blood vessels) of both bone grafts. This is, to our knowledge, the first time that this comparison is made. We found that maxillary tuberosity bone (cancellous) graft compared to mandibular retromolar bone (cortical) graft, showed increased bone vitality and vascularization 4 months post-MSFE, likely due to faster bone remodeling or earlier start of new bone formation **(Figure 1)**. This is in agreement with findings by others that cortical bone graft, compared to cancellous bone graft, show delayed vascularization due to lack of porosity and consequent inhibition of vascular ingrowth.[5] It would be highly interesting to also investigate the bone regenerating process in biopsies taken at later time-points post-MSFE. Further studies are recommended to assess whether bone vitality and vascularization at the dental implant site affect clinical outcomes, *e.g.* primary stability, and implant survival and success. Based on those results, dental implant placement and loading protocols might be adjusted. Earlier dental implant placement and/or loading may lead to higher patient satisfaction. It might also stimulate the bone remodeling process and lamellar bone formation around the implant.[6]

In **Chapter 3**, we also showed that the number of osteocytes in the grafted area after MSFE is related to the type of autologous bone graft. A lower total number of osteocytes was found in the grafted area of the retromolar graft compared to the tuberosity graft, which may be the result of reduced diffusion of oxygen and nutrients due to delayed vascularization in the retromolar bone graft. Since mechanosensitive osteocytes play a crucial and governing role in the

micro-environment (niche) of the bone regeneration site,[7] the bone regeneration niche may be improved effectively and rapidly when osteocytes are optimally stimulated.

In **Chapter 4**, we demonstrated significant local differences in osteocyte surface area and orientation in residual native jaw bone after MSFE using ß-tricalcium phosphate (ß-TCP) bone substitute, which seemed to relate to local differences in tensile strain magnitude and orientation. It was shown that the osteocyte surface area was 1.5-times larger in the gap (two teeth adjacent to the implant site), than in the free-ending locations (one tooth adjacent to the implant site). Osteocyte morphology has been related to its mechanosensitivity.[8,9] Moreover, the elongated osteocytes in gap locations were more cranially-caudally oriented, resulting from high and uniformly directed tensile strain. Osteocytes are aligned to the collagen fiber orientation, which may correspond to the orientation of the tensile strain in the bone.[10,11] These findings suggest that the osteocytes in maxillary implant sites are affected by loading on adjacent teeth. Moreover, mechanical loading-regulated crosstalk between osteocytes and MSCs has been demonstrated.[12,13] Note that mechanical loading may not only affect osteocyte function, but also (pre)osteoblast behavior.[14,15] These findings suggest that accelerated dental implant loading might enhance the biomechanical stimulation of osteocytes and (pre) osteoblasts in the micro-environment (niche) of bone regeneration sites. Therefore, optimal biomechanical stimulation of osteocytes and (pre)osteoblasts might lead to accelerated bone regeneration at the dental implant site. Future studies are needed to elucidate the mechanism underlying the effect of mechanical loading on local bone cells at the bone regeneration site. In addition, we demonstrated that tuberosity bone graft in MSFE showed enhanced number of blood vessels and osteocytes compared to retromolar bone graft **(Chapter 3)**. These findings suggest that the type of bone grafting material in MSFE might affect the number of osteocytes in the grafted area by local vascularization potential. Therefore, vascularization strategies in jaw bone regeneration are highly recommended to be further investigated.

Bone formation has been related to angiogenesis in patients who underwent MSFE.[16–18] Autologous bone graft shows the highest bone regeneration potential compared to bone substitutes in MSFE. It is generally thought that the use of autograft in bone regeneration supports the neovascularization between graft and recipient site.[19] Vascularization of bone substitute in MSFE solely depends on the recipient's vascularity by angiogenesis. Enhanced blood vessel formation has been observed in autologous bone graft versus bone substitute at 3-months post-MSFE,[20] but similar blood vessel formation at 8–10 months post-MSFE.[16,21] To improve blood vessel formation in bone substitutes to levels similar to autologous bone, cellular bone tissue engineering has recently been proposed and actively pursued. Cellular tissue engineering/ regenerative medicine for oral and maxillofacial bone regeneration is moving rapidly into clinical application, such as adult MSCs originating from bone marrow (BMSCs), adipose tissue (ASCs), or dental tissue (DSCs) for MSFE,[22–26] alveolar cleft reconstruction,[27–31] jaw defect reconstruction,[32] periodontal defect regeneration,[33,34] mandibular condylar fracture regeneration,[35] and tooth socket preservation.[36,37] The application of human embryonic stem cells[38–40] and human induced pluripotent stem cells[41] for bone regeneration in the oral and maxillofacial region has only been investigated in *in vitro* and/or *in vivo* animal studies, but not in human studies. In **Chapter 2**, we reviewed important advancements of stem cell application and vascu-

larization in bone tissue regeneration in the oral and maxillofacial region. Cost-effectiveness and patient morbidity are challenges in clinical application of cellular bone tissue engineering. In this regard, the SVF of human adipose tissue is considered a promising single source for a heterogeneous population of essential cells with, amongst others, osteogenic and angiogenic potential. SVF-based vascularization strategies intend to enhance vascular ingrowth from the surrounding host tissue into the implanted graft by stimulating angiogenesis.[17] SVF is obtained from adipose tissue by digestion during a 45-60 min period,[22] providing a heterogenous population of cells showing osteogenic and angiogenic potential.[17,22] SVF-seeded scaffolds are bioactivated through a highly heterogeneous cell population, including native ASCs, mature endothelial cells, and hematopoietic cells.[42] SVF also contains macrophages, that secrete a multitude of vascular growth factors and cytokines.[43] SVF overcomes multiple drawbacks of other adult stem cells, *e.g.* BMSCs and DSCs. In contrast to BMSCs and DSCs, SVF can be applied in a one-step surgical procedure without costly and time-consuming culture expansion, due to the large quantities that can be harvested. Moreover, the frequency and potential of ASCs, compared to BMSCs, are less prone to ageing[44]. In this thesis (**Chapters 5 and 6**), we investigated patients who had received SVF harvested through adipose tissue liposuction under general anesthesia in a previous phase-I study.[22] General anesthesia has been used to avoid complications during adipose tissue procurement and MSFE surgery. Adipose tissue liposuction through local anesthesia could broaden the applicability of SVF by decreasing the treatment burden for the patients, and improving the cost-effectiveness of the treatment. Whether different types of local anesthesia do affect the osteogenic and angiogenic potential of SVF is not clear. Lidocaine anesthesia has been shown to result in contradictory results regarding ASC survival.[45–48] Lidocaine buffered by sodium bicarbonate[47], and ropivacaine[48] has been suggested as alternatives for lidocaine, which might improve ASC survival. Future investigation of SVF survival and quality, *e.g.* osteogenic and angiogenic potential, after local anesthesia are needed before clinical application in cellular bone tissue engineering can be considered. SVF-supplementation is more promising for clinical application than BMSCs and DSCs, since it is more cost-effective, and causes less patient morbidity.

We have previously shown that SVF supplementation of calcium phosphate bone substitute has a pro-angiogenic effect in patients treated with MSFE, compared to calcium phosphate bone substitute only.[17] To the best of our knowledge, differences in blood vessel formation and bone regeneration potential between bone substitute, either or not supplemented with SVF, and autologous bone graft ('gold standard') in MSFE are unknown. [49] In **Chapter 5**, we demonstrated that the highest osteoid volume was observed in tuberosity bone graft, and lowest in calcium phosphate bone substitute at 4–6 months post-MSFE (**Figure 1**). Similar osteoid volume was observed in retromolar bone graft and calcium phosphate bone substitute with SVF-supplementation (**Figure 1**). Highest bone volume was observed in retromolar bone graft, and lowest in calcium phosphate bone substitute at 4–6 months post-MSFE (**Figure 1**). Similar bone volume was observed in tuberosity bone graft and calcium phosphate bone substitute with SVF-supplementation (**Figure 1**). SVF-supplementation increased vascularization and osteoid volume in calcium phosphate bone substitute to a similar level of using retromolar bone graft at 4–6 months post-MSFE (**Figure 1**). This suggests that SVF-supplementation enhanced the vascu-

larization and bone regeneration potential of calcium phosphate bone substitute to a similar extent as retromolar bone graft at 4–6 months post-MSFE.

Although the potential of ASCs evokes high expectations for the application of cellular bone tissue engineering (**Chapter 2**), clinical evidence of abdominal derived-ASC-application for oral and maxillofacial bone regeneration is limited to a few successful short-term outcomes (≤3-year follow-up).[22,35,50] To the best of our knowledge, no long-term results have been reported. Stem cell-application in regenerative medicine has raised safety concerns, *e.g.* tumorigenic potential and biodistribution.[51] Therefore, clinical studies investigating long-term safety and efficacy are crucial before continuing with clinical application of (adipose) stem cells. In **Chapter 6**, we demonstrated for the first time the 10-year safety of SVF-supplementation in combination with calcium phosphate bone substitute in patients who underwent MSFE for jawbone reconstruction. No adverse effects or pathology were found based on general health questionnaires, clinical and radiological assessments. None of the patients report any graft-related problems after MSFE, and showed 92.9–100% dental implant survival rate (100% following 6-months follow-up), which confirmed the successful long-term clinical outcomes after SVF-supplementation in jawbone reconstruction. Our long-term results were in contrast to unsatisfying long-term results (≥6-year follow-up) of ASC-application in cranioplasty, *i.e.* graft resorption and late infection.[52] Regardless of stem cell-application, it should be noted that compared to MSFE, the cranioplasty surgical site has a different nature, *i.e.* large critical sized, tumorigenic defect.[52] The encouraging finding that SVF-supplementation showed enhanced bone regeneration in the short-term (previous phase-I study[22]), and led to no abnormalities, clinically and radiologically, in the long-term, warrants further studies to investigate whether further optimizations can be accomplished, *e.g.* by higher dosages of SVF, altering scaffold properties, or application of other adipose tissue processing methods. These will be addressed in more detail in the "future perspectives" section.

In summary, the results presented in this thesis provide new insights in bone formation and vascularization in jaw bone regeneration using different bone grafting materials, either or not supplemented with SVF, for dental implant placement. These new insights could have important implications for the development of new strategies in cellular bone tissue engineering in the fields of oral and maxillofacial surgery and orthopedics.

LIMITATIONS OF THE STUDIES

Chapters 3, 4 and 5 were retrospectively conducted studies, which resulted in several limitations related to the study design. Patients underwent MSFE using autologous bone graft or calcium phosphate bone substitute only, were treated unilaterally. To exclude inter-patient variation, a "split-mouth" model would be more favorable to compare different bone grafting materials. To reduce possible patient-related confounders in the comparison between the different bone grafting materials, we monitored several parameters, *e.g.* sex, age, and residual bone height pre-MSFE. No statistical differences were found. Therefore, we assumed that these possible patient-related confounders did not affect our results. Moreover, the surgeons were not blinded for the type of bone grafting material during MSFE, which might result in potential observer bias. Unfortunately, blinding of surgeons for the intervention was not possible. To exclude bias, data collection and analysis were performed blinded for bone grafting material. Another limitation was that we were only able to analyze biopsies harvested at one time point, preventing to assess the dynamics of the remodeling process in the different types of bone grafting materials. However, the observed differences in bone formation and vascularization between different bone grafting materials in MSFE, based on (immuno)histological data at 4–6 months post-MSFE (**Chapters 3 and 5**), warrant future studies investigating the bone regeneration process at different time points. No clinical follow-up was carried out for the patients treated with MSFE using autologous bone graft or only calcium phosphate bone substitute (**Chapters 3**–**5**). Therefore, our conclusions were only based on (immuno)histological data. These data revealed highly interesting and relevant results on the cellular level regarding jaw bone regeneration that warrant future studies combining clinical follow-up with (immuno) histological data.

Chapter 6 was a long-term follow-up of patients who participated in an earlier conducted phase-I clinical study.[22] The design of the earlier phase-I clinical study resulted in several limitations of the long-term follow-up study. During the earlier phase-I clinical study, the surgeons were not blinded for the type of graft during MSFE, and had prior knowledge of the research aims. This possibly resulted in potential observer bias. Unfortunately, blinding of surgeons for the intervention was not possible. To exclude bias at 10-year follow-up, data collection and analysis at 10-year follow-up were performed blinded. Another limitation was that no baseline radiographic and probing data after the first year of dental implant loading were recorded. These data were only retrieved at 10-year follow-up, preventing determination of onset and progression of peri-implant disease. Our conclusion was not affected by lacking baseline data, since there was no difference in the prevalence of peri-implantitis between study and control sides. Therefore, SVF-supplementation did not affect the prevalence of peri-implantitis at 10-year follow-up.

Chapter 7

CONCLUSIONS

The clinical studies in this thesis have contributed to new insights in bone formation and vascularization in jaw bone regeneration using different bone grafting materials, either or not supplemented with SVF, for dental implant placement. SVF-supplementation increased vascularization and osteoid volume in calcium phosphate bone substitute to a similar level of using retromolar bone graft in patients who had undergone MSFE. Therefore, SVF-supplementation might accelerate dental implant placement and loading. The successful 10-year long-term clinical and radiological follow-up of patients treated with MSFE using SVF-supplemented calcium phosphate bone substitute, provides powerful leads to extent the clinical application of SVF.

FUTURE PERSPECTIVES

The overall aim of this thesis was to investigate bone formation and vascularization in jaw bone regeneration using different bone grafting materials, either or not supplemented with SVF, for dental implant placement. Therefore, we conducted several clinical studies investigating the application of autologous bone grafts, bone substitutes, and adipose stem cells in MSFE. Our findings showed that autologous bone grafts are superior in bone formation and vascularization potential compared to a calcium phosphate bone substitute, and should still be considered the 'gold standard' bone grafting material in MSFE. Calcium phosphate bone substitutes supplemented with SVF showed enhanced vascularization compared to calcium phosphate bone substitute only. SVF-supplementation enhanced bone regeneration in the short-term, and demonstrated to be safe during 10-year follow-up. Therefore, SVF-supplementation in combination with calcium phosphate bone substitutes is promising for future clinical applications in jaw bone regeneration. Further optimization of SVF-supplementation with calcium phosphate bone substitute in jaw bone regeneration may, therefore, be assessed as follows:

1. Higher SVF-dosages and different time-points of biopsy harvesting in a new phase-I study to find the most effective and safe SVF-dosage in MSFE. Our data demonstrated 10-year long-term safety of SVF-supplementation with calcium phosphate bone substitute in patients treated with MSFE. One SVF dosage was chosen based on feasibility, safety, and efficacy studies of the one-step surgical procedure using SVF in a goat spinal fusion model.[53] To broaden our understanding of the bone regeneration process after SVF-supplementation, different time-points of biopsy harvesting are recommended.
2. Bioactive stimulation of SVF by growth factors, functionalized proteins and/or cellular matrix-derived peptides to enhance bone formation and vascularization potential of SVF. Our data demonstrated enhanced bone formation of SVF-supplementation to calcium phosphate bone substitute (ß-TCP/BCP) in patients treated with MSFE. Osteogenic growth factor, *e.g.* BMP-2 and 1,25-dihydroxyvitaminD_3, pre-incubation of human-ASCs seeded on ß-TCP and BCP scaffolds had a long-lasting stimulating effect on osteogenic differentiation.[54,55] Thus, it may be hypothesized that osteogenic "priming" of ASCs improves osteogenic differentiation of ASCs within the SVF, which may be particularly relevant in loading-compromised areas. Angiogenic growth factors and proteins, *e.g.* vascular endothelial growth factor, basic fibroblast growth factor, platelet-derived, growth factor, and angiogenin, might benefit the vascularization potential of SVF. Bioactive peptides are suggested to have similar potency, but more stability than growth factors and proteins.[56]
3. Enhancing bioactivation of SVF-seeded scaffolds by adding microvascular fragments to increase vascularization potential. Our data suggest enhanced vascularization potential of SVF-supplementation to calcium phosphate bone substitute (ß-TCP/BCP) in patients treated with MSFE. Recently, it was shown that digestion of adipose tissue for only 10 min provides a mixture of single cells and microvascular fragments.[57,58] These microvascular fragments exhibit the unique feature of rapidly reassembling into new microvascular networks following transplantation, since they still represent intact vessel segments. Microvascular fragments have been suggested to stimulate vascular ingrowth as well as outgrowth.[57,59,60]

Therefore microvascular fragments might possess higher vascularization potential than SVF.[57,58] We postulate that adding of adipose tissue-derived microvascular fragments might increase the vascularization potential of the graft, by stimulating vascularization (angiogenesis and vasculogenesis) from the graft towards the host. Further *in vitro* and *in vivo* research needs to confirm these findings.

4. Enzymatic preparation of ASC is still the most used method which in most countries is, however, considered as "more than minimal manipulation".[61] An alternative method is by disaggregating the adipose tissue mechanically into small fat particles, so-called microfragmented fat (MFAT).[62] Intact microarchitecture of MFAT preserves a similar or even higher number of regenerative cells than the enzymatically derived stromal vascular fraction (SVF).[63] This approach is now being investigated for bone reconstruction in alveolar cleft patients by combining BCP granules with MFAT derived from intraoperatively harvested adipose tissue from the buccal fad pad,[64] and may represent an interesting and cost-effective alternative for enzymatically digested adipose tissue.
5. Biomechanical stimulation of osteocytes at the bone regeneration site (niche). Our data indicated local differences in osteocyte surface area and orientation in maxillary jaw bone in patients treated with MSFE, which may be related to tensile strain magnitude and orientation. The exact underlying mechanisms are unclear. Moreover, mechanical loading-regulated crosstalk between osteocytes and MSCs has been demonstrated.[12,13] The maxillary sinus area is considered as a loading-compromised area. Therefore, increased biomechanical stimulation of osteocytes, *e.g.* by accelerated dental implant placement and loading protocols, may effectively improve the bone regeneration site (niche).

REFERENCES

1. Pjetursson BE, Tan WC, Zwahlen M, Lang NP. A systematic review of the success of sinus floor elevation and survival of implants inserted in combination with sinus floor elevation: Part I: Lateral approach. *J Clin Periodontol.* 2008;35(Suppl 8):216–240. doi:10.1111/j.1600-051X.2008.01272.x
2. Misch CM. Comparison of intraoral donor sites for onlay grafting prior to implant placement. *Int J Oral Maxillofac Implants.* 1997;12(6):767–776.
3. Raghoebar GM, Meijndert L, Kalk WWI, Vissink A. Morbidity of mandibular bone harvesting: A comparative study. *Int J Oral Maxillofac Implants.* 2007;22(3):359–365.
4. Tolstunov L. Implant zones of the jaws: Implant location and related success rate. *J Oral Implant.* 2007;33(4):211–220.
5. Fleming JE, Cornell CN, Muschler GF. Bone cells and matrices in orthopedic tissue engineering. *Orthop Clin North Am.* 2000;31(3):357–374. doi:10.1016/S0030-5898(05)70156-5
6. Degidi M, Scarano A, Piattelli M, Perrotti V, Piattelli A. Bone remodeling in immediately loaded and unloaded titanium dental implants: A histologic and histomorphometric study in humans. *J Oral Implantol.* 2005;31(1):18–24.
7. Cao W, Helder MN, Bravenboer N, Wu G, Jin J, Ten Bruggenkate CM, Klein-Nulend J, Schulten EAJM. Is there a governing role of osteocytes in bone tissue regeneration? *Curr Osteoporos Rep.* 2020;18(5):541–550. doi:10.1007/s11914-020-00610-6
8. Vatsa A, Breuls RG, Semeins CM, Salmon PL, Smit TH, Klein-Nulend J. Osteocyte morphology in fibula and calvaria - Is there a role for mechanosensing? *Bone.* 2008;43(3):452–458. doi:10.1016/j.bone.2008.01.030
9. Bacabac RG, Mizuno D, Schmidt CF, MacKintosh FC, Van Loon JJWA, Klein-Nulend J, Smit TH. Round versus flat: Bone cell morphology, elasticity, and mechanosensing. *J Biomech.* 2008;41(7):1590–1598. doi:10.1016/j.jbiomech.2008.01.031
10. Marotti G. Osteocyte relevance orientation in human lamellar bone and its to the morphometry of periosteocytic lacunae. *Metab Bone Dis Relat Res.* 1979;1(4):325–333.
11. Kerschnitzki M, Wagermaier W, Roschger P, Seto J, Shahar R, Duda GN, Mundlos S, Fratzl P. The organization of the osteocyte network mirrors the extracellular matrix orientation in bone. *J Struct Biol.* 2011;173(2):303–311. doi:10.1016/j.jsb.2010.11.014
12. Eichholz KF, Woods I, Riffault M, Johnson GP, Corrigan M, Lowry MC, Shen N, Labour MN, Wynne K, O'Driscoll L, Hoey DA. Human bone marrow stem/stromal cell osteogenesis is regulated via mechanically activated osteocyte-derived extracellular vesicles. *Stem Cells Transl Med.* 2020;9(11):1431–1447. doi:10.1002/sctm.19-0405
13. Brady RT, O'Brien FJ, Hoey DA. Mechanically stimulated bone cells secrete paracrine factors that regulate osteoprogenitor recruitment, proliferation, and differentiation. *Biochem Biophys Res Commun.* 2015;459(1):118–123. doi:10.1016/j.bbrc.2015.02.080
14. Jin J, Seddiqi H, Bakker AD, Wu G, Verstappen JFM, Haroon M, Korfage, JAM, Zandieh-Doulabi B, Werner A, Klein-Nulend J, Jaspers RT. Pulsating fluid flow affects pre-osteoblast behavior and osteogenic differentiation through production of soluble factors. *Physiol Rep.* 2021;9(12):1–19. doi:10.14814/phy2.14917
15. Jin J, Jaspers RT, Wu G, Korfage JAM, Klein-Nulend J, Bakker AD. Shear stress modulates osteoblast cell and nucleus morphology and volume. *Int J Mol Sci.* 2020;21(21):1-22. doi:10.3390/ijms21218361

16. Boëck-Neto RJ, Artese L, Piattelli A, Shibli JA, Perrotti V, Piccirilli M, Marcantonio Jr E. VEGF and MVD expression in sinus augmentation with autologous bone and several graft materials. *Oral Dis.* 2009;15:148–154. doi:10.1111/j.1601-0825.2008.01502.x

17. Farré-Guasch E, Bravenboer N, Helder M, Schulten EAJM, Ten Bruggenkate CM, Klein-Nulend J. Blood vessel formation and bone regeneration potential of the stromal vascular fraction seeded on a calcium phosphate scaffold in the human maxillary sinus floor elevation model. *Materials (Basel).* 2018;11(1):116. doi:10.3390/ma11010161

18. Kamolratanakul P, Mattheos N, Yodsanga S, Pornchai J. The impact of deproteinized bovine bone particle size on histological and clinical bone healing outcomes in the augmented sinus: A randomized controlled clinical trial. *Clin Implant Dent Relat Res.* 2022;24:361–371. doi:10.1111/cid.13083

19. Tetè S, Vinci R, Zara S, Zizzari, V, De Carlo A, Falco G, Tripodi D, Cataldi A, Mortellaro C, Gherlone E. Long-term evaluation of maxillary reconstruction by iliac bone graft. *J Craniofac Surg.* 2011;22(5):1702–1707.

20. Degidi M, Artese L, Rubini C, Perrotti V, Iezzi G, Piattelli A. Microvessel density in sinus augmentation procedures using anorganic bovine bone and autologous bone: 3 Months results. *Implant Dent.* 2007;16(3):317–325. doi:10.1097/ID.0b013e3180de4c5f

21. Artese L, Piattelli A, Stefano DA, Piccirilli M, Pagnutti S, Alimonte ED, Perrotti V. Sinus lift with autologous bone alone or in addition to equine bone: An immunohistochemical study in man. *Implant Dent.* 2011;20(5):383–388. doi:10.1097/ID.0b013e3182310b3d

22. Prins HJ, Schulten EAJM, Ten Bruggenkate CM, Klein-Nulend J, Helder MN. Bone regeneration using the freshly isolated autologous stromal vascular fraction of adipose tissue in combination with calcium phosphate ceramics. *Stem Cells Transl Med.* 2016;5(10):1362–1374.

23. Bertolai R, Catelani C, Aversa A, Rossi A, Giannini D, Bani D. Bone graft and mesenchimal stem cells: Clinical observations and histological analysis. *Clin Cases Miner Bone Metab.* 2015;12(2):183–187. doi:10.11138/ccmbm/2015.12.2.178

24. Pasquali PJ, Teixeira ML, Oliveira TA De, De Macedo LGS, Aloise AC, Pelegrine AA. Maxillary sinus augmentation combining bio-oss with the bone marrow aspirate Concentrate: A histomorphometric study in humans. *Egypt Dent J.* 2015;64(1):107–118. doi:10.1155/2015/121286

25. Kaigler D, Avila-Ortiz G, Travan S, Taut, Andrei D, Padial-Molina M, Rudek I, Wang F, Lanis A, Giannobile WV. Bone engineering of maxillary sinus bone deficiencies using enriched CD90+ stem cell therapy: A randomized clinical trial. *J Bone Miner Res.* 2015;30(7):1206–1216. doi:10.1002/jbmr.2464

26. Y Baena RR, D'Aquino R, Graziano A, Trovato, Letizia T, Aloise AC, Ceccarelli G, Cusella G, Pelegrine AA, Lupi SM. Autologous periosteum-derived micrografts and PLGA/HA enhance the bone formation in sinus lift augmentation. *Front Cell Dev Biol.* 2017;5:1–7. doi:10.3389/fcell.2017.00087

27. Bajestan MN, Rajan A, Edwards SP, Aronovich S, Cevidanes LHS, Polymeri A, Travan S, Kaigler D. Stem cell therapy for reconstruction of alveolar cleft and trauma defects in adults: A randomized controlled, clinical trial. *Clin Implant Dent Relat Res.* 2017;19(5):793–801. doi:10.1111/cid.12506

28. Al-Ahmady HH, Abd Elazeem AF, Bellah Ahmed NEM, Shawkat WM, Elmasry M, Abdelrahman, Mostafa A, Abderazik MA. Combining autologous bone marrow mononuclear cells seeded on collagen sponge with nano hydroxyapatite, and platelet-rich fibrin: Reporting a novel strategy for alveolar cleft bone regeneration. *J Craniomaxillofac Surg.* 2018;46(9):1593–1600. doi:10.1016/j.jcms.2018.05.049

29. Khalifa ME, Gomaa NE. Dental arch expansion after alveolar cleft repair using autogenous bone marrow derived mesenchymal stem cells versus autogenous chin bone graft. *Egypt Dent J.* 2018;643(1):107–118.

30. Behnia H, Khojasteh A, Soleimani M, Tehranchi A, Atashi A. Repair of alveolar cleft defect with mesenchymal stem cells and platelet derived growth factors: A preliminary report. *J Craniomaxillofac Surg.* 2012;40(1):2

31. Khojasteh A, Kheiri L, Behnia H, Tehranchi A, Nazeman P, Nadjmi N, Soleimani M. Lateral ramus cortical bone plate in alveolar cleft osteoplasty with concomitant use of buccal fat pad derived cells and autogenous bone: Phase I clinical trial. *Biomed Res Int.* 2017;2017:6560234. doi:10.1155/2017/6560234

32. Talaat WM, Ghoneim MM, Salah O, Adly OA. Autologous bone marrow concentrates and concentrated growth factors accelerate bone regeneration after enucleation of mandibular pathologic lesions. *J Craniofac Surg.* 2018;29(4):992 J Craniomaxillofac Surg. 997. doi:10.1097/SCS.0000000000004371

33. Baba S, Yamada Y, Komuro A, Yotsui Y, Umeda M, Shimuzutani K, Nakamura S. Phase I/II trial of autologous bone marrow stem cell transplantation with a three-dimensional woven-fabric scaffold for periodontitis. *Stem Cells Int.* 2016;2016:6205910. doi:10.1155/2016/6205910

34. Ferrarotti F, Romano F, Gamba MN, Quirico A, Giraudi M, Audagna M, Aimetti M. Human intrabony defect regeneration with micrografts containing dental pulp stem cells: A randomized controlled clinical trial. *J Clin Periodontol.* 2018;45(7):841–850. doi:10.1111/jcpe.12931

35. Castillo-Cardiel G, López-Echaury AC, Saucedo-Ortiz JA, Fuentes-Orozco C, Michel-Espinoza LR, Irusteta-Jiménez L, Salazar-Parra M. González-Ojeda A. Bone regeneration in mandibular fractures after the application of autologous mesenchymal stem cells, a randomized clinical trial. *Dent Traumatol.* 2017;33(1):38–44. doi:10.1111/edt.12303

36. Monti M, Graziano A, Rizzo S, Perotti C, Del Fante C, D'Aquino R, Redi CA, Y Baena RR. In vitro and in vivo differentiation of progenitor stem cells obtained after mechanical digestion of human dental pulp. *J Cell Physiol*. 2017;232(3):548–555. doi:10.1002/jcp.25452

37. D'Aquino R, Trovato L, Graziano A, Ceccarelli G, Cusella de Angelis G, Marangini A, Nisio A, Galli M, Pasi M, Finotti M, Lupi SM, Rizzo S, Y Baena RR. Periosteum-derived micro-grafts for tissue regeneration of human maxillary bone. *J Transl Sci.* 2016;2(2):125–129. doi:10.15761/jts.1000128

38. Liu X, Wang P, Chen W, Weir MD, Bao C, Xu HHK. Human embryonic stem cells and macroporous calcium phosphate construct for bone regeneration in cranial defects in rats. *Acta Biomater.* 2014;10(10):4484–4493. doi:10.1016/j.actbio.2014.06.027

39. Bourne S, Buttery LDK, Xynos ID, Episkopou V, Winston RM, Hughes SPF, Polak JM. Selective differentiation of osteoblasts and in vitro bone formation from murine embryonic stem cells. *Tissue Eng.* 2001;7(1):89–99.

40. Rutledge K, Cheng Q, Pryzhkova M, Harris GM, Jabbarzadeh E. Enhanced differentiation of human embryonic stem cells on extracellular matrix-containing osteomimetic scaffolds for bone tissue engineering. *Tissue Eng Part C Methods.* 2014;20(11):865–874. doi:10.1089/ten.tec.2013.0411

41. Ardeshirylajimi A. Applied induced pluripotent stem cells in combination with biomaterials in bone tissue engineering. *J Cell Biochem.* 2017;118(10):3034–3042. doi:10.1002/jcb.25996

42. Zuk PA, Zhu M, Mizuno H, Huang J, Futrell JW, Katz AJ, Benhaim P, Lorenz HP, Hedrick MH. Multilineage cells from human adipose tissue: Implications for cell-based therapies. *Tissue eng.* 2001;7:211–228. doi:10.1089/107632701300062859

43. Cho CH, Koh YJ, Han J, Sung, Hoon Ki L, Hyuek JL, Morisada T, Schwendener RA, Brekken RA, Kang G, Oike Y, Choi TS, Suda T, Yoo OJ, Ko GY. Angiogenic role of LYVE-1-positive macrophages in adipose tissue. *Circ Res.* 2007;100(4). doi:10.1161/01.RES.0000259564.92792.93

44. Dufrane D. Impact of age on human adipose stem cells for bone tissue engineering. *Cell Transplant.* 2017;26(9):1496–1504. doi:10.1177/0963689717721203

45. Grambow F, Rutkowski R, Podmelle F, Schmoeckel K, Siegerist F, Domanski G, Schuster MW, Domanska G. The impact of lidocaine on adipose-derived stem cells in human adipose tissue harvested by liposuction and used for lipotransfer. *Int J Mol Sci.* 2020;21(8):2869. doi:10.3390/ijms21082869

46. Wang WZ, Fang XH, Williams SJ, Stephenson LL, Baynosa RC, Khiabani KT, Zamboni WA. Lidocaine-induced ASC apoptosis (tumescent vs. local anesthesia). *Aesthetic Plast Surg.* 2014;38(5):1017–1023. doi:10.1007/s00266-014-0387-2

47. Francis A, Wang WZ, Goldman JJ, Fang XH, Williams SJ, Baynosa RC. Enhancement of viable adipose-derived stem cells in lipoaspirate by buffering tumescent with sodium bicarbonate. *Plast Reconstr Surg Glob Open.* 2019;7(3):1–6. doi:10.1097/GOX.0000000000002138

48. Goldman JJ, Wang WZ, Fang XH, Williams SJ, Baynosa RC. Tumescent liposuction without lidocaine. *Plast Reconstr Surg Glob Open*. 2016;4(8):1–6. doi:10.1097/GOX.0000000000000830

49. Stumbras A, Krukis MM, Januzis G, Juodzbalys G. Regenerative bone potential after sinus floor elevation using various bone graft materials: A systematic review. *Quintessence Int.* 2019;50(7):548–558. doi:10.3290/j.qi.a42482

50. Sándor GK, Tuovinen VJ, Wolff J, Patrikoski M, Jokinen J, Nieminen E, Mannerström B, Lappalainen OP, Seppänen R, Miettinen S. Adipose stem cell tissue-engineered construct used to treat large anterior mandibular defect: A case report and review of the clinical application of good manufacturing practice-level adipose stem cells for bone regeneration. *J Oral Maxillofac Surg.* 2013;71(5):938–950. doi:10.1016/j.joms.2012.11.014

51. Heslop JA, Hammond TG, Santeramo I, Tort Piella A, Hopp I, Zhou J, Baty R, Graziano EI, Proto Marco B, Caron A, Sköld P, Andrews PW, Baxter MA, Hay DC, Hamdam J, Sharpe ME, Patel S, Jones DR, Reinhardt J, Danen EHJ, Ben-David U, Stacey G, Björquist P, Piner J, Mills J, Rowe C, Pellegrini G, Sethu S, Antoine D, Cross MJ, Murray P, Williams DP, Kitteringham NR, Goldring CEP, Park BK. Concise review: Workshop review: Understanding and assessing the risks of stem cell-based therapies. *Stem Cells Transl Med.* 2015;4(4):389–400. doi:10.5966/sctm.2014-0110

52. Thesleff T, Lehtimäki K, Niskakangas T, Huovinen S, Mannerström B, Miettinen S, Seppänen R, Öhman J. Cranioplasty with adipose-derived stem cells, beta-tricalcium phosphate granules and supporting mesh: Six-year clinical follow-up results. *Stem Cells Transl Med.* 2017;6:1576–1582.

53. Kroeze RJ, Smit TH, Vergroesen PP, Bank RA, Stoop R, Van Rietbergen B, Van Royen BJ, Helder MN. Spinal fusion using adipose stem cells seeded on a radiolucent cage filler: A feasibility study of a single surgical procedure in goats. *Eur Spine J.* 2015;24(5):1031–1042. doi:10.1007/s00586-014-3696-x

54. Overman JR, Farré-Guasch E, Helder MN, Ten Bruggenkate CM, Schulten EAJM, Klein-Nulend J. Short (15 minutes) bone morphogenetic protein-2 treatment stimulates osteogenic differentiation of human adipose stem cells seeded on calcium phosphate scaffolds in vitro. *Tissue Eng Part A.* 2012;19(3-4):571–581. doi:10.1089/ten.tea.2012.0133

55. Mokhtari-Jafari F, Amoabediny G, Dehghan MM, Helder MN, Zandieh-Doulabi B, Klein-Nulend J. Short pretreatment with calcitriol is far superior to continuous treatment in stimulating proliferation and osteogenic differentiation of human adipose stem cells. *Cell J*. 2020;22(3):293–301. doi:10.22074/cellj.2020.6773

56. Abdal Dayem A, Lee S Bin, Lim KM, Kim A, Shin HJ, Vellingiri B, Kim YB, Choo SG. Bioactive peptides for boosting stem cell culture platform: Methods and applications. *Biomed Pharmacother.* 2023;160:114376. doi:10.1016/j.biopha.2023.114376

57. Später T, Frueh FS, Nickels RM, Menger MD, Laschke MW. Prevascularization of collagen-glycosaminoglycan scaffolds: Stromal vascular fraction versus adipose tissue-derived microvascular fragments. *J Biol Eng.* 2018;12(1):113. doi:10.1186/s13036-018-0118-3

58. Vezzani B, Shaw I, Lesme H, Yong L, Khan N, Tremolada C, Péault B. Higher pericyte content and secretory activity of microfragmented human adipose tissue compared to enzymatically derived stromal vascular fraction. *Stem Cells Transl Med.* 2018;7(12):876–886. doi:10.1002/sctm.18-0051

59. Frueh FS, Später T, Scheuer C, Menger MD, Laschke MW. Isolation of murine adipose tissue-derived microvascular fragments as vascularization units for tissue engineering. *J Vis Exp.* 2017;2017(122):1–7. doi:10.3791/55721

60. Shepherd BR, Chen HYS, Smith CM, Gruionu G, Williams SK, Hoying JB. Rapid perfusion and network remodeling in a microvascular construct after implantation. *Arter Thromb Vasc Biol.* 2004;24(5):898–904. doi:10.1161/01.ATV.0000124103.86943.1e

61. Trivisonno A, Alexander RW, Baldari S, Cohen SR, Di Rocco G, Gentile P, Magalon G, Magalon J, Miller RB, Womack H, Toietta G. Concise review: Intraoperative strategies for minimal manipulation of autologous adipose tissue for cell- and tissue-based therapies. *Stem Cells Transl Med.* 2019;8(12):1265–1271. doi:10.1002/sctm.19-0166

62. Sesé B, Sanmartín JM, Ortega B, Matas-Palau A, Llull R. Nanofat cell aggregates: A nearly constitutive stromal cell inoculum for regenerative site-specific therapies. *Plast Reconstr Surg*. 2019;144(5):1079–1088. doi:10.1097/PRS.0000000000006155

63. Vezzani B, Shaw I, Lesme H, Yong L, Khan N, Tremolada C, Péault B. Higher pericyte content and secretory activity of microfragmented human adipose tissue compared to enzymatically derived stromal vascular fraction. *Stem Cells Transl Med.* 2018;7(12):876–886. doi:10.1002/sctm.18-0051

64. Natsir Kalla DS, Alkaabi SA, Fauzi A, Tajrin A, Nurrahma R, Müller WEG, Schröder HC, Wang XH, Forouzanfar T, Helder MN, Ruslin M. Microfragmented fat (MFAT) and BCP for alveolar cleft repair: A prospective clinical trial protocol. *JMIR Res Protoc*. In press

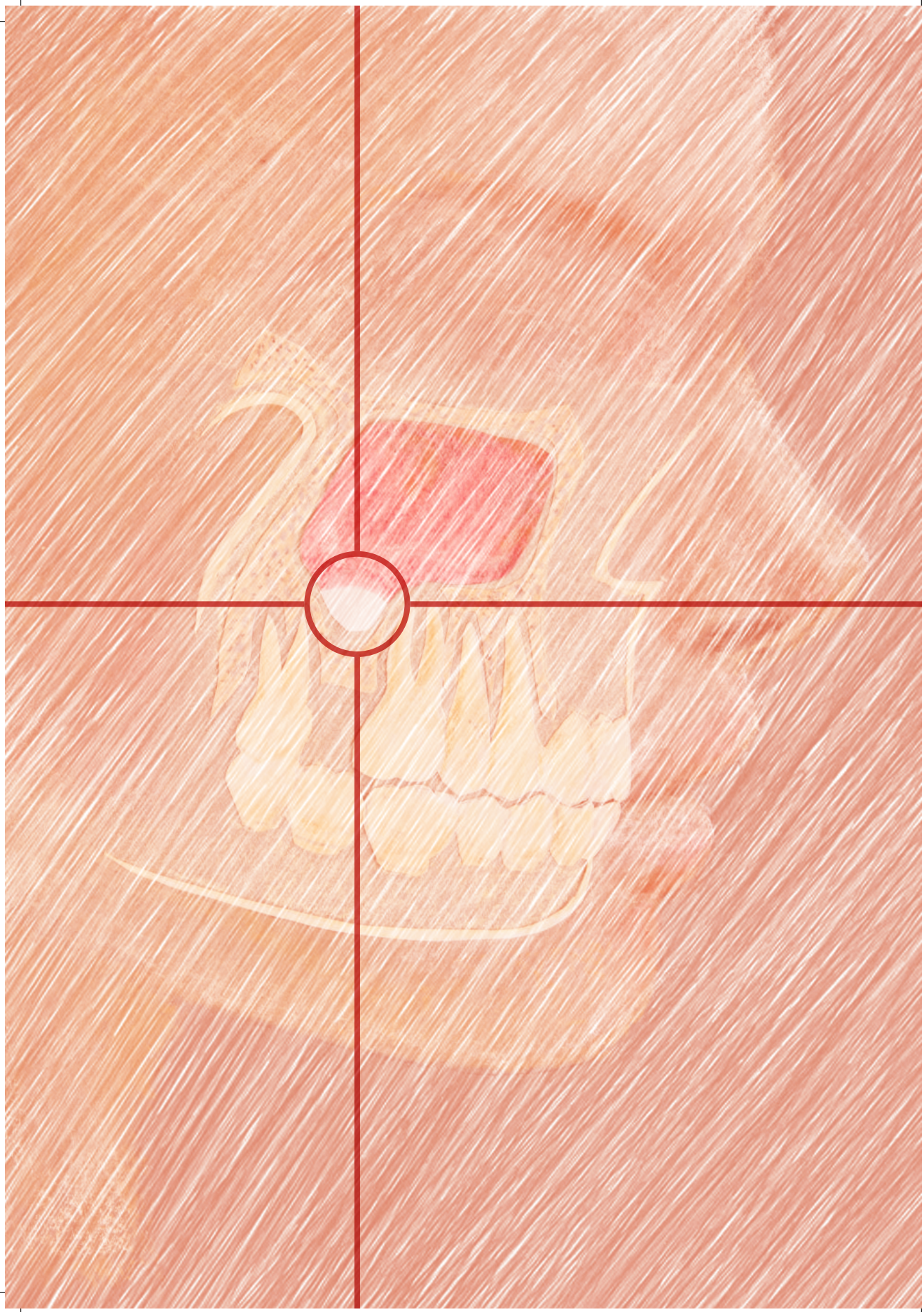

APPENDIX

SUMMARY

The demand for dental implants to replace missing teeth has strongly increased over the last 30 years, and is expected to further increase in the next decade. Insufficient local jaw bone volume resulting from bone loss due to systemic or local causes, is a common problem for dental implant placement. Maxillary sinus floor elevation (MSFE) is carried out to restore insufficient alveolar bone height in the lateral maxilla to allow dental implant placement. Autograft (autologous bone graft), allograft, xenograft, and/or synthetic bone substitute, are currently used bone grafting materials in MSFE. Autologous bone graft results in more satisfactory jaw bone regeneration outcomes compared to bone substitute. Their associated drawbacks, *e.g.* patient morbidity and limited availability, encourage the search for suitable alternatives with similar bioactivity. The ideal bone regeneration material with sufficient biomimetic properties, excellent bone regeneration potential, and limited drawbacks, *e.g.* low patient morbidity, sufficient availability, and low cost, has not been developed yet.

Cellular bone tissue engineering using mesenchymal stem cells (MSCs) seeded on bone substitute in patients treated with MSFE has shown to increase bone formation compared to bone substitute only. A major challenge in cellular bone tissue engineering is still the vascularization of the implanted graft. The stromal vascular fraction (SVF) containing adipose tissue-derived mesenchymal stem cells (adipose stem cells; ASCs) is currently considered as a highly promising source of adult stem cells with osteogenic and angiogenic potential for cellular bone tissue engineering. Moreover, mechanosensitive osteocytes play a crucial role in the micro-environment (niche) of the bone regeneration site. Therefore, increased understanding of the relation between mechanical loading and osteocytes is needed to develop future strategies using MSCs to induce functional bone tissue for dental implant placement. It is desirable that SVF containing ASCs shows similar bioactivity as autologous bone graft, as well as long-term safety, to be a suitable alternative for the currently used bone grafting materials, *i.e.* autologous bone graft and/or bone substitute, in jaw bone regeneration.

In this thesis, we investigated bone formation and vascularization in jaw bone regeneration using different bone grafting materials, either or not supplemented with SVF, for dental implant placement. MSFE was used as a human experimental model for the application of different bone grafting materials. MSFE was also used as a human split-mouth model to compare the application of SVF-supplemented calcium phosphate bone substitute with calcium phosphate bone substitute only in jaw bone regeneration.

In **Chapter 2**, the advancements in stem cell application, vascularization, and bone regeneration in the oral and maxillofacial region, with emphasis on the human jaw, were reviewed.

Important advancements have been made in stem cell application, but adequate graft vascularization is still a major challenge. The clinically applied sources of stem cells for bone tissue engineering originate from bone marrow, adipose tissue, and dental tissues. The SVF of human adipose tissue is a promising single source for a heterogeneous population of essential cells for osteogenesis and angiogenesis. Besides, adipose tissue-derived microvascular fragments (MF) are suggested as a promising cell source for vascularization strategies, due to their correct native cell ratios. Enhanced vascularization of tissue-engineered grafts can be

achieved by different mechanisms: vascular ingrowth directed from the surrounding host tissue to the implanted graft, vice versa, or concomitantly. The classical vascularization strategies focus on enhancing vascular ingrowth into the implanted graft directed from the surrounding host tissue to the implanted graft. MF may have stimulating actions on both vascular ingrowth and outgrowth, since they contain angiogenic stem cells as well as vascularized matrix fragments. Both adipose tissue-derived SVF and MF are cell sources with clinical feasibility due to their large quantities that can be harvested and applied in a one-step surgical procedure. Furthermore, appropriate *in vitro* models to study bone tissue engineering are lacking. The development of engineered *in vitro* 3D models mimicking the bone defect environment would facilitate new strategies in bone tissue engineering. Successful clinical application of stem cell applied cellular bone tissue engineering requires innovative future investigations enhancing vascularization.

In **Chapter 3**, we demonstrated that compared to retromolar bone, tuberosity bone graft showed increased bone vitality and vascularization (number of blood vessels) in patients treated with MSFE. (Immuno)histomorphometrical analysis of bone biopsies taken 4 months post-MSFE prior to dental implant placement were carried out. The use of tuberosity bone graft in MSFE resulted in 10% higher osteoid volume in the center and at the cranial side of the grafted area, and 150%–300% higher total number of blood vessels in the total grafted area compared to retromolar bone graft. We hypothesized that the increased bone vitality and vascularization in tuberosity bone graft, was likely due to faster bone remodeling or earlier start of new bone formation in tuberosity than retromolar bone graft. Therefore, our histological data suggest that tuberosity bone graft might perform better in enhancing bone regeneration than retromolar bone graft, since more osteoid was deposited, more blood vessels were formed, and a more active remodeling process was initiated. A shorter healing period before dental implant placement and loading might be feasible, if tuberosity bone graft is used in MSFE.

In **Chapter 4**, we demonstrated differences in the surface area and orientation of osteocytes, in particular, in the areas of the maxillary bone that are related to the tensile strain magnitude and orientation. Gap and free-ending implant locations of patients treated with MSFE using β-tricalcium phosphate bone substitute (ß-TCP) were compared, using three-dimensional finite element modeling and histomorphometrical analysis of bone biopsies retrieved 8 months post-MSFE prior to dental implant placement. Firstly, the finite element model of the maxilla predicted larger, differently directed tensile strains in the gap versus free-ending implant locations. Secondly, a more cranial-caudal orientation and a larger surface area of osteocytes in the single gap than in the free-ending implant locations were found. No differences were found in mineralized residual native bone volume and the number and morphology of the osteocytes between single gap and free-ending implant locations. Our data provide, for the first time, a view on the relationship between tensile strain and osteocyte morphology and orientation in maxillary bone, which might contribute to a better understanding of the cellular processes that lead to different bone qualities in various dental implant positions, and eventually to the success of dental implants in the maxilla. The exact implication of the osteocyte orientation on dental implant success, however, is complex and deserves further investigation.

In **Chapter 5**, we demonstrated differences in vascularization and bone regeneration potential between calcium phosphate bone substitute either or not supplemented with SVF versus autologous bone graft 4–6 months post-MSFE. Histological analysis was carried out on human bone biopsies retrieved 4–6 months post-MSFE prior to dental implant placement. Patients treated with MSFE using retromolar bone graft, tuberosity bone graft, ß-TCP, biphasic calcium phosphate bone substitute (BCP), ß-TCP supplemented with SVF, and BCP supplemented with SVF (n=5) were compared. Calcium phosphate bone substitute supplemented with SVF in MSFE resulted in similar blood vessel number and osteoid volume as retromolar, but not as tuberosity bone graft 4–6 months post-MSFE. Blood vessel number and osteoid volume were lower in calcium phosphate than autologous bone graft biopsies in the cranial area. Moreover, bone volume was lower in calcium phosphate bone substitute than autologous bone graft biopsies. Bone volume was similar in calcium phosphate bone substitute supplemented with SVF as in tuberosity, but lower than in retromolar bone graft biopsies. We hypothesized that the similar vascularization and bone regeneration potential observed in calcium phosphate bone substitute supplemented with SVF and retromolar bone graft, was due to a potential vasculogenic, angiogenic, and osteogenic effect of SVF-supplementation. Our histological data suggest that calcium phosphate bone substitute supplemented with SVF might perform similarly as retromolar bone graft in MSFE, since comparable blood vessel number and osteoid were observed. Therefore, calcium phosphate bone substitute supplemented with SVF might be promising to replace autologous bone graft for enhanced bone regeneration in MSFE.

In **Chapter 6**, we demonstrated for the first time the 10-year safety of SVF-supplementation in combination with calcium phosphate bone substitute in patients treated with MSFE using the lateral window technique for jawbone reconstruction. All 10 patients previously participating in a phase-I trial were included in this 10-year follow-up. They received either ß-TCP (n=5) or BCP (n=5) with SVF-supplementation on one side (study). Bilaterally-treated patients (6 of 10; 3 ß-TCP, 3 BCP) received only calcium phosphate on the opposite side (control). Clinical and radiological assessments were performed on 44 dental implants at 1-month pre-MSFE, and 0.5–10-year post-MSFE. No adverse effects and pathology were found based on general health, clinical, and radiological assessments. Forty-three dental implants (98%) remained functional. One dental implant failure was observed, which was unlikely related to SVF-supplementation. Control and study sides showed similar peri-implant soft tissue quality, sulcus bleeding index, probing depth, plaque index, keratinized mucosa width, as well as marginal bone loss (0–6 mm), bone graft height loss (0–6 mm), and bone graft volume reduction. Peri-implantitis was observed around six implants in three patients (control: 4; study: 2). In conclusion, SVF-supplementation showed enhanced bone regeneration in the short-term (previous study), and led to no abnormalities clinically and radiologically in the long-term. Future studies with more patients and higher SVF-dosages are recommended to improve efficacy and open new possibilities for a variety of cell-based bone tissue engineering applications.

In conclusion, the results of the clinical studies in this thesis have contributed to new insights in bone formation and vascularization in jaw bone regeneration using different bone grafting materials, either or not supplemented with SVF, for dental implant placement. SVF-supplementation increased vascularization and osteoid volume in calcium phosphate bone substitute to

a similar level of using retromolar bone graft in patients who had undergone MSFE. Therefore, SVF-supplementation might accelerate dental implant placement and loading. The successful 10-year clinical and radiological follow-up of patients treated with MSFE using SVF-supplemented calcium phosphate bone substitute, provides powerful leads to extent the clinical application of SVF. The new insights provided in this thesis could have important implications for the development of new strategies in cellular bone tissue engineering in the fields of oral and maxillofacial surgery and orthopedics.

SAMENVATTING

De vraag naar tandheelkundige implantaten ter vervanging van ontbrekende gebitselementen is de laatste 30 jaar sterk toegenomen. Naar verwachting zal deze vraag komend decennium nog verder stijgen. Onvoldoende kaakbotvolume als gevolg van botverlies door systemische of lokale oorzaken, is een veelvoorkomend probleem bij het plaatsen van tandheelkundige implantaten. Een sinusbodemelevatie (SBE) wordt uitgevoerd om het verticale botvolume in de zijdelingse delen van de bovenkaak te vergroten ten behoeve van het plaatsen van een tandheelkundig implantaat. Autoloog bottransplantaat, allogeen, xenogeen en/of synthetisch botsubstituut zijn bottransplantatiematerialen die worden gebruikt voor een SBE. Het gebruik van autoloog bottransplantaat resulteert in een betere kaakbotregeneratie dan wanneer alleen botsubstituut wordt gebruikt. De nadelen van het gebruik van een autoloog bottransplantaat, zoals donorplaats morbiditeit en beperkte beschikbaarheid, leiden ertoe dat er naar geschikte alternatieve botregeneratiematerialen met vergelijkbare bioactiviteit gezocht wordt. Het ideale botregeneratiemateriaal met adequate biomimetische eigenschappen, uitstekend botregeneratiepotentieel, en weinig nadelen, zoals lage morbiditeit, voldoende beschikbaarheid en lage kosten, is tot op heden nog niet ontwikkeld.

Het is aangetoond dat het toevoegen van mesenchymale stamcellen (MSC's) aan een botsubstituut bij patiënten die een SBE ondergaan, meer botvorming geeft dan het gebruik van alleen een botsubstituut. Een grote uitdaging bij de bot *tissue engineering* is nog steeds het verkrijgen van een goede vascularisatie van het geïmplanteerde materiaal. De stromale vasculaire fractie (SVF), die uit vetweefsel afkomstige mesenchymale stamcellen (vetstamcellen; ASC's) bevat, wordt momenteel beschouwd als een veelbelovende bron van volwassen stamcellen met osteogeen en angiogeen potentieel voor cellulaire bot *tissue engineering*. Bovendien spelen mechanosensitieve osteocyten een cruciale rol in de micro-omgeving (niche) van het botregeneratiegebied. Daarom is een beter begrip van de relatie tussen mechanische belasting en osteocyten nodig, om toekomstige behandelstrategieën te ontwikkelen waarbij MSC's worden gebruikt om functioneel botweefsel te induceren ten behoeve van de plaatsing van tandheelkundige implantaten. De toepassing van SVF (met daarin ASC's) kan een geschikt alternatief zijn voor de huidige kaakbotregeneratiematerialen, *d.w.z.* autoloog bottransplantaat en/of botsubstituut, indien het op de lange termijn vergelijkbare biologische activiteit en veiligheid vertoont met een autoloog bottransplantaat.

Dit proefschrift is gericht op de vascularisatie en botvorming bij kaakbotregeneratie waarbij verschillende bottransplantatiematerialen worden gebruikt, al dan niet aangevuld met SVF, ten behoeve van de plaatsing van tandheelkundige implantaten. De SBE werd als model gebruikt om verschillende botregeneratiematerialen te onderzoeken. Tevens werd het SBE-model gebruikt als een humaan *"split-mouth"* model om het gebruik van een calciumfosfaat botsubstituut met de toevoeging van SVF te vergelijken met enkel calciumfosfaat botsubstituut bij kaakbotregeneratie.

In **Hoofdstuk 2** wordt de huidige stand van zaken beschreven met betrekking tot het aanbrengen van stamcellen, de vascularisatie en de botregeneratie in het orale en maxillofaciale gebied, met de nadruk op de humane kaak. Er zijn belangrijke vorderingen gemaakt bij

de toepassing van stamcellen, maar een adequate vascularisatie van het betreffende bottransplantaat blijft een grote uitdaging. Stamcellen voor bot *tissue engineering* kunnen worden verkregen uit beenmerg, vetweefsel en tandweefsel. SVF uit menselijk vetweefsel levert een veelbelovende heterogene populatie van essentiële cellen op voor de osteogenese en angiogenese. Bovendien worden van vetweefsel afgeleide microvasculaire fragmenten (MF) gesuggereerd als een veelbelovende bron van cellen voor het stimuleren van vascularisatie, vanwege de juiste natuurlijke verhoudingen van de cellen. De vascularisatie van *tissue engineered* transplantaten kan op verschillende manieren worden verbeterd: vasculaire ingroei van het omliggende gastheerweefsel naar het geïmplanteerde transplantaat, en/of *vice versa*. De klassieke strategieën om de vascularisatie te verbeteren, richten zich op het versterken van de vaat ingroei van het omliggende gastheerweefsel in het geïmplanteerde transplantaat. MF kunnen een stimulerende werking hebben op zowel vaat in- als uitgroei, aangezien MF zowel angiogene stamcellen als gevasculariseerde matrixfragmenten bevatten. Van vetweefsel afgeleide SVF en MF zijn beide celbronnen met klinische toepasbaarheid vanwege de grote hoeveelheid die kan worden geoogst en toegepast in een éénstaps chirurgische procedure. Geschikte *in vitro* modellen om bot *tissue engineering* te bestuderen ontbreken momenteel. De ontwikkeling van geconstrueerde *in vitro* 3D-modellen die de omgeving van een botdefect nabootsen, zou nieuwe strategieën voor cellulaire bot *tissue engineering* mogelijk kunnen maken. Succesvolle klinische toepassing van op stamcellen gebaseerde cellulaire bot *tissue engineering* vereist innovatief toekomstig onderzoek dat de vascularisatie zou kunnen verbeteren.

In **Hoofdstuk 3** hebben we aangetoond dat een bottransplantaat uit het tuber maxillae, in vergelijking met retromolaar bot, een verhoogde botvitaliteit en vascularisatie laat zien bij patiënten die een SBE hebben ondergaan. We hebben een (immuno)histomorfometrische analyse uitgevoerd op botbiopten die 4 maanden na de SBE, voorafgaand aan het plaatsen van een tandheelkundig implantaat, werden genomen. We zagen dat het gebruik van een tuber maxillae-bottransplantaat bij SBE resulteerde in een 10% hoger osteoïd volume in het midden en aan de craniale zijde van het getransplanteerde gebied, en een 150%–300% hoger (totaal) aantal bloedvaten in het gehele getransplanteerde gebied in vergelijking met een retromolaar bottransplantaat. Onze hypothese was dat de verhoogde vitaliteit en vascularisatie bij een tuber maxillae-bottransplantaat waarschijnlijk het gevolg is van een snellere botremodellering of een eerdere start van nieuwe botvorming in het tuber maxillae-bottransplantaat dan in retromolaar bottransplantaat. Onze histologische gegevens suggereren dat een tuber maxillae-bottransplantaat tot een betere botregeneratie leidt dan een retromolaar bottransplantaat, aangezien er meer osteoïd wordt afgezet, meer bloedvaten worden gevormd en een actiever remodelleringsproces wordt geïnitieerd. Wanneer tuber maxillae-bottransplantaat wordt gebruikt bij een SBE, is mogelijk een kortere genezingsperiode haalbaar vanaf SBE tot het moment van tandheelkundige implantaat plaatsing en belasting.

In **Hoofdstuk 4** hebben we verschillen aangetoond in het oppervlak en de oriëntatie van osteocyten, met name in regio's van het maxillaire kaakbot gerelateerd aan de grootte en oriëntatie van de trekkracht. De implantaatposities in een diasteem en vrij-eindigende situatie werden vergeleken bij patiënten die een SBE hebben ondergaan met β-tricalciumfosfaat (ß-TCP) als bottransplantatiemateriaal. In dit onderzoek werd gebruik gemaakt van

driedimensionale eindige-element analyse (*finite element analysis)* en werd een histomorfometrische analyse uitgevoerd van botbiopten die acht maanden na SBE, vóór plaatsing van een tandheelkundig implantaat, werden genomen. Ten eerste voorspelde de eindige-element analyse van de bovenkaak grotere trekspanningen met een andere oriëntatie in het diasteem dan in de vrij-eindigende implantaatposities. Ten tweede zagen we dat osteocyten in een enkelvoudig diasteem een meer craniale-caudale oriëntatie en een groter oppervlak hadden dan osteocyten in vrij-eindigende implantaatlocaties. Er waren geen verschillen in gemineraliseerd residuaal natief botvolume, en in osteocyt aantal en morfologie tussen een enkelvoudig diasteem en vrij-eindigende implantaatlocaties. Onze bevindingen geven inzicht in de relatie tussen trekspanning en osteocyt morfologie en oriëntatie in maxillair bot, hetgeen zou kunnen bijdragen aan een beter begrip van de cellulaire processen die leiden tot verschillen in botkwaliteit op verschillende implantaatposities en uiteindelijk tot het succes van tandheelkundige implantaten in de bovenkaak. De exacte betekenis van de oriëntatie van osteocyten bij het succes van tandheelkundige implantaten is echter complex en vergt nader onderzoek.

In **Hoofdstuk 5** hebben we verschillen aangetoond in de vascularisatie en het botregenererend vermogen tussen een calciumfosfaat botsubstituut, al dan niet aangevuld met SVF, versus een autoloog bottransplantaat 4–6 maanden na een SBE. Een histologische analyse werd uitgevoerd op botbiopten die 4–6 maanden na de SBE, vóór plaatsing van het tandheelkundige implantaat, werden verkregen. Patiënten die een SBE ondergingen met retromolaar bottransplantaat, tuber maxillae-bottransplantaat, ß-TCP, bifasisch calciumfosfaat (BCP), ß-TCP aangevuld met SVF en BCP aangevuld met SVF werden vergeleken. Het gebruik van een calciumfosfaat botsubstituut aangevuld met SVF bij SBE resulteerde in een vergelijkbaar aantal bloedvaten en osteoïdvolume met retromolaar bot, maar minder dan bij tuber maxillae-bottransplantaat 4–6 maanden na de SBE. Het aantal bloedvaten en het osteoïdvolume waren lager in het craniale gedeelte van het botbiopt bij gebruik van een calciumfosfaat botsubstituut dan een autoloog bottransplantaat. Bovendien was het botvolume lager in de onderzochte botbiopten bij gebruik van een calciumfosfaat botsubstituut dan bij een autoloog bottransplantaat. Bij gebruik van een calciumfosfaat substituut aangevuld met SVF en tuber maxillae-bot was het botvolume vergelijkbaar, maar lager dan bij een retromolaar bottransplantaat. Vergelijkbare vascularisatie- en botregeneratie potentie werd waargenomen bij gebruik van calciumfosfaat botsubstituut aangevuld met SVF en retromolaar bottransplantaat. Dit is mogelijk het gevolg van een vasculogeen, angiogeen en osteogeen effect van de SVF-toevoeging. Onze histologische gegevens suggereren dat calciumfosfaat botsubstituut aangevuld met SVF dezelfde uitkomst zou kunnen geven als retromolaar bottransplantaat bij SBE, aangezien een vergelijkbaar aantal bloedvaten en osteoïdvolume werd waargenomen. Daarom zou calciumfosfaat botsubstituut aangevuld met SVF veelbelovend kunnen zijn om een autoloog bottransplantaat te vervangen voor een betere botregeneratie bij SBE.

In **Hoofdstuk 6** hebben we de lange termijn-veiligheid (follow-up van 10 jaar) aangetoond van SVF-toevoeging in combinatie met een calciumfosfaat botsubstituut bij patiënten die een SBE ondergingen. Alle 10 patiënten die eerder hadden deelgenomen aan een fase I-studie werden opgenomen in deze 10-jaar follow-up studie. Ze kregen ofwel ß-TCP (n=5) ofwel BCP (n=5) met SVF-toevoeging aan één zijde (studie). Bilateraal behandelde patiënten (6 van de

10; 3 ß-TCP, 3 BCP) kregen daarnaast calciumfosfaat aan de andere zijde (controle). Klinische en radiologische beoordelingen werden uitgevoerd op 44 tandheelkundige implantaten 1 maand vóór de SBE en 0.5 tot 10 jaar na de SBE. Er werden geen nadelige effecten en pathologie gevonden op basis van algemene gezondheids-, klinische en radiologische beoordelingen. Drieënveertig tandheelkundige implantaten (98%) bleven functioneel. Eén tandheelkundig implantaat faalde, hetgeen niet gerelateerd was aan de SVF-toevoeging. Controle- en onderzoekszijden toonden vergelijkbare kwaliteit van de peri-implantaire mucosa, bloedingsindex, pocketdiepte, plaque-index, breedte van de gekeratiniseerde mucosa, evenals peri-implantair botverlies (0–6 mm), verlies van bottransplantaathoogte (0–6 mm) en vermindering van het bottransplantaatvolume. Peri-implantitis werd waargenomen rond zes implantaten bij drie patiënten (controle-zijde: 4; studie-zijde: 2). Concluderend, SVF-toevoeging toont een verbeterde botregeneratie op de korte termijn (eerdere fase-I studie) en leidt op de lange termijn niet tot afwijkingen, noch klinisch noch radiologisch. Toekomstige studies met meer patiënten en hogere SVF-doseringen zijn nodig om de werkzaamheid van SVF te verbeteren en nieuwe mogelijkheden te exploreren voor een verscheidenheid aan cellulaire bot *tissue engineering*.

Concluderend kan gesteld worden dat de resultaten van de klinische studies in dit proefschrift meer inzicht hebben gegeven in de vascularisatie en botvorming bij kaakbotregeneratie, door gebruik te maken van verschillende bottransplantatiematerialen, al dan niet aangevuld met SVF, ten behoeve van de plaatsing van tandheelkundige implantaten. SVF-toevoeging verhoogde de vascularisatie en het osteoïdvolume bij het gebruik van calciumfosfaat botsubstituten tot een vergelijkbaar niveau als retromolaar bottransplantaat bij patiënten die SBE hadden ondergaan. Derhalve kan SVF-toevoeging mogelijk de botregeneratie versnellen, zodat het plaatsen en belasten van tandheelkundige implantaten eerder mogelijk wordt. De lange termijn patiëntveiligheid van calciumfosfaat botsubstituten met SVF-toevoeging bij SBE werd aangetoond door de 10-jarige klinische en radiologische follow-up van patiënten. Deze succesvolle uitkomst biedt nieuwe aanknopingspunten voor klinisch vervolgonderzoek met SVF. De inzichten in dit proefschrift zouden van groot belang kunnen zijn voor de ontwikkeling van nieuwe strategieën voor cellulaire bot *tissue engineering* binnen de kaakchirurgische en orthopedische disciplines.

AUTHORS' CONTRIBUTIONS

Chapter 2 was published in: *Stem Cells International 2019;2019:6279721*
Bone tissue regeneration in the oral and maxillofacial region: A review on the application of stem cells and new strategies to improve vascularization
Authors:
Vivian Wu (VW), Marco N. Helder (MH), Nathalie Bravenboer (NB), Christiaan M. ten Bruggenkate (CB), Jianfeng Jin (JJ), Jenneke Klein-Nulend (JK), Engelbert A.J.M. Schulten (ES)
Authors' contributions:
Conceptualization, VW, MH, NB, CB, JK, ES; Investigation, VW; Supervision, MH, NB, CB, JK, ES; Writing-original draft preparation, VW; Writing-review and editing, MH, NB, CB, JJ, JK, ES; All authors have read and agreed to the published version of the manuscript.

Chapter 3 was published in: *International Journal of Oral Science 2018;10(1):2*
Osteocyte morphology and orientation in relation to strain in jaw bone
Authors:
Vivian Wu (VW), René F.M. van Oers (RO), Engelbert A.J.M. Schulten (ES), Marco N. Helder (MH), Rommel G. Bacabac (RB), Jenneke Klein-Nulend (JK)
Authors' contributions:
Conceptualization, VW, RO, ES, MH, RB, JK; Funding acquisition, JK, ES, MH, RB; Investigation, VW, RO; Supervision, VW, ES, MH, JK; Writing-original draft preparation, VW; Writing-review and editing VW, RO, ES, MH, RB, JK; All authors have read and agreed to the published version of the manuscript.

Chapter 4 was published in: *Clinical Implant Dentistry and Related Research 2023;25(1):141–151*
Bone vitality and vascularization of mandibular and maxillary bone grafts in maxillary sinus floor elevation: A retrospective cohort study
Authors: Vivian Wu (VW), Engelbert A.J.M. Schulten (ES), Marco N. Helder (MH), Christiaan M. ten Bruggenkate (CB), Nathalie Bravenboer (NB), Jenneke Klein-Nulend (JK)
Authors' contributions:
Conceptualization, VW, ES, MH, CB, NB, JK; Funding acquisition, JK, ES, MH, NB, CB; Investigation, VW, ES, MH, CB, NB, JK; Supervision, ES, MH, CB, NB, JK; Writing-original draft preparation, VW; Writing-review and editing, ES, MH, CB, NB, JK; All authors have read and agreed to the published version of the manuscript.

Chapter 5 was prepared as:
Vascularization and bone regeneration potential of calcium phosphate bone substitutes either or not adipose stem cell-supplemented versus autologous bone grafts in maxillary sinus floor elevation: A retrospective cohort study
Authors:
Vivian Wu (VW), Marco N. Helder (MH), Engelbert A.J.M. Schulten (ES), Christiaan M. ten Bruggenkate (CB), Jenneke Klein-Nulend (JK), Nathalie Bravenboer (NB)

Authors' contributions:
Conceptualization, VW, MH, ES, CB, JK, NB; Funding acquisition, JK, ES, MH, NB, CB; Investigation, VW; Supervision, MH, ES, CB, JK, NB; Writing-original draft preparation, VW; Writing-review and editing, MH, ES, CB, JK, NB; All authors have read and agreed to the final version of the manuscript.

Chapter 6 was published in: *Stem Cells Translational Medicine 2023;szad045*
Long-term safety of bone regeneration using autologous stromal vascular fraction and calcium phosphate ceramics: A 10-year prospective cohort study
Authors:
Vivian Wu (VW), Jenneke Klein-Nulend (JK), Nathalie Bravenboer (NB), Christiaan M. ten Bruggenkate (CB), Marco N. Helder (MH), Engelbert A.J.M. Schulten (ES)
Authors' contributions:
Conceptualization, VW, JK, NB, CB, MH, ES; Funding acquisition, JK, ES, MH, NB, CB; Investigation, VW, CB, ES; Supervision, JK, NB, CB, MH, ES; Writing-original draft preparation, VW; Writing-review and editing JK, NB, CB, MH, ES; All authors have read and agreed to the final version of the manuscript.

LIST OF ABBREVIATIONS

AB	autologous bone
ASC	adipose stem cell
B.Ar	bone area
bFGF	basic fibroblast growth factor
Bloodves	bloodvessels
BMP	bone morphogenetic protein
BMSC	bone marrow stem cell
β-TCP	β-tricalcium phosphate
BCP	biphasic calcium phosphate
CaP	calcium phosphate
CBCT-scan	cone beam computed tomography scan
Micro-CT	micro-computed tomography
CGF	concentrated growth factor
COL	collagen sponge
DBBM	demineralized bovine bone matrix
DSC	dental stem cell
EPC	endothelial progenitor cell
EPSC	embryonic stem cell
FDBA	freeze dried bone allografts
FE	finite element
GMP	good manufacturing practice
GMSF	grafted maxillary sinus floor
HA	hydroxyapatite
IPSC	induced pluripotent stem cell
IL	interleukin
KM	keratinized mucosa
Lac	osteocyte lacunae
MF	microvascular fragments
MFAT/NFAT	microfragmented adipose tissue/nanofat
MSC	mesenchymal stem cell
MSFE	maxillary sinusfloor elevation
NB	native bone
O.Ar	osteoid area
PI	plaque index
PD	probing depth
PDGF	platelet derived growth factor
PLGA	poly(lactic-co-glycolic acid)
PRF	platelet-rich fibrin
PRP	platelet-rich plasma
RNB	residual native bone

RI	region I
RII	region II
RIII	region III
Ocl	osteoclasts
Ot	octeocytes
Pt	patient
RANKL	receptor activator of nuclear factor-κB ligand
ROI	region of interest
SBE	sinusbodemelevatie
SBI	sulcus bleeding index
SEM	standard error of the mean
SD	standard deviation
SI	silica
SVF	stromal vascular fraction
TNF-α	transforming necrosis factor-α
TRAcP	tartrate-resistant acid phosphatase
T.Ar	total area
TZ	transition zone
VEGF	vascular endothelial growth factor

DANKWOORD

Doctor of Philosophy (PhD) is een Anglo-Amerikaanse variant op de academische titel doctor, de hoogste academische graad. Philosophy omvat hier de bredere en originele betekenis van het Oudgriekse woord philosophia (φιλοσοφία), wat letterlijk betekent liefde voor wijsheid.

Nog voordat ik tandarts werd, wist ik dat ik mij wilde specialiseren in de implantologie én dat ik wilde promoveren uit liefde voor wijsheid. Het eerste is reeds succesvol geschied. Het bewijsstuk van het tweede ligt voor u: de thesis gebaseerd op het verrichte onderzoek van de afgelopen vier jaar. Toen ik in 2019 aan mijn wetenschappelijke avontuur startte, besefte ik mij nog niet dat het promotietraject een "project of life" zou worden. Vele avonden, weekenden en vakanties heb ik hieraan opgeofferd. Ik ben gepast trots en tevreden met het eindresultaat.

"You can't be what you can't see" is een gevleugelde uitspraak over hoe het werkt met rolmodellen: iemand moet je voorgaan, zodat je kunt zien wat er mogelijk is. Mijn rolmodellen in mijn persoonlijke en professionele leven hebben mij geholpen om anders naar het leven te leren kijken. Zij hebben mij geleerd hoe ik kan nadenken over wie ik ben, wat ik doe en wat ik wil. Ik ben ontzettend dankbaar voor alle rolmodellen en kansen die ik heb gekregen in de verschillende fases van mijn leven. Ik wil mijn **familie**, **vrienden**, **kennissen**, **opleiders**, **collegae en patiënten** hartelijk danken voor het vertrouwen, de steun en de wijsheid die hebben bijgedragen tot de totstandkoming van dit proefschrift. Dit proefschrift is een ode aan eenieder die in mij heeft geloofd.

Prof.dr. J. Klein Nulend, Beste Jenneke, In 2013 had ik, als student Tandheelkunde, het geluk om met u kennis te maken. U heeft mij begeleid bij mijn eerste stappen in de wetenschap, mijn master thesis. Dit werk leverde uiteindelijk mijn eerste wetenschappelijke publicatie op in een vooraanstaand wetenschappelijk tijdschrift en nominaties voor verschillende wetenschappelijke prijzen. Toendertijd is mijn wens om te promoveren ontstaan. Ik ben u ontzettend dankbaar voor al uw tijd en energie die u in mij en mijn promotietraject heeft gestoken, en het vertrouwen dat u mij heeft gegeven. Ik prijs mezelf gelukkig dat ik u als mijn eerste promotor had. U heeft mij geleerd wat nodig is om te excelleren in de wetenschap. Dit zal ik de rest van mijn carrière bij mij dragen.

Prof.dr. E.A.J.M Schulten, Beste Bert, U bent voor mij een rolmodel van een vooraanstaande clinicus die hoogstaand wetenschappelijk onderzoek verricht. Tijdens mijn master thesis en promotietraject inspireerde u mij met de translatie van klinische vraagstukken naar fundamenteel onderzoek, en vice versa. Ik ben u zeer dankbaar voor uw toewijding aan mijn promotietraject als tweede promotor. Niet alleen inhoudelijk, maar ook textueel, leidde u mij naar precisie en correctheid.

Dr. M.N. Helder, Beste Marco, Als expert op het gebied van de toepassing van stamcellen bij botregeneratie, inspireerde jij mij veelal met vernieuwende wetenschappelijke inzichten. Jij was als mijn copromotor, kritisch maar ondersteunend in mijn promotietraject. Door cruciale vragen te stellen en logisch te redeneren leerde jij mij wetenschappelijk onderzoek te verrichten op een hoog niveau.

Dr. N. Bravenboer, Beste Nathalie, Mijn histologische kennis, inzicht en vaardigheden heb ik onder jouw vleugels kunnen ontwikkelen. Een groot deel van mijn promotieonderzoek heb ik op jouw prachtige lab mogen uitvoeren. Naast jouw professonele begeleiding als copromotor, ben ik erg dankbaar voor jouw persoonlijke steun afgelopen jaren. De deur naar jouw kamer stond altijd open. Je bent voor mij een voorbeeld van een succesvolle vrouwelijke wetenschapper die zeer prettig is in de omgang: “hard on the issue, soft on the person”.

Prof.dr. C.M. ten Bruggenkate, Beste Chris, Het was een eer om u als supervisor tijdens mijn promotietraject te hebben. U bent zowel klinisch als wetenschappelijk een groot voorbeeld voor mij. Uw ervaring in de implantologie is van onschatbare waarde. Ik ben ontzettend dankbaar voor uw betrokkenheid bij mijn promotietraject, ondanks de belemmeringen van de ‘Coronatijd’ trachtte u mijn promotietraject zoveel mogelijk te bespoedigen.

Hooggeleerde en zeergeleerde leden van mijn promotiecommise: **dr. A.D. Bakker**, **prof.dr. G.M. Raghoebar**, **prof.dr. K. de Groot**, **prof.dr.ir. S.C.G. Leeuwenburgh**, **prof.dr. J.W.M. Niessen**, **prof.dr. P.A. Nolte**, **prof.dr. I. Heyligers**, Ik dank u hartelijk voor het lezen en beoordelen van mijn proefschrift. Ik voel me vereerd dat ik mijn promotietraject mag eindigen met zo’n vooraanstaande promotiecommissie.

Dr.ir. R.F.M. van Oers, Beste René, Veel dank voor onze interdisplinaire samenwerking en jouw technische inzichten over ‘finite element analysis’, die uiteindelijk hebben geleid tot mijn master thesis en eerste wetenschappelijke publicatie. Ik heb jouw begeleiding als zeer prettig en leerzaam ervaren.

Prof.dr. R.G. Bacabac, Dear Mel, It was a great honour working with you. Our interdisciplinary and international cooperation was truly inspiring. I am grateful for your time and effort.

H.W. van Essen, Beste Huib, Veel dank voor jouw geduldige begeleiding bij de immunokleuringen in het lab. Dankzij jouw hulp heb ik een totaal onbekende vaardigheid eigen kunnen maken, die ik veelvulldig heb toegepast in mijn promotietraject.

M.A. van Duin, Beste Marion, Hartelijk dank voor al jouw hulp bij het gereedmaken van mijn biopten en coupes. Tijdens mijn master thesis en promotietraject heb jij mij tevens geleerd om met de microscoop te werken. Een essentiële vaardigheid tijdens mijn promotietraject.

Dr. F.A.S. van Esterik en **Dr. E. Farré-Guasch**, Beste Francis en Elisabet, Veel dank voor het verschaffen en uitleggen van data uit eerdere studies. Jullie eerdere werk was voor mij een inspiratiebron.

Mijn **OCB-collegae** wil ik hartelijk danken voor de samenwerking, adviezen en steun. **Jinfeng** en **Wei**, ik wil jullie in het bijzonder danken voor jullie directe hulp en betrokkenheid bij de totstandkoming van mijn proefschrift. **Sue**, **Teun**, **Ton**, **Victor**, **Tijmen**, **Chen**, **Yuanyuan**, **Ivana**, **Carolyn** en **Cindy** met plezier kijk ik terug op een inspirerende en gezellige tijd met jullie. **Behrouz**, **Jolanda**, **Ineke** en **Cor**, veel dank dat jullie deur altijd openstond voor hulp.

Dr. H. Brand en **Dr. J.A.M. Korfage**, Beste Henk en Hans, Hartelijk dank voor al jullie hulp en steun achter de schermen bij de totstandkoming van mijn proefschrift.

Dr.ir. G.J. Streekstra en **dr.ir. J.G.G. Dobbe**, Beste Geert en Iwan, Dankzij jullie heb ik inmiddels een ander besef van '3D'. Ik waardeer jullie tijd en inzet enorm die jullie in mijn promotietraject hebben gestoken.

Dr. R.G. Gorter, Beste Ronald, Via het *honours programme* bracht jij mij in contact met Jenneke, wat uitiendelijk het begin was van dit proefschrift. Ik ben jou dankbaar voor alle kansen die jij mij in het *honours programme* hebt geboden.

Oud-opleiders in de orale implantologie: **Prof.dr. D. Wismeijer**, Beste Daniël, Ik ben jou zeer dankbaar voor de kans die jij mij hebt gegeven om de opleiding MSc. Orale Implantologie en Prothetiek te volgen. Vanzelfsprekend, speel jij een onontbeerlijke rol in mijn carrière als implantoloog. **Dr. Tahmaseb**, Beste Ali, Mijn eerste dierexperiment en ITI-consensus meeting was onder jouw vleugels. Veel dank voor alle leerzame momenten en steun. **Dr. E. Blom**, Beste Erik, Jij bent een voorbeeld voor mij op veel vlakken. Het belang van klinisch handelen met wetenschappelijk inzicht heb jij altijd onderstreept. Onze nervus lateralisatie was memorabel! **J.H.P. Cossé**, Beste Johan, Ik hoor nog steeds jouw stem in mijn gedachte, wanneer ik een patiënt aan het behandelen ben. Ik heb veel bewondering voor jou als chirurg en jouw nuchtere benadering van het vak. Wellicht hoor ik ook ooit nog eens jouw stem tijdens het rijden (911). **P.W. van Elsas**, Beste Pieter, Als mijn mentor tijdens de opleiding heb jij mij vanaf dag één scherp gehouden door kritische vragen te stellen gestoeld op wetenschap. Veel dank dat ik mocht delen in jouw onuitputbare kennis en ervaring. **E. Rikken**, Beste Enrique, Mijn eerste laterale sinusbodemelevatie was onder jouw vleugels. Je kwam speciaal ervoor op een donderdag naar ACTA, een bijzonder moment. Hartelijk dank voor alle toewijding aan mijn opleiding. **H. Kuit**, Beste Haakon, Als opleider inspireerde, motiveerde en steunde je mij, veel dank hiervoor. Je bent een groot voorbeeld voor mij als vooraanstaande clinicus en "pink tissue-expert", en wellicht ook als golfer binnenkort. **J. Huigen**, Beste Jeroen, Mijn eerste implantaat heb ik met jou geplaatst. Veel dank voor alle leerzame momenten en fijne begeleiding. **S. Umanjec-Korac**, Beste Sanja, Ik heb veel ontzag voor hoe jij jouw carrière hebt ontwikkeld. Je bent een voorbeeld voor veel (jonge)

vrouwen. **H.R. Hoogeveen**, Beste Robin, Kort maar krachtig was jij mijn opleider. Ik bewonder jouw “down-to-earth” mentailiteit. Veel dank voor alle constructieve feedback.

Lieve **collegae van de Orfeokliniek**, Ik wil jullie hartelijk danken voor de collegiale samenwerking, en een aantal collegae in het bijzonder: **R.M. Mulié**, Beste Mul, de beste ortho van Nederland! Veel dank voor uw vertrouwen in mij. Ik ben u zeer dankbaar voor alle kansen en grote steun die u mij heeft gegeven afgelopen jaren. Het is een eer om met u te mogen samenwerken en van uw jarenlange kunde en kennis te leren. **Albert**, veel dank voor de fijne en leerzame samenwerking. Jij hebt mij in het zadel hebt geholpen in mijn opstartfase in de kliniek. **Calin** en **Zoï**, jullie zijn mijn zeer gewaardeerde endo-buddies, veel dank voor de collegiale samenwerking en gezelligheid. **Henry** en **Herman**, hartelijk dank voor de feilloze ortho-implanto samenwerking. **Kees**, bedankt voor de gezelligheid en collegialiteit die jij hebt meegebracht op de werkvloer. **Liesbeth**, hartelijk dank voor jouw ontzettend positieve steun en collegialiteit. **Selma** en **Sandra**, jullie zijn de duizendpoten in de kliniek. Veel dank dat ik jullie altijd mag storen met verzoeken voor hulp en de gezelligheid en gekkigheid die mijn dag maken. **Claire**, **Lucinda** en **Mariesa**, dankzij jullie professionele contact met de patiënten en verwijzers is de implantologie hard gegroeid. Dreamteam **Gill** en **Margreth**, teamwork makes the dream work! Ik ben jullie veel dank verschuldigd voor jullie tomeloze inzet dag in, dag uit. Dankzij jullie hebben ik implantologische successen kunnen behalen en hebben wij daarmee veel patiënten geholpen. Samen presteren wij op top niveau. En dat ik er soms moe uit zag, komt dus door dit proefschrift. **Caro**, Je past feilloos in het dreamteam. Ik vind je een geweldige assistent. **Dorleen**, **Floor**, **Elly**, **Fahima** en **Patricia**, dank voor al jullie inzet bij mijn behandelingen. **Babette**, dank voor alle gezelligheid op de werkvloer en het delen van al jouw ervaringen in toerisme. **Chantel**, **Rosita** en **Gustavo**, veel dank dat jullie er (achter de schermen) voor zorgen dat mijn implantologische behandelingen soepel kunnen verlopen. **Matthieu**, hartelijk dank voor jouw vertrouwen en het in goede banen leiden van de kliniek.

Verwijzers, ik wil jullie hartelijk danken voor het vertrouwen dat jullie mij hebben gegeven, en in het bijzonder: **Hans Man in ’t Veld**, **Ghizlane Aarab**, **Arlies Nieuwenhuijse**, **Magchiel Hoogendoorn**, **Paul Delsing**, **Jos Crooijmans**, **Tajana Westerhof**, **Menar Handy**, **Pim Smits**, **Kiki Oei**, **Angelique Dao**, **Ivy Liu** en **Yu Ming Chung**. Zonder jullie, als verwijzers van het eerste uur, had ik mijn carrière in de implantologie niet kunnen opstarten. Het is een eer om jullie patiënten te mogen behandelen.

Lieve ACTA-vriendinnen *(est. 2010)*: **Daniëlle**, wij zijn vriendinnen sinds dag 1 van onze opleiding Tandheelkunde op ACTA. Woorden schieten tekort als ik mijn waardering van onze vriendschap wil beschrijven. Jij hebt naast mij gestaan op verschillende moeilijke en mooie momenten in mijn leven. Ik ben trots dat jij wederom, als paranimf, aan mij zij staat tijdens mijn promotie. Veel dank voor alle steun en hulp. **Lieneke**, als partners hebben wij samen onze eerste tandheekundige behandelingen uitgevoerd op ACTA. Mijn waardering is groot dat ik nog steeds jouw patner mag zijn op implantologisch gebied. Als collega bewonder ik jouw ondernemerschap, als vriendin bewonder ik jouw hart van goud. **Fleur**, wij zijn een fantastisch team, of het

nou gaat om het schrijven van een bachelor scriptie, filosoferen over onze levens of opzetten van een vakantie. Ik hoop dat ik nog heel lang van jouw positieve energie en aligner-restauratieve tandheelkundige kennis mag genieten. **Eveline**, jij bent mijn favoriete "gele persoon". Jouw enthousiasme en sociale vaardigheden zijn een groot voorbeeld voor mij. Je bent een geweldige tandarts. Ik waardeer enorm dat wij op implantologisch gebied samenwerken, veel dank voor jouw vertrouwen. **Janine**, wij hebben samen veel meegemaakt op het land en water. Onze vriendschap is hartverwarmend. Ik heb me erg gesteund gevoeld door jouw oprechte interesse in mij en mijn promotietraject. **Valerie**, ondanks dat je niet meer om de hoek woont, voelt het altijd als ik jou spreek en/of zie dat er geen dag voorbij is gegaan. Veel dank dat je altijd voor me klaar staat. Ik heb veel ontzag voor hoe je je eigen weg hebt gevonden en alle ballen hoog houdt, wat ben je een doorzetter.

Lieve Leydse Liefs (est. 2004): **Elisa**, **Merle**, **Meret**, **Amy**, **Nikki** en **Barbara**, we go way back. Ik vind het ontzettend bijzonder dat wij nog steeds de belangrijke momenten in ons leven met elkaar delen. We zitten allemaal in verschillende professies, fases van ons leven en zelfs in verschillende landen, maar onze vriendschap brengt ons weer samen terug naar Leiden. Ik heb mij altijd erg gesteund gevoeld door onze vriendschap.

Lieve **Raissa** en **Annemiek**, Afgelopen 10 jaar is onze vriendschap sterk gegroeid. Jullie steun in mijn persoonlijke en professionele leven betekent veel voor mij. Jullie zijn voorbeelden van twee succesvolle carrière vrouwen die tevens weten te genieten van het leven. Rais, extra dank voor de PhD-related "onderonsjes". Deze waren een grote steun voor mij. Ik kijk uit naar nog veel leuke momenten met julie. Ik ben trots om jullie vriendin te zijn!

Lieve **Aisha**, Sinds de opleiding zijn we dikke maatjes in de implantologie en privé. Samen struinen we congressen af voor een gezonde mix van work en pleasure. Ik bewonder hoe jij jouw carrière combineert met jouw gezinsleven. Ik vind dat je het fantastisch doet!

Lieve **Michael** en **Femke**, **Steven** en **Jessica**, **Philip** en **Annemijn**, **Reynier** en **Quirine**, **Rutger** en **Kaire**, Dank voor jullie vriendschap en interesse in mijn promotieonderzoek.

Lieve **oom Klaas** en **tante Gien**, Jullie hebben vanaf mijn geboorte een belangrijke rol gespeeld in mijn leven. Ik ben ontzettend dankbaar dat jullie mijn peetouders zijn, en op belangrijke momenten in mijn leven als familie voelen. Heel veel dank voor al jullie betrokkenheid, wijze raad en steun.

Lieve **Gerlof**, **Loes**, **Fokke**, **Katja**, **Fedde** en **Kee**, Ik prijs mij gelukkig met het liefdevolle en warme bad waarin ik ben terecht gekomen. Veel dank voor alle mooie en fijne momenten van samenzijn en jullie oprechte steun en interesse in mij en mijn promotietraject.

Lieve **Duco**, Corona heeft de wereld veranderd, maar ook ons leven. Ons leven is nu samen. En samen zijn wij op ons best: yinyang. Ik heb zin in de dag van morgen, omdat ik benieuwd

ben wat ons dat gaat brengen. Ik put veel liefde, energie en vertrouwen uit onze relatie. Ik ben dankbaar voor jouw directe en indirecte bijdrage aan de totstandkoming van mijn proefschrift. Jij bent mijn wandelende textuele hulp en mijn emotionele steun en toeverlaat. 2023 is een mijlpaal voor ons beiden. Ik ben heel trots op jou en ons, en kijk uit naar een toekomst vol geluk. Ik hou van je!

Lieve **George**, Vroeger was ik altijd jouw grote zus, nu ben jij vaak mijn grote broer! Bedankt dat je onvoorwaardelijk voor mij klaarstaat. Ik heb respect voor jouw technische inzichten, doorzettingsvermogen en sociale vaardigheden. Jij hebt een bewonderingswaardige bachelor thesis geschreven over de osteocyt, toen nog onwetende dat jou een wetenschappelijke opleiding te wachten staat. Je zult een geweldige tandarts worden. Ik kijk er naar uit om in de toekomst nauw met je samen te gaan werken.

Lieve **Papa** en **Mama**, Jullie zijn mijn grootste rolmodellen. Jullie hebben mij van jongs af aan aangemoedigd om groots te durven dromen, en mij het vertrouwen gegeven dat ik alles kan bereiken wat ik wil. Oneindige dank en waardering voor al jullie zorgen en de kansen die jullie mij hebben gegeven. Alle inspirerende gesprekken aan de keukentafel hebben mijn carrière een vliegende start gegeven. Zonder jullie had ik nu niet gestaan, waar ik nu sta. Bedankt voor het liefdevolle en zorgeloze gezin waarin ik mocht opgroeien, en nog steeds in thuis mag komen. Ik hou van jullie!

ABOUT THE AUTHOR

Vivian Wu

19-11-1992, Amsterdam

Vivian Wu holds a MSc honours degree in Dentistry from the Academic Centre for Dentistry Amsterdam (ACTA, 2016), and a MSc degree in Oral Implantology and Prosthodontics (ACTA, 2019). At the age of 26, she was the youngest implantologist ever in The Netherlands. Currently, Vivian works both part-time as a dentist/implantologist in a private clinic specializing in complex dental treatments, and as part-time PhD-candidate at ACTA. Vivian conducts translational research within a network of (inter)national interdisciplinary collaborators on the application of autologous bone grafts, bone substitutes, and adipose stem cells for jaw bone augmentation to allow dental implant placement. Vivian's proven track record makes her a promising rising talent in science. She co-authored the 2018 International Team for Implantology (ITI) consensus statements, and published in leading scientific journals. Moreover, Vivian was chosen by Elsevier Weekblad as one of the '30-under-30' brightest and talented young people of 2021 who will dictate the country's future.

PUBLICATIONS

Wu V, Van Oers RFM, Schulten EAJM, Helder MN, Bacabac RG, Klein-Nulend J. Osteocyte morphology and orientation in relation to strain in jaw bone. *International Journal of Oral Science*, 2018;10(1):2. doi:10.1038/s41368-017-0007-5.

Tahmaseb A, **Wu V**, Wismeijer D,Coucke W, Evans C. The accuracy of static computer-aided implant surgery: A systematic review and meta-analysis. *Clinical Oral Implants Research*, 2018;29Suppl16:416–435. doi:10.1111/clr.13346.

Wismeijer D, Joda T, Flügge T, Fokas G, Tahmaseb A, Bechelli D, Bohner L, Bornstein M, Burgoyne A, Caram S, Carmichael R, Chen CY, Coucke W, Derksen W, Donos N, El Kholy K, Evans C, Fehmer V, Fickl S, Fragola G, Gimenez Gonzales B, Gholami H, Hashim D, Hui Y, Kökat A, Vazouras K, Kühl S, Lanis A, Leesungbok R, van der Meer J, Liu Z, Sato T, De Souza A, Scarfe WC, Tosta M, van Zyl P, Vach K, Vaughn V, Vucetic M, Wang P, Wen B, **Wu V**. Group 5 ITI Consensus Report: Digital technologies. *Clinical Oral Implants Research*, 2018;29Suppl16:436–442. doi:10.1111/clr.13309

Wu V, Helder MN, Bravenboer NB, Ten Bruggenkate CM, Jin J, Klein-Nulend J, Schulten EAJM. Bone tissue regeneration in the oral and maxillofacial region: A review on the application of stem cells and new strategies to improve vascularization. *Stem Cells International*, 2019;2019:6279721. doi:10.1155/2019/6279721.

Wu V, Schulten EAJM, Helder MN, Ten Bruggenkate CM, Bravenboer NB, Klein-Nulend J. Bone vitality and vascularization of mandibular and maxillary bone grafts in maxillary sinus floor elevation: A retrospective cohort study. *Clinical Implant Dentistry and Related Research*, 2023;25(1):141–151. doi:10.1111/cid.13142.

Wu V, Klein-Nulend J, Bravenboer NB, Ten Bruggenkate CM, Helder MN, Schulten EAJM. Long-term safety of bone regeneration using autologous stromal vascular fraction and calcium phosphate ceramics: A 10-year prospective cohort study. *Stem Cells Translational Medicine,* 2023;szad045. doi:10.1093/stcltm/szad045.